The structural and elemental composition of inhaled particles in ancient Egyptian mummified lungs.

A thesis submitted to the University of Manchester for the degree of Ph. D.
in the Faculty of Life Sciences

2012

Roger Douglas Montgomerie

Contents

Chapter 2 Materials

Chapter 3 Methods

Chapter 4 Results

Chapter 6 Conclusions and Future Work

Abbreviations

ESEM	Environmental Scanning Electron Microscope
EDX	Energy Dispersive X-ray Analysis – an elemental analysis technique
EVG	Miller's elastic – a variation of the elastic Van Giesen histological stain.
FTIR	Fourier Transform Interferometry – chemical bond analysis technique
H+E	Haemalum and Eosin – a histological stain
ICP-MS	Inductively Coupled Plasma Mass Spectrometry – an elemental analysis technique
LA-ICP-MS	Laser Ablative Inductively Coupled Plasma Mass Spectrometry – a variation of the elemental analysis tehnique
TB	Toluidine Blue – a histological stain
WD-EPMA	Wavelength Dispersive Electron Probe Micro-Analysis

Abstract

Since the first modern investigations into Egyptian mummies in the 1970s, anthracosis and silicosis have regularly been found in mummified lungs (Tapp, 1975; Walker et al, 1987). Anthracosis, lung irritation caused by carbon particles, is well researched in modern populations but very little is known about the disease in ancient times. Similarly, little is known about the prevalence of silicosis, caused by the inhalation of particles of silicon, in ancient times. It has been assumed that carbon was inhaled through the combustion of fuel for cooking and illumination whilst silicon came from the desert environment.

This study aims to test these assumptions by characterising the shape, size and elemental composition of the organic and inorganic particles contained within ancient lung tissue. When these particles are compared against surrogate carbon and silicon particles, it may be possible to identify them and reveal their aetiology.

Surrogate carbon particles were produced through controlled combustion of fuels the ancient Egyptians are likely to have used. The modern silica containing sand was collected from various archaeological sites in Egypt. A sonication method was used to extract particles from ancient tissue. After extraction, individual ancient particles were isolated and examined for size and shape analysis using light microscopy. The surrogate particles were examined in the same manner. The particles were then imaged using environmental scanning electron microscopy (ESEM) and elemental profiles determined by energy dispersive X-ray analysis (EDAX). Bulk analysis by mass spectrometry was then employed to qualitatively and quantitatively analyse the elements contained within ancient lung particles and the modern surrogates. Electron probe micro-analysis (EPMA) was used to map the deposition and elemental composition of inorganic compounds in sections of ancient lung. Further information on the bonds and chain length of soots were obtained through FTIR and Raman spectroscopy.

Results have shown the presence of anthracosis and birefringent particles in all ancient lung tissues examined by this study. Both organic and inorganic ancient particles have been found to be respirable (ie, less than 10 microns in diameter) and were present in the lung pre-mortem. EDX and ICP-MS results show the inorganic particles to consist of aluminium silicates (sand) and calcium carbonate (limestone). FTIR and Raman spectroscopy were not accurate enough to detect the ancient or surrogate soot bonds and were not suited to this study.

Declaration

No portion of the work referred to in the thesis has been submitted in support of an application for another degree or qualification of this or any other university or other institute of learning.

Copyright statement

Acknowledgements

I would like to thank John Denton and Dr Keith White for all their time, patience, knowledge and help throughout my project. I would also like to thank Prof Rosalie David, Angela Thomas, and everyone at the KNH centre for their help, support and friendship

I would also like to thank Dr Alan Cox and Neil Bramall at Sheffield, Centre for Analytical Sciences for their help with the ICP-MS techniques, Dr Richard Cutting and Dr John Waters for their assistance with the ESEM, Dr David Ellis and Dr Elon Correa for FT-IR, Dr Lorna Ashton for her help with Raman, Dr John Charnock for his help with WD-EPMA.

I would like to thank my parents and family for all their love, help and advice throughout my PhD. Finally I would like to thank Joanna for all her love and support that kept me going through all the hard times.

Chapter 1

Introduction

1.1 Mummification in Ancient Egypt

Lung disease caused by the inhalation of modern pollutants, including particulates, is well researched and documented. However, relatively little is known about particulate lung disease or the nature of the inhaled particulates in ancient Egypt (or the rest of the ancient world; Molina and Sokhi, 2011). This includes the sources of both inorganic and organic inhaled particulates and the extent of lung diseases in the ancient population. Through their burial practices, particularly the preservation of tissues through intentional mummification using natron, plus accidental mummification in desert conditions following internment, the ancient Egyptians have presented scientists with an exciting opportunity to study the extent and degree of inhalation of particulates and their associated pathologies in antiquity.

1.1.1 *Background*

Egypt existed as a distinct political entity for approximately 3500 years from around 3150BC to 550AD, and over this time Egyptologists recognise seven major periods (Shaw, 2000) which are summarised in Table 1.1. The Old, Middle and New Kingdoms were times of political stability and economic and agricultural prosperity whereas the Intermediate Periods were characterised by political and economic disruption, sometimes accompanied by loss of centralised control, famine, invasion and occupation (Kemp, 2000).

From at least the 3rd Dynasty of the Old Kingdom the ancient Egyptians practiced mummification with the intention of preserving the bodies of their dead for the afterlife. This religious practice often involved the evisceration, and the dehydration of the corpse by natron salt, and culminated in wrapping the corpse in linen bandages whilst various religious rites were performed (Riyad, 1973). The eviscerated abdominal and thoracic organs were treated similarly and stored in organ packages or canopic jars ("Canopic" results from the erroneous association by nineteenth century Egyptologists with the ancient Greek legend of Canopus, (David, 1999)). The organ packages were placed inside the mummy while the canopic jars were usually stored in a nearby canopic chest.

Table 1.1 Chronology of Ancient Egypt using Shaw's dating system (Shaw, 2000).

Period	Date
Old Kingdom	3150 BC
1st Intermediate Period	2180 BC
Middle Kingdom	2055 BC
2nd Intermediate Period	1650 BC
New Kingdom	1550 BC
3rd Intermediate Period (with Persian influence)	1069 BC
Greco-Roman Period	332BC to 550AD

Aufderheide (2003) separated the multiple methods of mummification into four categories, only two of which can be applied to ancient Egypt: spontaneous ("natural") and anthropogenic ("artificial") mummification. Artificial mummification aims to mimic natural mummification by stopping or slowing down the usual decay processes that affect a recently deceased body in order to preserve the corpse's appearance and physical state.

Putrefaction and autolysis are the two main processes of decomposition and are both driven primarily by enzymatic action. Autolysis occurs shortly after death when lysozymes, a class of intracellular enzymes stored within cells in specialised organelles called lysosomes, are released (Vass, 2001). Lysozymes are regulated during life by the cell and are used in immunological reactions and other processes such as programmed cell death and the breakdown and recycling of protein (Artal-Sanz et al, 2006). When released in large amounts, lysosomal enzymes attack peptide bonds in proteins causing damage and eventual death to the parent cell and sometimes other cells in the vicinity. Putrefaction is the secondary decomposition process and occurs when bacteria and fungi from

endogenous (for example, faecal or intestinal), or external environmental sources begin to digest the body tissues. The digestive enzymes released by fungi or bacteria cause damage similar to autolysis, for example, karyolysis (destruction of the nucleus) and thereby render the tissues available for the micro-organism's nutrition requirements (David and David, 1995).

The ancient Egyptians developed an artificial mummification process that attempts to arrest the two main decomposition processes by evisceration and dehydration. The most putrefying substances in the body, for example, bacterial flora in the intestines and the stomach's hydrochloric acid, were removed by evisceration. Putrefaction is also greatly retarded by dehydration of the corpse with natron salt. Natron is a mineral of hydrous sodium carbonate ($Na_2CO_3 \cdot 10H_2O$) and is often found crystallized with other salts. Natron not only dehydrates the corpse but also changes the chemical environment rendering most bacteria inactive. Though all bacteria need water, the minimum water content and oxygen tension they require to function varies. However, the change in hydrogen ion concentration (and therefore pH) from natron ensures disruption of cellular processes in the bacteria, including those able to survive at very low concentrations of liquid water (Potts, 1994).

1.1.2 *Natural mummification*

The earliest attempts at mummification by the ancient Egyptians were presumably entirely unintentional. In the Pre-dynastic Period (before c3100BC), the Egyptians buried their dead on the border between the uncultivated desert and their settlements on the fertile banks of the Nile. Pre-dynastic graves were simple shallow pits in which the corpse was placed, usually in a crouched "foetal" position, along with clothes and other possessions. The grave would be covered with a reed mat, a layer of sand or both. Heat from the sun and the porous desert sand ensured the quick evaporation and absorption of bodily fluids from the newly buried corpse. This type of mummification is called natural or "spontaneous" and produces mummies with characteristically dark-brown tanned leather-like soft tissues (Aufderheide, 2003; David, 2008). It is unclear when or why the Egyptians started to practice intentional mummification. The development of intentional

mummification techniques was likely driven by the pharaohs and other members of the high elite (who in this early period were probably related to the monarch) who, presumably for reasons of prestige, religious practice, or both began to construct increasing monumental and elaborate tombs. These tombs called "mastabas" were initially mud brick lined pits in the desert covered with large stone slabs. The burial pit was overlain by a flat roofed rectangular superstructure of mud brick or, subsequently, sometimes of stone. Later mastabas developed into multi-layered, usually subterranean structures of mud-brick or stone (Reisner, 1934). Mastaba tombs were much cooler and more humid than traditional desert pits which meant putrefying bacteria that were unable to attack the corpse due to rapid desiccation, were able to proliferate and decompose the body. Presumably, this was noticed and the elite therefore took steps to ensure their happiness and well being in the afterlife by intentionally preserving the body following death. The ancient Egyptians believed, in common with most modern religions, that a person's body and soul separated after death. However, they believed the soul consisted of three separate parts and two parts still depended on the body for sustenance and well-being in the afterlife. These three parts were called the "*akh*", the "*ka*" and the "*ba*". The *akh* went to heaven after death and remained there in the company of the god Osiris. The *ka* stayed in the body and lived in the area around the tomb whilst the *ba* journeyed in a bark with the sun god Ra and resided in the deceased's body during the day and the heavens at night (Riyad, 1973).

Figure 1.1 The Ba, represented as a human-headed bird, sometimes with the facial likeness of the deceased, visits the mummy which harbours the Ka (Canadian Museum of Civilization, 2010).

These beliefs meant that at least one of the three parts of the soul depended on the body being in a good state of preservation at any one time. Obviously, if the body was to decay, then the soul would not have a place to reside and this would lead to an awful and undesirable afterlife. Therefore statues of the dead and wall paintings of the deceased drawn according to a religious "canon of proportions" were included in the tomb to harbour the *ka* and *ba* in the case of the body being damaged. At certain periods, Egyptian priests would also rescue damaged or vandalised mummies from robbed tombs, repair them and place them in newly built or existing tombs to create mummy caches. The best example of this is the DB320 cache at Deir El-Bahri, which was found by archaeologists in 1881 and contained the mummies of around fifty kings, queens and noblemen, including the pharaoh Ramses II (Feldtkeller et al, 2003).

As tombs became more complex, the need for intentional mummification became necessary and it is well documented that artificial mummification started to be practiced regularly during the 3rd Dynasty (c2770 BC) after several centuries of experimentation (Quirke and Spencer, 1992).

Artificial Mummification

Although there is no ancient Egyptian account of the mummification process, it has been described in detail by two Greek travelers and historians; Herodotus and Diodorus, who visited Egypt in the fifth and first centuries BC respectively. Three mummification processes were described by Herodotus and he separated them by their cost and effectiveness in preserving the body.

The most expensive method was as follows:

1) The corpse was placed on an operating table in the "*per nefer*", the "House of Mummification" or more correctly "the house of beauty", stripped of clothing and prepared for the mummification process.
2) Excerebration was carried by cutting the brain with a sharp hook via the ethmoid bone and removing it from the skull with another instrument

shaped like a spoon. This step was not always carried out effectively, even on the elite. There is also evidence that this practice was not always carried out before the New Kingdom as even the elite of the 18th dynasty did not have this procedure carried out (Brier, 1996). It is unknown why excerebration was developed as the brain neither greatly increases decomposition of the corpse nor was the brain assigned any religious significance by the Egyptians.

3) The viscera were removed by making an incision in the left side of the abdomen with a sharp stone and removing the contents of the abdomen including the stomach, spleen, intestines, liver and sometimes the kidneys. The removal of these organs would have hindered putrefaction and autolysis and presumably the ancient Egyptians were aware of this. Once the abdomen had been emptied, the diaphragm was cut and the lungs were taken out. The heart due to its religious significance as the seat of emotion and thought was left in situ.
4) The body cavities and the extracted viscera were cleaned with palm wine and spices. Fermented palm wine would probably have contained around 14% ethyl alcohol, and could have acted as a sterilising agent. This would have therefore further hindered decomposition processes.
5) The viscera were then emptied of their contents, again hindering putrefaction, and rewashed with palm wine and spices. After the washing, they were placed in natron salt on an inclined table and dehydrated for about forty days. Natron, used for the embalming process, is a naturally occurring salt consisting mainly of sodium carbonate with traces of sodium sulphate, bicarbonate and chloride and was readily available in ancient Egypt (Currie, 2006). This salt would have quickly dehydrated the organs to produce dried-out husks. As well as desiccating the organs, the salt also produces an alkaline environment of pH 12-13 which would be hostile to most bacteria and other micro-organisms (Currie, 2006).

   After the forty days the organs were anointed with perfumed oil and coated with resin, before being bandaged. These individually bandaged organs could then be either placed into small anthropoid coffins, like those of Tutankhamen, or, more commonly, into organ packages or sealed canopic jars. The canopic jars were sealed with stoppers in the shape of a human

head and put under the protection of the four sons of Horus. This practice persisted until the end of the 18th Dynasty when these designs were replaced with the representative heads of the Four Sons of Horus. Hapy (with the head of an ape) guarded the lungs; Imsety (with the head of a human) guarded the liver; Qebeh-senwef (hawk-headed) guarded the intestines whilst Duamutef (the jackal head) protected the stomach (Riyad, 1973). The canopic jars/anthropoid coffins were then placed in a single canopic chest.

6) The body cavity was packed with temporary stuffing materials such as natron packets to aid internal dehydration, linen packets for absorbing fluids that may have pooled in the cavity and gum-resin packets to cover the corpse's odour during the dehydration process.
7) The body was then dehydrated by placing it upon an inclined bed, known as the bed of mummification, and placing dry natron upon, in and around the body. The inclined bed further aided the dehydration by allowing excess bodily fluids and water to easily drain away from the body (Riyad, 1973). Between forty to seventy days the body was removed from the mummification bed. Natron was removed and any temporary stuffing material was transferred from the corpse into special jars which were later buried near or around the tomb, along with other items involved in the mummification process.
8) The permanent stuffing materials were then added to the body. These materials included resin or resin soaked linen for the skull's cranial cavity and linen bags of resin, cassia, cinnamon, sawdust, myrrh and natron for the abdominal and thoracic cavities. The incision that had been made to remove the organs from the abdomen would be sealed and covered with a small gold plate or beeswax containing the protective "*wedjat*" eye symbol.
9) The body was anointed with cedar oil and rubbing fragrant substances, such as, myrrh and cinnamon, presumably to cover the smell of putrefaction.
10) Facial openings, for example, the ears, nose and eyes, were packed with resin soaked linen or beeswax in an attempt to restore a lifelike appearance.

11) The skin was smeared with molten resin (for example, bitumen) which would make the skin stronger and sealed any open pores, making the corpse water and moisture-proof.
12) The now chemically treated corpse was wrapped in its characteristic linen bandages with amulets in specific anatomic locations, for example, over the abdominal incision, and specific bandage layers to provide good fortune and spiritual protection for the corpse (Riyad, 1973). The mummified corpse and any physical representations of the deceased would be magically awakened in the “Opening of the Mouth” ceremony prior to the sealing of the tomb where priests would perform a magical rite allowing the corpse and the associated statues of the deceased to regain the use of the eyes, mouth and ears in the afterlife (Quirke and Spencer, 1992).

Herodotus describes this as the most expensive and exclusive method of mummification used only by nobles and royalty. It would have produced a mummy with soft tissues and internal organs in a well preserved state. The other two methods would have produced mummies of considerably lower quality and preservation.

The middle cost option is similar to the most expensive method except for two important modifications; the excerebration and evisceration steps were omitted completely. Instead of removing the internal organs from the body and dehydrating them individually, the internal cavities were simply filled with oil. However, the body was still treated externally with natron and underwent the same religious rituals as the more expensive method (Garner, 1979). This process would have produced a mummy with differing results. Treatment of the body with natron may have preserved the soft tissues, but this method would have left the internal organs in a poor state of preservation. Arguably, filling the body cavities with oil may have reduced putrefaction, depending on the anti-bacterial properties of the oil. As the internal organs were not desiccated, autolysis could still have occurred and it is unlikely the stomach, liver and abdominal contents would have been preserved at all. Although there appears to have been very little written on mummification using this method, the literature agrees that the abdominal organs probably deteriorated and came away when the oil was drained off (Abdel-

Maksoud and El-Amin, 2011). In contrast, the thoracic organs have and probably would have been better preserved. The lack of evidence is possibly due to studies focusing largely on elite mummies or that this mummification method produced mummies with soft tissues that are not sufficiently preserved for scientific analysis. In my opinion, this type of mummification would probably allow sufficient preservation of lung to allow studies such has reported here to be undertaken.

The third option was the cheapest and least effective mummification technique. Again there were two differences to the most expensive process: no excerebration or evisceration steps. In this method, the abdominal cavity was simply washed out with an unidentified liquid before the entire body was treated externally with natron (Harris and Weeks, 1973). This unidentified fluid is thought to have been either water or a dilute salt solution (Garner, 1979). Again, even though the external soft tissues may have preserved, this method would have left the internal organs in a very poor state of preservation. Washing the internal organs with water or a salt solution is unlikely to have hindered either autolysis or putrefaction. The only beneficial effect could have been an enema-like reaction removing faecal matter from the body. Without desiccation or sterilization, the internal organs would have degraded long before the body was buried.

There has been some criticism about the accuracy of these accounts of the mummification process. It is argued that Herodotus and Diodorus were foreign travellers and did not see the mummification process first-hand, since it was still a secretive procedure at that time and was protected by an “embalmer’s oath” according to the Hawara papyrus (Brier and Wade, 2001). As the information was passed on from father to son and protected by an oath, Herodotus’ and Diodorus’ information had to have been provided by an unknown, anonymous source whose accuracy and veracity cannot be confirmed (Brier and Wade, 2001). It has also been argued that the mummies from the 5th century BC onwards are mummified to a lower standard and therefore less preserved than mummies from the earlier periods (David and David, 1995). However, it is generally accepted that both Herodotus’ and Diodorus’ accounts of the process are reasonably accurate as they have been supported by both embalming materials and medical instruments found by archaeologists plus inscriptional evidence such as the mural on the northern exposure wall of a Ptolemaic Period temple at Kom Ombo (Nunn, 1996)

(Figure 1.2). Although no Pharaonic Period instruments have been found, the ancient Egyptians had at least four words for medical-related knives and medical papyri make numerous references to the "knife treatment" "*djua*" (Nunn, 1996).

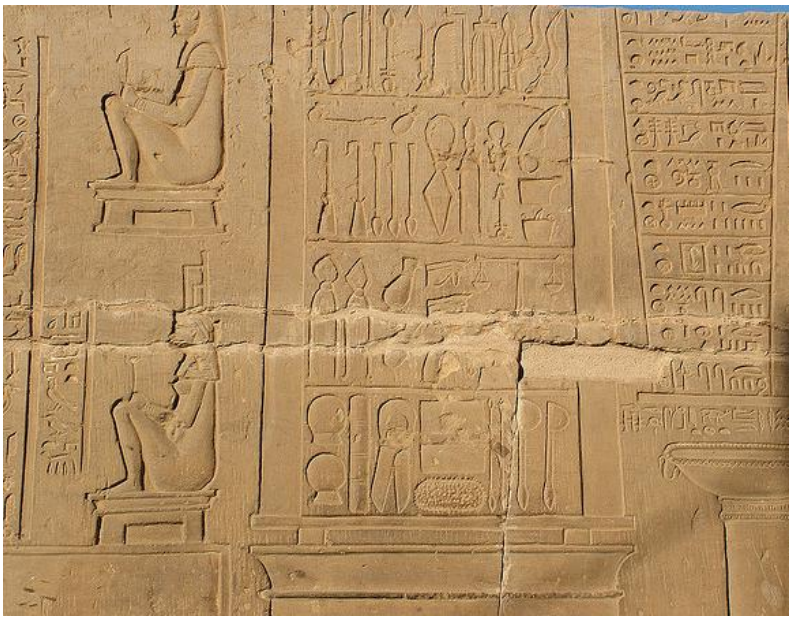

Figure 1.2 Depiction of medical and mummification tools (central register) in a mural on the northern rear wall of the temple of Sobek/Haroeris at Kom Ombo (Ptolemaic dynasty, second century BC; image from Gains Heritage, 2010).

Mummification and the "democratisation" of the afterlife

After several centuries of experimentation, the intentional mummification process started to be practiced regularly during the 3rd Dynasty (c2770 BC) (Quirke and Spencer, 1992). However, due to the time and cost, it is thought that it was only carried out on members of the ruling dynasty (Harris and Weeks, 1973).

Over the next one thousand years, mummification techniques were continually being refined and perfected. Excerebration (removal of the brain) started in the New Kingdom (18th Dynasty c1550 BC) although it was not always carried out, even on the elite (Hirata, 2005). The art of mummification peaked in the 21st Dynasty (c1070-940 BC) with the introduction of facial packing which further enhanced the life-like appearance of the mummy and facilitated recognition by the *Ba* (David and David, 1995). After this peak, the quality of mummification declined until it was stopped in the Coptic Period (David and David, 1995; Corbelli, 2006)

by the Christians as part of their suppression of native religious belief and practices.

Although intentional mummification was initially reserved for royalty of Egypt, the “nobility” (the often a hereditary elite of high officials, increasingly independent of the king) began to adopt royal burial customs during the Old Kingdom, and this was accelerated after the fall of the Old Kingdom in 2180 BC (Seidlmayer, 2000). This started a slow and gradual process called the “democratisation of the afterlife”. Over the following centuries admission to the afterlife and its associated practices became available to an increasing number of people from the higher social classes (Seidlmayer, 2000). This eventually enabled mummification to become a mass-producing industry for middle class burials during the Greco-Roman period (David and David., 1995). This would suggest that any study of intentionally mummified material would have a bias towards the more elite classes of ancient Egyptian society, increasingly so as one moves back in time. This means that the particles these mummified persons were exposed to in life are likely to be different to some but not all of the particles encountered by non-elite groups.

The non-elite include peasant farmers and labourers, especially those engaged on the extensive state-sponsored construction projects that characterized the Old, Middle and New Kingdoms and, to a lesser extent, the Ptolemaic and Roman Periods. Although artificial mummification was presumably not common among such groups (Wilson, 1965), numerous examples of mummies from such non-elite social classes have come from burial sites where spontaneous mummification has occurred. The Dakhleh Oasis in Egypt’s western desert, for example, contains spontaneous mummies from non-elite classes from the New Kingdom to the Coptic Period (Kaper and Zoest, 2006).

A specific review of the significance and mummification of the lungs can be found in Section 2.1.2.

1.1.3 *Egyptian society and particle exposure*

Despite the passage of three and a half thousand years, the day-to-day life of an average Egyptian did not alter markedly between the Old Kingdom and the Greco-Roman period, including the late Roman period from which some of the naturally mummified material used in this study is derived. This continuity in living conditions and lifestyle was due to the conservatism of Egyptian culture and its slow and stable development of technology (Wilson, 1965). This conservatism is shown by the ancient Egyptian language which altered very little in two thousand years from the Old Kingdom to the New Kingdom, which is very surprising to a modern individual where lifestyle changes happen in decades not millenia (Wilson, 1965). This strict adherence to traditional practices enables individuals from different times and geographical areas of ancient Egypt to be studied as an entity as living conditions, agricultural practices, quarrying, construction activities and religious rites - and hence exposure to particulates - did not change radically. Such conservatism extended to the type of crops cultivated and the type of materials used for construction and decoration. The only differences in exposure of particulates could come from new fuels that were introduced through trade or invasion. For example, olive oil does not appear to have an ancient Egyptian name before the 17th Dynasty and was presumably introduced through trade at this time (Lucas, 1962).

The following summary examines the various social groups that constituted ancient Egyptian society, with particular reference to similarities and differences in particulate exposure. Very little research has been carried out into the particles, both organic and inorganic, that the ancient Egyptians may have been exposed to. Research, thus far, has centred on two areas of interest; lamp designs and lamp fuels (Serpico and White, 2000; Vogelsang-Eastwood, 2000; Shier, 1978). No studies have examined the exposure of different social classes to disease-causing particles.

Dependence on artificial illumination

It has been argued that the majority of ancient Egyptians would have risen and gone to bed with sunrise and sunset (Hayes, 1953). However, while it is probable that lighting was more extensively used by the elite of Egyptian society, it appears that even the poorest home would have had some form of artificial lighting. Three pieces of evidence testify to the acceptance of artificial lighting as a part of normal life by the ancient Egyptians. The hieroglyph for the letter "H" is a lamp wick (Figure 1.3) (Fischer, 1977). This wick composed of a coiled piece of flax or rope can be found on numerous temples and monuments throughout Egypt and must have been recognisable to most if not all Egyptians.

Figure 1.3 The hieroglyph "H" is a stylised representation of a lamp wick (Uponreflection.com, 2009).

Secondly common Egyptian house designs, (as shown in Figures 1.4a and b) possessed very small, highly-placed windows that would not have provided much natural illumination making artificial light a necessity for anyone wishing to carry out work indoors. Finally, one of the most widely known stories from ancient Egypt is that of the "Tale of the Two Brothers". In this 19th Dynasty story, the elder brother, Anubis, notices something is wrong as he returns home from working in the fields, because the lights in his house are not lit (Erman, 1894, Mair, 2008). This tale shows that artificial light was used and accepted even by Egyptians working as farmers and, possibly, labourers. Unfortunately, the view that artificial lighting was just for the elite has been held due to the lack of physical evidence found at archaeological sites. The reasons for the lack or misidentification of this evidence will be discussed further in section 1.24. The following sections examine different sections of ancient Egyptian society, not only to assess the likely degree

of artificial illumination they employed but also the various sources of organic and inorganic particles that could be present in their lungs.

Housewives

Most peasant Egyptians lived in small, enclosed mud-brick dwellings with small, high windows (Davies, 1929; Kemp, 2000). These dwellings consisted of one or two storeys with very few or no windows on the ground floor. It is thought that cooking may have been carried out in a non-covered area (i.e. an area without a roof) in the house or even possibly on the roof itself in an effort to remove heat and smoke from the house (Davies, 1929). An example of these house designs from Thebes can be seen in the illustrations of the papyrus of Nakht from the 18th Dynasty (1550-1295 BC) (Figure 1.4a). A recent example of this design taken in a photo from Khargeh in 1928 can be seen in Figure 1.4b. These designs are thought to be typical of the average Egyptian's house from the Old/Middle Kingdoms onward.

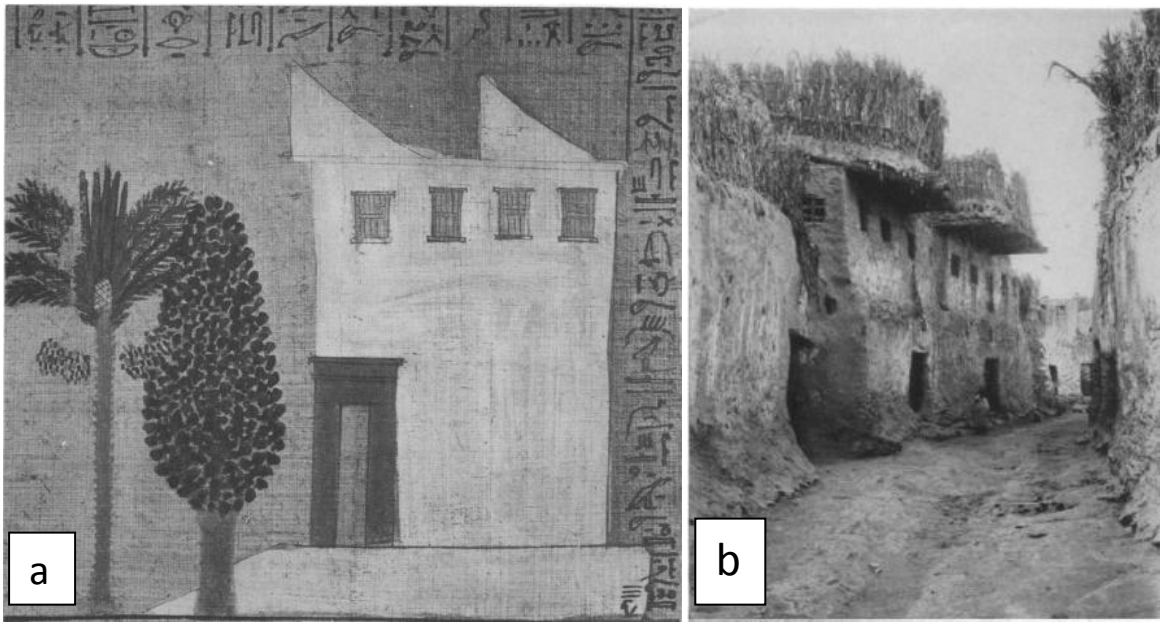

Figure 1.4 a) Illustration from the papyrus of Nakht (18th Dynasty Thebes) (Davies, 1929) of an ancient Egyptian house. b) A similar house design to (a) in the village of Khargeh near the Dakhleh Oasis in 1928 (Davies 1929).

Ancient Egyptian women were not allowed to perform manual labour or work in the fields and would carry out work in or around the home (Robins, 1993). Therefore, they were probably exposed to soot from the cooking fire and possibly mud brick particles from the home environment. Additionally the small windows would have

necessitated artificial lighting for any cooking or food preparation indoors. Soot from cooking fire has been argued to have been found in ancient Egyptian and Roman mummies (Capasso, 2000). If everyday cooking was carried out in a partially roofed area, it is likely that the small windows could not provide adequate ventilation for fires and significant amounts of smoke may have been trapped in the building. Additionally, if the windows could have been regularly closed or blocked because of bad weather, for example, to keep out desert sand during the "Khamsin" wind season, this would have further compounded smoke pollution. This lack of ventilation inside the houses would have ensured that non-elite ancient Egyptians were exposed to constantly high concentrations of smoke. Modern studies, based predominantly on women from Africa and Bangladesh, show that cooking fires burning a mixture of dung, plant and shrub material (equivalent to what the ancient Egyptians are likely to have burnt) produce a dangerous smoke with a high concentration of particles. When exposed to this smoke for sufficient periods, pneumoconiosis with the appearance of both anthracosis and silicosis can form (Grobbelaar and Bateman, 1991). Elite Egyptians had separate kitchen areas and servants to do the cooking and so will have had less exposure to smoke from cooking fires.

Farmers/Manual Labourers

This section of society was the most numerous. Peasant (subsistence) farmers have been estimated as much as constituting 80% of ancient Egyptian society during the Pharaonic Period (Allen, 1997). They lived in houses such of similar design to those shown in figure 1.4, although the degree of ornamentation such as the (stone) door posts and lintel shown in Figure 1.4(a) would have been confined to the wealthy. The house's design indicates poor ventilation for those living inside the house and they would have been exposed to smoke and fumes from any lighting or cooking source. The "Tale of the Two Brothers" features two brothers who own and work a farm and details that the elder brother's wife routinely lit up the house every night. This would suggest that this section of society used artificial illumination extensively.

Farmers working the fields in ancient (and modern) times will have been exposed to a number of inorganic particles. The Nile valley was only cultivated to a maximum of thirteen miles in breadth (e.g. David, 1999). This means that most farmers would have been within a few miles of the banks of the Nile and could have inhaled fine alluvial silt deposited by the river. Additionally the farmers may have been exposed to cellular components of plants known as phytoliths. Phytoliths can be released in a respirable form during crop burning and have been shown to cause respiratory irritation, as shown in a modern study of Canadian farmers (Becklake, 2007). Phytoliths will be examined further in Section 1.3.1. Farmers would have also been exposed to sand from the surrounding desert environment.

Manual labourers would have been involved with everyday building construction as well as quarrying and construction of larger public monuments and pyramids. Such groups could include farmers due to the use of corvée labour in which peasants were conscripted to work on state-sponsored construction projects during the Nile inundation season (Ezzamel, 2004). Figures 1.5a and b show the known locations of ancient quarries in Upper and Lower Egypt respectively. The majority of the quarries were located on the border between the cultivated Nile valley and the surrounding desert. Not only was this because the Egyptians did not wish to waste valuable farming pasture but also because the quarries needed access to the Nile in order to transport the heavy stone to other parts of Egypt (Arnold, 2001). The Egyptians practiced open-cast quarrying where the soft (limestone, sandstone) or hard (granite, quartzite) rocks were divided from the surrounding stone by trenches and split from the surface below before being transported off-site (Arnold, 2001). Subsequent stone working was either carried out by copper or bronze chisels for the soft rocks and dolorite tools for the harder rocks (Arnold, 2001).

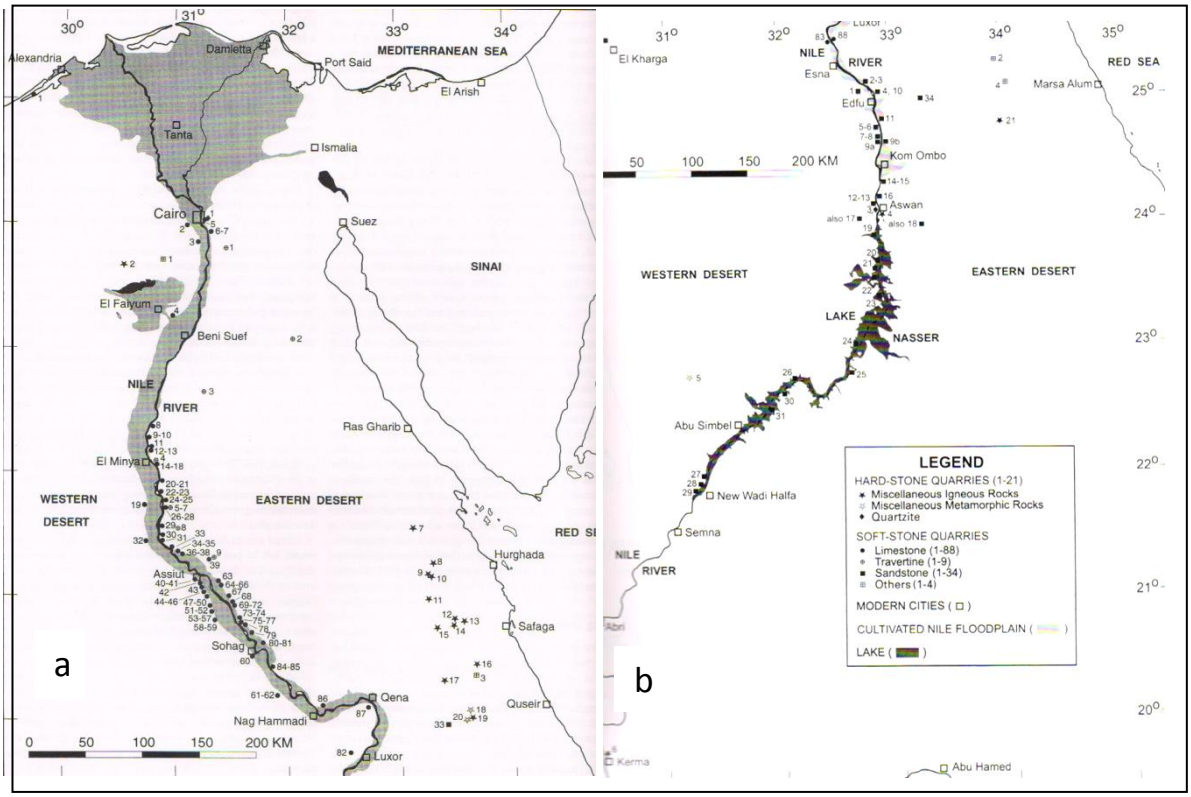

Figure 1.5 Known locations of ancient quarries in Egypt: a) quarries in the delta and down to Luxor, b) Luxor down to Nubia (Taken from Nicholson and Shaw, 2000).

During the quarrying and stone-working process labourers are likely to have been exposed to many different forms of inorganic particles. They will have inhaled particles from excavating and splitting the rocks when quarrying, handling and manipulating the stone blocks during transportation and dressing the stone at the construction site. Additionally they will have been exposed to sand from the deserts surrounding the quarries and perhaps the silt from the banks of the river Nile.

Labourers involved in mining and tomb cutting would have involved the use of some form of artificial illumination. The gold mines at Bir Umm Fawakhir are not very long (around 100m) and are cut straight into the mountainside. The mine shows no signs (i.e. soot) of being illuminated by lamps (Meyer, 1997). It is possible that reflective surfaces were employed to light the mines, much like they are used by modern Egyptians at tourist sites. Despite the lack of physical evidence for artificial lighting in gold mining, there is plenty of literary evidence for lighting used in tomb cutting and decorating. Workmen's villages, such as Deir el-

Medina, have provided papyri, pottery sherds and ostraca which detail the widespread use of lighting at such sites (McDowell, 1999; Mair, 2008). These records include purchase details, receipts of delivery, storage and distribution plans and consumption rates of the workers. For example, one ostracon found in Tomb 5 in the Valley of the Kings acknowledges the delivery of two-hundred oil lamps for the workers decorating and cutting the tombs (Weeks, 2000; Mair, 2008). Cerny (1973) deduced that over any given period the number of wicks issued in the morning and afternoon were equal. This suggests that the worker's day was split up into two sections with a lunch-break in between (Cerny, 1973). The number of wicks allocated alters between tombs and probably depended on different numbers of workers or possibly different-sized tombs. The Egyptians recorded that they used up to 64 wicks per day in the third month of excavation and decorating (McDowell, 1999). Given the poor ventilation of the tombs themselves, this would indicate that workers carving out tombs would have had a long exposure to soots from illumination.

Craftsmen

Craftsmen were highly valued in ancient Egypt and were provided accommodation near to the construction sites they worked on (McDowell, 1999). They could have been exposed to particles specific to their craft, for example, copper particles from a copper smelter or lead fumes from manufacturing lead vessels. Tomb painters and decorators presumably were exposed to soot from lamps during the decoration of tombs and the interiors of temples. As detailed above, tomb decorators in the Valley of the Kings used over 60 lamp-wicks a day and were working in these conditions for at least three months (McDowell, 1999). Further evidence that craftsmen used artificial illumination can be found in "the Satire on Trades" where a scribe Dua-Khety tries to persuade his son Pepy to follow in his footsteps by insulting other professions. He describes a "*carpenter who bears the adze*" who "*is wearier than a field-hand ... There is no end to his work ... At night-time he (still) must light his (lamp)"* (Simpson et al,1972; Mair, 2008). A possible exception to this may be stonemasons. They produced dressed stone for buildings including architectural elements such as cornices and column drums (all dressed and carved in situ), plus monumental sculptures. They would have to have worked

outdoors and probably would not have had much exposure to soot from illumination.

Like the other social groups, craftsmen would have had heavy exposure to inorganic particles such as sand from the desert and mud-brick dust from the home environment.

Priests

Light held magical properties for the ancient Egyptians and were involved in a variety of rituals. The temples were not extensively lit by natural light for liturgical reasons which would have meant any light-source would have been artificial (Rawlinson, 1880). A photograph of the interior lighting in the virtually intact

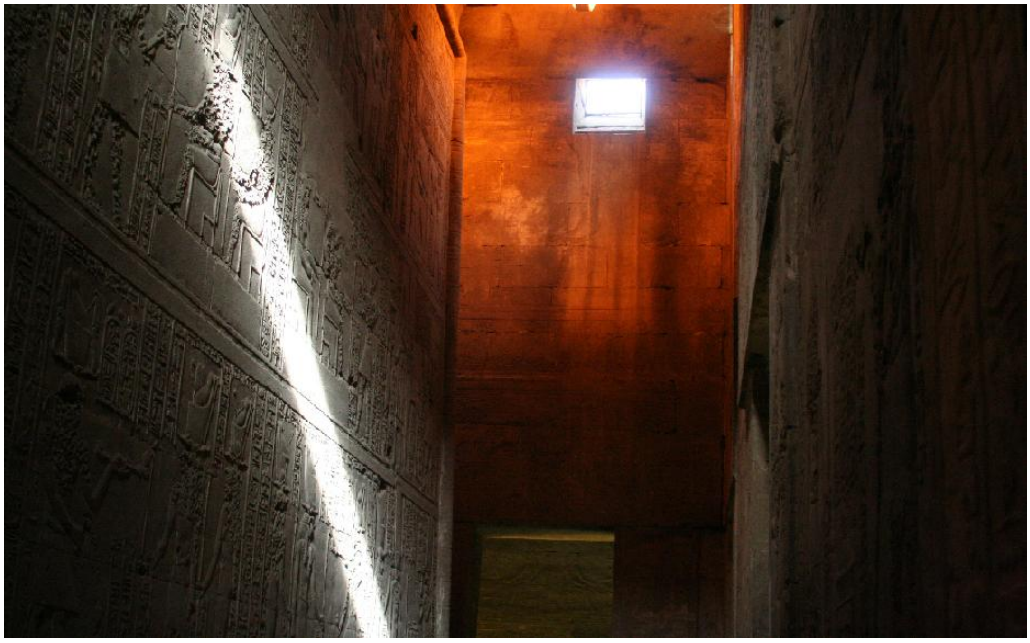

Figure 1.6 Photograph of the interior of the temple of Horus at Edfu showing the limited amount of natural light (Author's own photograph).

Ptolemaic temple at Edfu can be seen in Figure 1.6. The small, highly-placed windows would have provided very limited light, making artificial lighting a necessity. These openings would also have provided very little ventilation ensuring that the priests were exposed to illumination soots. Torches and burning incense were used extensively in religious rites, for example as described in the "Chapter of the Four Torches" from the Book of the Dead (Budge, 1895). Although priests would have been in contact with soots from many different sources, the amount of soot that they were exposed to could vary greatly between individuals because

the priesthood was a part-time occupation until the Late Kingdom and the vast majority of priests only worked six-month shifts in temples (Arnold, 1996). Even in the Late Kingdom and onwards only senior priests would spend all year in the temples. Junior priests would still be part-time workers and presumably their exposure would be less. The level of exposure could also vary by sex, as female priests and chantresses were involved in different rituals (using different fuels) to their male counterparts. Priests may have also come into contact with cooking soot as part of their temple duties as some prepared food as votive offerings for deities.

Inorganic particles that the priests would have had contact with would include desert sand and possibly mud-brick dust from the six months when the priests were not residing in temple complexes.

The Elite

Royalty, nobles and senior administrators or scribes enjoyed considerably better living conditions than the majority of the Egyptian population. These roles were not mutually exclusive and it was not uncommon for an important Egyptian to hold at least three or four titles. The elite had bigger and better housing with improved ventilation and they usually had separate kitchens where cooking would be performed by servants (Davies, 1929). It is therefore doubtful they would have been exposed to as much illumination or cooking soots as the average Egyptian. Even though the elite attended certain religious ceremonies, they probably would not have been exposed to as much religious soots as members of the priesthood. Although their exposure to soot was less, the composition and structure of soot in their lungs could be distinguished from other sections of society by the fuels they used. It is far more likely that the elite could have afforded olive oil for illumination for example; something presumably beyond the spending power of the average Egyptian (Serpico and White, 2000).

Like the other sections of Egyptian society, members of the elite would have been exposed to desert sands and mud-brick dust.

Summary

My personal interpretation of the probability of exposure of the various ancient Egyptian social classes to potential combustion products of fuels has been summarised in the tables below. Table 1.2 summarises exposure to organic particles and Table 1.3 shows exposure to inorganic particles.

Table 1.2 Likelihood of exposure of ancient Egyptian social classes to organic particles. Red, high probability of exposure; yellow, medium probability chance of exposure; green, low probability of exposure.

Source	Organic						
	Heating	Illumination				Crafts	Religious
Profession	Wood	Castor	Olive	Palm	Sesame	Beeswax	Goose
Labourer							
Farmer							
Housewife							
Craftsmen/ Painter/Decorator							
Junior Priest							
Senior Priest							
Elite (royals/nobles)							

Table 1.3 Likelihood of exposure of ancient Egyptian social classes to inorganic particles. Red, high probability of exposure; yellow, medium probability chance of exposure; green, low probability of exposure.

Source	Inorganic					
Profession	Desert Sand	Quarry	Limestone	Metals	Phytoliths	Mud Brick
Housewife						
Farmer						
Labourer						
Craftsmen						
Junior Priest						
Senior Priest						
Elite (royals/nobles)						

1.1.4 *History and Geography of the mummified samples*

Ancient mummified Egyptian tissue is a valuable and finite resource. As such, it is very hard to procure. All effort must be made to ensure that as many non-destructive tests are carried out as possible and that little tissue is destroyed. The ideal samples for this project would be obtained from mummies, both spontaneous and artificial, from all the periods of Egyptian history and from all strata of Egyptian society. These samples would show if the differences between spontaneous and artificial mummification alter the preservation of the tissue and amount of particulates in lung tissue which may reflect the social environment at the time of mummification. Samples from a variety of Egyptian historical periods would reveal shifts in reliance on a certain fuel type to another over time. There should be variation between the lungs of individual from different social classes. For example, it is reasonable to assume that a priest would have more incense-based carbon particulates than a labourer.

The mummified samples examined in this study were obtained from the Manchester International Mummy Tissue Bank and were provenanced to be from the Dakhleh Oasis and Kulub Narti. The locations of the Dakhleh Oasis (25.5˚N and 29.1˚E) and Kulub Narti (20.4˚N and 30.2˚E) are shown on Figure 1.7. These samples were chosen because of their availability, their different geographical locations (one site in the desert and one adjacent to the River Nile), and different historical periods. All the mummies appear to have been spontaneously mummified and some were wrapped (Aufderheide, 2003). The mummies from both sites all appear to be of the same class; and none appear to be from wealthy or elite groups.

Figure 1.7 Map of modern Egypt and the northern Sudan showing the location of the Dakhleh Oasis and Kulubnarti (Google maps).

The Dakhleh Oasis was used as a trading post by merchants and caravans travelling across the western desert of Egypt and gave them access into West Africa. The oasis had its first known contact with the Pharaonic state in 2200BC (Hubschmann, 2010). Dakhleh and the nearby Kharga Oases were known to be

areas of unrest throughout the Pharaonic Period; however, the flow of trade increased over time and reached its peak in the Greco-Roman Period when the town became an important trading hub surrounded by a large area of agricultural land (Hubschmann, 2010). Excavations at a Ptolemaic temple at Amheida, a town populated from the Old Kingdom to Greco-Roman times and located on the periphery of the oasis, found wheat, barley, grape, olive tree, date palm, fig, lentil, flax, cotton, safflower, coriander, rosemary and a variety of grass weeds (Hubschmann, 2010). A map of the Dakhleh Oasis region can be seen in Figure 1.8.

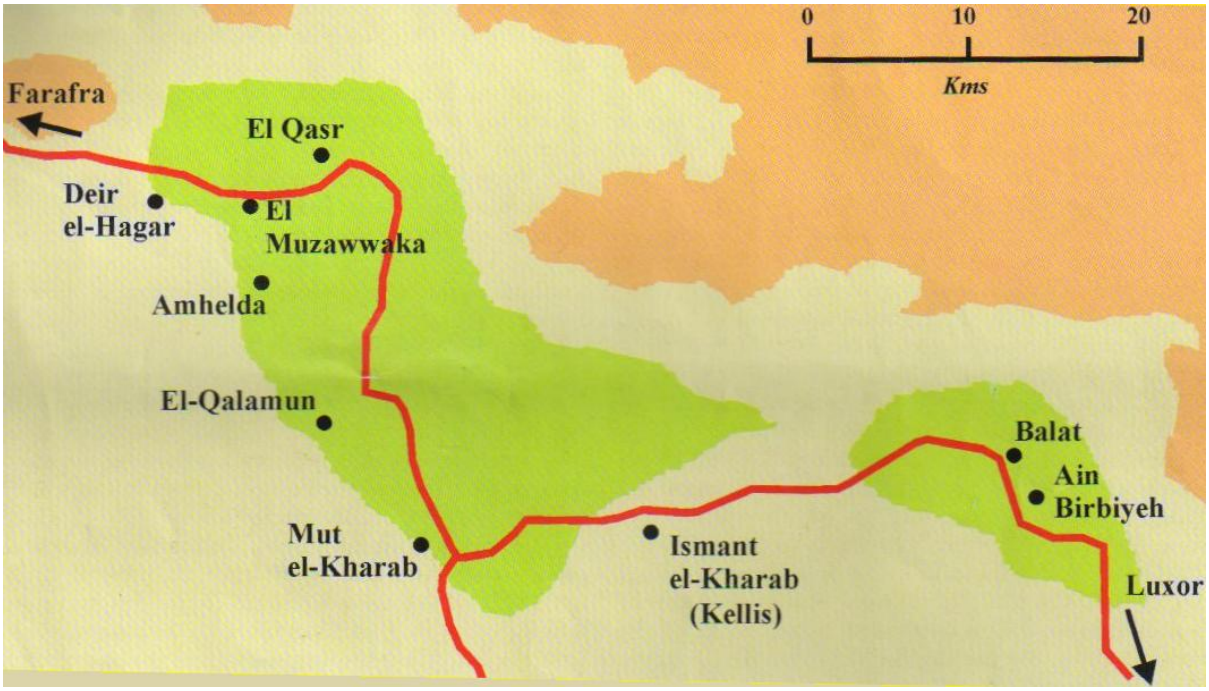

Figure 1.8 Map of the Dakhleh Oasis region showing the position of the Kellis cemeteries. The green areas show the extent of modern cultivation (Shelldrick, 2007).

The samples used in this project are from the Kellis I cemetery. This Greco-Roman cemetery consists of over 24 small tombs cut into the face of a sandstone terrace. The tombs are approximately one metre high and two to three metres square. The entrance is supported by two upright stones and closed by a coarse rectangular coverstone (Aufderheide et all, 2004). A photograph of tombs from El Muzawakka (near Kellis) in Figure 1.9 shows the typical style of the tombs found in

the Dakhleh Oasis. Fifteen mummies were excavated from tombs 1 to 12 in 1993 and thirty-four mummies from tombs 16 to 21 in 1998 (Aufderheide et al, 2004).

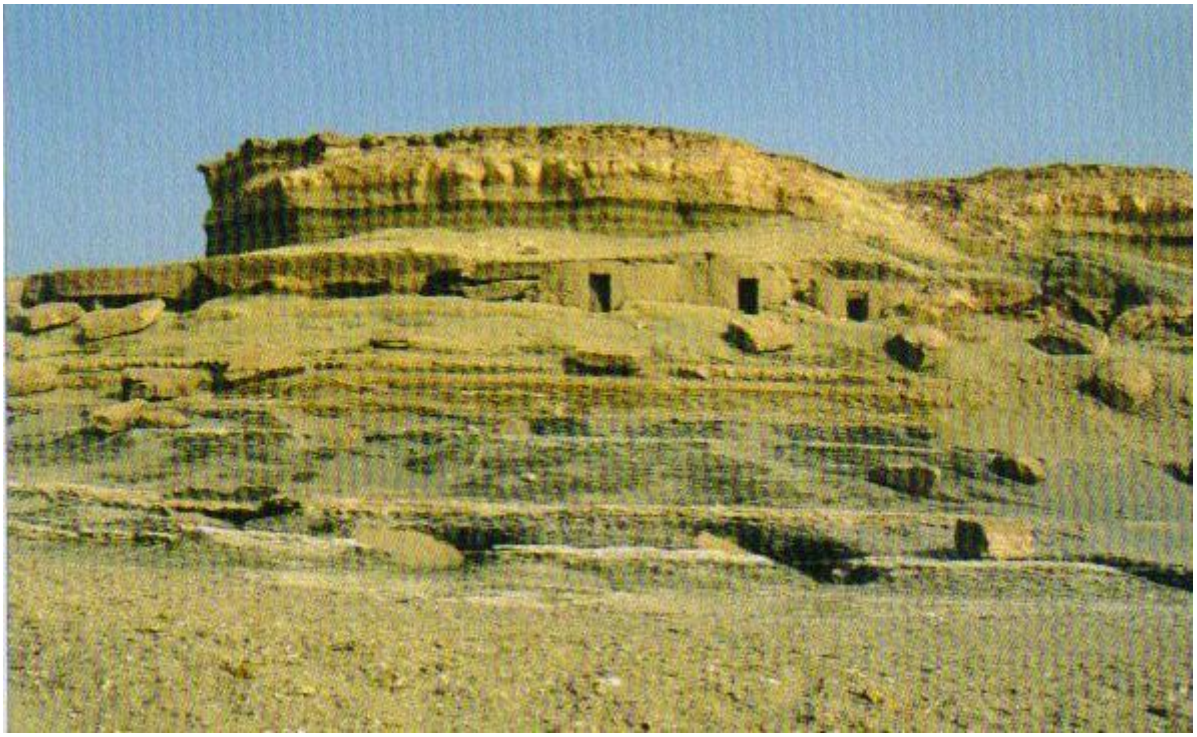

Figure 1.9 Tombs cut into a limestone terrace at El Muzawakka in the Dakhleh Oasis. These tombs are similar to the tombs found at the Kellis cemeteries (Shelldrick, 2007).

Although all the mummies found at the Kellis cemeteries appear to have been wrapped at one time, the mummification methods vary with individuals. The wrapping process appears to involve large sheets of linen which were applied with resin to the corpse and then secured with long thin linen bands. No two mummies' wrappings are alike and the low standard of embalming corresponds to that typical of the Greco-Roman time period (Aufderheide, et al, 2004). Damage, including dismemberment and unwrapping, from plundering in antiquity has also hindered attempts to analyse the Dakhleh mummification methods (Aufderheide, et al, 2004). The mummification process was caused by desiccation by the sun and produced characteristic changes in the internal organs. The lungs collapse into a 2 to 3mm thick plaque-like structure which sticks to the posterior wall of the inner lining of the thoracic cavity (Aufderheide, et al, 2004). Mummies with intact chests and abdomens were chosen for this project to ensure correct identification and sampling of the lung tissue.

Kulubnarti is a seasonal island situated in Upper Nubia between the second cataract and the Dal cataract of the Nile in modern-day Sudan. During the high Nile flood season it is completely separated from the west bank of the Nile and is located 640km north-west of Khartoum in an area known as Batn el-Hajar ("Belly of Rocks"). It can be seen in Figure 1.10. The island is still inhabited and has been so since late Christian times (c550AD) (Anderson, 2008).

Kulubnarti possesses three Christian/Medieval Period settlements designated as 21-S-2, 2-S-9, and 21-S-10. The settlement at 21-S-2 contains four castle-houses and two churches which can be seen in Figure 1.11. All three settlements were excavated in 1969 by the University of Kentucky. The cemeteries of the churches contain over two-hundred spontaneously mummified mummies from the late Roman Period and were excavated in 1979 (Anderson, 2008; Mulhern, 2000). The mummies were of non-elite origin (Mulhern, 2000).

Figure 1.11 Settlement 21-S-2 on the Island of Kulubnarti (Anderson, 2008).

1.2 Anatomy and Mummification of the Lungs

1.2.1 *Anatomy*

Human lungs consist of a right and left lung (with three and two lobes respectively), the trachea, the bronchus and the bronchioles (Peros-Golubicic and Sharma, 2006). The bronchioles become smaller and eventually the terminal bronchioles end in alveoli. The process of respiration occurs in the alveoli contained within the lobes of the lungs. The anatomy of the human lungs can be seen in Figure 1.12 and the anatomy of the alveoli and terminal bronchioles can be seen in Figure 1.13.

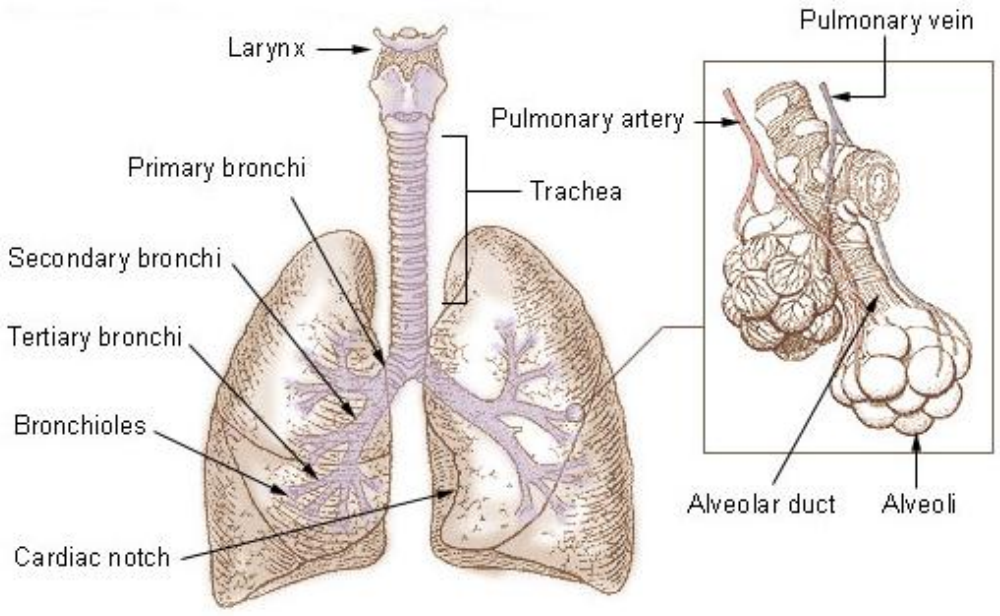

Figure 1.12 Gross anatomy of the human lung (U S National Cancer Institute, 2006)

When the diaphragm (a muscular sheet at the bottom of the ribcage) contracts, the lungs expand and air is drawn in. Air travels from the trachea through the bronchus and bronchioles into the lungs. Alveolar bronchioles lead the air into alveolar ducts and finally the alveoli where oxygen and carbon dioxide diffuse in and out of the blood. Alveoli are elastic air-filled sacs with an excellent blood supply to ensure a high diffusion rate during the respiration process. Humans

possess three-hundred million alveoli with a combined surface area of 70 m^2 (Notter, 2000).

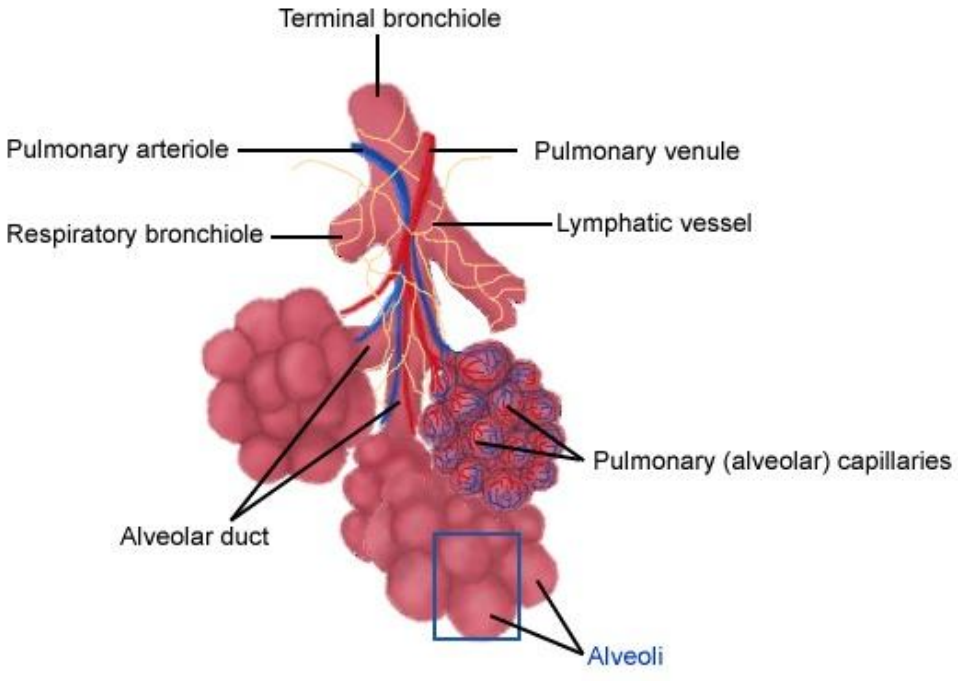

Figure 1.13 Anatomy of terminal bronchioles and alveoli of the human lung (St George's University of London, 2013).

Due to the volume changes and flexing required for the breathing process, the lungs are primarily composed of flexible collagen and elastin fibres. As alveoli make up the vast majority of the internal structures, a large percentage of the mummified lung tissue found in this and other studies will contain collapsed alveoli with some bronchioles. Alveoli contain two types of cells: type I cells act as the surface for gas exchange and type II secrete surfactant which aids gas exchange and also lubricates the alveolar sac (Ward and Nicholas, 1984). Tissue from the trachea could also be found as it does not appear to have been removed during mummification (Cockburn, 1985). The alveoli and the interstitial tissue should contain any particles that have entered and remained within the lungs. Alveolar wall tissue contains both elastin and collagen and the interstitial tissues between alveoli and other structures contain a 2:1 ratio of collagen types I and III (Lang et al, 1994).

Collagen fibres are often intra- and inter-molecularly cross-linked giving them a high tensile strength which in turn gives the lung its structural strength. Strong

cross-linked bonds between lysine or hydroxylysine side groups of the collagen molecule gives collagen a high chemical resistance (Stanley et al, 1975) and lung tissue is considered one of the most resistant of all organs following natural and artificial mummification (Walker at al, 1987; Stanley et al, 1975).

Elastin fibres are also intra and inter-molecularly cross-link bonded although the cross-links produce different conjugate groups to collagen (Stanley et al, 1975). These fibres not only give lung tissue the necessary elastic potential during the respiration process but also preserve very well; they have been demonstrated to have excellent preservation in samples from mummies that are almost 2000 years old (Montes et al, 1985).

1.2.2 *Mummification of the lungs*

When the Egyptians mummified their dead, the heart and the kidneys were often left in situ. The reason the heart (ancient Egyptian: '*ib*) was not removed was because the ancient Egyptians believed it was the "seat of the mind" and of the highest religious importance, especially in the afterlife. It has been debated whether the kidneys were left in situ because of their awkward anatomical placement within the body or because they were not recognized as organs (David and David., 1995).

The lungs were therefore often the only organ of the thoracic cavity to be mummified by the ancient Egyptians (David and David., 1995). For the most expensive mummification method described by Herodotus, an incision was made in the left side of the abdomen with a sharp stone and the contents of the abdomen including the stomach, spleen, intestines, liver were removed. Once the abdomen had been emptied, the diaphragm was cut and all the thoracic contents were removed including the lungs but excluding the heart. It appears that the lungs were cut beneath the trachea, as intact elements of the trachea remain in the majority of mummies (Cockburn, 1985; Cesarani et al, 2003).

The contents of the abdomen, including gastro-intestinal tract were probably removed due to their contents, such as the stomach with its associated hydrochloric acid and digestive bacteria, would have led to very rapid putrefaction

of the corpse. However, because ancient Egyptian religious beliefs required the preservation of the whole body to ensure continued existence in the afterlife the organs were preserved, and placed under the protection of specific deity in a canopic jar. The jar would then be placed in a canopic chest. An example of the canopic jars and chest that accompanied the mummy of Henutmehyt can be seen in Figure 1.14

Figure 1.14 The canopic jars and chest of Henutmehyt (c 1250 BC, 19th dynasty; British Museum, 2009) showing the jar containing the intestines (protected by the hawk-headed deity Qebeh-senwef and that containing the stomach (protected by the jackal headed deity Duamutef – stopper removed). The jar containing the lungs is still in the canopic chest.

In spontaneous mummification the preservation was caused by desiccation by the sun and the hygroscopic properties of sand. An example of an autopsy of a spontaneously-mummified mummy can be seen in Figure 1.15. The lungs are easily visible as a thin flat sheet of material in their original anatomical position within the thoracic cavity.

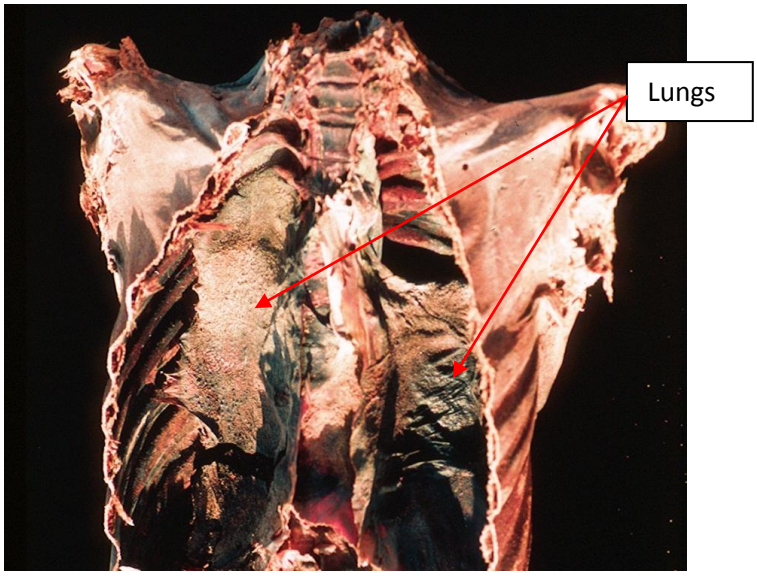

Figure 1.15 An autopsy photograph showing the preserved mummified organs of the thorax and abdomen of a mummy from the Kellis II cemetery at the Dakhleh Oasis (Courtesy of Prof A. Aufderheide).

1.2.3 *Lung Particulates*

Many small or large particles can enter the body through the process of breathing. The body has several defence mechanisms for filtering inhaled air including nasal hairs, throat and lung mucus. The main defence of the lungs against bacteria and particles is the mucociliary escalator. The mucociliary escalator extends from the larynx to the terminal bronchioles and consists of ciliated epithelium and goblet cells. Goblet cells secrete mucus which traps particles and bacteria while ciliated epithelia use their cilia (6 µm long tail-like appendage organelles) to push the mucus up to the throat where it can be swallowed or spat out. However, this mucus cannot filter out all particulates of less than ten microns in aerodynamic diameter (Clarke and Pavia, 1980). Aerodynamic diameter is a property used to describe the often irregular shapes of particulates as if they were perfect spheres and allows the behaviour of particulates to be predicted and modelled (Clarke and Pavia, 1980).

Particulates are defined as tiny particles of liquids or solids suspended in a gas and are also known as fine particles or particulate matter. Particulates differ in definition to aerosols in that aerosols refer to both the particles and the gas

together. Particles with a diameter less than ten microns (PM10s) are the largest particles that can enter the inner lung. It is therefore reasonable to assume that any individual particles found in mummified lung should be less than ten μm in diameter and that any larger particles are likely to be post-mummification contamination. Now the key groups of inhaled particulates and their associated diseases will be examined.

Silicosis

Sand is a very common granular or crystalline material which occurs naturally due to erosion and usually consists of a mixture of fine rock particles. Examples of sand grains can be seen in the electron micrograph below (Figure 1.16) which shows the difference in size and shape between grains in one very small sample of sand. One of the most common elements in sand is silicon. Silicon is usually present in the natural environment as the salt form (silicate) of aluminium, magnesium, calcium or iron and as silica (silicon dioxide, SiO_2). When silicon-containing compounds enter the lungs, they induce a localised toxic effect called silicosis (a variant of pneumoconiosis) (Aston, et al, 2000). This toxicity results from two effects of silicon deposition in the lungs. Firstly macrophages (white blood cells) phagocytose the silicon containing compounds causing an inflammatory response by releasing tumour necrosis factors (TNFs) and associated proteins such as interleukin-1 and leukotriene B4. These proteins induce fibroblasts to produce collagen around the silicon-containing particles which result in fibroses and large silicotic nodules (Cassel et al, 2008). The second effect results from the positive charge of silicon-containing particles which can produce free radical reactions and the creation of damaging chemicals, such as, hydrogen peroxide (Bagchi, 1992). This immune response and its fibroses within the interstitial tissues can be used to differentiate it from anthracosis (Walker et al, 1987). Silicates are less toxic to lung tissue than pure silica but can still cause fibrosis (induced by irritation) if the deposit is large enough (Walker et al, 1987).

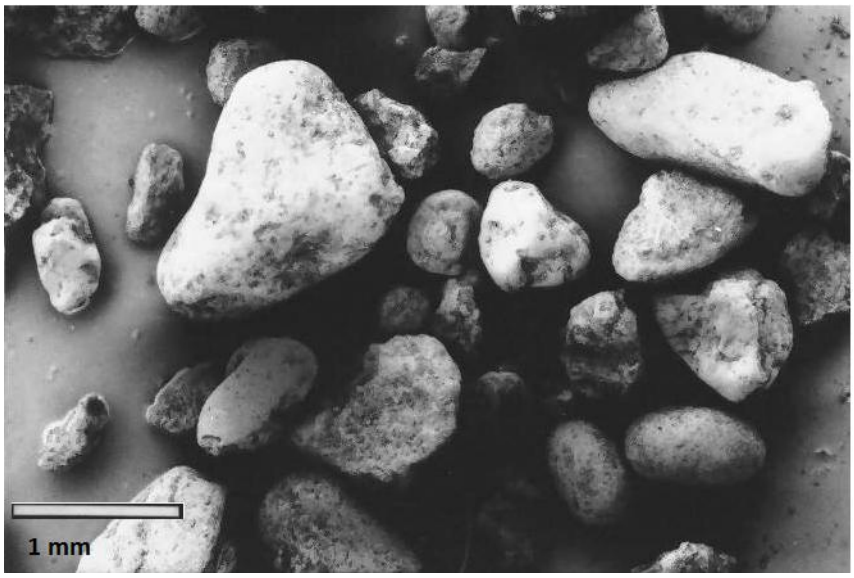

Figure 1.16 Typical sand grains (scale in millimetres) (Suthren, 2007)

The fibrotic tissue surrounding the silica particles is called a nodule and is formed from concentric rings of collagen fibre (Dunnill et al, 1996). A silicotic nodule in a section of modern lung tissue stained with Haematoxylin and Eosin stain can be seen in Figure 1.17. It appears as a large pink bundle of collagen surrounded by darker interstitial tissue. Both silica and silicon-containing compounds are birefringent.

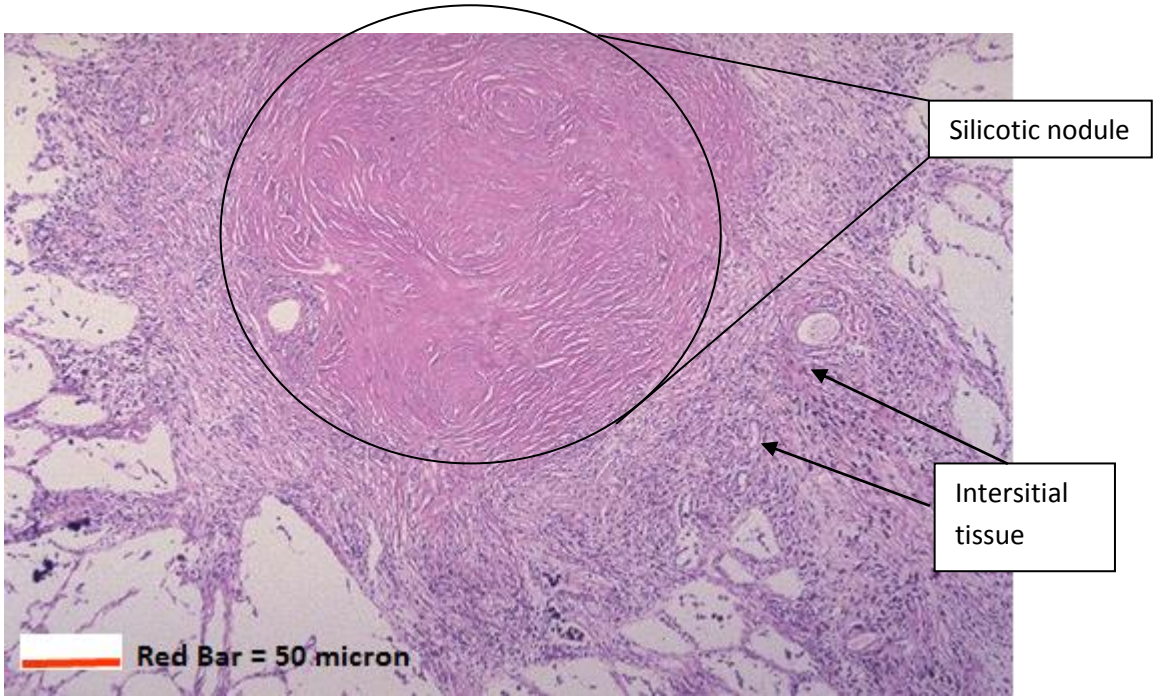

Figure 1.17 A silicotic nodule surrounded by interstitial lung tissue stained with haematoxylin and eosin (Klatt, 2009).

Contamination can greatly affect any effort to study silica in mummified lungs. There are two important criteria which must be borne in mind when examining such ancient material: silicates entering the lungs before death will be fine particulates of less than ten microns while post-mortem contamination will have a range of sizes, including some greater than the PM10 value. The second criterion is that silica deposited before death will be in alveolar fibrotic areas while post-mortem silica will be found in the larger bronchial lumens (Aufderheide, 2003).

Anthracosis

Although the lungs have an effective defence mechanism in the form of the mucociliary escalator, the lungs can be overwhelmed with particulates. Inhalation of a smoke or an aerosol with high concentrations of small particles can usually overwhelm this defence. There is often large variation in the size and composition of smoke particles, but most particles are carbon-based compounds. These smoke

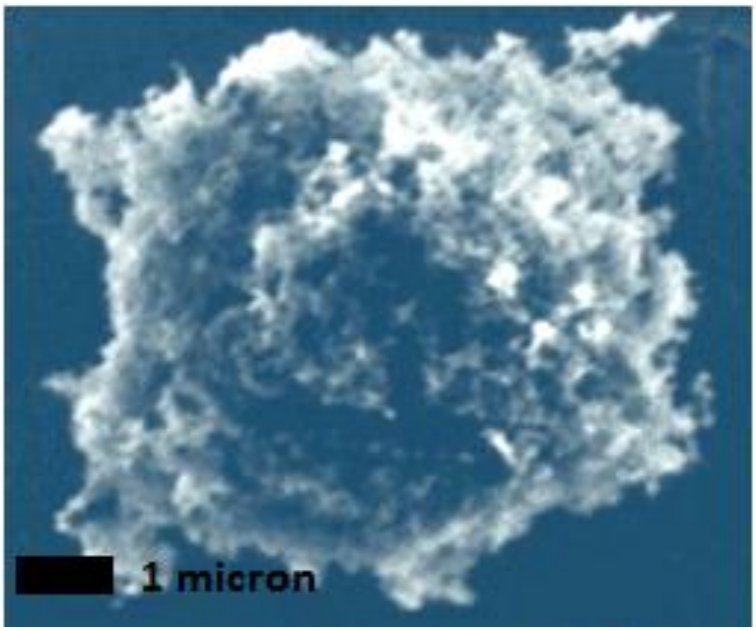

Figure 1.18 Electron micrograph of a carbon pm10 particulate from petrol combustion (Kay, 1996)

particles cannot be removed by macrophages as they are not biodegradable. These macrophages then congregate in the periphery of the alveolar sacs where they undergo apoptosis (cell death) and deposit the particles. They stain the lungs

a characteristic dark brown/black colour. An electron micrograph of a carbon pm10 particulate derived from petrol combustion can be seen in Figure 1.18. Most carbon particulates are approximately spherical in shape.

Lung discolouration increases with continued smoke inhalation and this can be used to estimate the extent of past smoke exposure. Anthracosis only refers to the deposition of carbon-based pigment in the lungs and does not necessarily imply loss of function or injury. Anthracosis can manifest in two main forms: simple anthracosis (shown in Figure 1.19), where carbon is deposited by wood or coal smoke in the absence of silica and causes little inflammation and functional impairment even with continual exposure. The second form, progressive massive fibrosis (PMF), is more serious. Silica (from rock being worked on by coal miners for example) causes irritation and the strong immune response (discussed above) that encourages fibrotic tissue to form around carbon deposits (Dunnill et al, 1996). Figure 1.19 shows human lung tissue stained purple with dark carbon deposits in the interstitial tissue.

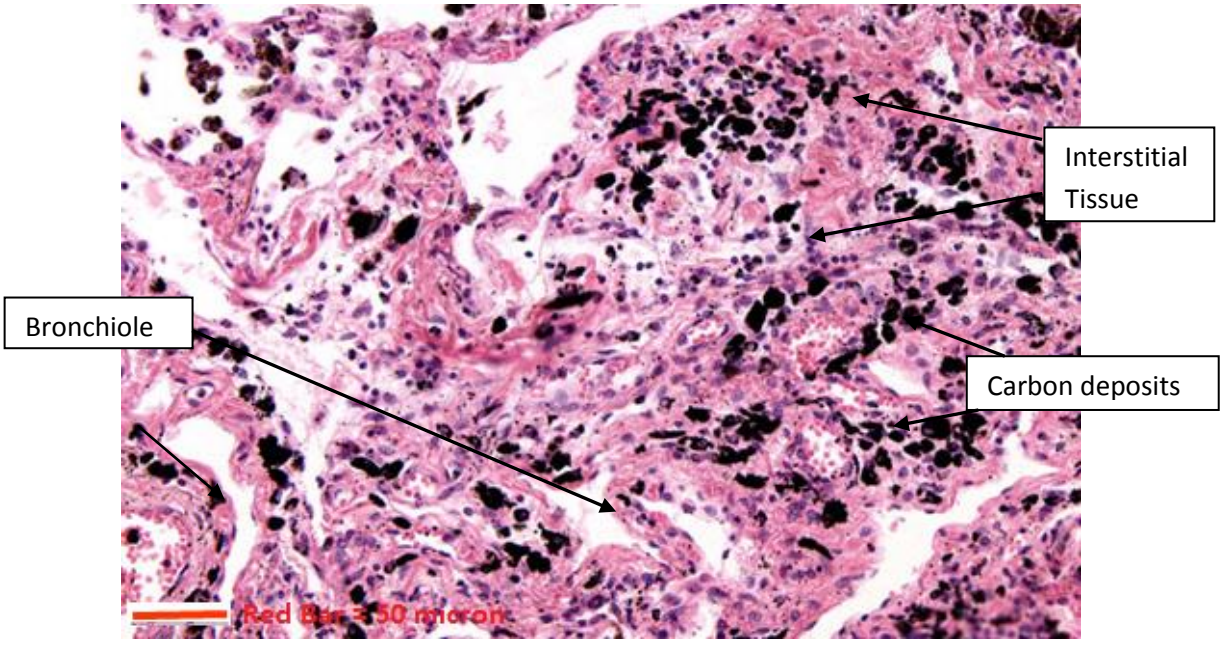

Figure 1.19 Simple anthracosis in human lungs stained with H+E (Nikon, 2009)

1.2.4 *Review of studies of mummified lungs*

To date, there have been no studies examining the difference in preservation between artificially and spontaneously mummified lung tissues. The only studies into mummification methods thus far have examined questions concerning artificial mummification, for example, whether natron was used in a solid or liquid form (Garner, 1979). It is still not known whether artificial or natural mummification results in better preserved lungs or if indeed there are any differences at all between them. This study will examine lung samples from both the artificial and spontaneous mummification processes in order to address these questions.

Inorganic particles and associated silicosis has been found in Egyptian mummies in several studies, including the study of Nekht Ankh from the Manchester Museum where it was termed “sand pneumoconiosis” (Tapp et al, 1975; Aufderheide, 2003). Walker et al, (1987) also found silicates in six samples of mummified lung from mummies dating from the 19th Dynasty to c200 BC; however, they attributed the silicate deposits as a coincidental finding and not as a direct cause of lung disease as no interstitial fibroses were found. Although simple anthracosis has been found in several Egyptian mummies from the New Kingdom (Shaw, 1938) and Walker et al, (1987) found PMF caused by both carbon and silicate in two lung samples from a total of six individuals, no investigation has identified and characterised the carbon deposits. These two lung samples came from a post 20th Dynasty canopic jar and a 20th Dynasty canopic coffin (Walker et al, 1987). Additionally no studies have been carried out into the source of the ancient silica particulates.

This project will be the first to characterise ancient inorganic and organic lung particles by size or shape. This project is also the first to perform elemental analysis on individual particles with a view to obtain an elemental “fingerprint” which can be compared against known inorganic and organic particles, the latter generated from sources used by the ancient Egyptians. No attempts have been previously made before to reproduce and characterise the soot that the ancient Egyptians may have inhaled.

1.3 Potential Sources of Lung Particulates

There were many possible sources of the particulate matter found in ancient Egyptian lungs. Ancient Egyptian culture had several different social classes and many different occupations within those classes (discussed in section 1.1 above). An individual might have been exposed to any number of sources, but if one source seems dominant then that might provide an insight into the individual's status or employment. For example, a mummy with a high amount of soot may have been exposed to open fire, incense burners or lamps providing lighting. If it was possible to further characterise the origin of the particles it may be possible to identify the specific profession or environmental conditions.

The mummies in this study are predominantly from non-elite backgrounds so probably would have been exposed to organic fuels that were common and relatively inexpensive in ancient Egypt. Due to their status it is also probable that the individuals were not exposed to soots from religious sources. All the mummies in this study would have been exposed to inorganic particles from either their mud-brick homes or the desert environment; however, the degree of their exposure would vary from individual to individual. Egyptians from the Dakhleh Oasis may have been exposed to more desert sand (due to its geography) than Egyptians from the Kulubnarti Island. It would also be possible that lungs from women would contain more mud-brick dust than their male counterparts as women led a more home-based lifestyle.

1.3.1 *Silica and silicate sources*

Sand

Due to Egypt's climate and geography, silica, in the form of sand is obviously a very common particulate often found in mummified lung tissue (Walker et al,

1987). Presumably there were three different types of particles that were inhalable: desert sand, particles from mechanical working of stone and erosion of mud bricks. Particles from mechanical working of stone would have affected only select groups such as quarry workers, stone masons and sculptors. A picture from Hierakonpolis showing Egypt's desert climate and sand dunes can be seen in Figure 1.19. Egypt's vast stretches of desert would have provided large amounts of inhalable sand.

Figure 1.19 Egypt's desert climate and sand at Hierakonpolis. Also shown is the remains of a mud-brick construction from the predynastic period which would provide a further potential source of particulates (Author's own photo).

These two types of sand grain have different abrasion histories and can be differentiated from each other by roundness (Pettijohn et al, 1987a). Roundness is defined as the curvature of the sand grain's corners (Pettijohn et al, 1987b). A well rounded grain may have travelled a long distance, with every journey contributing to the abrasion of its edges or may have received intensive abrasion in an environment where rounding was rapidly accomplished. Beach and sand dunes are considered special environments where such rapid rounding occurs (Pettijohn et al, 1987). A silicate particle which is less rounded (i.e. sides with sharper angles) could have been produced by, for example, mechanical wear from quarrying or manipulation of stone by ancient Egyptian workers. A comparison of the composition of ancient silica and silicates to samples of sand from modern

Egypt using light microscopy and scanning electron microscopy should allow identification of the geographical and abrasion origins of the ancient silica. When this information is combined with archaeological or documentary evidence of a mummy, it could provide new details on the individual's occupation and social status.

Phytoliths

A less obvious source of inhalable silica is the burning of crops. Barley and wheat contain silicon-rich structures within their stems and glumes (a type of modified protective leaf known as a "bract") called phytoliths (Piperno, 2006). These structures are found in stems and protective leaves of plants and are considered to give the plant added strength and protection against herbivorous animals. The phytolith's shape is unique to the species and can even allow botanists to distinguish between wild and cultivated varieties of plant (Piperno, 2006). A phytolith recovered from ancient maize can be seen in Figure 1.20a. The phytoliths appears as an angular, dagger blade-like crystal. This shape is indicative of maize phytoliths. Both the stems and glumes form the waste and chaff during the processing stage of cereal production and would have been burnt in the fields by the ancient Egyptians. Charred remains of chaff stems and glumes have been found as evidence of deliberate episodes of crop burning in ancient times (Murray, 2000). These burning practices are still practiced by modern farmers (Figure 1.20b). Inhalation of grain dust, including phytoliths, has been found to be detrimental to the lungs of modern farmers in Canada (Becklake, 2007). Assuming that the phytoliths are also released in a respirable form by

Figure 1.20 Ancient maize phytoliths (scale: 1 μm) (Rosen, 1998) (a) and modern Egyptian farmer burning chaff in a field near Luxor (Author's own photo) (b).

combustion, it may be present in the lungs of ancient Egyptian farmers. Another source of respirable phytoliths could be from the inhalation of a suspension of phytoliths created from the grinding and milling of maize during bread and flour production. These flour particles have been indicated in causing respiratory illness in modern developing world populations (Grobbelaar and Bateman, 1991). Barley and wheat were grown as cereal crops by the ancient Egyptians from the Pre-dynastic Period to the modern day (Murray, 2000).

An experimental component of this project will attempt to combust the chaff and waste from barley and wheat to see if phytoliths are released in a respirable form and to identify these by shape, size and composition.

1.3.2 *Carbon sources*

The most probable way that the ancient Egyptians inhaled carbon was in the form of soot and smoke from the combustion of carbon-rich fuels. The three main applications for these fuels were providing heat, illumination and religious use.

Heat for living and cooking would have been partially provided by the combustion of wood. The woods used by the Egyptians included cedar, acacia and juniper (Hepper, 1990: 45). However, since wood was scarce in ancient Egypt, it is far more likely that the Egyptians would have burnt a mixture of dung, scrubland plants and farm waste, for example, chaff and glumes from crops such as those used by African populations today (Grobbelaar and Bateman, 1991). Additionally the resins available from trees do not appear to have been used for combustion purposes (Lucas, 1962).

Illumination in ancient Egypt was provided domestically by lamps and ceremonially by torches (Wilson, 1936). These lamps burnt a variety of vegetable oils, including castor, linseed and olive as well as animal fats, including cattle, sheep, goat and pig (Serpico and White, 2000). These clay lamps sometimes absorbed the fuel which has allowed the residues to be analysed by Gas Chromatography Mass Spectrometry (GC-MS). Copley et al (2005) used GC-MS to analyse residues from ten Egyptian lamps found at Third Intermediate Period (664 – 323 BC) sites at Qasr Ibrim and identified residues indicative of radish oil, castor oil, animal fat and

possibly linseed oil. These lamps were thought to have no religious role or connotations and were used only for illumination.

Religious services in ancient Egypt involved both incense burning, and illuminating lamps (Rawlinson, 1880). Lamps and torches were used in a variety of different religious services and light itself held a certain magical power. Examples of these rites include a chapter of the Book of the Dead called “the Chapter of the Four Torches” in which an incantation to be recited over four torches (lit during daylight) to ensure the deceased’ soul will not perish and that his soul will “flourish like Osiris” (Budge, 1895; Mair 2008). Scenes from Hatshepsut’s barque shrine (the ‘Red Chapel’) depict a ritual where a senior priestess, the God’s Wife of Amun, uses flames to symbolically destroy Egypt’s enemies (Tyldesley, 1996; Mair, 2008). A blessing found in an inscription from the 18th Dynasty tomb of Paheri at Kab states “Mayest thou go forth every morning and betake thyself home (?) every evening; may a light be lighted for thee at night-time until the light (of the sun) rises upon thy breast” which further implies that light held a protective magical power for the ancient Egyptians (Taylor and Griffith, 1894, Mair, 2008).

As Egyptian religious practice employed lamps for both liturgical and illumination purposes, the temples, including the so-called mortuary temples dedicated to the cult of the reigning/deceased Pharaoh and his protective deity, would have been subject to smoke and soot. These temples were also not very well ventilated and lit by natural light for liturgical reasons (Rawlinson, 1880) which resulted in a thick layer of soot being deposited on the roofs and walls. This soot layer can be seen in most temples, including the temple of Seti I at Abydos (Figure 1.21) where small windows in the roof of the vault would have provided limited ventilation. Examination and characterisation of such soot should be extremely useful as it would contain evidence of the fuels and incense the Egyptians burnt in antiquity. It should be noted, however, that such soot could have been contaminated by later conversion and occupation of abandoned temples by Coptic Christians and others (Meinardus, 2003). This is almost certainly the case at Abydos where the tombs were inhabited by Egyptians until the 19th century. There is some debate over the incense used by the Egyptians: although only pistacia resin has strong archaeological evidence from offering bowls in Amarna and amphorae labelled as “*sntr*” (incense) (Serpico, 2000). However, frankincense and myrrh have also been

suggested (Serpico, 2000). The results from this project could be used to inform the incense debate.

Figure 1.21: Roof of Seti I's temple at Abydos showing soot deposits on the vaulted roof (Author's own photo). The lighter areas are modern restorations of the roof.

This project will attempt to recreate the smoke particles that may have been inhaled by the ancient Egyptians in order to compare them against ancient samples. The modern recreations will be created through controlled combustion of incense and oils particular to Egypt and the collection of their soot and smoke. The ancient samples will be retrieved from mummified tissue and soot deposits from temple sites in Egypt.

It has been suggested that the following fuels were used by the ancient Egyptians in lamps.

Castor Oil

The castor plant (*Ricinus communis)* is thought to be indigenous to Egypt and seeds have been found in tombs and settlements dating back to the Badarian era (Predynastic period around 4400 to 4000 BC) (Lucas, 1962). Castor oil has been mentioned by the Greek and Roman authors Strabo, Pliny and Herodotus. Herodotus specifically mentioned that this oil was used in lamps and may have been employed in various religious ceremonies (Lucas, 1962). Castor oil is liquid at room temperature and consists primarily of unsaturated Ricinoleic acid. It will not burn with a sooty flame (Santhanam et al, 2012).

Olive Oil

Olive oil derived from the olive (*Olea europaea)* is not mentioned in Ancient Egypt until a wall painting in the 18th Dynasty. There does not appear to be a word for this oil in ancient Egyptian until the 19th Dynasty (Lucas, 1962). The Greek traveller and philosopher, Theophrastus, mentions gardens of olive trees growing in the Thebaid region of Egypt in the 3-4th century BC. Olive oil is also mentioned by Pliny, Strabo and Herodotus (Lucas, 1962). It has been suggested that the scarcity of olive oil before this time may have made it one of Egypt's earliest bulk imports from the Aegean region (Serpico and White, 2000). If this is correct then olive oil may have been very expensive which would have limited its use to the elite classes of Egyptian society. Olive oil is liquid at room temperature and consists primarily of unsaturated oleic acid which suggests it will not burn with a sooty flame (Mailer, 2006).

Palm Oil

The oil palm (*Elaeis guineensis)* is native to West Africa and palm oil has been found in large quantities in Egyptian tombs dating back to 3000BC (Friedel, 1987). There is some debate over whether it is palm oil or merely palmitic acid which is a breakdown product of many different plant-derived oils (Friedel, 1987). Palm oil was widely used by ancient Egyptians in later periods; for example, it was employed extensively in the mummification processes described by Herodotus. Palm oil is a liquid at room temperature and has very saturated palmitic fatty acids (Sundram, 2002). This fuel would probably burn with a sooty flame.

Sesame Oil

The Roman naturalist and philosopher Pliny the Elder correctly identifies and mentions sesame oil imports (from *Sesamum indicum)* from ancient Egypt. Evidence of crushed sesame seeds has been found in Egypt in ancient times and indicates that they knew how to process and acquire the oil from seeds (Bedigian and Harlan, 1985). Sesame oil is a liquid at room temperature and consists mainly of unsaturated oleic and linoleic acid (Nzikou et al, 2009).

Animal fats

Although all animals possess a certain amount of fat, the most abundant sources of animal fat available to the ancient Egyptians would have come from their domesticated animals which were also used for meat and hide production. These animals included cows (*Bos taurus*), sheep (*Ovis aries*), goat (*Caprica hircus*), pig (*Sus domesticus*) and donkey (*Equus asinus*) which would have been available from Predynastic times (Serpico and White, 2000). Geese (*Anser spp* and *Branta spp*) and ducks (*Anas spp*) could also have been a potential source of fats. It is unknown how the ancient Egyptians rendered fat from animals but any fat they rendered would be full of saturated fatty acids (Serpico and White, 2000). This would have burnt with a very sooty flame.

Beeswax

The ancient Egyptians were extensive keepers of bees to provide honey as a sweetener in food and drink. They also used beeswax as a binder for paint, glue and for fixing hair wigs. Although there is no recorded use of beeswax as candles, beeswax has been found in several houses in Amarna and its presence there has not been explained (Lucas, 1962). Beeswax is solid at room temperature and is made of long-chained aliphatic alcohols (Christie, 2012).

1.3.3 *Lamp design and development*

Lamps were used by the ancient Egyptians not only as a way to provide illumination but also as part of religious ritual and offerings. A variety of materials including granite, limestone, calcite and clay were used to produce these lamps varying both in design and size (Petrie et al, 1895; Robins, 1939; Mair, 2008).

Herodotus, in the 5th century BC, described Egyptian lamps as an open bowl (with or without a spout) featuring a floating wick supported by a layer of salt covering the lamp fuel (Robins, 1939). This simple design ensured that the salt not only kept the wick upright when the lamp was alight (thus removing the need for a spout) but also protected the lamp fuel from external contamination. It has been argued that the addition of salt to the lamp fuel reduced the sootiness of the flame and this project will attempt to examine if this is indeed correct. One possible issue with this design is the unknown value of salt to the average ancient Egyptian. Salt (sodium chloride) is one of the oldest known flavouring agents and was an expensive commodity in both ancient Greece and the Roman Empire (Smith, 1953). Although the Egyptians used large amounts of natron salt in the mummification process it was not used for food flavouring as it contained little sodium chloride and had a disagreeable taste. Was salt so common that most Egyptians could use it for their household lamps? There appears to be no satisfactory evidence to answer this question.

The oldest identified Egyptian lamp was found in a settlement near Asyut dated to the Badarian era (Predynastic Period, 4400 to 4000 BC) (Lucas, 1962). A thick, black greasy residue was found in a red clay bowl which featured a spout and three handles. This was identified as a lamp by the excavator Brunton and it has been argued that castor oil seeds, found in a nearby tomb, provided the oil fuel (Brunton, 1928; Lucas, 1962). A drawing of the lamp can be seen in Figure 1.22a.

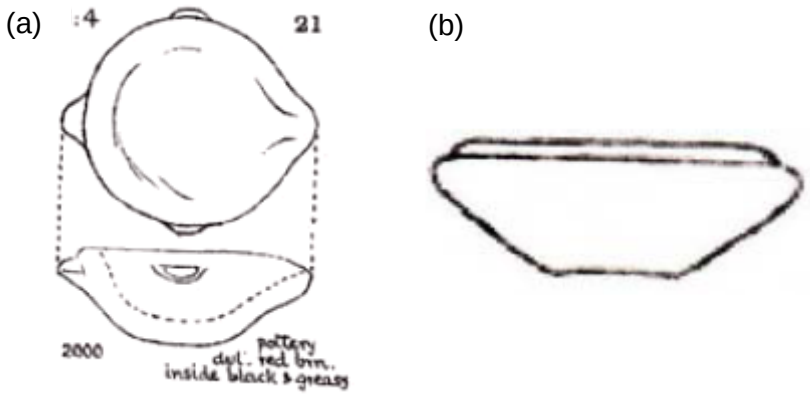

Figure 1.22 Drawing of the lamp found at the Badarian settlement (a); an Old Kingdom lamp identified by Quibell (b) (Both reproduced from Mair, 2008).

Another example of an early lamp of similar design (Figure 1.22b) was found by Quibell in 1895 when he uncovered a rough granite bowl in an Old Kingdom burial site at Deir el-Ballas in Upper Egypt. The lamp was identified by a soot stain and the presumed remnants of a wick inside the bowl (Petrie and Quibell, 1895). A similar design from the Greco-Roman Period can be seen in Figure 1.23. It seems that this simple design persisted throughout Egypt's history and may have been used by the vast majority of the Egyptian population. Further support for the extensive use of this simple design over an extended period of time is the absence at Amarna of the more elaborate Greco-Roman designs (Serpico and White, 2000).

Figure 1.23: Simple Egyptian lamp from Greco-Roman period (Petrie Museum, 2009c)

The specifics of this design would also explain why very few examples of artificial lighting in ancient Egypt before the Greco-Roman Period have been found. As a floating wick would leave very few burn marks or residue inside the bowl, it would be very hard to identify the vessel as a lamp. It is very possible that any lamps found by archaeologists have been grouped in with ordinary household containers from the excavation site. In addition, it appears as if ordinary household containers could also have been used as substitute lamps so this could further confuse their identification.

Lamp design changed dramatically during the Ptolemaic Period and by the 3rd Century BC lamps were becoming mass produced (Shier, 1978). Two typical Greco-Roman Period examples can be seen in Figure 1.24.

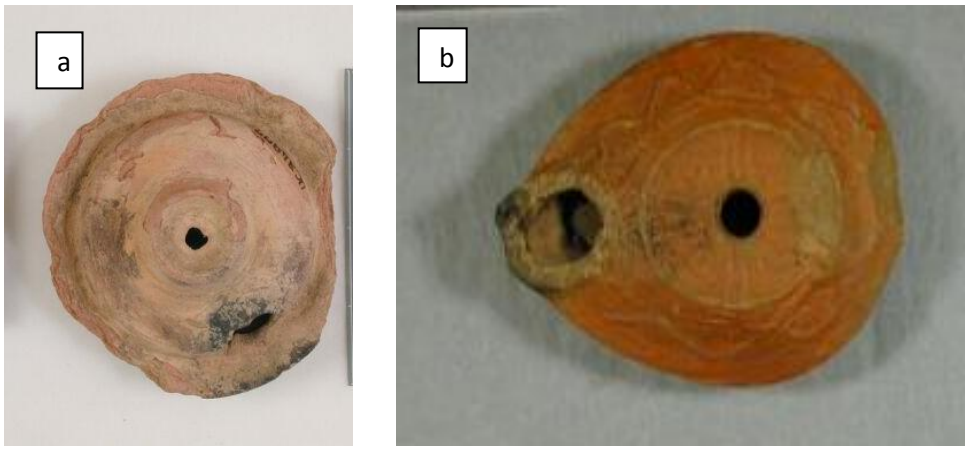

Figure 1.24a,b. Two Egyptian lamps in the Greek style from the Greco-Roman period (Petrie Museum, 2009a)

The first Greco-Roman lamp differs from the ancient design by having a covered reservoir with a central hole for refilling the oil and a hole on one side for the wick. Figure 1.21b shows a more ornate sealed lamp in a classical Greek style characterised by an elliptical shape and a nozzle to accommodate the wick. These lamps were ubiquitous and presumably were used by all members of society.

The wick for ancient Egyptian lamps was usually made of a twisted length of flax or cloth which was twisted back upon itself and allowed to sit in the oil. (Vogelsang-Eastwood, 2000). Figure 1.25 shows a cloth wick from Tel el Amarna (18th Dynasty, approx. 1350 BC). Wick length is proportional to the burn duration and could have been used as a way of measuring time. Tomb workers were reputed to have wicks that burnt for four hours and the end of the lamp indicated the end of their shift (Strouhal, 1992). At the workman's village at Deir el-Medina, the workmen were given linen and old clothes and allowed to manufacture their own wicks (Manniche, 1999).

Figure 1.25: Cloth wick from Amarna (scale bar is in cm) (Serpico, 2009)

Incense burners usually consisted of simple bowls with direct or out-turned lips in which the incense was placed and combusted. An example of an incense burner with visible residue and combustion marks can be seen in Figure 1.26. This example would be typical of those found in temples throughout Egypt's history (Serpico, 2009).

Figure 1.26: Incense burner from Amarna (shown with a 5cm scale bar) (Serpico, 2009)

1.4 Aims and Objectives

1.4.1 *Aims*

- To assess differences in quality of preservation of lung tissue and their associated particles across the different types of mummification (intentional and spontaneous)
- To assess evidence of disease of particulate origin in ancient Egyptian lung tissue.
- To characterise the particles found in ancient Egyptian lung tissue, including with reference to surrogate (modern) particles
- Use this information as an indicator of the social status and living conditions of ancient Egyptians
- To review evidence for use of artificial lighting and cooking in enclosed environments (and hence exposure from the resulting soot) in ancient Egypt

1.4.2 *Objectives*

- Examine ancient particles in situ in mummified lung tissue
- Create surrogate particles from fuels that may have been used by the ancient Egyptians
- Develop biological model to assess changes made to particles during intentional mummification process. Model will also provide tissue for development of particle extraction method.
- Extract ancient particles from mummified lung tissue
- Characterise and compare in situ and ex situ particles by size, shape and elemental composition
- Compare surrogate and ancient particules by size, shape and elemental composition
- Examine inscriptions and evidence from excavation for the use of artificial lighting and cooking in enclosed environments by different social groups and hence the extent of exposure of the population as a whole.

1.5 Investigative techniques and methods to be used in this study

As no one method can reveal the size, shape and elemental composition of the ancient lung particles and the modern surrogate particles, multiple methods must be employed to examine the lung tissue and its inhaled particles. Additionally, mummified material is a valuable finite resource and care must be taken not to waste it. It would be highly desirable to choose non-destructive methods or at least methods which leave the samples available for subsequent examination by other techniques. If these aims are impractical then the smallest amount of tissues that will give the definitive answer must be used.

1.5.1 *Surrogate particle production*

This study will use modern surrogate soots produced in the laboratory, phytoliths and sand samples from Egypt as comparisons against particles contained within ancient lung tissue. When the size, shape and elemental composition of ancient particles are examined and compared against their modern counterparts, it may be possible to deduce the aetiology of the ancient particles.

Generation of surrogate carbon particles for analysis

The surrogate soot produced by this study should come from fuels the ancient Egyptians may have used. The soot must also be captured in a way where the size and shape of the soot is unaltered and is free from elemental contamination.

Sand and phytoliths particles for analysis

Modern sand samples will be collected from various archaeological sites around Egypt. These sands will show the possible variations in physical and elemental composition of sand between the different geographical areas of Egypt. Their size, shape and elemental composition will be analysed and compared to inorganic crystalline particles found in ancient lung tissue.

Phytoliths will be extracted from modern samples of crops used by the ancient Egyptians, for example, barley, and also compared against ancient inorganic particles.

1.5.2 *Biological model for particle deposition*

It is unknown to what extent the intentional mummification process affects the physical and chemical properties of organic and inorganic lung particles. This study will attempt to introduce organic and inorganic particles into the lungs of a deceased animal. The lungs will then be intentionally mummified in the laboratory under controlled conditions. After mummification is complete, the animal tissue will be prepared in the same fashion as Egyptian mummified tissue and examined histologically. The pre and post-mummification particles will then be compared by size, shape and elemental composition to see if any changes have taken place. Additionally, any remaining material from this model can be used as practice tissue for the particle extraction method.

1.5.3 *Ancient lung particle extraction*

As anthracosis presents itself visually as large clumped deposits of dark particles (see Section 1.2.3) it will be necessary to isolate the individual particles so they can be analysed accurately. Particle extraction can be achieved by digestion of the lung tissue by proteolytic enzymes, or by physical methods, such as sonication. Enzyme digestion is an established method where a proteolytic enzyme, such as, trypsin or papain, breaks down tissue by hydrolysing peptide bonds between proteins (Mihalyi, 1953). This method, although used extensively for ancient DNA extraction, has not been used on mummified lung material before (David, 2008)

Sonication is an alternative method that uses ultrasound to disrupt cellular membranes allowing the cellular contents to be released. It has been previously used to break down paraffin-mounted tissue for DNA extraction and analysis but has not been used on mummified tissue (Heller et al, 1991).

1.5.4 *Histology*

Histology is a well established technique that has been applied successfully to mummified tissue. Histology uses chemical stains to display contrast between the components, architecture and relationships of cells and allows details (that are usually transparent and lack contrast) to be observed using light microscopy. Histology has been widely used on mummified tissue for over one hundred and fifty years. After the pioneering work of Czermack (in 1852), Ruffer successfully experimented with rehydration techniques on Egyptian mummified tissue (Ruffer**,** 1910). After Ruffer's work, not many histological studies of Egyptian mummies were carried out until the 1970s. Since the renewal of interest in the 1970s, for example, the Manchester Museum Mummy Project led by Rosalie David, many histological investigations have been regularly carried out on mummified tissues (David, 1978; Tapp, 1979). These studies have provided an abundance of information of ancient disease including parasites, such as, schistosomiasis (also known as Bilharzia), and the presence of atherosclerosis in mummies (Lambert-Zazulak, 2000). Histology has been carried out on mummified lung tissue and was used by Tapp (1979) and Walker et al (1987) to identify anthracosis and other lung pathologies.

Typical sample preparation

The first preparation step for both modern and rehydrated ancient tissue is fixation. This step has several aims: to prevent autolysis and putrefaction of the tissue, to prevent any shape or volume change, to provide enough structural stability to allow processing and to allow easy staining of the section without radically altering its pre-fixed appearance (Bancroft and Stevens, 1996). Fixation can also improve staining quality and clarity by encouraging certain stains by acting as mordants and also subtly changing the refractive indices of cellular components to enhance contrast (Drury and Wallington, 1980). A mordant is a substance that acts like a bridge between the dye and the sample material and allows them to easily bond.

Mummified sample preparation

However for mummified tissue, an extra step is necessary to those described above. Mummified tissue is hard, brittle and discoloured. It bears no resemblance to its original appearance either macro or microscopically (see figure 1.27a). For these reasons and to aid tissue processing, it must be rehydrated. When a piece of tissue is rehydrated it regains some of its original appearance and morphology (figure 1.27b) allowing the tissues' architecture and staining characteristics to return (Mekhota and Vermehren**,** 2005). It also softens during the rehydration process allowing for easier cutting. Although many chemicals and methods have been tried and tested over the years as rehydration solutions, there is no agreed universally standard rehydration solution and it often varies from study to study (Currie, 2008).

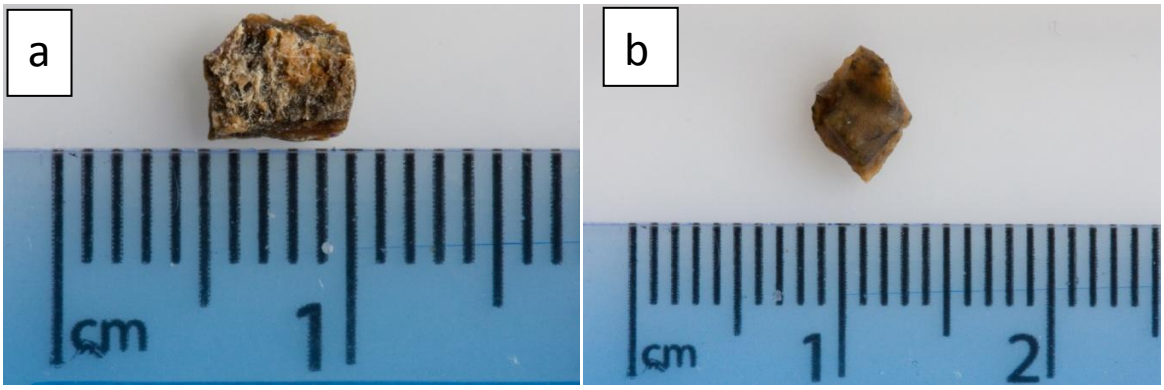

Figure 1.27 Section of mummified tissue from Nekht-Ankh (mummy 11724) before (a) and after tissue processing (b). The tissue in (b) is noticeably softer in appearance.

After the tissue has been fixed, the tissue is placed in a tissue cassette for processing. Processing results in the tissue being embedded in a solid medium, for example, paraffin wax, that can support the tissue but is still sufficiently soft to be cut by a microtome blade (Bancroft and Stevens, 1996). There are four stages:

1) Dehydration – the removal of water,
2) Clearing – the removal of the dehydrating agent and replacement with a solvent that is miscible with the embedding medium,
3) Impregnation – replacing the clearing agent with the molten embedding medium,

4) Embedding – solidifying the molten embedding medium.

The dehydration stage removes any aqueous fixative fluids from the tissue because these may hinder the penetration of paraffin wax into the tissue. A series of alcohols are added to remove water through hydrophilic attraction or to effect dehydration by repeatedly diluting the water present in the sample. These alcohols are used in order of increasing strength to minimise any damage done to tissues by water diffusion currents (Bancroft and Stevens, 1996). The alcohols used in the dehydrating process are not miscible with paraffin wax so an additional step where a substance that is miscible with both is added. This substance is a hydrocarbon based solvent which makes the tissue appear translucent as it replaces the dehydrating agent, hence its name “clearing” agent. There are several clearing agents available including chloroform, xylene and toluene (Bancroft and Stevens**,** 1996).

After dehydration and clearing, the tissue needs to be impregnated with an embedding medium to replace the clearing agent and enable cutting of the sample with a microtome. Paraffin wax (mixed with co-polymers) is the most widely used medium for soft tissues because of its high availability, low viscosity and a wide range of melting temperatures. Plastic resin is used for hard tissue samples due to their similar hardness. The only disadvantage is that the tissue needs to be heated in order to be impregnated and therefore shrinkage and thermal damage may occur. No standard procedure for processing mummified tissue exists and the processing method tends to vary from study to study (Currie, 2008).

After the tissue sample has been successfully treated and impregnated with an embedding medium, it must be cut to produce a section of 5-20 microns thickness that can be mounted onto a slide and stained. Soft tissue samples can be cut by either a rotary or base-sledge microtome to produce ribbons of sample sections. The ribbons are then separated into individual sections and can be mounted onto a slide using a water bath or an albumin-based glue. Before the section can be stained, the paraffin wax must be removed by a clearing agent and must also be rehydrated. This was achieved by putting the section into three successive containers (‘washes’) of xylene, then through a graded series of alcohols beginning with 100% and then immersing in distilled water for rehydration.

Staining

An unstained tissue section will appear transparent and colourless under a light microscope and any structures present in the tissue will indistinguishable. Staining of the tissue allows these structures to be seen by either altering the contrast of the tissue or its colour. A stain causes this colour change through changing the wavelengths of light that are absorbed by the tissue. This absorption is caused by the dye molecules which bind to the specific parts of the cells. This colour causes the cells to be seen in colour and allows cellular components and structures to be identified and in some cases the number of cells in a section to be quantified.

Unfortunately there is not a stain that will reveal all the structural details of a tissue. The stain should be selected on the basis of the tissue component(s) that are to be identified, be permanent bonding, coloured or fluorescent and, most importantly, reproducible (Drury and Wallington, 1980). Tissue staining involves reactions between the solid tissue section phase and the liquid stain phase. The stain dye or molecule usually shows some degree of affinity for a specific cellular component and bonds to it (Bancroft and Stevens, 1996). When choosing stains for a histological examination, one must also choose stains that are appropriate for the tissue. All mummified tissue suffers from some degree of degradation however connective tissues, such as, collagen and muscle fibres, are the cellular components most resistant to degradation and the most successful stains on mummified material are likely to show these connective tissues. Nuclei are generally not preserved in mummified tissue which makes differentiation of cell types and sometime distinguishing individual cells difficult or impossible.

Post staining preparation

After staining, any excess stain must be removed and the section protected by a cover slip before it can be examined with a light microscope. This is achieved by putting the section into three successive containers of distilled water, and graded series of alcohols and then immersing in xylene. This is essentially the reverse of pre-staining procedure. The mounting medium for the coverslip is hydrophobic and makes these final steps necessary.

Examination with light microscopy

The stained and mounted slides can then be viewed in a light microscope. The images can be viewed at varying magnifications (from 2x to 40x) and with different types of illumination (bright field and polarised). Images can be captured through a digital camera and an attached computer and imaging package. Software packages can be used to analyse the images from the microscope and calculate values, such as, area, length, breadth, or roundness of features in the image.

Bright field illumination is the standard method of illumination where white light is transmitted through the slide from below. Some of the transmitted light is absorbed by the section and contrast is provided by areas that have absorbed significant amounts of light (dark areas) and areas with little absorbance (bright areas). Polarised light is produced by putting a polarising filter (which only allows a certain oscillation of light through) over the light source and an identical filter orientated at 90^0 difference from the first filter with the specimen between the two. Polarised light can interact with anisotropic substances to produce a bright, glowing effect called birefringence. If an object is birefringent, this indicates that the substance has an ordered structure, for example, a crystal lattice. Sand and inorganic particles in the lung may have an ordered crystal structure and may be made visible through polarised light (Bradbury and Bracegurdle, 1998). Another method of viewing transparent particles and structures is differential interference contrast microscopy (DIC). In DIC, a complex series of polarised filters is used to demonstrate the difference in optical length and density in a section. The resulting image shows a three-dimensional, almost topographical image of the section with depth depending on the optical density of the section.

Histology has two major advantages in the field of examining mummified tissue: it restores mummified tissue to something more closely resembling its original appearance and it requires very small samples compared to other destructive analytical techniques. Samples for histology are fairly easy to obtain as they can be retrieved by taking scrapings, corings or small pieces of the original mummy tissue. They can also be taken endoscopically with radiological images for guidance (Currie, 2006).

The major disadvantage is that histology produces a two-dimensional image of a three-dimensional structure and this can lead to some mistakes and confusion when interpreting the image and deducing its identity. There is not one stain that will reveal or display all the information present within a sample, meaning that multiple sections of the same sample must be tested with multiple stains. Also the rehydration process will only restore the tissue to its pre-desiccated state and as the tissue may not have been desiccated immediately after death, the tissue may be badly degraded and not suitable for examination. Some additional expansion and contraction damage to the tissue can be caused by diffusion currents during the tissue processing methods so care must be taken.

1.5.5 *Histological stains used in this study*

Haemalum & Eosin (H&E) stain

Haemalum and eosin can show cellular details and components ranging from cell nuclei and other basophilic structures to muscle striations and elastic fibres. Nuclei within the cell are stained blue or black by the haemalum whilst the eosin counter-stains connective tissues and cytoplasm with varying intensities of pinks, oranges and reds. This stain is not without its disadvantages. The H&E stain is not good for staining hydrophobic structures and areas, such as those rich in fats (Kiernan, 2010; Bancroft and Stevens, 1996). However, this is not a disadvantage in the examination of mummified tissue as most lipids have long since putrefied. Another possible disadvantage for H&E is that haemalum is very sensitive to acid and the presence of acid may reduce the visibility of nuclei. As nuclei from mummified material are almost always deteriorated, this could lead to some very poor staining of these sections (Bernard Shaw, 1938).

Toluidine Blue at pH 4.2

Toluidine blue is normally an orthochromatic “architectural” stain. The dye usually displays the general structural information of the sample in differing shades of blue although some connective tissue polysaccharides and cartilage matrixes will stain purple. This colour variation is due to dye-dye molecule interactions and is termed “metachromasia”. Post staining exposure of the slide to light will cause fading of the stain so care must be taken during storage (slides were stored in the dark) and

examination under a light microscope. Toluidine Blue has been successfully used on mummified tissue, especially bone, to show differences in general structure and possible pathologies, such as, osteoporosis and arthritis. (Drury and Wallington, 1980; Bancroft and Stevens, 1996 and Strouhal et al, 2003). Toluidine blue has been chosen in this study for its simplicity and proven success with mummified tissue.

Miller's elastic stain

Miller's elastic stain consists of a mixture of three dyes (Victoria blue 4R, new fuchsin and crystal violet) in a solution with resorcin, dextrin and ferric chloride. It is thought that the resorcin-fuchsin complex forms hydrogen bonds with elastin fibrils staining them black (Miller, 1971). Counterstaining with Picro-sirius red allows the rest of the tissue to be visualised. This stain was selected for investigation as elastic fibres are generally well preserved in mummified tissue (Walker et al, 1987).

One step MSB

One step MSB is a trichrome (meaning "three colour") stain and displays the presence of fibrin in any tissue and also differentiating its age by colour. Fibrin is made from fibrinogen and they interact with each other in various ways in haemostasis causing platelet aggregation and the formation of a protective scab over a wound (Dugan, et al. 2006). Fibrin is usually found in solution with blood plasma. The stain has three components: the yellow, red and blue dye. The small yellow dye molecule along with phosphotungstic acid stains red blood cells and early deposits of fibrin. The acid stops the yellow dye molecule from bonding and staining muscle, collagen and other connective tissue. Muscle and mature fibrin are stained red by the middle-sized red dye molecule, and collagen staining is prevented by residual phosphotungstic acid. Old fibrin and collagen deposits are then stained by the final treatment of the large blue dye molecule (Bancroft and Stevens, 1996). This method can be applied to ancient Egyptian mummified materials to specifically stain and display muscles and connective tissues (Zimmerman, 1972). An error that may occur is the misidentification of old fibrin as collagen. MSB is useful as it can help differentiate degrees of degradation within a

sample as the different sized dye molecules are pore-filling and will reveal the size of pores made in the tissue by putrefaction and autolytic damage.

1.5.6 *Environmental Scanning Electron Microscopy (ESEM)*

ESEM is an imaging technique which can be used to examine samples at very high magnifications (up to 500,000 times) but it is generally used at much lower magnifications. The basic principle of an ESEM is as follows. Electrons are produced by a metal filament, accelerated by a voltage, directed by electromagnetic fields and fired down the column towards the specimen. The electrons hit and interact with the surface layer of the specimen for up to a depth of one micron (like conventional SEM). Possible interactions can be seen in figure 1.28.

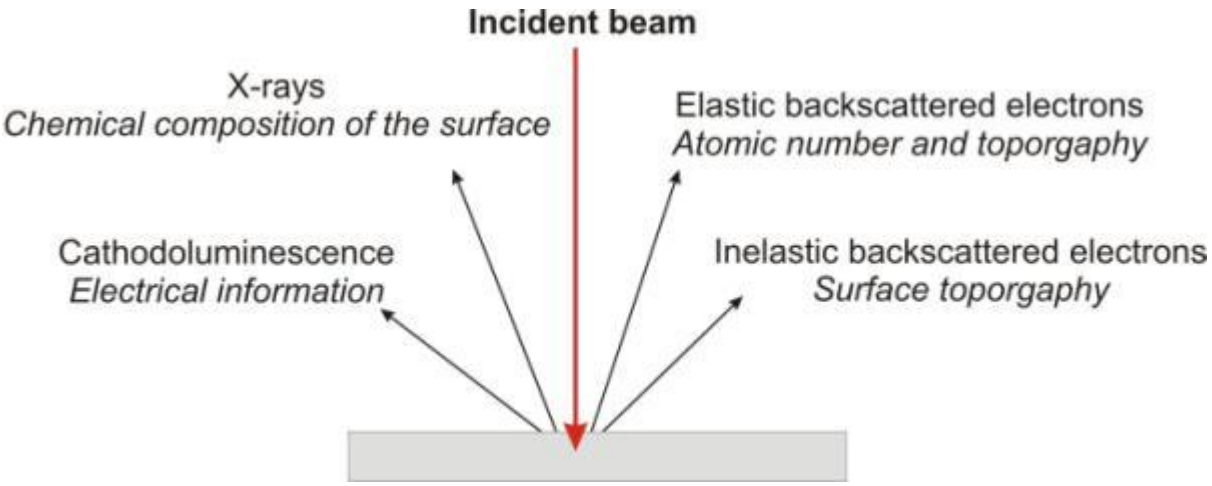

Figure 1.28 Possible interactions of an incident electron beam with the surface of a sample. Inelastic backscattered electrons are the most useful products for imaging the surface details of a sample (CNX.org, 2012).

For ESEM, measuring the inelastic backscattered (also known as secondary) electrons is the most commonly used way for imaging the surface details of a sample. As the electron beam is fired across the surface of the sample in a raster pattern, the intensities and energies of the secondary electrons are detected by the gaseous electron detector. The detector is a uniform electric field (of known voltage) between two separate plates. When electrons (from the sample)

encounter the field, the voltage and current alter. This change is detected and the results are displayed as a black and white image where dark areas are areas that produced few electron and white areas produced large amounts.

ESEM can provide very detailed, high magnification, black and white images of samples. It has been used extensively with mummified material as diverse as cartonnage to hair (McCreesh et al, 2011). Its major advantage over a conventional SEM is that it has a partially pressurised specimen chamber that allows wet or uncoated samples to be imaged. The absence of carbon coating therefore allows precious mummified samples to be re-examined using other analytical means. Its main disadvantages are that it is not capable of the high magnification in conventional SEM and that the black and white images produced by both ESEM and SEM make tissue and particles harder to visualise than stained or unstained light microscopy images.

1.5.7 Energy Dispersive X-ray Analysis (EDX)

EDX is a non-destructive technique for elemental analysis that is usually attached to a SEM or ESEM. EDX has been used to identify unknown residues on mummified hair (McCreesh et al, 2011). It is both a qualitative and quantitative technique, meaning that it will show the presence of an element and how much of that element is present but only under very controlled conditions. It is therefore suitable for “elementally fingerprinting” soots and other particles both in- and ex situ and comparing them against each other.

The basic principles are similar to that of ESEM. Electrons are produced by a metal filament, accelerated by a voltage and fired down the column towards the specimen. The electrons then hit and interact with the surface layer of the specimen for up to a depth of one micron. However, instead of secondary electrons, characteristic x-rays are produced (see Figure 1.28 above). These characteristic x-rays have energies which correspond to specific elements and once they are collected and measured, an EDAX spectrum can be produced, displayed and stored.

The advantages of EDX are that it is quick and a specific area or particle can be targeted for analysis. The limitations of EDX are that it is a relatively insensitive technique (compared to mass spectrometry); it cannot scan large areas and that certain elements, for example carbon, are almost invisible to the detector. Since this study is more interested in the trace elements that may be present in ancient soot and other particles rather than the carbon content, the third limitation is not too serious. EDX is also destructive in that the electron beam heats the material, both changes its composition and damaging the structure. This limitation is less of a disadvantage with modern or isolated ancient soot, but will limit its use in the analysis of irreplaceable mummified tissues sections.

1.5.8 Inductively Coupled Plasma Mass Spectrometry (ICP-MS)

Mass spectrometry is an established bulk analysis method where a solublised sample is ionised in the plasma which is at 8,000 ^{0} k^{to} where ions are produced. The ions are then separated by their mass to charge ratio (m/z) in a quadropole mass spectrometer. After separation, the ions are detected qualitatively and quantitatively by their abundance and m/z by a detector to produce a mass spectrum. The composition of the sample can then be deduced from this spectrum via cross referencing with a library of known spectra (Gross, 2004). In an ICP-MS, the ions from the samples are carried by an inert gas through the plasma (usually Ar or He) which passes through a quadropole and to the detector. This plasma is created by passing an inert gas through an induction created electrical arc. The quadropole (a strong electromagnet) is used to separate the ions by their m/z before they reach the detector. The signals from the detector are then used to produce a mass spectrum. The high accuracy of this method means it can help identify elements in Egyptian artifacts or mummies by fingerprinting different composition. For example, this has been done with resins on mummification bandages (Harrall and Lewan, 2002).

Recent advancements include the time-of-flight analyser which can separate ions also using an electromagnetic field but in a different way. Current mass spectrometers can also analyse large molecules of over 100 kDa (kiloDaltons) in size and have a sensitivity range of up to several parts per billion (ppb) or parts per trillion (ppt) depending on the element being investigated (Dass, 1994;

Robinson et al, 2004). The ability to analyse large and complex molecules along with various ways of producing and separating ions allows for many different samples types to be tested. Ancient samples that have been successfully examined vary from inorganic and metallic materials to mineral and biological samples, such as, plants and soil (Molinero et al, 1997; Carneiro et al, 2008).

A major disadvantage for the use of mass spectrometry in Egyptology is the destruction of the sample in the ionisation process. This does not necessarily present a problem in other areas, such as biology or chemistry, as samples can be regrown or synthesised again. However the large variety of samples that can be analysed, the high sensitivity and versatility of this method means it will be a valuable technique in this project.

The following elements have been chosen to be scanned for in this project; Aluminium and silicon were chosen for their high affinity to each other in nature and the possible presence of these alumino-silicates in the lung. Boron was chosen as a positive identifier for the use of natron in the mummification process (Currie, 2008). Calcium and magnesium were chosen to show calcium carbonates and other common rocks, such as, gypsum. Nickel, cobalt, chromium, cadmium, uranium and manganese are fairly common elements in the earth's crust and their presence in soil or rocks can be used to distinguish the geographical location of a sample. Phosphorus and sulphur can indicate the presence of phosphate or sulphate type rocks. Iron has been chosen because haemosiderin (a storage complex of iron) can be an indicator of disease and inflammation. Copper, gold, lead and mercury were chosen as indicators of profession eg, presence of gold could suggest the individual worked with or smelted gold.

1.5.9 Laser Ablative Induction Coupled Plasma Mass Spectrometry (LA-ICP-MS)

This method consists of an ICP-MS used with a laser ablator to produce ions. The laser is used to vapourise the sample and the vapour is carried through into the temperature oven by the flow of the plasma. This method has several advantages over normal mass spectrometry: the main being the high ionisation efficiency of the laser (almost 100% ionisation) which produces predominantly single positively-charged ions. These ions produce relatively simple spectra allowing easy analysis

of the results (Robinson et al, 2004). Additionally the laser allows for spot analysis or the analysis of a linear path through the sample which is very useful for this study as it may allow for specific regions or particles in ancient mummified lungs to be examined.

1.5.10 Electron Probe Micro-Analysis (EPMA)

EPMA is a technique, similar in principle to ESEM and EDX, which can produce elemental maps of a solid resin-mounted sample. These elemental maps can show the physical location and intensities (and therefore relative amounts) of up to ten elements over the same area. This technique is therefore very useful for identifying the ancient inorganic particles as in addition to identifying which elements are present it shows which are co-localised with each other; for example, a pairing of calcium and sulphur could indicate the presence of gypsum particles in the lungs. This technique has been applied to mummified material from Swedish bogs (Turner-Walker and Peacock, 2008) but not to remains from ancient Egypt.
A sample mounted in resin is placed in the specimen chamber and pumped to vacuum. Electrons are produced by a metal filament, accelerated by a voltage, magnified by lenses and fired towards the specimen. The electrons then hit and interact with the surface layer of the specimen for up to a depth of one micron. Characteristic x-rays are produced by the incident electron beam. These characteristic x-rays have energies which correspond to specific elements and are collected by detector. As the beam scans over the desired area of the sample in a raster pattern, this eventually produces an elemental map of the desired area. The difference between EPMA and EDAX is that the detector only detects one specific element in one pass of the area. As the EPMA only possesses four detectors, this means an area must be scanned multiple times to detect more than four different elements.
However, EPMA is very sensitive compared to EDAX and additionally can produce detailed maps of the distribution of elements and therefore, the elements localised within the inorganic and organic particles in a mummified sample. The major limitation for its use with mummified material is the requirement for the sample to be embedded in resin. Although the method is non-destructive, embedment in

resin makes the material difficult or impossible to use for analysis by other techniques.

1.5.11 Fourier Transform InfraRed Spectroscopy (FTIR)

FTIR is a non-destructive technique which can “fingerprint” a wide range of sample types. The FTIR absorption spectra allow the identification of molecular bonds and chemical groups in a sample which when compared to known “fingerprinted” spectra can facilitate the identification of the sample. Although the FTIR fingerprints may not identify the constituent compounds of the lung particles, the fingerprints will be specific and unique to a sample type. The aim is to allow the surrogate soots, surrogate fuels and ancient soots to be directly compared against each other. This method has been previously applied to mummified material but only to skin and hair samples to establish whether or not resins had been applied during the intentional mummification process (Fornaciari et al, 1998; Cotte et al, 2005).

FTIR is based on the principle that when an infrared beam is passed through a sample, functional groups within the sample will absorb the radiation and vibrate by either stretching, deforming, or bending. When these absorptions are detected, the region of absorptions can be used as a fingerprint and directly compared against the fingerprints of other known substances or samples to establish its identity. Most information and fingerprints are taken from the mid-IR range (wavenumber of 4000 to 600cm^{-1}) as vibrations are seen as sharp peaks (Ellis and Goodacre, 2006). Sections of mummified tissue are mounted on calcium fluoride slides and spot analysis carried out through an attached light/IR microscope. Samples of soot and ancient particles can be loaded as either solids or liquids on the surface of an attenuated total reflectance (ATR) crystal.

The advantages of FTIR are that it is a rapid method which can be used on a variety of samples and requires little sample preparation.

1.5.12 Raman Spectroscopy

Raman spectroscopy is a non-destructive technique that can be used to “fingerprint” a variety of samples. It is similar in principle to FT-IR; however instead

of measuring the absorption of an infrared beam, it measures the energy exchange between the beam and the sample. Raman spectroscopy can show the presence of chemical species which can be identified by cross-referencing the fingerprint against libraries of known spectra (Ellis and Goodacre, 2006). The fingerprints produced by Raman spectroscopy may not identify the particles within ancient lung but should allow the surrogate soots and the ancient soots to be directly compared. Raman has not yet been used on mummified lung tissue or ancient lung particles although it has been used to analyse Egyptian mummy skin samples (Smith and Clark, 2004).

The principle behind Raman spectroscopy is as follows: when an infrared laser (in the visible to mid-IR range) is focused onto a sample, the exchange of energy between the beam and sample results in a measurable Raman shift in the wavelength of the incident laser. This Raman shift (also known as the inelastic light scattering effect) is complementary to FT-IR and can show similar peaks with additional information. For example, peaks from Raman spectra may present themselves with higher intensities than their FT-IR counterparts and show the presence of benzene rings or other functional groups (Ellis and Goodacre, 2006).

The advantages of Raman spectroscopy are that it is suitable for a variety of samples both liquid (for example, a suspension of water and surrogate soot) and solid (for example, a tissue section) with very little sample preparation. Additionally, the Raman spectrometer can be attached to a light microscope allowing spot analysis of clearly identified sections of mummified tissue. The limitations of Raman spectroscopy are that the beam needs to be focussed exactly onto the sample. If not focussed correctly, the spectrometer can receive false signals from the long distance objective lens. The Raman effect is also very weak, with only 1 in every 10^6 to 10^8 photons undergoing inelastic scattering, and this can lead to very long collection times (Ellis and Goodacre, 2006).

1.6 Structure of Thesis

This thesis consists of five further chapters. *Chapter two* describes the materials used in the study. Provenance and information on the ancient lung tissue used will also be given along with a brief description of why the tissues are suitable for study. Tabulation and geographical background information will be provided on sand and mud brick samples from modern Egypt. There will also be a description of the modern fuels that were combusted and their suitability for this project.

Chapter three will detail the methodologies used in this project. This will include details and explanations of the histology of ancient tissue, the extraction protocol for extracting organic and inorganic particles from ancient lung tissue and the production of surrogate soot particles from modern fuels. More established methodologies, such as Inductively Coupled Plasma Mass Spectrometry (ICP-MS),Environmental Scanning Electron Microscopy (ESEM), Energy Dispersive X-ray Analysis (EDAX) and Electron Probe Micro-Analysis (EPMA) will also be briefly outlined.

Chapter four will present the results of this project. Key histological and ESEM images and descriptions of ancient lung tissue, and both ancient and surrogate particulates will be presented and described. Size/shape data of both inorganic and organic ancient particulates will be examined. Surrogate sample size/shape analysis will also be tabulated and the results will include combusted lamp oil particulates, inorganic particulates and mud brick dust. The EDAX spectra of particles will be presented to show their typical elemental composition. EPMA maps of particles in ancient lung tissue will present spectra of particles to show their typical elemental composition and distribution within lung tissue. Additionally there will be a summary table showing size/shape data on particles with pictures and EDAX spectra which will allow for easy comparison of all the particles.

Chapter five will contain the discussion and analysis of the results from chapter four, whilst *Chapter six* will outline the key conclusions and also identify any key areas that would benefit from further study.

Chapter 2

Materials

2.1 Mummified remains

All samples of mummy tissues have been acquired through the International Mummy Tissue Bank in Manchester (Lambert-Zazulak et al, 2003). The tissue from the Dakhleh Oasis was deposited by Professor Aurderheide of Minnesota University, USA in 2002. The samples from the British Museum were deposited in 2006. The University of Colorado deposited the Kulubnarti material in 2004. Samples DO45 and DO46 from the Dakhleh Oasis were deposited by Professor Zimmerman of Villanova of University in Pennsylvania in 2010.

The samples are detailed below in reverse chronological order from the most recent to the most ancient.

2.1.1 *Kulubnarti material - S82, S85 and S195*

S82, S85 and S195 have been previously identified as lung material by Patricia Rutherford when the samples were donated to the tissue bank (Adams, et al, 1999). These samples are from three mummies of unknown age and sex from the island of Kulubnarti (see Introduction, section 1.1.4). The excavators consider that the mummies came from the late Roman Period (500-550AD) as this was when the cemetery was primarily used (Mulhern, 2000). Although there is no record of the mummification type, the individuals were probably spontaneously mummified in common with the other mummies from Kulubnarti (Turner et al, 1997). The lack of wrapping and intentional mummification suggests the individuals were probably of non-elite status. The Kulubnarti samples were chosen for this study as they are known to be lung tissue samples and have not been examined before.

2.1.2 *Dakhleh Oasis material - DO45 and DO46*

Sample DO45 and DO46 are taken from the right and left lung respectively of a male inhabitant of the Dakhleh Oasis (see Introduction section 1.1.4). The mummy is thought to have come from the Greco-Roman Period (332BC to 395AD) as this is when the cemetery was primarily used. Unfortunately the age of the individual could not be deduced from the remains (Zimmerman, 2010). The social status of

the mummy is unclear but is possibly elite as the mummy appears intentionally mummified according to the examination notes of Prof Zimmerman (Zimmerman, 2010). This tissue was chosen for the study as anthracosis and anthracotic particles have previously been found in these samples (Zimmerman, 2010) but were not characterised. These two specimens will also allow a direct comparison of particle distribution in one individual.

2.1.3 *Dakhleh Oasis material from the Kellis cemetery (material provided by Prof Aufderheide)*

A-4

Sample A-4 is thought to be from the right lung of a non-elite woman, aged 20 to 22 years old who was spontaneously mummified following her burial at the Kellis cemetery near the Dakhleh Oasis (Aufderheide, 2003; see also Introduction, section 1.1.4). This mummy and all the others detailed below from this site dates to the Greco-Roman Period as this was the period during which the cemetery was used. Unfortunately the particular mummy could not be dated further. This sample was chosen because it was of very few female samples available from the Dakhleh Oasis. It was also specifically labelled as lung by Aufderheide and has not been examined before.

A13

Mummy A13 was a male aged 50-60 from the Kellis cemetery, was excavated in 1993 and dates from the Greco-Roman Period. It has not been examined before and was chosen as it is one of the eldest (of age at death) available and hence should have had a longer exposure to particles than most other mummy samples examined in this study.

A-102

Sample A-102 comes from a young boy aged 9 to 13 years old of non-elite status. Despite possessing some wrappings is thought to be spontaneously mummified (Aufderheide, 2003). He was excavated in 1998 and dates to the Greco-Roman Period. This sample was chosen because it was one of the youngest age (at death) samples available and should arguably show less exposure to particles

than the other mummified lung tissues. The lung tissue was identified by Aufderheide and has not been examined before. Figure 2.1 shows the mummy and its wrappings before autopsy. The mummy was intact and therefore facilitated identification and removal of the lungs.

Figure 2.1 Image of Mummy A-102 showing its wrappings and state of preservation. (courtesy of A. Aufderheide)

A105

Mummy A105 was a male aged 50 to 60 years old. The type of mummification for this individual could not be determined as the mummy consists only of a torso with a head and one arm. This Greco-Roman Period (332BC to 395AD) mummy is probably of non-elite status. This mummy was chosen as it is one of the eldest (at death) available and although it has not been examined before the lung should contain many particles after years of exposure to soot and sand.

A108

Mummy A108 was a male aged 21 to 25 years old (at age of death) and probably of non-elite status due to its lack of intentional mummification. This sample was chosen as it has never been examined for anthracotic or silicotic particles.

A110

A110 was a 30-40 year old male dated to the Greco-Roman Period. The lung sample has not been examined before. It was chosen as it is one of the few

mummies from the Kellis cemetery that was intentionally mummified and may be of a higher social status than the other mummies from the Dakhleh Oasis.

A111

Mummy A111 is a male mummy probably of non-elite status and was spontaneously mummified. This individual was aged twenty to twenty-five years old when he died. This mummy was chosen as the lung sample has not yet been examined before.

Figure 2.2 Mummy A126 shown pre-autopsy. The mummy was a 20-25 yr old man from the Dakhleh Oasis. (Courtesy of A. Aufderheide).

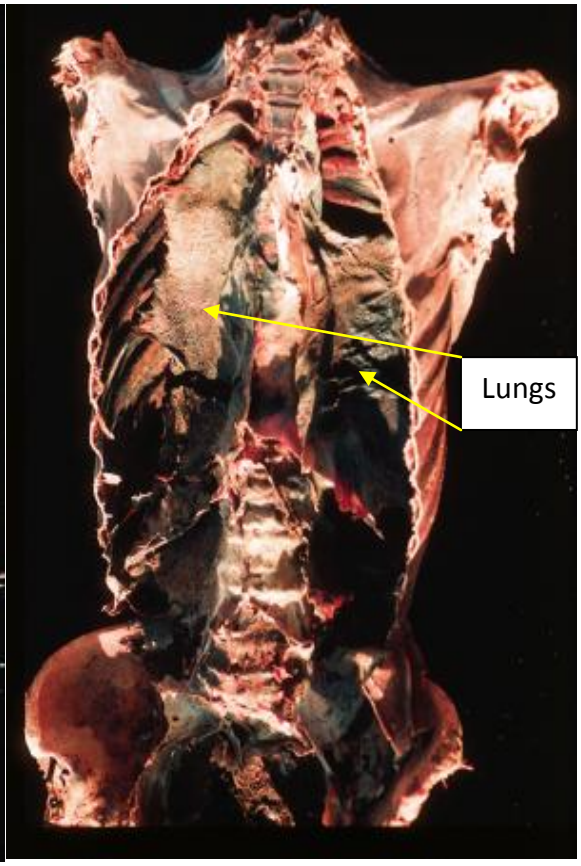

Figure 2.3 Mummy A126 shown post-autopsy. The lungs are clearly visible in the thoracic cavity. (Courtesy of A. Aufderheide).

A-126

Sample A-126 is a right lung of a man, aged 40 to 50 years old dating back to the Greco-Roman period (332BC to 395AD) and was spontaneously mummified. Photographs of the mummy pre- and post-autopsy, can be seen in Figures 2.2 and

2.3. The sample from this mummy was chosen because it has not been examined for anthracosis, silicosis or pneumoconiosis before.

A132

Mummy A132 was chosen as it is the youngest (of age at death) sample available. This three to five month old infant again dates to the Greco-Roman period. Although the infant was wrapped, it appears the mummy was spontaneously mummified and is probably of non-elite origin. Due to the young age of the mummy, it is not possible to determine its sex. This mummy was chosen as it should have had the least amount of exposure to sand or soot particles due to its short lifespan. The wrapped mummy can be seen in figure 2.4.

Figure 2.4 A132 shown pre-autopsy. The mummy was of a 5-6 month old infant and was found intact (Courtesy of A. Aufderheide).

2.1.4 Intentionally mummified lung material

MM 1777

Sample MM 1777 is taken from the posterior of the thoracic cavity wall of a 25th Dynasty (c760 BC) female mummy named Asru (figure 2.5). She was aged between 50 to 60 years old when she died and was intentionally mummified. She worked as a priestess of Amun at Thebes. This lung sample was chosen as this

mummy would represent an elite individual who may have additionally been exposed to soots arising from participation in religious rituals.

Figure 2.5 The mummy of Asru as displayed in the Manchester Museum. Asru was aged 50 to 60 yrs old and probably buried at Thebes.

BM 51813

Sample BM 51813 is taken from the Canopic jar of a Theban priestess of the 19th Dynasty (c1250 BC) named Henutmehyt. This lung sample was chosen because a previous examination showed that it contained anthracosis (Walker et al, 1987) although the internalised particulates have not been characterised. This lung sample also comes from an individual who was intentionally mummified and was from an elite background and would have probably been exposed to further soot during her religious duties. Therefore, the individual could have been exposed to a greater number of soots than most of the non-elite mummies. The Canopic chest and two Canopic jars from Henutmehyt can be seen in Figure 1.1.4 above.

MM 11724

Sample MM 11724 is taken from the thoracic cavity of the second of the “two brothers” displayed at the Manchester Museum, Khnum-Nakht. Khnum-Nakht was

a “Great Waab-Priest” of the God Khnum at Rifeh during the 12th Dynasty (c1990-1802BC). He was aged around sixty years old at death. He was intentionally mummified and of elite status. This sample was chosen as this individual was of elite status and his age at death would ensure that he had been exposed to particles for a long period of time. The Great Waab Priest was overseer of the ordinary (Waab) priests and therefore is likely to have been exposed to temple soot from temple lighting and rituals.

BM 34193

This sample is material taken from a pottery canopic jar found in Egypt. The jar possessed a human-headed stopper and unfortunately there is no provenance to associate it with a particular mummy. However, as the sample presents to its intentional mummification, it is probable that the mummy was of elite status. Although the stopper was not in the likeness of Hapy, this canopic jar was found to have lung material (Walker et al, 1987). This sample was chosen as it contains anthracotic particles (Walker et al., 1987) and may come from an elite background, meaning the individual may have been exposed to different soots to the individuals from the Dakhleh Oasis or Kulubnarti.

BM 37949

This sample consists of material taken from a limestone canopic jar with an eagle-headed stopper of the deity Qebeh-senwef. There is no provenance to associate it with a mummy. However, due to the presence of intentional mummification, it is probable that the mummy was of elite status. The stopper would suggest the mummy was mummified after the 18th Dynasty (Riyad, 1973). Despite coming from a canopic jar with the wrong stopper (Qebeh-Senwef is protector goddess of the intestines), it was chosen because previous examination had identified lung tissue (Walker et al, 1987). Anthracotic particles were identified by Walker but they were not characterised.

Details of the Dakhleh Oasis samples are summarised in Table 2.1 and the samples from other geographical areas in Table 2.2.

Table 2.1 Summary of the Dakhleh Oasis samples' provenance showing time period, sex, age at death, name, mummification type, location and social status (if known). (G-R = Greco-Roman Period)

Mummy	Period	Sex	Age	Name	Mummified	Location	Likely social status
DO-45	G-R ~200AD	M	unknown	?	Yes	Dakhleh Oasis	Non-elite
DO-46	G-R ~200AD	M	unknown	?	Yes	Dakhleh Oasis	Non-elite
A4	Ptolemaic/G-R	F	20-22	?	Spontaneous	Dakhleh Oasis	Non-elite
A13	Ptolemaic/G-R	M	50-60	?	Spontaneous	Dakhleh Oasis	Non-elite
A102	Ptolemaic/G-R	M	nine to 13	?	Spontaneous	Dakhleh Oasis	Non-elite
A105	Ptolemaic/G-R	M	50-60	?	Unknown	Dakhleh Oasis	Non-elite
A108	Ptolemaic/G-R	M	21-25	?	Spontaneous	Dakhleh Oasis	Non-elite
A110	Ptolemaic/G-R	M	30-40	?	Yes	Dakhleh Oasis	Non-elite
A111	Ptolemaic/G-R	M	20-25	?	Spontaneous	Dakhleh Oasis	Non-elite
A126	Ptolemaic/G-R	M	20-25	?	Spontaneous	Dakhleh Oasis	Non-elite
A132	Ptolemaic/G-R	Infant	3-5 months	?	Yes	Dakhleh Oasis	Non-elite

Table 2.2 Summary of the samples from Kulubnarti, Thebes, and Rifeh samples' provenance showing time period, sex, age at death, name, mummification type, location and social status (if known).

Mummy	Period	Sex	Age	Name	Mummified	Location	Likely social status
S82	Christian ~550AD	?	?	?	Unknown	Kulub Narti	Non-elite
S85	Christian ~550AD	?	?	?	Unknown	Kulub Narti	Non-elite
S195	Christian ~550AD	?	?	?	Unknown	Kulub Narti	Non-elite
BM 51813	19th Dynasty	F	?	Henutmehyt	Yes	Thebes	Elite
MM 1777	25th Dynasty	F	50-60	Asru	Yes	Thebes	Elite
MM 11724	12th Dynasty	M	40	Nekht-Ankh	Yes	Rifeh	Elite
34193	Unknown	?	?	?	Yes	Unknown	Elite
37949	Unknown	?	?	?	Yes	Unknown	Elite

2.2 Inorganic Samples from Egypt

The samples of inorganic particles to be analysed in this study were collected from various archaeological sites around Egypt in 2010. The samples were chosen to represent the various types of sand present at those sites and therefore presumably similar to those to which people in ancient times living at these sites would have been exposed to. Mud brick samples were also collected, as it is likely that dust from this very friable material would also have been inhaled. Mud bricks were universally used in the construction of residential and commercial buildings, including those of the high elite and royalty; the exception being temples and tomb superstructures that were usually largely built of stone. The sand and mud brick samples used in this study were stored and transported in sterile plastic bags to minimise contamination.

2.2.1 *Sand samples*

Sample from Karnak

The sample was chosen because of its fine granular appearance. It was taken from recent excavations of a Greco-Roman site adjacent the first pylon of the temple of Amun-Re at Karnak and can be seen in Figure 2.7.

Figure 2.7 The Greco-Roman baths near the temple of Karnak where the soil sample was taken on the lower right hand side (Author's own photo).

Sample from Beni-Hassan

This sand was taken from the base of the steps up to the Middle Kingdom tombs located in the cliffs at Beni-Hassan and features a variety of different sized particles.

Sand Sample 1 from Tel-el Amarna

This sand consists of a variety of particles ranging from very small to gravel sized. It was taken from base of Northern Tomb cliffs (Figure 2.8) and chosen for its proximity to the tombs and main areas of Amarna.

Figure 2.8 The site where sand sample 1 was taken near the Northern Tomb cliffs of Amarna (Author's own photo).

Sample 2 from Northern Palace at Amarna

This sand consists of sand grains of various sizes. It was taken from the base of the raised embankment surrounding the palace excavation site.

Sample from Tuna-Elgebal

This very fine, homogeneous desert sand can be found on paths to Amarna boundary stela at Tuna el-Gebel (figure 2.9).

Figure 2.9 The desert sand found at the Amarna boundary stela at Tuna-Elgebal (Author's own photo).

2.2.2 *Mud Brick Samples*

Sample 1 from Northern Palace at Amarna

Figure 2.10 Mud brick 1 from the Northern Palace at Amarna (Author's own photo)

Figure 2.11 Mud brick 2 from the Northern Palace at Amarna (Author's own photo).

The appearance of a small piece of a mud brick is shown in figure 2.10. The original brick would have been larger and more rectangular. It was taken from the Northern Palace at Amarna and is made from mud and small, fine aggregates

Sample 2 from Northern Palace at Amarna

Figure 2.11 shows the appearance of a large portion of a mud brick. The original brick would have been larger and more rectangular. It is made from mud, plant material and small, fine aggregates which was taken from the Northern Palace at Amarna.

Sample 3 from Dahshur pyramid

Figure 2.12 shows a mud brick from the pyramid of Amenemhat II from the Royal necropolis at Dahshur in Egypt. The mud brick appears darker and contains larger pieces of plant material than the Amarna mud bricks.

Figure 2.12 Mud brick fragment from Dahshur pyramid.

2.3 Surrogate Fuels

The following fuels were used in this study to provide surrogate soot of the type that the ancient Egyptians have been exposed to. Information from the literature supporting the selection of these fuels can be found in Section 1.3.2 of the Introduction. Table 2.3 contains a summary of the degree of saturation, chain length and constituents of these fuels can be found at the end of this section.

Beeswax

Although there is little evidence for the use of beeswax candles in ancient Egypt, this fuel was included in this study to provide an example of a non-liquid, animal-derived soot as fuels of animal origin were used. Beeswax is solid at Egyptian room temperature (25˚C) and melts at 62 to 64˚C. Its primary constituents are palmitoleate, palmitate, hydroxypalmitate, and long chain oleate esters of aliphatic alcohols (Christie, 2012). The beeswax for this project was purchased from Fred Aldous, Manchester, U.K.

Castor oil

Castor oil was widely available in ancient Egypt and has been found in tombs from Pre-Dynastic times (Lucas, 1962). This fuel was chosen because it represents a non-elite fuel to which most of the Egyptian population could have been exposed. Castor oil is a liquid at Egyptian room temperature and consists primarily of ricinoleic acid, with small amounts of linoleic acid, oleic acid, stearic acid and palmitic acid (O'Shea, 2012). The castor oil for this project was purchased from Pukka Herbs Ltd, Bristol, U.K.

Olive oil

Olive oil seems to have been introduced into Egypt during the 19th Dynasty, around 1200 BC, but seems to have been an expensive commodity until the introduction of the olive tree in the 4th century BC (Lucas, 1962). This fuel was chosen as its soot would not be expected to be found in any mummies before the 19th Dynasty and is likely to occur predominantly in elite Egyptians until the Greco-Roman Period. Olive oil has a low degree of saturation compared to other vegetable oils. Its main constituents are oleic acid, palmitic acid, linoleic and

stearic acid (Mailer, 2006). The olive oil for this project was purchased from Healthy Oils, London, U.K.

Palm oil

Palm oil was used throughout Egypt in ancient times and was used extensively in later periods, for example, in Herodotus' mummification methods (Rawlinson, 1880). As a commonplace fuel, palm oil was chosen as it may be present in mummies of all social classes and time periods. The major constituents of palm oil are palmitic acid, oleic and linoleic acid (Sundram, 2002). It is a liquid at Egyptian room temperature. The palm oil for this project was purchased from Pukka Herbs Ltd, Bristol, U.K.

Sesame oil

Sesame oil was an important export from Egypt to the Greeks according to the Revenue Laws of Ptolemy II Philadelphus in 259BC (Dalby, 2003). It continued to be exported when Egypt became part of the Roman Empire and is mentioned by Pliny the Elder in the 1st century AD (Bedigian and Harlan, 1986). It has been chosen as a fuel that would have been popular in later periods. It consists primarily of oleic and linoleic acid (Nzikou et al, 2009). The sesame oil for this project was purchased from Suma Wholefoods, Elland, U.K

Table 2.3 Summary of fuels used to produce the surrogate soot in this study. The table shows the major and minor constituents of the fuels along with their relative saturations and state at room temperature. Alter this depending on results – size, shape, etc

Fuel	Beeswax	Castor oil	Olive oil	Palm oil	Sesame oil
Major constituents (>15%)	Oleate esters (35-80%) Free wax acids (14-16%)	Ricinoleic acid (89%)	Oleic acid (72%)	Palmitic acid (44%) Oleic acid (36%)	Oleic acid (35-50%) Linoleic acid (35-50%)
Minor constituents (<15%)	Hydrocarbons (10-14%)	Linoleic acid (4%) Oleic acid (3%) Stearic acid (1%) Others/uknown (3%)	Palmitic acid (8-15%) Linoleic acid (6-9%)	Linoleic acid (9%) Stearic acid (6%) Others unkown (5%)	Palmitic acid (7-12%)
Percentage saturation	Unknown	11%	13%	59%	18%
Percentage of non-saturation	Unknown	89%	87%	41%	82%
State at room temp	Solid	Liquid	Liquid	Solid	Liquid

Chapter 3

Methods

3.1 Histology

Histology is a well established technique that has been applied successfully to mummified tissue for over a hundred years. Histology uses chemical stains to allow details about the components, architecture and relationships of cells to be visualised and observed using light microscopy. These stains are necessary due to the lack of inherent contrast in unstained tissue. The principles underlying histology were previously discussed in the Introduction, Section 1.5.4..

3.1.1 *Rehydration and fixation of ancient samples*

The first stage of sample preparation of histology for modern tissue samples is fixation. Fixation stabilizes the tissue and prepares it for subsequent processing and it also preserves the tissue by arresting bacterial growth and preventing putrefaction. However, mummified tissue requires an additional step: rehydration. Rehydration restores some of the tissue's original appearance and morphology and also leads to a softening of the tissue (Mekhota and Vermehren**,** 2005). This softening ultimately makes subsequent processing and cutting (sectioning) of the tissue easier.

This study used a solution of 1% sodium lauryl sulphate in formal saline to rehydrate and fix the mummified samples in one processing step. The formal saline solution consisted of 0.9g of sodium chloride in 100 ml of distilled water containing 10% formalin (Currie, 2008. The formalin solution is made commercially by passing formaldehyde gas through water resulting in a solution containing 40% formaldehyde gas in solution. This rehydrating solution was found by previous researchers to produce the best results as it uses the optimal non-ionic detergent for arresting the growth of bacteria and other putrefying organisms during rehydration (Currie, 2008). This is essential as, left uninhibited, bacteria would putrefy the tissue during rehydration. The protocol for rehydration is outlined below (Currie, 2008).

1) 20ml of the rehydrating solution (1% sodium lauryl sulphate in formal-saline) was added for every gram of tissue and placed in a sample container.

2) The sample was left for 48 hours and then removed from solution. The sample was then stored in formalin. This allowed the tissue to be stored for convenience until sufficient numbers of ancient tissue were ready to be processed.

3.1.2 *Tissue processing and sectioning*

Processing

After fixation, the tissue must be processed so that the tissue is embedded in a medium that allows it to be easily sectioned by a microtome. Usually this process requires the tissue in aqueous solution to be put through a series of dehydrating alcohols to remove water before it can be embedded. However, as most embedding materials are also immiscible with alcohol, another step must be added where the alcohol is removed before embedding. No standard procedure for processing mummified tissue exists and the processing method tends to vary from study to study (Tapp, 1979, Walker et al, 1987). The tissue in this study was processed by a Citadel 2000 tissue processor using the solutions outlined in table 3.1. This study uses industrial methylated spirits (IMS) (95% ethanol with 5% methanol) as the dehydrating agent and was chosen for its easy availability and its efficacy as a dehydrating agent. Xylene was chosen as the clearing agent to remove the alcohol. Xylene was also chosen due to its miscibility with the embedding medium and its ready availability. Paraffin wax with added co-polymers was chosen as the embedding medium because of its high availability, low viscosity and a wide range of melting temperatures. The addition of copolymers ensures that the paraffin wax would only form micro-crystals when cooled rapidly. If large crystals were to form upon cooling, they could not only damage the tissue but also impede the sectioning process due to tearing.

The sample was removed from the formalin storage solution and placed into solution 1 in the automated tissue processor. The first solution of 50% formol saline and 50% IMS washed out any residual sodium lauryl sulphate from the rehydration and fixation process. The next five IMS containers removed water from the sample. The first solution of IMS absorbed the largest amount of water and

progressive IMS containers absorbed less water until all water has been removed from the sample. At this point the clearing process began and xylene was used to remove the alcohol prior to tissue embedding. The majority of the alcohol was removed in the first two xylene containers. After the third xylene container, the sample was ready to be impregnated by molten paraffin wax. After this process was complete, the tissue cassette was removed and stored for 48 hours in a vacuum oven set at a pressure of 2 Bars.

Table 3.1 Concentrations of IMS, xylene, and wax plus the processing times for the processing of mummified material.

Container	Fluid	Time (hours)	Stage
1	50% Formol-saline/ 50% IMS	0	Washing
2	100% IMS	1.5	Dehydrating
3	100% IMS	1.5	Dehydrating
4	100% IMS	1.5	Dehydrating
5	100% IMS	1.5	Dehydrating
6	100% IMS	1.5	Dehydrating
7	Xylene	1.5	Clearing
8	Xylene	1.5	Clearing
9	Xylene	1.5	Clearing
10	Xylene	1.5	Clearing
11	Paraffin Wax	1.5	Impregnation
12	Paraffin Wax	1.5	Impregnation

Preparation of sample ribbons and slides

After tissue processing was complete and the sample had been impregnated with the paraffin wax the embedded tissue was orientated and mounted onto a tissue cassette to facilitate sectioning. Mounting was achieved by using a Leica blocking station (Leica Ltd, Cambridge, England; Figure 3.1).

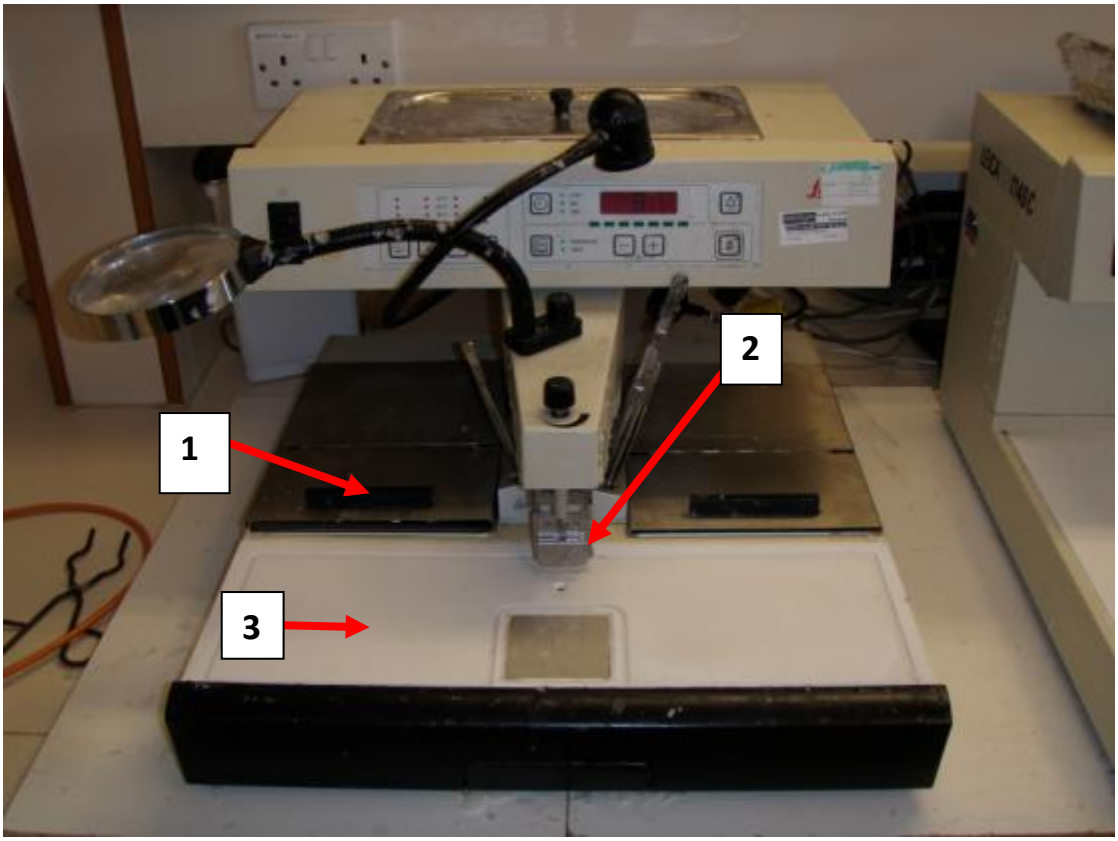

Figure 3.1 A Leica blocking station. The wax reservoir (1), wax dispenser (2) and cold plate (3) can be seen.

1) The tissue cassette was stored in a vacuum oven at 65°C and a pressure of-2 Bars. The low vapour pressure and relatively high temperature of the oven aided impregnation of the tissue by the paraffin wax and ensured that any volatile substances left over from the tissue processing steps evaporated off.
2) The cassette was removed from the oven and placed into the molten paraffin reservoir of the docking station (Figure 3.1). A metal mould (of appropriate size relative to the size of the tissue sample) was chosen and half-filled with molten paraffin wax from the wax dispenser (Figure 3.1).
3) The tissue sample was then removed from the tissue cassette and carefully placed in the bottom of the mould. If possible, effort was made to ensure that tissue was placed in the optimal angle for the best sections to be taken. For example, a section of skin should be cut transversely to show a cross-section of the different layers of epidermis and dermis. The metal mould was then filled to the brim with molten wax and the base of the tissue

cassette placed on top. This tissue cassette holds the tissue containing block in place when sectioning with a microtome.

4) If the tissue moved when the wax was added, the excess wax would be poured off until the metal mould was half-full. The mould would then be placed on the cold section of the blocking station for a very short period until the bottom of the wax had coagulated. This coagulated wax could then be used to hold the tissue in place when the mould was filled up with more molten wax.
5) The metal mould was then put on the blocking station's cold plate to quickly cool the paraffin and prevent damage from crystal formation. The solid wax tissue block was then stored in a freezer for 30 minutes to shrink the wax aiding removal from the metal mould.

Sectioning and mounting

1) The metal mould was removed from the freezer and placed on the laboratory bench. The metal mould was inverted and lightly tapped until the wax block fell out. Any excess wax was trimmed off.
2) The tissue block was placed in the chuck of a rotary microtome. The microtome was used to produce thirty 5μm thick sections of the sample. The sections were produced in the form of a long ribbon of attached sections. The ribbon was placed between two sheets of wax paper to reduce static electricity and contamination.
3) Ten consecutive sections (with no obvious tears or wax folds) were separated from each other and chosen to be mounted. The sections were mounted using a water bath or albumin. For the albumin method, Mayer's albumin and water was spread by a finger over the centre of a microscope slide. The section was introduced and teased over the area of albumin. In the water bath method, separated sections were floated in a water bath (at 40˚C). A microscope slide was placed in the bath and the section was floated onto it. The albumin method was used to mount sections not onto a glass slide but onto 200micron Mylar sheet for Laser Ablative Inductively Coupled Plasma Mass Spectrometry (LA-ICP-MS) to ensure that the section containing the particles had good adherance. Mylar sheet was used as glass (which contains many elements was unsuitable) and the plastic

only contains undetectable organic groups. The water bath method was used to mount sections for all other analytical methods.

4) After the ten sections had been mounted onto ten slides, the slides were placed onto two hot plates. The first hot plate (at 50˚C) was designed to aid evaporation of any remaining water and to partially melt the paraffin wax and remove bubbles between the wax and slide. The second hot plate (at 70˚C) is a step unique to mounting mummified tissue, and is used to “fuse” the section to the slide (Denton, 2009). This is because the usual adherents of tissue sections (for example, proteins) are seriously degraded in mummified tissue.

3.1.3 *Pre-staining preparation*

Before the section can be stained, the paraffin wax must be removed by a clearing agent and then rehydrated as the stains used in this study were all water-soluble. Removal of the wax was achieved by placing the slides containing the tissue sections into three successive containers of xylene, rehydrating through a graded series of alcohols and finally immersing in water.

Wax removal Stage

1) The slide was immersed in the first xylene container for 2 minutes.
2) The slide was removed, shaken slightly to remove excess xylene and then immersed in the second xylene container for 30 seconds.
3) The slide was removed, shaken slightly to remove excess xylene and immersed in the third xylene container for 30 seconds.

Xylene removal stage

1) The slide was removed from the xylene container and shaken well to remove excess xylene. The slide was then immersed in the first container of IMS for two minutes.
2) The slide was removed, shaken slightly to remove excess IMS and immersed in the second IMS container for 30 seconds.
3) The slide was removed, shaken slightly to remove excess IMS and immersed in the third IMS container for 30 seconds.

Rehydration stage

1) The slide was removed from the IMS container and shaken well to remove excess IMS. It was then immersed for two minutes in the first container of distilled water.
2) The slide was removed, shaken slightly to remove excess water and immersed in the second water container for 30 seconds.
3) The slide was removed, shaken slightly to remove excess water and then immersed in the final water container for 30 seconds.

3.1.4 *Post-staining procedure*

Although most stains are aqueous, the mounting medium used to adhere the coverslip to the microscope slide and section is not, so water must be removed from the slide. This process is essentially the opposite of the pre-staining procedure.

Dehydration stage

1) The slide was immersed in the first container of IMS for two minutes.
2) The slide was removed, shaken slightly to remove excess IMS and immersed in the second IMS container for 30 seconds.
3) The slide was removed, shaken slightly to remove excess IMS and immersed in the third IMS container for 30 seconds.

IMS removal stage

1) The slide was removed from the IMS container and shaken well to remove excess. The slide was then immersed in the first xylene container for 2 minutes.
2) The slide was removed, shaken slightly to remove excess xylene and immersed in the second xylene container for 30 seconds.
3) The slide was removed, shaken slightly to remove excess xylene and immersed in the last xylene container for 30 seconds.

Mounting

1) A small amount of XAM mounting medium was applied to a cover slip and placed medium side up on a clean piece of tissue paper. The slide (with the

stained sample over the glued cover slip) was then pressed onto the cover slip and held firmly down for 5 seconds.

3.1.5 *Histological stains to be used in this study*

All reagents were obtained from Sigma-Aldrich Ltd. (Dorset, UK) unless stated otherwise.

Haemalum & Eosin (H&E) stain (Harris, 1900)

The principle for this stain has been previously described in the Introduction chapter, section 1.3.5.

Materials

Harris' Haemalum (VWR International, Lutterworth, UK)

1% Alcoholic eosin

1% acid alcohol

Method

1) The sections were taken to water (see section 2.9).
2) The slides were stained in a coplin jar containing modified Harris' Haemalum for 4-7 minutes. The staining time depended on how well the tissue took up the stain.
3) They were then rinsed in hot running tap water.
4) The slides were differentiated in 1% acid alcohol until the background appeared clear following removal of any loosely bound haemalum.
5) The sections were then 'blued' in hot tap water. The tap water has made the pH of the section more basic and allowed the haemalum to be visualised again.
6) The slides were then counterstained in 1% alcoholic eosin Y for 1 minute.
7) The sections were dehydrated, cleared and mounted (section 2.10).

Result

Nuclei and basophilic structures – Blue.

Background – Pink.

Toluidine Blue pH 4.2 (Wolman, 1971)

The principle for this stain has been previously described in the Introduction chapter, section 1.3.5.

Materials

Stock – 0.5% Toluidine Blue (VWR International, Lutterworth, UK) in distilled water

Working solution – 0.05% Toluidine Blue

Method

1) The sections were taken to water (see section 2.9).
2) They were stained in a coplin jar containing the working solution (10 ml of 0.5% Toluidine Blue in 90ml of water) for 10 minutes.
3) They were then rinsed in water, dehydrated, cleared and mounted (see section 2.10).

Result

Nuclei and other components – Blue.

Metachromatic substances – Red, pink, green or purple.

Miller's elastic stain (Miller, 1971)**:**

The principle for this stain has been previously described in the Introduction chapter, section 1.3.5.

Materials

Miller's Elastic Stain (R.A. Lamb, London, UK)
1% potassium permanganate
5% oxalic acid
IMS
Xylene
Picro-sirius red

Method

1) The sections were taken to water (section 2.9).
2) The slides were stained in a coplin jar containing 1% potassium permanganate for 5 minutes. They were then rinsed in water for 2 minutes.
3) The slides were submerged and stained in 5% oxalic acid for 5 minutes.
4) The slides were rinsed again in water for 5 minutes and then rinsed in IMS for 2 minutes.
5) The slides were left to stain in a coplin jar containing Miller's elastic stain for 3 hours.
6) They were then rinsed in IMS until all the excess stain was removed (roughly 30 seconds).
7) The slides were rinsed again in water for 2 minutes.
8) They were then counterstained in Picro-sirius red for 5 minutes.
9) The slides were cleared and mounted (xylene stage of section 2.10 onwards).

Results

Elastic fibres – Blue/black
Collagen – Red
Muscle – Yellow

3.1.6 *Examination of histological slides using light microscopy*

The slides were examined using a Leica RMDB light transmission microscope (Leica Ltd, Cambridge, England). Images were captured by a Delta Infinity X camera (Lumenera Corporation, Ontario Canada) and Leica Qwin software (Leica Ltd, Cambridge, England).

1) The slide was examined using a 10x lens and bright field illumination.
2) The general architecture of the slide was observed and images taken.
3) Any areas of interest were examined at higher magnifications (X40, X100) and images taken. If particles were found within the sections, the slide would also be examined using polarised light (to demonstrate birefringence) or DIC (to enhance contrast).

3.2 Biological model for particle deposition

3.2.1 *Preparation*

For this study, a biological model was designed to allow, respectively, soot and clay particles of a known size and shape to be introduced into rat lungs. The principles behind this model have been previously described in Introduction, Section 1.5.2. The lungs were then mummified with the aid of natron salt. The aim of this experiment was to produce mummified lungs that could demonstrate any size or shape alterations to the particles caused by the intentional mummification process. Additionally the tissue could also be used as practice material for the enzymatic extraction method (see Introduction section 1.5.3).

The lungs for this study were acquired from rats that were killed for a separate study examining cardiac myocytes and would otherwise have been disposed of. The male Wistar rats were ordered from Charles River Laboratories (U.K.). The rat used weighed between 225 and 250g and their age would have been between 6 - 8 weeks old. The animals were killed by stunning and cervical dislocation. Care and use of the animals was in accordance with Schedule 1 of the Animals (Scientific Procedures) Act 1986.

1. The lungs (including the bronchus and trachea) were excised from a rat less than five minutes after death. No preservative was added so that no additional fluid would enter the lungs..
2. The bronchus was cut so that both bronchi were exposed. The pipette tip of a Gilson Pipetman P200 filled with 150µl of solution was placed inside the lumen of a bronchus. The bronchus was tied using a cable tie (Figure 2.22) and the pipette was used to introduce the solution into one half of the lungs. The soot solution consisted of 0.02g of soot (collected by glass plate from the smoke plume of an olive oil burning lamp) in 1ml of saline stock solution (0.9g sodium chloride in 100ml of distilled water). The clay solution of 5g of clay in 10ml of saline stock solution. These solutions were chosen as the optimum particle solutions for analysis by light microscopy. A control saline solution (100ml of distilled water and 0.9g sodium chloride) was also run to show any changes on the lung tissue caused by the intentional mummification process without particles.

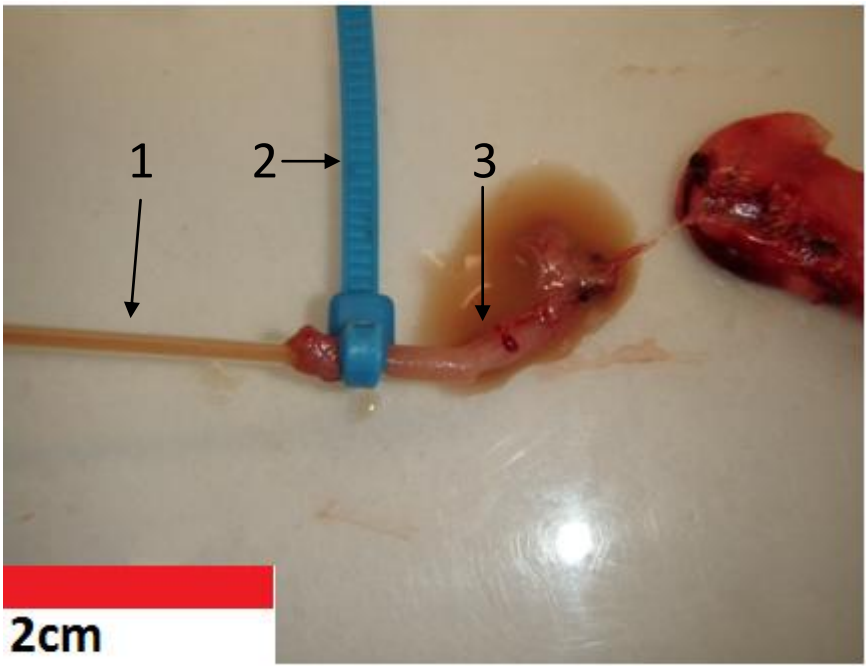

Figure 3.2 A pipette tip (1) that has been secured by a cable tie (2) to the bronchus of a rat lung (3). Unfortunately the bronchus has detached from the lung spilling the surrogate clay solution.

3. A glass pipette was heated over a Bunsen burner flame and then drawn out to produce a long thin tapered tip. This pipette was then inserted into the bronchus. The pipette bulb was lightly compressed fifty times to inflate and

deflate the lungs to imitate breathing. Care was taken not to pump the lung too hard and hence damage the alveoli. The left lung was insufflated first and the right lung second.

4. The lobes were then stored in 40% neutral buffered formalin solution prior to tissue processing. The lung were then weighed on a balance, placed in a Tupperware container onto a bed of artificial natron. The lungs were then fully covered with natron. The natron was made to the following formulation: 50% sodium carbonate, 30% sodium bicarbonate, 10% sodium chloride and 10% sodium sulphate (Currie, 2008). The amount of natron added was equal to ten times the weight of the lung.
5. The Tupperware containers were then covered with thin tissue paper (to act as a permeable membrane) and put into a food dehydrating oven at 40˚C which was judged to be an average ambient temperature for a *per nefer* (Marota et al, 2002).
6. The containers were left for 28 days which has been judged a sufficient time for mummification models (Currie, 2008; Abdel-Makhsoud et al, 2011). They were then removed from the oven, weighed, photographed and placed in a 1% sodium lauryl sulphate in formal saline rehydrating solution (with a ratio of 20mls to every gram of tissue) prior to tissue processing.

3.2.2 *Extraction of particles contained within lung tissue*

Papain method

Papain is a cysteine protease that is often used in laboratories and is an established technique for lung for tissue digestion (Vaccaro and Brody, 1979). It was used for this study due to its effectiveness and its optimum pH of 7 which would reduce any changes to particles during the extraction process. This method was used exclusively on lung tissue from rats which allowed the method to be refined and practiced before being employed on ancient tissue.

1) The left lobe of rat lung (typically weighing 0.3 to 0.4g) was cut and placed in a sample container. 20mls of 1% aqueous papain solution (for every gram of lung tissue) was then added to the container.
2) The container was placed in a 37˚C incubator and incubated for 48 hours.

3) After 48 hours, 1ml of 10% thymol solution (for evey gram of tissue) was added to the container. The container was then stored in a refrigerator at 4˚C.

Sonication method

Unfortunately, the papain method resulted in sample solutions being contaminated with bacteria, presumably due to the incubation period. The method of particle isolation used in this study was developed after an incident where an unstained section of lung tissue on a slide covered by a coverslip was ruptured and its contents spilt after making accidental contact with the bottom of a microscope lens. It was subsequently noted that mummified tissue is sufficiently weak that a little external pressure can break the tissue and release its contents. The extraction method for this study therefore uses sonication to physically remove the particles out of the tissue.

As each section of mummified lung contains tens of thousands of particles, five sections per extraction were judged adequate in order that mummified material was not wasted. Before the sections can be sonicated in a commercial ultrasonic cleaner, the embedding medium of paraffin wax has to be removed so xylene was therefore added prior to sonication. After undergoing sonication, the mummified tissue will have broken down and the contents released. The sample was then centrifuged to concentrate the soot and tissue into a pellet which allows the supernatant of xylene (with paraffin wax in solution) to be removed. A fresh wash of xylene was added to the eppendorf to remove any excess paraffin wax. It was then subject to a series of washes of xylene, followed by a graded series of industrial methylated spirits (IMS) until the pellet was transferred to distilled water. The pellet was sonicated during each wash to ensure that the soot particulates and tissue did not aggregate. Once the pellet is in distilled water, it was then placed in a refrigerator and stored at 10˚C. The substrate was then ready to be pippetted onto a substrate for further analysis.

1) A cassette of ancient lung tissue was removed from the freezer, any excess wax trimmed off and the cassette placed in a rotary microtome. The microtome was used to produce five 5μm thick slices of the sample.

2) The five tissue sections were then introduced into a 1.5ml eppendorf tube. The eppendorf was filled with 1ml of xylene and allowed to stand for 1 minute.
3) The eppendorf was then placed in a sonicator which was filled up with 30cm^3 of water. The eppendorf was then sonicated for 1 minute.
4) The eppendorf was then placed into a microcentrifuge (with a weighed counter-balance) and centrifuged at 1000g for 30 seconds.
5) The supernatant was carefully removed using a pipette and an additional 1ml of xylene added. The eppendorf was then sonicated again for 15 seconds, placed into a microcentrifuge and centrifuged at 1000g for 30 seconds.
6) The supernatant was carefully removed using a pipette and 1ml of industrial methylated spirits (IMS) added. The eppendorf was sonicated again for 15 seconds, then placed into a microcentrifuge and spun at 1000g for 30 seconds.
7) Step 6 was repeated; however after another cycle of sonication and centrifugation, distilled water was added to replace the IMS.
8) After a final cycle of sonication and centrifugation, the distilled water was removed by pipette and replaced by 1ml of distilled water. The contents of the original eppendorf were removed into a new labelled eppendorf and stored in a refrigerator at 4˚C.

3.3 Surrogate particle production

This study used modern surrogate soot as a comparison against the ancient soots. This comparison required the production of two types of surrogate soot: soot for size/shape analysis and soot for elemental analysis.

3.3.1 *Generation of particles for size/shape analysis*

There are many factors affecting the size and shape of soot produced by a flame. These factors include the diameter of the wick, temperature of the flame, diffusion rate of the fuel through the wick and availability of oxygen (see Introduction section 1.5.1). It was decided that the best approach was to attempt to combust the fuels as authentically as possible using modern lamps modelled after the ancient

Egyptian types, using double-twisted cotton wicks like those found at Amarna (see Introduction section 1.3.3). The fuels used in the experiment were obtained from commercial sources. The lamps for this study were provided by an outreach programme with Moseley Hollins High School. In this programme, Art students (taught by David Ingham) and Science students (taught by Andy Fenton) studied and produced facsimiles in clay or terracotta. The lamps the students produced were based on those found at Amarna and can be seen in Figure 3.3.

Figure 3.3 A clay lamp produced by students at Mossley Hollins High School to act as a burning vessel for this project (Author's own photo).

The method of producing and capturing the soot for this study is as follows. A lamp was filled with fuel and a double-twisted wick soaked in the fuel for an hour. This ensured the wick was impregnated with the fuel. The wick was then lit and allowed to burn for five minutes. A spray of water and detergent was sprayed across the top of the smoke plume and the spray captured in a container on the other side of the lamp. The spray when passing through the smoke plume captures the soot from the combustion process. The spray was passed as close to the top of the smoke plume as possible and care was taken not to extinguish the flame. A 2.5% solution of detergent sodium dodecyl sulphate (with distilled water) was used to ensure that the soot particles did not aggregate, nor that any fuel residues adhered to the soot. In the case of beeswax, it was not possible to use the lamp so a beeswax candle was made. The same protocol was carried out using the candle flame rather than a lamp flame. This method is diagrammatically represented in Figure 3.4.

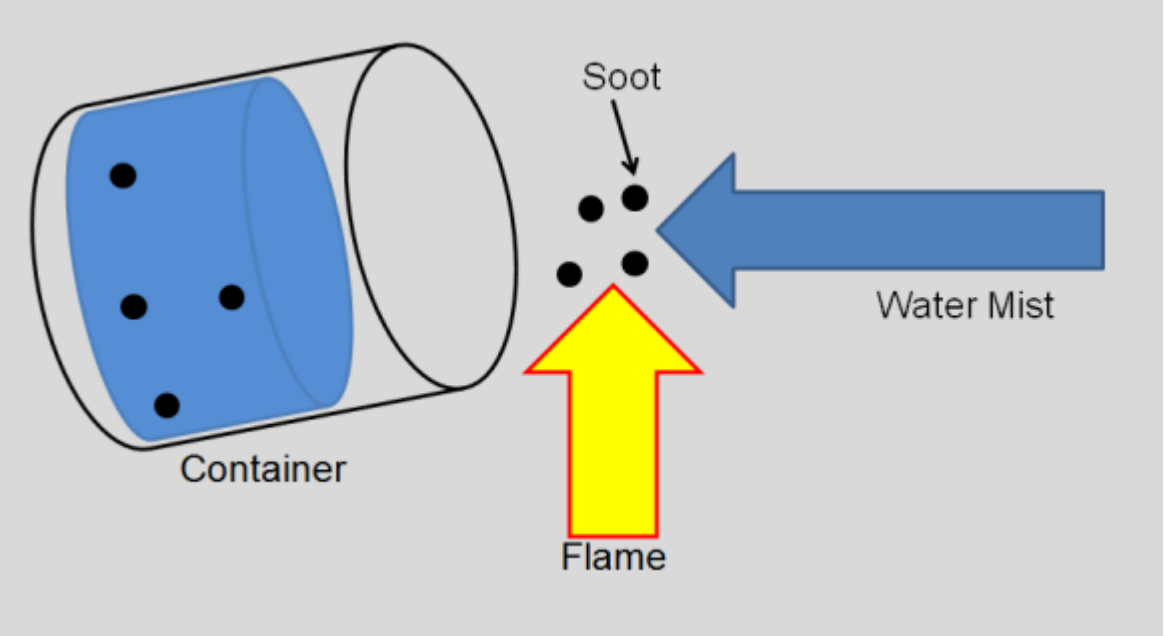

Figure 3.4 Diagram showing the method for producing soot particles for size/shape analysis. A spray of water mist is passed through the smoke plume of a burning lamp. Any soot produced by the flame, is captured by the spray, which itself is captured in a container**.**

After the soot had been collected, the soot suspension in water was decanted into a sterile flask and sealed. The suspension was allowed to sediment. Prior to analysis the flask was unsealed and placed at a 30 degree angle to aid collection. A pipette was introduced into the flask and used to pipette the soot suspension onto a microscope slide (for size/shape analysis using light microscopy) or a carbon tab (for scanning electron microscopy). For light microscopy slides, glycerol was used as the mounting medium as it is miscible with water (unlike XAM) and has a refractive index that renders soot more visible.

3.3.2 *Generation of particles for elemental analysis*

When soot particles produced by the size/shape analysis method were examined using EDAX for elemental analysis, it was found that they contained very high signals for sulphur and sodium. This contamination was found in all the samples examined and was determined to be a systematic contaminant caused by the detergent (sodium dodecyl sulphate) used in the water spray. It appears that this detergent adsorbed to the soot particles during the collection stage.
Therefore a new method was developed. Since the soot produced by this method is only to be used for bulk elemental analysis, the size and shape of the soot

particles produced does not matter. The method employed in this study for production of soot for elemental analysis therefore used a glass plate suspended over the smoke plume of a lamp flame to capture large amounts of soot. This soot is then scraped off using a scalpel and collected in an eppendorf tube. The soot created by this method is free from foreign contaminants and can be easily manipulated onto an ESEM carbon tab or other substrate for further analysis.

1) The fuel reservoir of a clay lamp was filled with the required fuel. A double-twisted wick was submerged in the fuel for an hour.
2) The wick was brought to the surface of the fuel and placed on the wick notch to the side of the lamps. Excess fuel was allowed to drain off for 10 minutes. The wick was then lit and allowed to burn for 5 minutes. For the beeswax candle, the candle was simply lit and left to burn for 5 minutes.
3) A glass plate was placed over the smoke plume and held there for 5 minutes.
4) The flame was extinguished and the glass plate placed soot-side up on the bench work surface. A scalpel was used to scrape the soot off the surface off the glass plate and into a labeled eppendorf.

3.3.3 *Phytolith production*

The modern phytoliths for this project were provided by dry ashing barley chaff. Dry ashing is a proven and common method for producing phytoliths for size and shape analysis and was chosen as its methodology closely resembles ancient Egyptian crop burning more than alternative methods, for example, acid extraction (Parr et al, 2001).

1) 500g of barley chaff was weighed out and placed in a clean barbeque. The barbeque was lit and allowed to burn for one hour.
2) The charred remains were collected and placed in a muffle furnace. The remains were ashed in the furnace at a temperature of 500˚C for three hours. This temperature is sufficient to remove most biological material but leave the phytoliths unaltered.
3) 0.5g of the ash was then transferred into a1.5ml eppendorf. 0.5ml of 10% HCl was added to the tube and allowed to stand for 5 minutes.

4) 1ml of distilled water was added and the eppendorf was spun at 1000g for 5 minutes. The supernatant was then discarded.
5) Step 4 was repeated three times.
6) The contents were then removed into a new labelled 1.5ml eppendorf.

3.3.4 *Particle/phytolith size and shape characterisation by light microscopy*

Particles were visualised using Leica RMDB light transmission microscope (Leica) at a magnification of 40x. An image-analysis software package Leica Quantimet (programmed by Leica and used at the University of Manchester) was used to analyse the images.

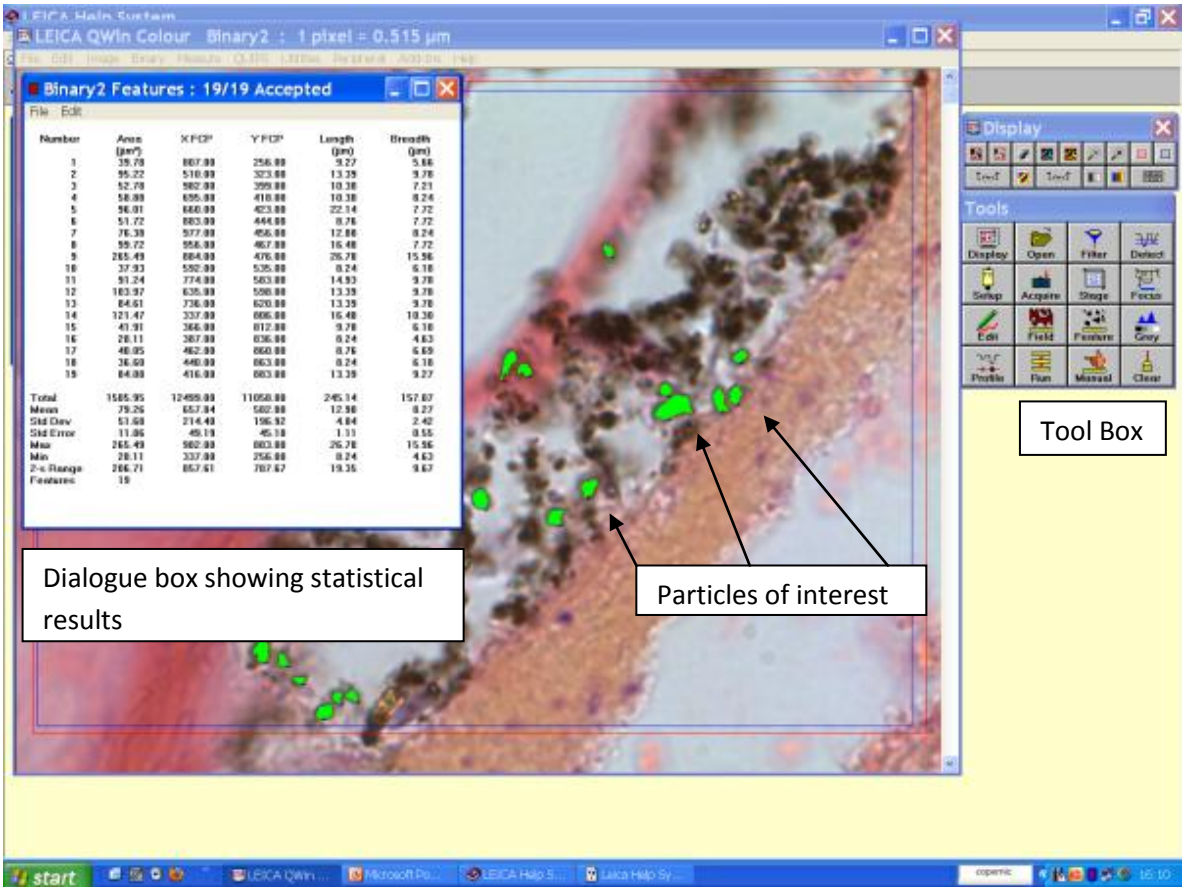

Figure 3.5 Image of Leica Quantimet. The background image consists of ancient lung tissue with dark anthracotic particles. The particles of interest are highlighted green and a dialogue box showing the statistical results of the analysis.

1) The slide was placed into the stage of a Leica RMDB light transmission microscope fitted with aDeltapix Infinity X digital camera and Leica

Quantimet image analysis software. The illumination was set to bright field and representative images of the whole sample were taken at X10 magnification. The illumination was changed to polarised light and the same images were captured again.

2) Images of particles were then taken using a 40x objective with bright field illumination. The same image fields were then captured again with polarised light. In total, 6 bright field and 6 polarised light images of particles were taken using a 40x objective.
3) The images were then imported into the Leica Quantimet image analysis software (figure 3.5). The image settings were set to 40x magnification and the particles were assigned a specific colour via the software tool box. Then the field measure option was used with the following parameters selected: length, breadth, area and roundness. All 6 bright field and all six polarized light images were processed in this manner. The microscope measures features using Feret diameters, also known as caliper diameters, which are defined as “the orthogonal distance between a pair of parallel tangents to the feature at the specified angle of the scan” (Leica, 1994). These can be seen diagrammatically in Figure 3.6. The features are defined as follows: length is “the length of the longest of the feret measurements”, and breadth is “the shortest of feret measurements”. The definition of roundness is “a dimensionless shape factor describing the circularity of a feature. A true circle would have a roundness of one (irrespective of size). All other objects will have a roundness of greater than one” (Leica, 1994).
4) Five different fields of the section (with at least 50 particles in them) were measured using the Quantimet software.
5) The produced data were imported into the Microsoft Excel 2007 spreadsheet package. The bright field data was used to provide a median of organic particles with a standard error of plus/minus one interquartile range (IQR). The polarised light data was used to provide a median of inorganic particles with a standard error of $\pm$ 1 IQR. These values were then analysed by the SPSS v16.0 statistical software package. The analysis included normality plots to assess the normality of the data and a Kruskal-Wallis test to demonstrate any significant differences between the lengths, breadths, areas and roundnesses of the different particles. A post-hoc test

consisting of a Mann-Whitney test with Bonferroni corrections was carried out to test the validity of the data.

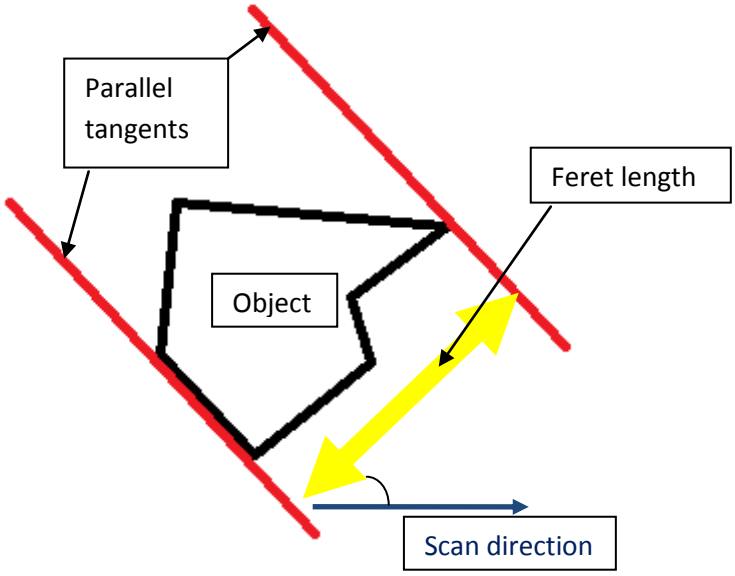

Figure 3.6 Diagram showing how feret diameters can measure the length of an object.

3.4 Electron microscopy and Elemental analysis

Scanning electron microscopy (SEM) was used to examine the surrogate soot, the modern sand and phytoliths, and the extracted and isolated ancient lung particles. A number of complementary analytical techniques were then used to examine the elemental composition of the internalised lung particulates, and to compare with the surrogate modern particulates. The advantages and limitations of each technique are described below.

3.4.1 *Environmental Scanning Electron Microscopy (ESEM)*

The principle behind this method has been previously discussed in Introduction section 1.5.6.

Procedure for ESEM samples

1) Analysis was carried out using a Phillips XL30 ESEM (Phillips, Aberdeen, Scotland) with standard Phillips ESEM software.

2) The specimen was examined at 200x 800x, 1600x and 3200x magnification at an acceleration voltage of 20 kV, a spot size of 4.0 and a chamber pressure of 1.0 Torr.

3.4.2 *Energy Dispersive X-ray Analysis (EDX)*

This study used EDX qualitatively and the principle behind this method has been previously discussed in Introduction section 1.5.7.

Procedure for EDX samples

1) Analysis was carried out using a Phillips XL30 ESEM (Phillips, Aberdeen, Scotland) with standard Phillips ESEM imaging software. The EDX software used was EDAX Genesis (Phillips, Aberdeen, Scotland).
2) The specimen was examined at an acceleration voltage of 20 kV and a spot size of 4.0 at a pressure of 1.0 Torr. Areas of interest were chosen in the imaging mode of the ESEM. The scanning mode was switched to “spot” only mode. The EDAX was then activated and ran for 100 seconds.
3) Ten EDAX spectra were recorded for each sample. These ten spectra were then imported into the Microsoft Excel 2007 spreadsheet package. The spectra were used to provide an average EDX spectrum of the examined particles with a standard error of ± SD.

Ten spectra were taken for each sample. This would typically consist of the spot analysis of ten different particles or features in the sample.

3.4.3 *Induction Coupled Plasma Mass Spectroscopy (ICP-MS)*

Induction Coupled Plasma Mass Spectroscopy (ICP-MS)

The principles behind ICP-MS have already been discussed in Introduction section 1.5.8.

Procedure for ICP-MS

1) Sample preparation was as follows; for the ancient tissue digests, a small piece of mummified tissue (weighing 0.03g) was digested in 2ml

concentrated Nitric acid with 0.5ml concentrated Perchloric acid. Samples were then heated to boil off the nitric acid and then the perchcloric acid was fumed at 200˚C for 30 minutes before cooling and making up to 15ml with distilled water. The mummified lung extracted particles were diluted to a concentration of 5% in Tetra Methyl Ammonium Hydroxide (TMAH) and Ethylene Diamine Tetra Acetic acid (EDTA) and made up to 15ml with distilled water. The TMAH/EDTA solution was prepared by diluting a 25% Tetra-Methyl-Ammonium-Hydroxide solution twenty-fold with water and the addition of 1g per litre of EDTA diammonium salt. For the surrogate fuels, 0.15g of fuel was extracted into 15ml of TMAH/EDTA solution. The surrogate soots and phytoliths sample were prepared by putting 0.05g of the sample into aqua-regia and they were made up to 25ml with distilled water.

2) The mass spectrometer was an Agilent HP 4500 ICP-MS (Agilent Technologies UK Ltd., Wokingham, England). The nebuliser gas was set to 1 litre per minute and the Argon plasma was set at a flow rate of 16 litres per minute.
3) The sample was introduced into the specimen chamber. As the sample was aerosolised and carried into the argon plasma, all selected elements were scanned for. This was carried out on five surrogate fuels, five surrogate fuels, six digestions of ancient lung material (including one control), six lung extracts and a sample of ashed phytoliths. The mass spectrum for all these samples were then recorded.

Laser-Ablative Induction Coupled Plasma Mass Spectroscopy (LA-ICP-MS)

LA-ICP-MS and the principles behind it have already been discussed in Introduction section 1.5.9.

Procedure for LA-ICP-MS

1) For the ancient tissues, a 20µm thick section of tissue was mounted onto a mylar slide using albumin. A 20µm thick section of tissue was chosen to provide a sufficient number of particles for analysis. The section was then

dewaxed using xylene. Samples of modern sand were mounted onto a mylar polymer slide using double-sided sticky tape. Mylar and sticky tape were used as they are invisible to the detector.

2) The start and finish points were drawn onto the mylar using a red pen. The mylar slide was introduced into the laser ablation chamber (New Wave RS UP 266 micron, UV laser, New Wave Research Co., Eynesbury, England). The laser was manually aimed at the start point and end point. The laser was set to 60% ablative energy (of a maximum 40 milli-Joules) with a spot size of 100µm. The laser was traversed across the sample at a scan speed of 40µm per second. The auxilliary gas used to introduce the ablated sample into the plasma was set to 1 litre per minute.
3) The mass spectrometer was an Agilent HP 4500 ICP-MS (Agilent Technologies UK Ltd., Wokingham, England. The nebuliser gas (used to create the plasma) was set to 1 litre per minute and the Argon plasma was set at a flow rate of 16 litres per minute.
4) As the laser ablated the sample the following ten elements were detected: aluminium, silicon, phosphorus, sulphur, boron, magnesium, calcium, mercury, gold, and lead. These elements were selected for the reasons described in the Introduction (section 1.5.8.). This was carried out on three ancient lung sections and five modern sand samples.
5) The mass spectrum for this sample was then recorded.

Electron Probe Micro-Analysis (EPMA)

The principles behind EPMA have been previously discussed in Introduction section 1.5.10.

1) A small piece of tissue was dehydrated and delipidised. This processing is necessary as water and lipids may impede the impregnation of the tissue by the mounting resin. The section was then mounted in London Resin White (hard grade, Agar Scientific, Stansted, United Kingdom) and polymerised for twenty-four hours at a temperature of 42˚C and a pressure of 2 bar (60 psi). The mounted tissue was then polished as the sample surface must be extremely smooth so that surface imperfections do not interfere with the surface/electron beam interactions. The resin block was polished roughly with

a Metaserv 200 and then hand-lapped with 1200 grit paste. The block's surface was brought to a fine polish using a Kent 3 polisher with 3 and 1µm diamond paste.

2) The EPMA instrument was a Cameca SX 100 (Acutance Scientific Ltd, Tunbridge Wells, United Kingdom) with Cameca signal processing software. The specimen was examined at an acceleration voltage set to 20 kV with a spot size of 4.0. The area for scanning was chosen as a 512 by 512 pixel box in imaging mode. Upon completion of the scan the signal processing software produces an elemental map of the sample.
3) The elements aluminium, silicon, calcium and phosphorus were chosen for the first scanning run. The elements iron, magnesium, lead and sulphur were chosen for the second run. Aluminium and silicon were chosen for their high affinity and the presence of alumino-silicates in the lung. Calcium and magnesium were chosen to show the presence of calcium carbonates and other common rocks, such as, gypsum. Phosphorus and sulphur can indicate the presence of sulphate or phosphate rocks. Iron has been chosen as haemosiderin (a storage complex of iron) can be an indicator of disease. Lead was chosen as an indicator of profession eg, presence of lead could suggest the individual worked with lead-based paints or objects.

3.5 Molecular analysis

3.5.1 *Fourier Transform InfraRed Spectroscopy (FT-IR)*

FTIR and the principles behind it have already been discussed in Introduction section 1.5.11.

Analysis of lung tissue

1) A 5 micron thick section of ancient tissue was floated transferred to a water bath at 37˚C to facilitate spreading of the sample and then floated onto the surface of a calcium fluoride disk. After drying on a hot plate at 50˚C for 20 minutes and a second at 70˚C for 15 minutes, the section was dewaxed and taken to water as outlined in section 3.5.

2) The mounting disk was placed onto the stage of a Hyperion 3000 light/IR microscope attached to a Bruker Optics Equinox 55 FTIR (Bruker Optics UK Ltd Coventry, UK) with Opus signal measuring software.
3) The microscope was aimed to a blank area of the disk, switched to IR mode and a background scan was created that was subtracted from subsequent scans of the tissue. The light microscope was used to visually identify areas of interest. The microscope was then switched to IR mode and 128 scans of a specified spot were carried out. The average of the 128 scans was then displayed on screen and saved.
4) Step 3 was repeated on 10 areas of each tissue, 10 areas of soot and 10 areas of soot and possible inorganic crystals.

Analysis of surrogate material

1) The ATR crystal was mounted in the central chamber of the FT-IR machine. The solid soot particles or 30µl of the solution of extracted ancient lung particles and distilled water were placed into the trough located just above the ATR crystal. Care was taken to ensure that the solid soot particles fully covered the ATR crystal.
2) The solid soot or extracted lung particle solution was then scanned 32 times. This step was repeated 2 more times. The sample was scanned three times

3.5.2 *Raman spectroscopy*

The principles behind Raman spectroscopy have already been discussed in Introduction section 1.5.12.

Analysis of ancient tissue sections

1) A 5 micron thick section of ancient tissue was transferred to a water bath at 37˚C and floated onto the surface of a calcium fluoride disk. After drying on a hot plate at 50˚C for 20 minutes and 70˚C for 15 minutes the section was then taken to water as outlined in section 3.5.

2) A suitable section of ancient tissue was chosen transferred to a calcium fluoride disk directly from the water-bath. The section was dewaxed and taken to water as outlined in section 3.5.
3) The disk was placed onto the stage of a Renishaw Raman microscope (Renishaw Plc. Old Town, Wotton-under-Edge, Gloucestershire, U.K.). The IR laser was set to use an excitation wavelength of 785 nm. The instrument was wavelength-calibrated with a silicon wafer focused under 50x objective lens and collected as a static spectrum centred at 521 cm^{-1} for 1 second.
4) The tissue section was viewed at 20x magnification. Areas of anthracotic pigment were selected and then focussed on at 50x magnification. The area was then probed with the laser (set at 785 nm) for 2 exposures of 30 seconds. An average of the two exposures was calculated and used to produce a Raman spectrum.

Analysis of surrogate material

1) For solid samples, for example, surrogate soot or sand, 0.5g of the specimen was placed into a 1ml vial shell. When examining liquid (fuel) samples, 0.5ml was placed into a 1ml vial shell.
2) The vial shell was placed into the stage of a Renishaw Raman microscope (Renishaw Plc, Wotton-under-Edge, Gloucestershire, U.K.). The IR laser was set to use an excitation wavelength of 785 nm. The instrument was wavelength-calibrated with a silicon wafer focused under the long distance 50x objective and collected as a static spectrum centred at 521 cm^{-1} for 1 second.
3) The specimen was focussed on at 50x and then probed by the laser. Solid samples were probed for five exposures of 12 seconds. Liquid samples were probed for six exposures of 10 seconds. Averages of these exposures were calculated and used to produce Raman spectra.

Chapter 4

Results

4.1 Surrogate particles

4.1.1 *Surrogate organic particles derived from the spray capture method*

Figure 4.1 shows a thinly spread suspension of surrogate soot particles from castor oil examined under the light microscope. The numerous soot particles in this representative image appear as rounded dark brown or black specks (red arrows) against a white background. The larger irregular-shaped particles are aggregate clumps composed of smaller pieces of soot (blue arrow).

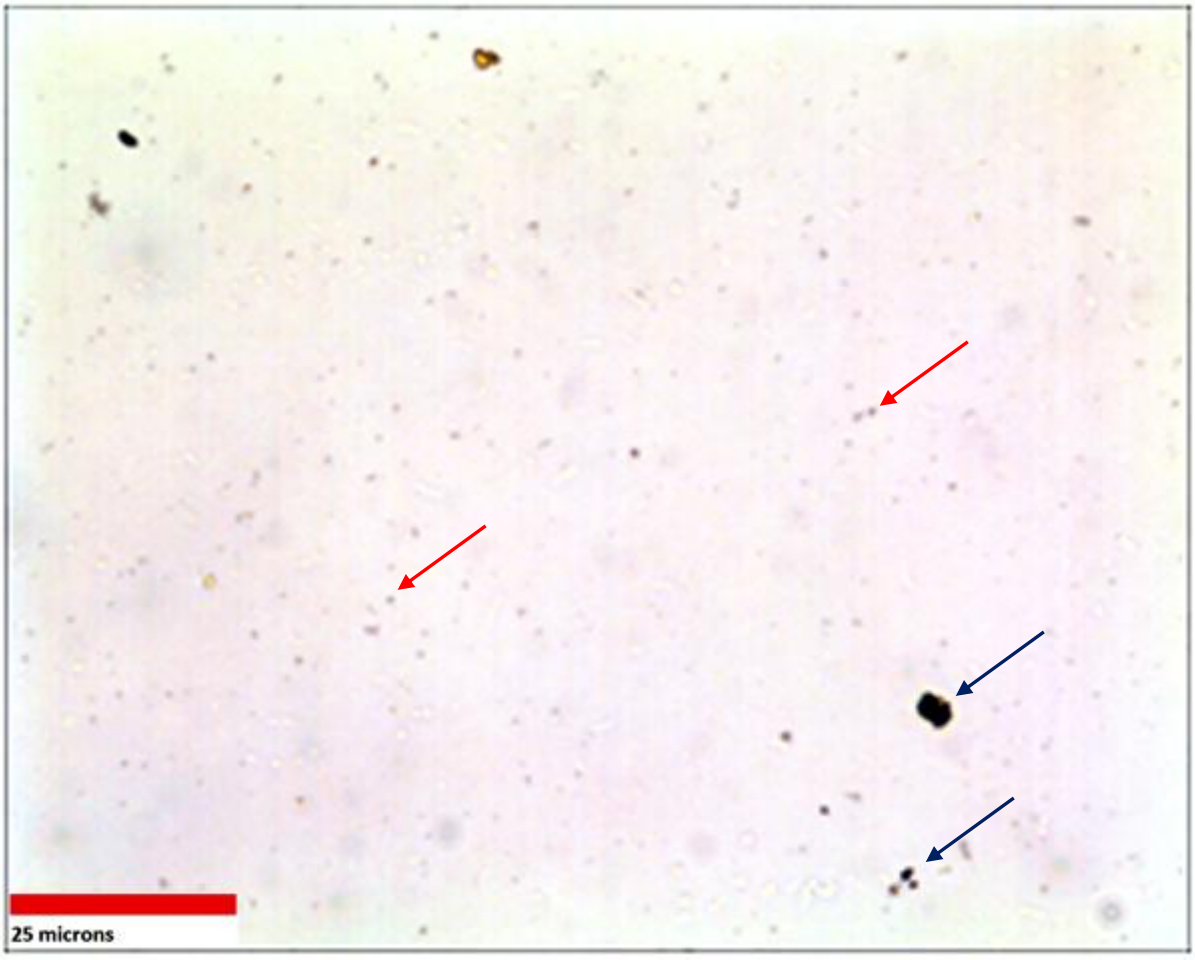

Figure 4.1 Light microscope image showing a suspension of castor oil soot consisting of individual soot particles (red arrows) and soot clumps (blue arrows).

Figure 4.2a, b, c, and d show the representative images of soot particles produced from the combustion of the remaining fuels - olive oil, palm oil, sesame oil and beeswax. The soot appears as dark brown or black specks on a white

background. Olive oil, sesame oil and beeswax have the largest number of large aggregates; castor oil has fewer aggregates whereas palm oil appears to have a noticeably lower numbers of aggregated particles.

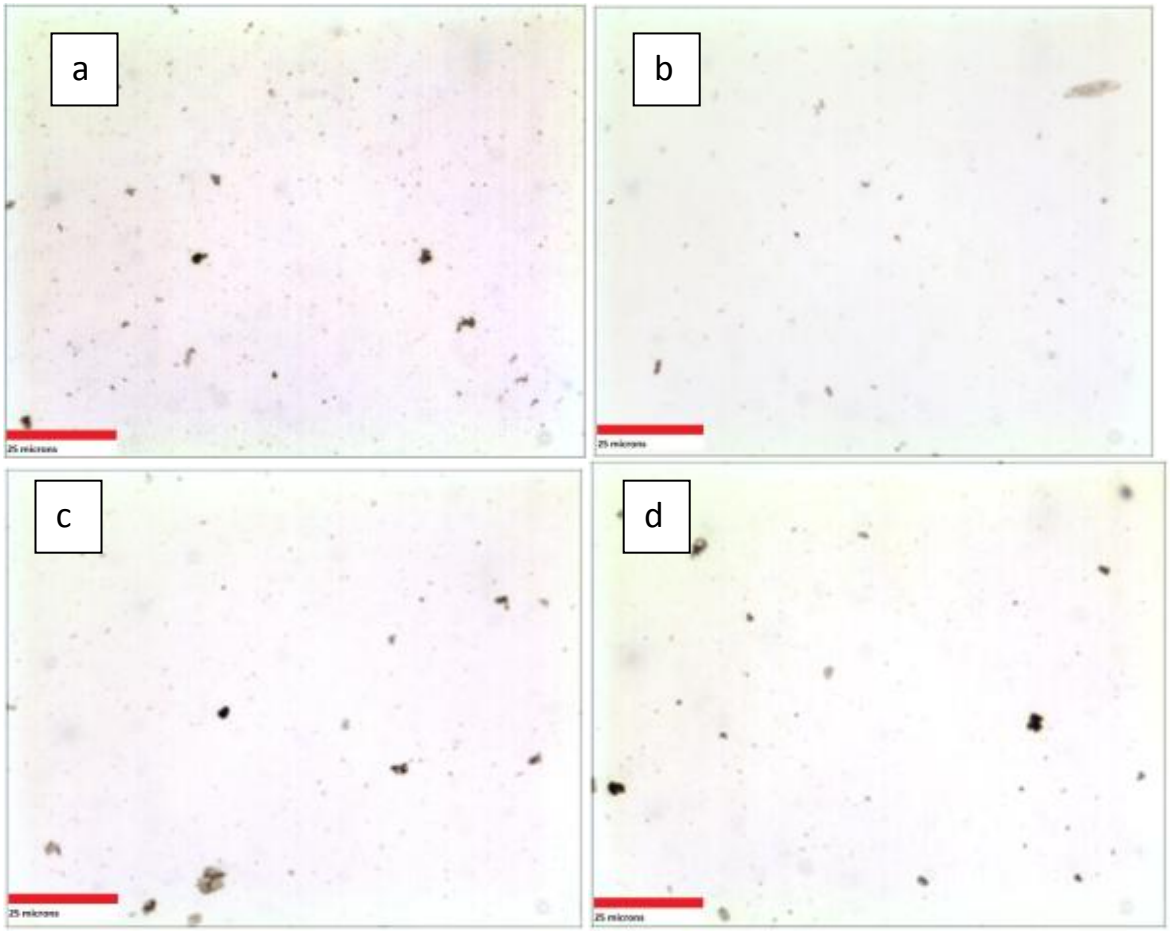

Figure 4.2. Light micrograph of soot particles arising from combustion of olive oil (a), palm oil (b), sesame oil (c) and beeswax (d). Scale bar = 25 microns.

It is apparent that the spray capture method is effective at collecting the particulates generated from the combustion of the surrogate fuels presumed to have been used and, hence, inhaled by the ancient Egyptians.

4.1.2 *Surrogate inorganic particles*

Here the aim was to differentiate the different types of sand grains of sizes likely to be inhaled using light microscopy, and hence to decide whether it was worthwhile attempting to characterise them further, and to distinguish similar particulates *in vitro* and *in vivo* from ancient material.

Sands from Egypt

Amarna

Figure 4.3 shows a suspension of sand from Amarna in glycerin and examined with a light microscope. The sand grains in this representative image appear to be of two different varieties; a light translucent colour (indicated by purple arrows) and a darker colour (indicated by red arrows). Both types of grains appear angular. Glycerin was used as the mounting medium as its refractive index enhanced contrast when viewing the sand grains.

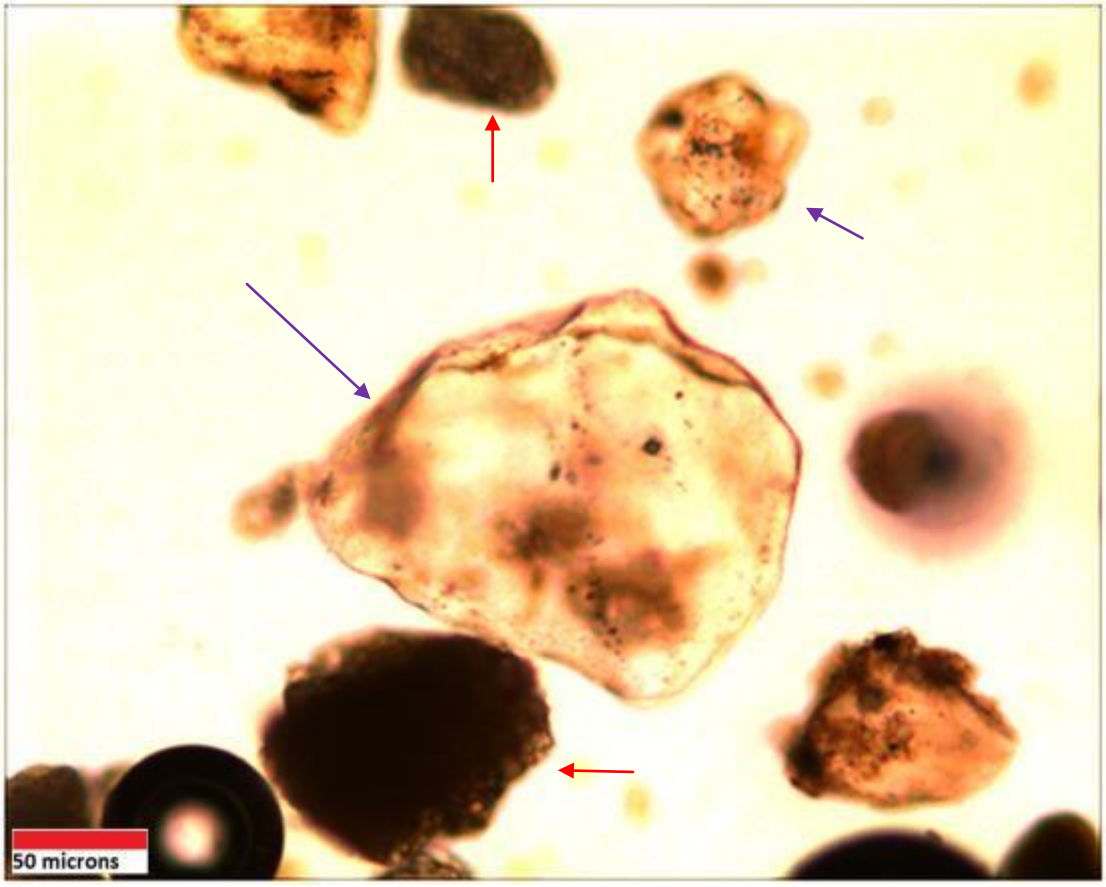

Figure 4.3: The appearance of sand from Amarna suspended in glycerin and examined with a light microscope. Two types of grain are visible in this representative image; a dark coloured grain and a light coloured grain.

Amarna North Palace, Beni Hassan and Karnak

Figure 4.4a, b, and c show suspensions of sand from Amarna North Palace, Beni Hassan and Karnak respectively in glycerin and examined with a light microscope. As expected, these samples appear to be mixtures of three different varieties of

sand grains; a light translucent colour (indicated by green arrows) and a brown colour (indicated by blue arrows) and a third black colour (indicated by red). All three types of grains appear angular and these images are representative of each sample of sand. Figure 4.4d shows a representative sample of sand from Tuna Al Gebel, again suspended in glycerine. The sand grains are large compared to the other sites and consist of two types: a translucent grain (indicated by a black arrow) and a milky-looking grain (indicated by a brown arrow).

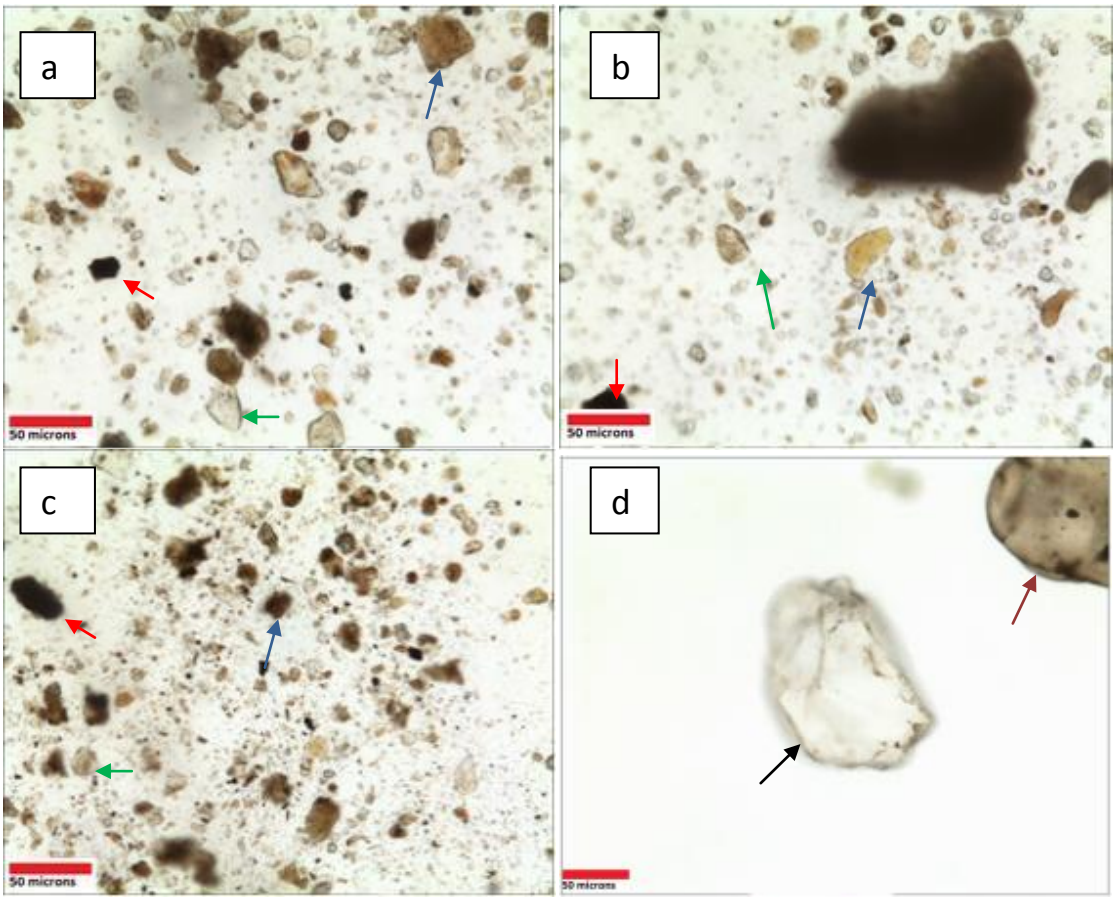

Figure 4.4 Representative images of sands from Amarna north palace (a), Beni Hassan (b), Karnak (c) and Tuna Al Gebel (d). All these sands were suspended in glycerin and examined with a light microscope. Scale bars are 50 microns.

Mud Brick

Figure 4.5a, b and c show suspensions of mud brick dust the Amarna North Palace bricks 1 and 2 and from the region of the Dahshur pyramid, respectively, and some difference are apparent. The particles were mounted in glycerin and examined with a light microscope. The Amarna North Palace samples appear to

be mixtures of three different varieties of sand grains; a light translucent colour (indicated by green arrows) and a brown colour (indicated by blue arrows) and a third black colour (indicated by red). All three types of grains appear angular and these images are representative of the whole sample. The Dahshur pyramid mud brick appears to consist of only two types of grain: a translucent grain (purple) and a dark grain (yellow).

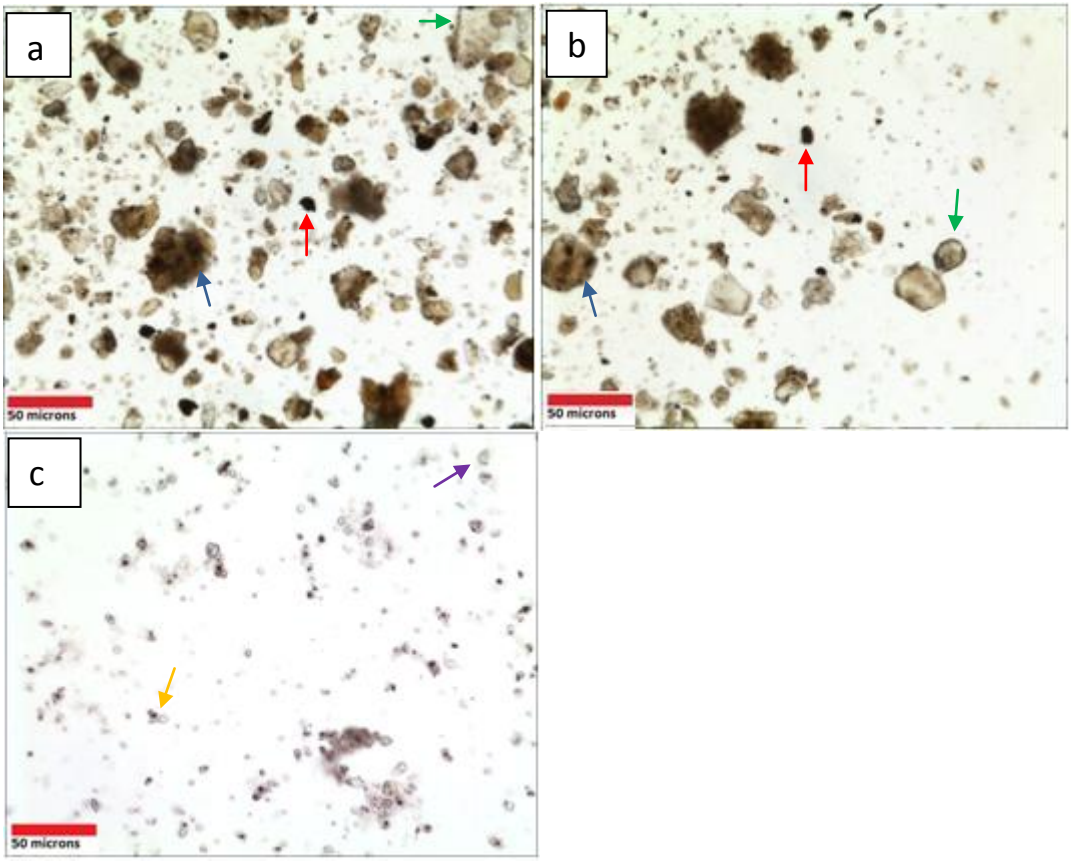

Figure 4.5 Representative images of mud bricks from Amarna North Palace mud brick 1 (a), Amarna North Palace mud brick 2 (b) and the Dahshur pyramid (c). Scale bars are 50 microns.

Phytoliths

A birefringent phytolith (1) visualised with polarised light (see Introduction section 1.3.4) can be seen against a dark background in Figure 4.6a. Phytoliths cannot be visualised easily using bright field illumination. Other remnants from the barley chaff that have also survived acid washing and high temperatures; for example, a sieve tube element (2) can be seen. The same field can be imaged using a quarter wave plate (figure 4.6b) which reveals the phytoliths to be positively birefringent.

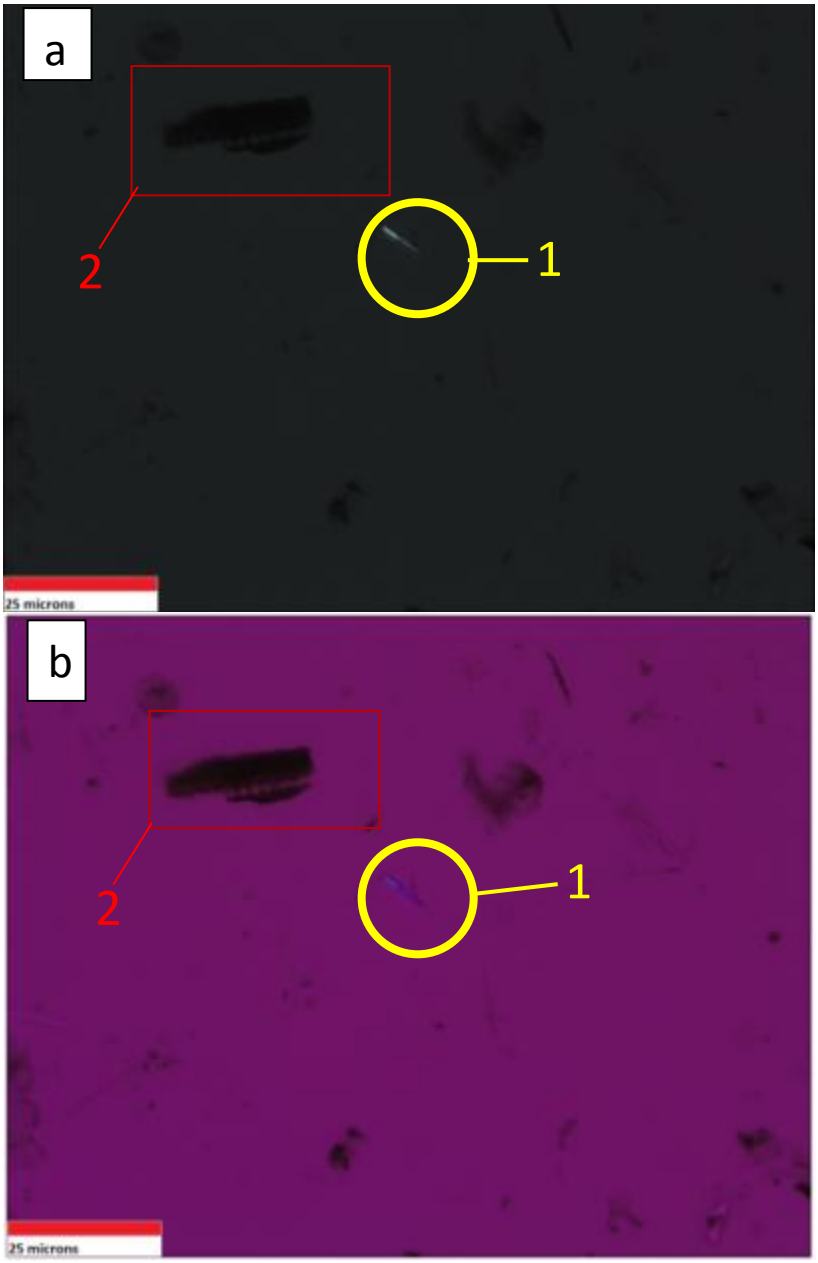

Figure 4.6 (a) Image of a birefringent phytolith (1) imaged with polarised light and (b) viewed with ¼ wave plate analysis. Plant remains such as a sieve tube (2) can also be seen in (a) and (b). The phytolith (1) can be seen to be positively birefringent blue object in (b). Scales bars are 25 microns.

4.2 Biological Rat lung model

This study employed a biological model using the rat to attempt to assess any physical or chemical changes that organic or inorganic particles could undergo during the intentional mummification process. A pair of rat lungs, insufflated with surrogate particles, was mummified for 28 days in artificial natron. After the 28 days, it was rehydrated, processed and examined histologically.

4.2.1 *Weight reduction*

When the rat lungs were mummified, they underwent a weight change with between 68 and 77% loss in weight following mummification with natron for 28 days. This weight change was proportional to the amount of water lost and demonstrated the efficacy of the method (Table 4.1). As expected, there was no difference in weight change resulting from insufflation of the lungs with surrogate particles

Table 4.1 The percentage loss in weight of rat lungs as a result of being mummified in artificial natron for 28 days.

Rat lung sample treatment	Pre-mummification Weight (g)	Post-mummification Weight (g)	Weight Change (%)
Clay 1	1.06	0.34	68%
Clay 2	1.27	0.35	72%
Soot 1	1.2	0.27	77%
Soot 2	1.36	0.33	76%
Control 1	1.38	0.41	70%
Control 2	1.18	0.28	76%

4.2.2 *Histology*

A representative image of rehydrated control rat lung tissue stained with Toluidine Blue (TB) is shown in figure 4.7. Alveoli and regular lung structure can be seen (1) along with areas of damaged tissue where it appears the alveoli have burst (2). These damaged areas are indicative of pressure-induced emphysema and most likely happened post-mortem during the insufflation process. It is possible that these areas of alveolar damage could be alveolar ducts (areas where the terminal bronchioles become alveoli and typical alveolar features are sparse). Partially stained mucus can be also seen (3) which would suggest an immune response was occurring in the rat just prior to death. Another possible explanation for the

areas of inflammation is that they are type II alveolar cells that were in the process of secreting surfactant.

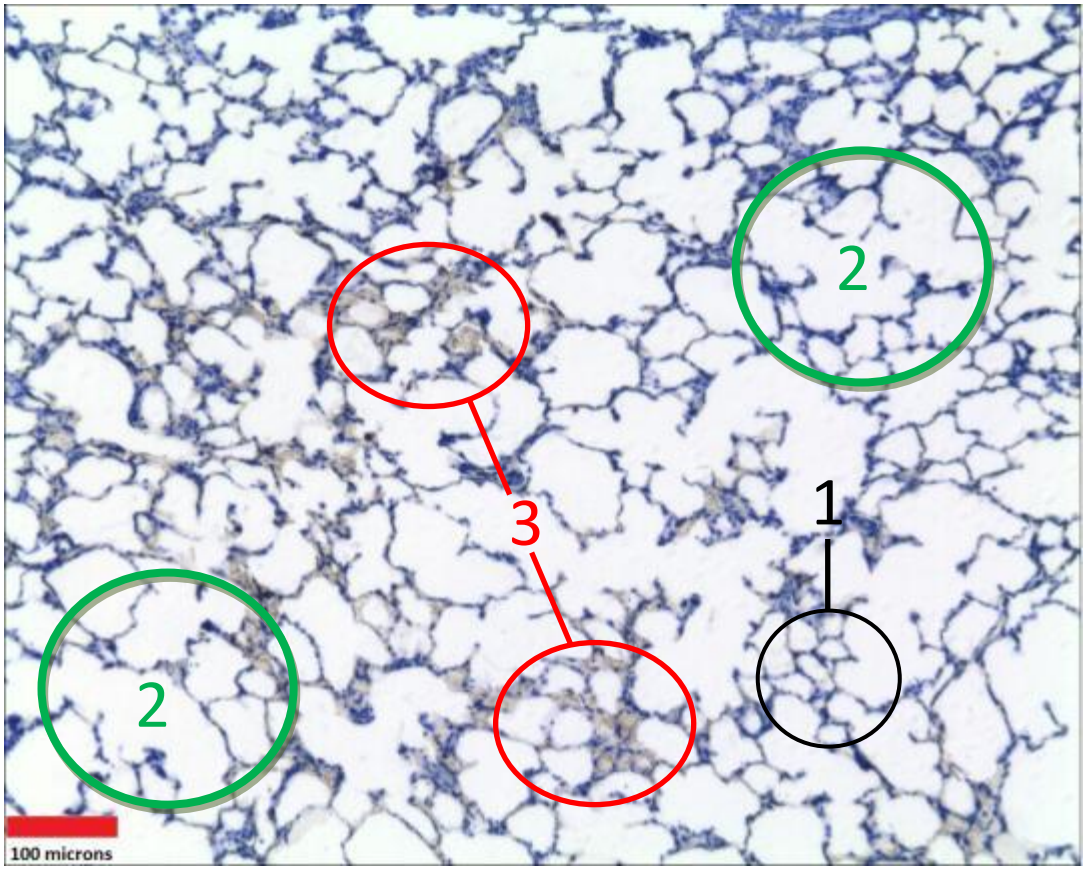

Figure 4.7 Representative image of rehydrated control rat lung tissue (TB). Normal lung structure (1) is present along with damaged areas/alveolar ducts (2) and areas with partially stained mucus or surfactant (3). Scale bar = 100 microns.

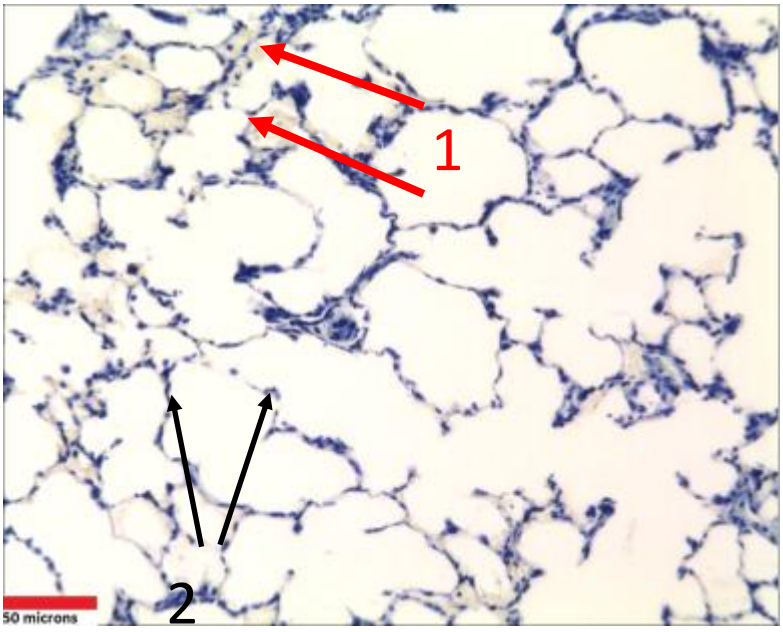

Figure 3.8 Control rat lung tissue showing mucus (2) and inflammatory cells (1). It is possible that these are type II cells (1) secreting surfactant (2).

When the same area is viewed at higher magnification, blue stained inflammatory cells (1) can be seen in the partially stained mucus (2). Scale bar = 50 microns.

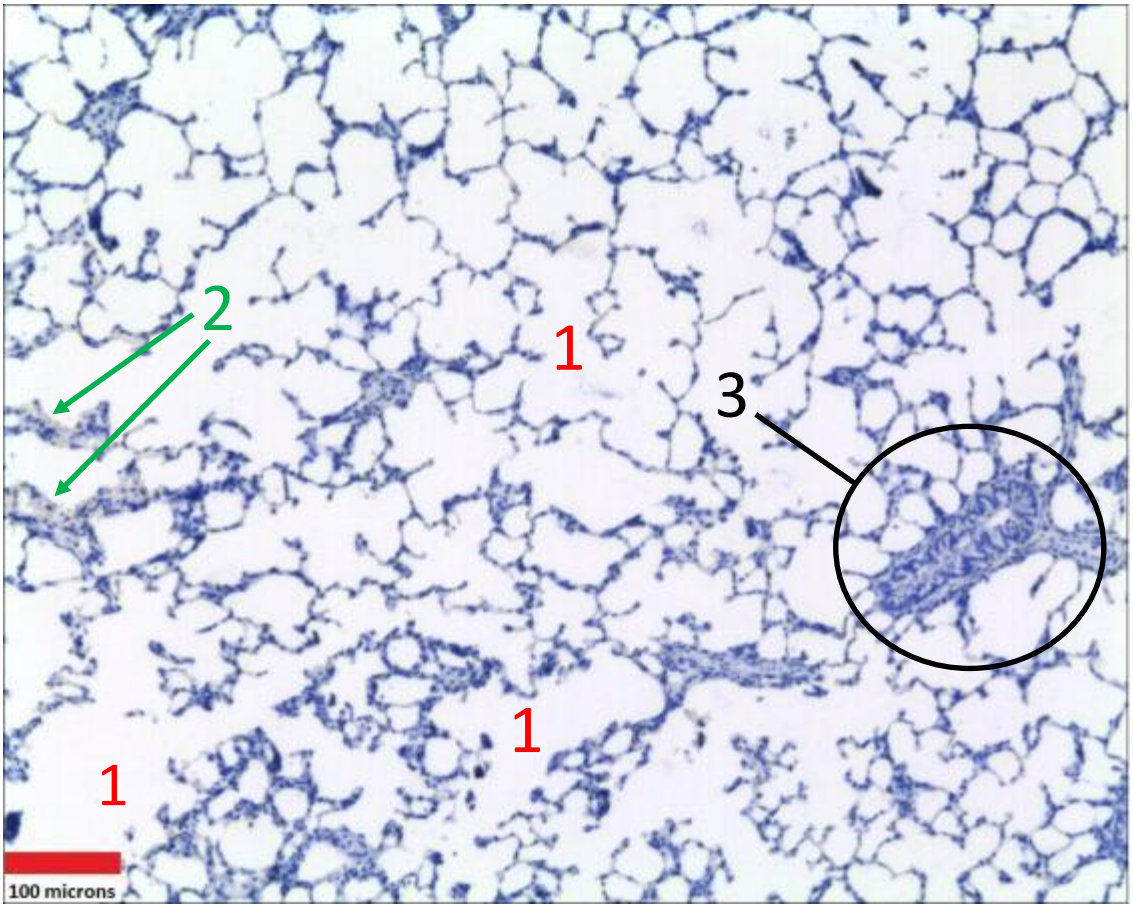

Figure 4.9 Rat lung tissue insufflated with soot solution (TB). Areas of lung damage can be seen (1) along with signs of inflammation/surfactant (2) and a bronchiole (3). No soot particles are visible.

Figure 4.9 shows a section of rehydrated section of rat lung that was insufflated with surrogate soot solution. No soot particles can be seen in this or other sections however. Alveolar ducts or areas of alveolar damage from pressure-induced emphysema (1) and areas of inflammation or surfactant (2) are present. Additionally, a dendritic bronchiole can be seen in this particular section (3).

A section of rehydrated rat lung, that was insufflated with surrogate inorganic particles, is presented after staining with Toluidine Blue in figure 4.10. No surrogate inorganic particles are visible. Very little intact alveoli can be seen however, bronchioles (1) and an arteriole (2) along with pressure induced

emphysema (3) are present. An immune reaction (indicated by blue-stained inflammatory cells) is also present near the arteriole and bronchioles (4).

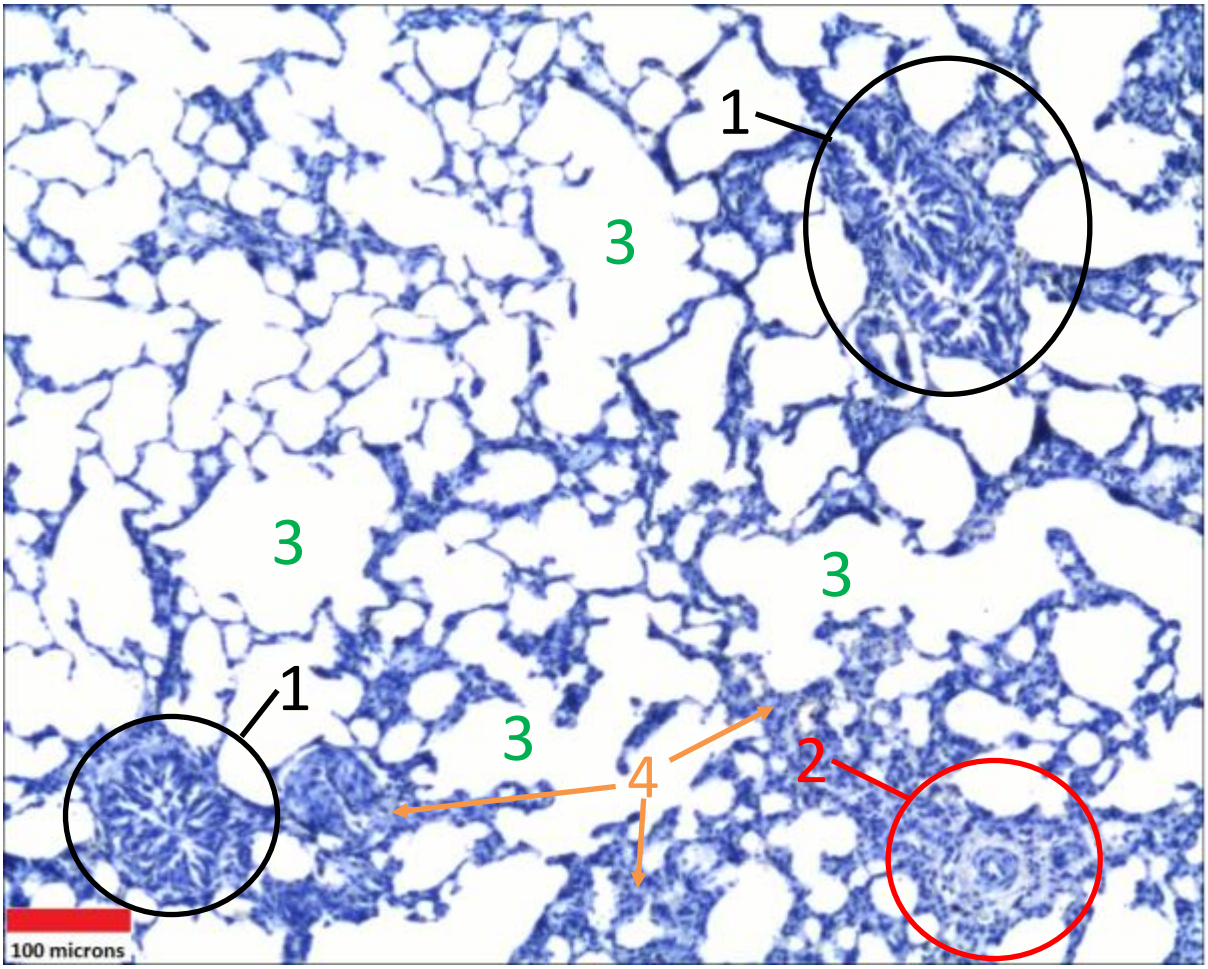

Figure 4.10 Rat lung tissue insufflated with surrogate inorganic particles (TB). No surrogate inorganic particles can be seen. Areas of damaged alveoli (3) along with bronchioles (1), arterioles (2) and inflammatory/type II cells (4) can be seen.

4.3 Ancient Tissue

4.3.1 *Histological examination of ancient lung material*

Kulubnarti material

Sample S82

Figure 4.11 shows a representative section of S82 stained with Toluidine Blue (TB). There is no identifiable tissue in the section apart from a few semi-continuous circular tube-like structures (1). Examination of these structures at

higher magnification reveals them to be plant sieve tubes (in a longitudinal view) and could be either xylem or phloem (1). The red lines indicate the general length and direction of the tubes. The rest of the material in the section appears as large darkly stained objects (2) or badly degraded tissue with little or no distinctive morphology. There appears to be no lung in this sample.

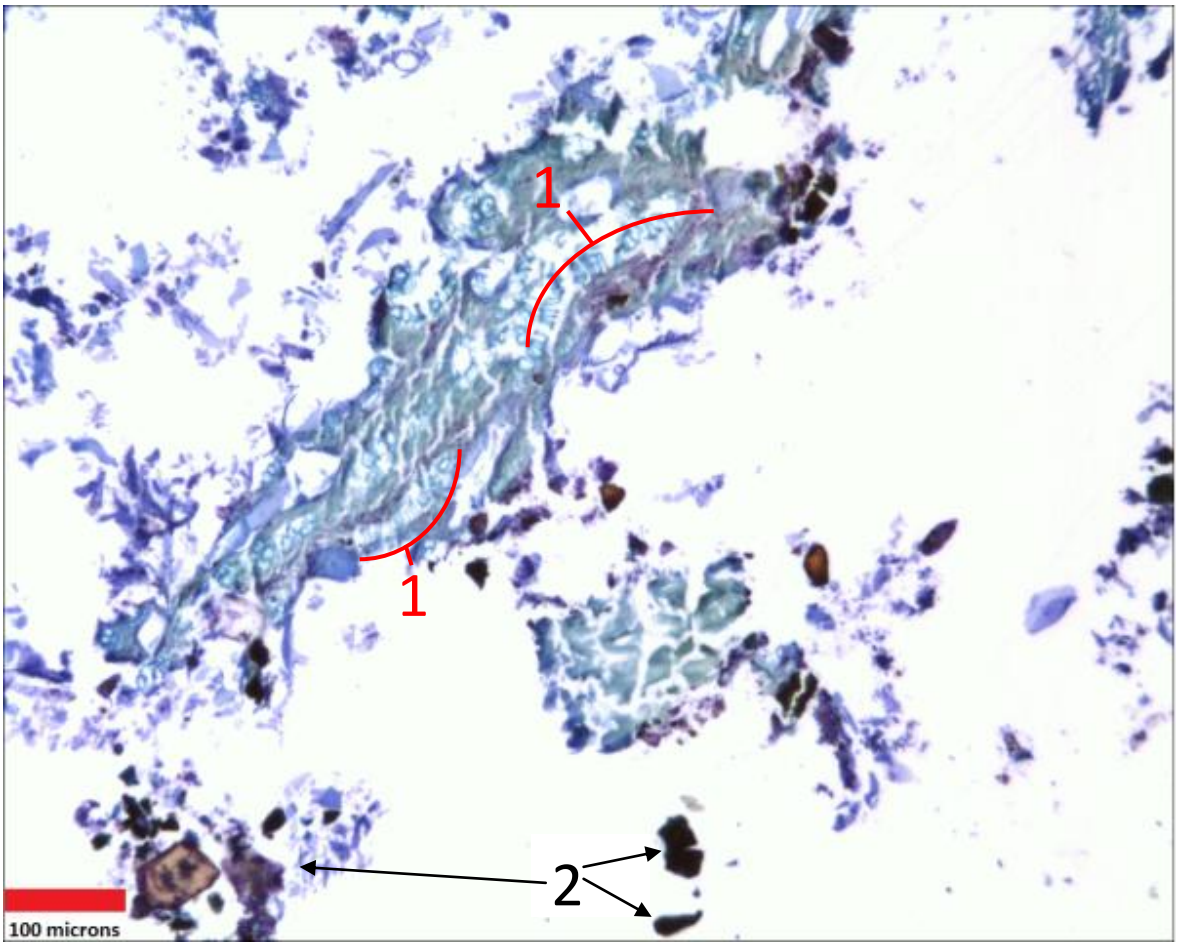

Figure 4.11 Representative image of material from mummy S82 (TB) showing plant (1) and dark-stained objects (2).

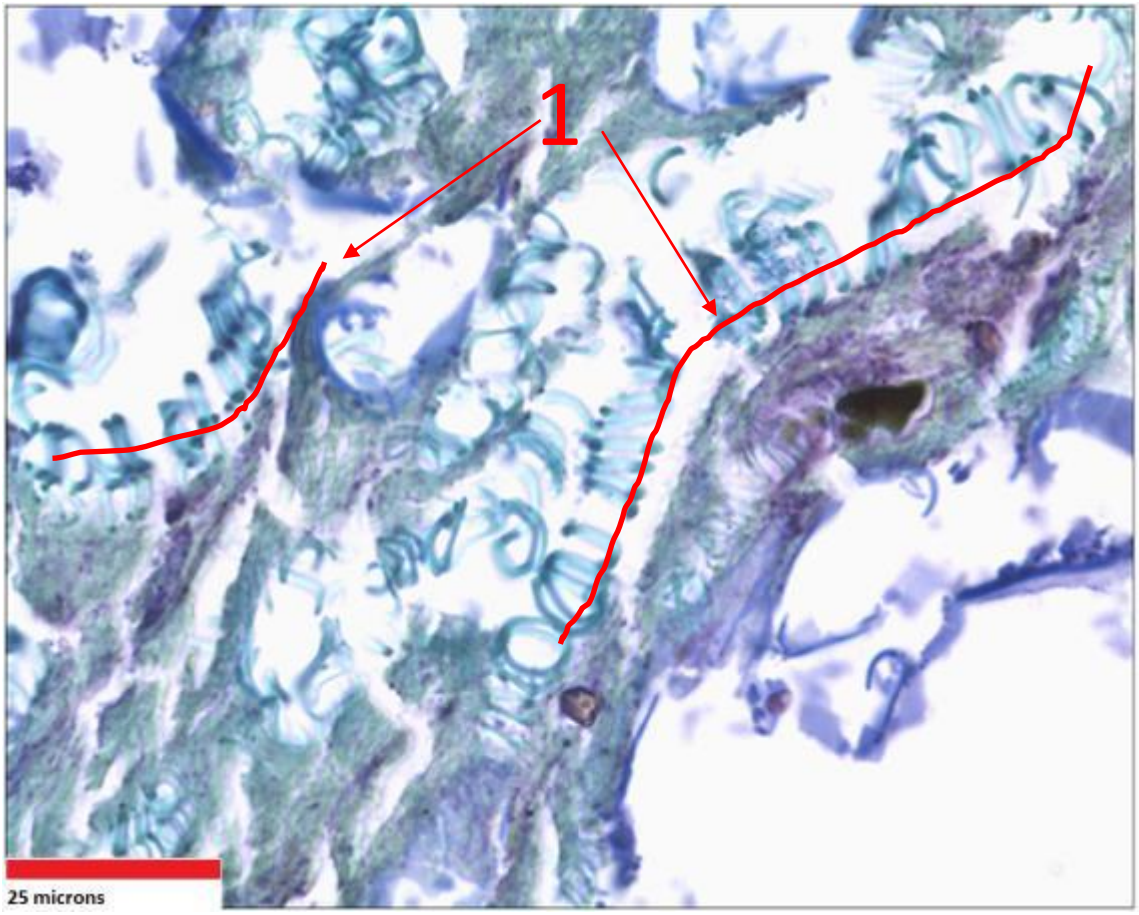

Figure 4.12 Badly degraded tissue with plant sieve tubes and segments (1) in material from mummy S82 (TB).

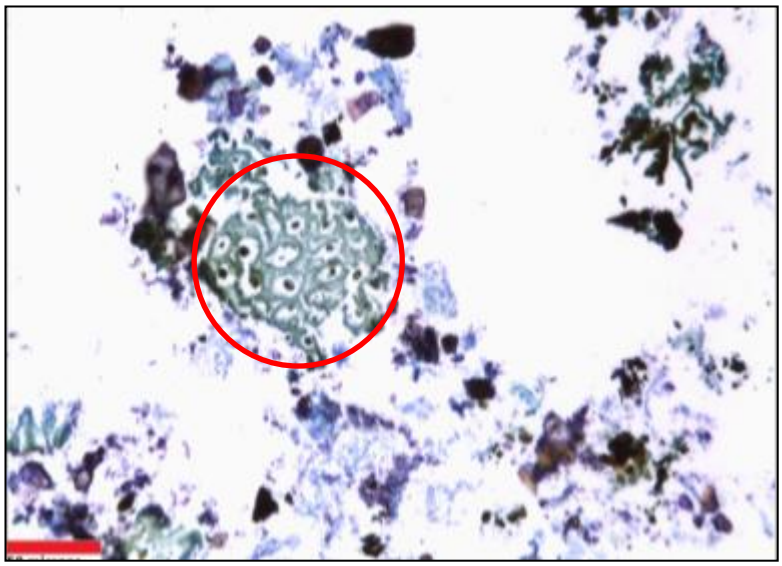

Figure 4.13 An area of plant sieve tubes (circled red) in material from S82 (TB). Scale bar = 50 microns.

Another area of plant material (circled red) surrounded by detritus and unidentifiable material can be seen in figure 4.13. This material could be the same plant sieve tube but viewed at a transverse angle. Given the plant material and unidentifiable matter present, the sample could be mummified excreta, also called coprolite.

Sample S85

Figure 4.14 shows the general architecture of sample S85. There is no identifiable tissue apart from some plant sieve tube sections (1).

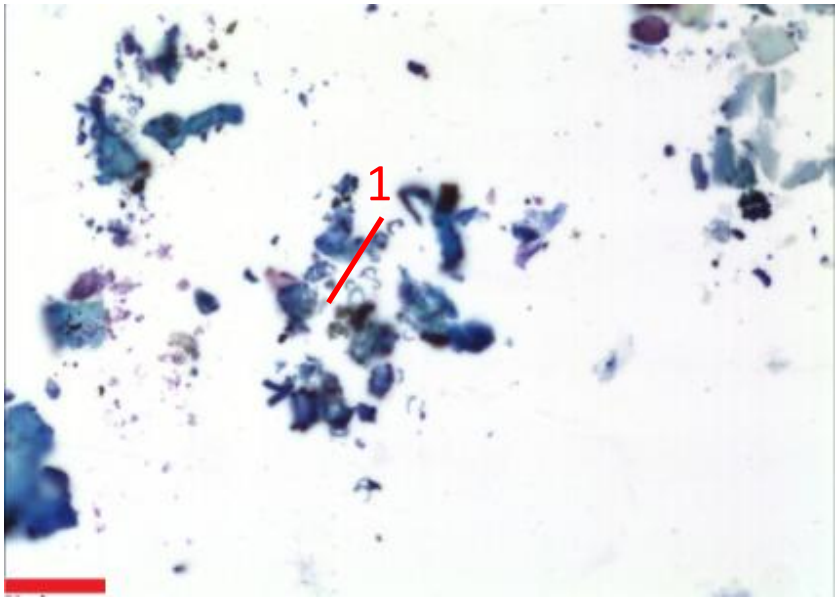

Figure 4.14 Plant tube section in material from S85 (1) (TB). The rest of the material is unidentifiable. Scale bar = 50 microns.

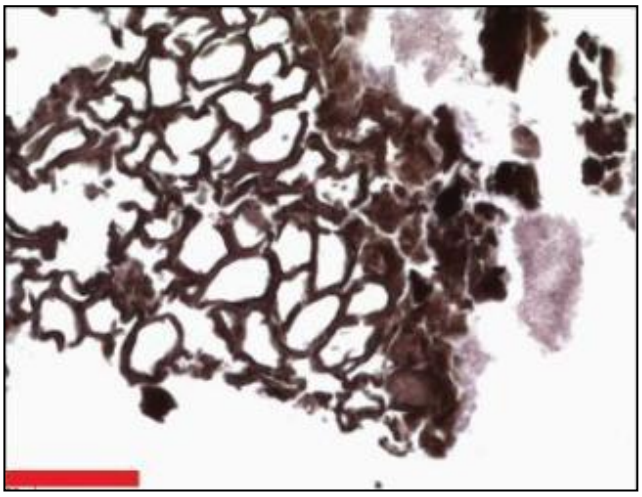

Figure 4.15 Plant material in material from S85 (H+E). Scale bar = 50 microns

Further plant material can be seen (with a hexagonal style arrangement) stained red by H+E in figure 4.15. The presence of badly degraded, unidentified material along with plant material would suggest this sample is coprolite.

Sample S195

Figure 4.16a shows a representative image of mummy S195 stained with TB and viewed with bright field illumination. All the material is unidentifiable apart from some possible plant material (arrows). When the same field is examined with polarised light, the plant material is revealed to be birefringent. This sample is once again probably coprolite.

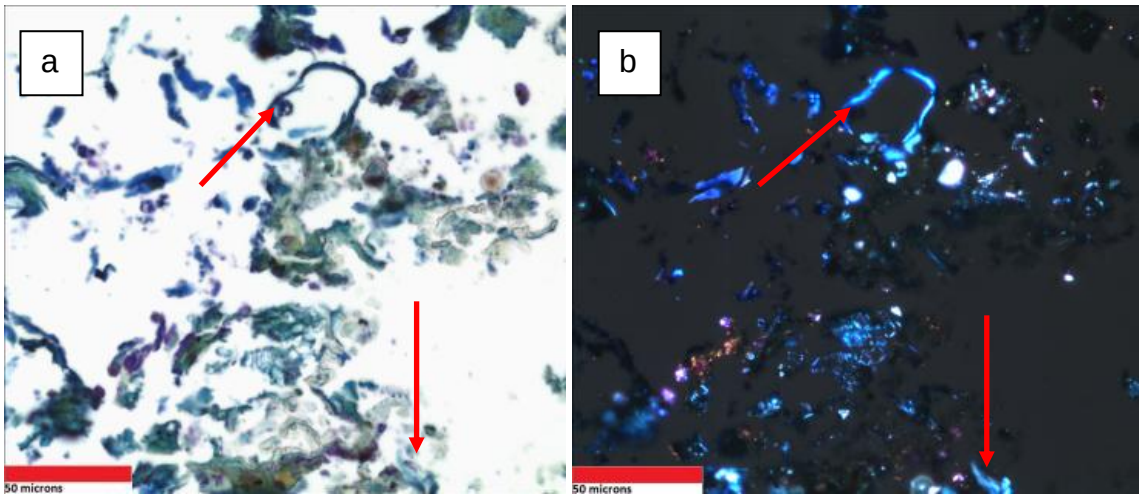

Figure 4.16 Representative image of material from S95 showing possible plant remains (arrows) with unidentified material (TB) under bright field illumination (a) and with polarised light (b). Scale bars = 50 microns

Dakhleh Oasis

Sample DO 45

Figure 4.17 shows a section of tissue from mummy DO45 stained with Miller's Elastic stain (M). The background consists of compacted lung tissue stained pink, with the elastic components stained purple. Dark deposits of anthracotic pigment (1) can be seen along with elastic tissue whose configuration suggests it may have been a larger vessel or bronchiole (2). There appear to be tears throughout the

lung tissue which are not necessarily indicative of the state of preservation but could have arisen from the sectioning of the wax block.

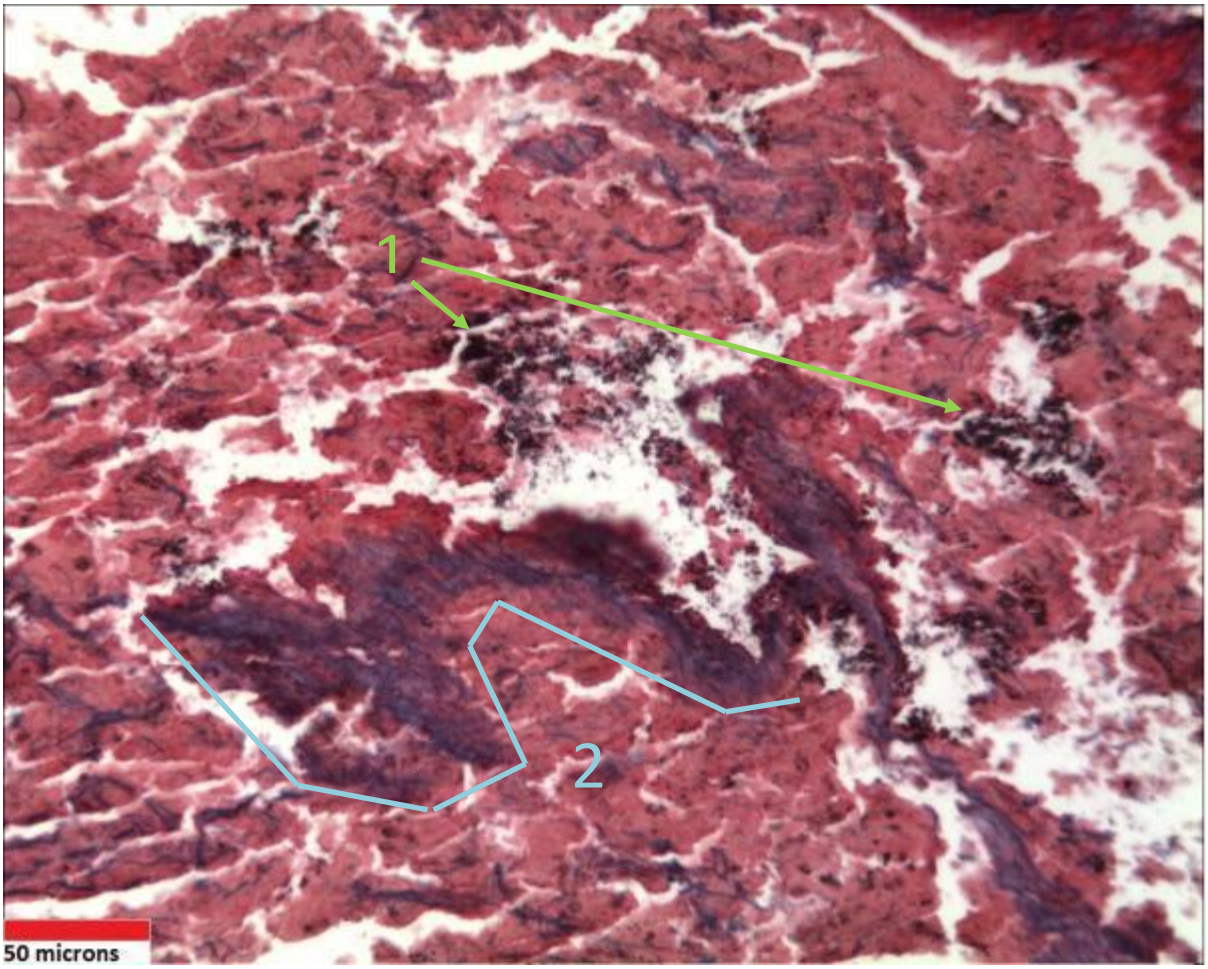

Figure 4.17 Image of DO45 (M) showing a pink background of compacted lung tissue with deposits of anthracotic pigment (1) and elastic tissue stained purple (2).

The dark anthracotic deposits are displayed at a higher magnification in figure 4.18. The deposits appear to be aggregates of individual particles (1) of dark pigment. There are areas of purple metachromasia in-between the individual particles of the larger deposits (2). This may indicate that there are particles of different charge and properties contained in the deposits. Additionally, a fungal body along with debris can be seen in the space between the areas of tissue (3).

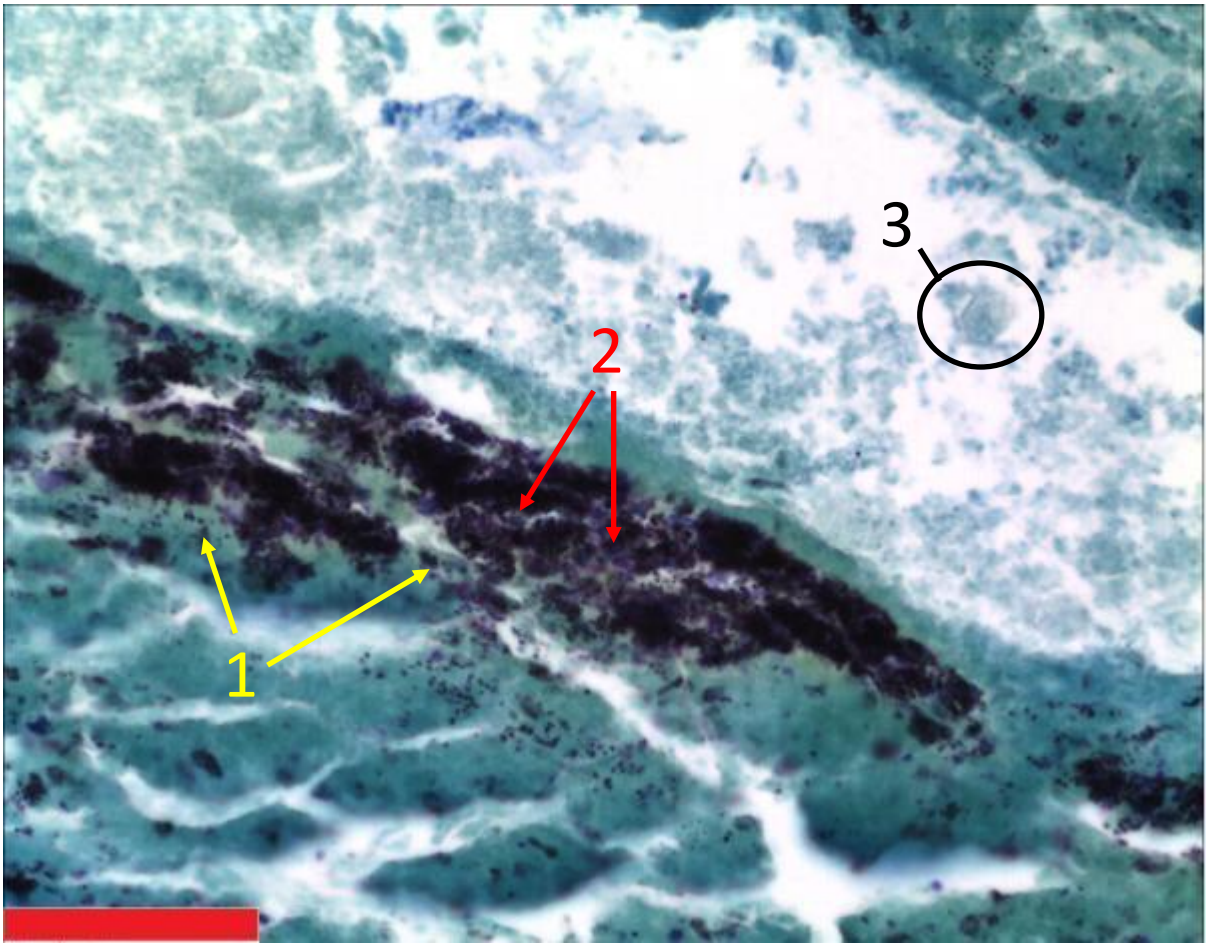

Figure 4.18 DO45 (TB) showing deposits of anthracotic pigment which are composed of smaller individual particles (1). Metachromasia (2) and a fungal spore (3) can also be seen. Scale bar = 50 microns.

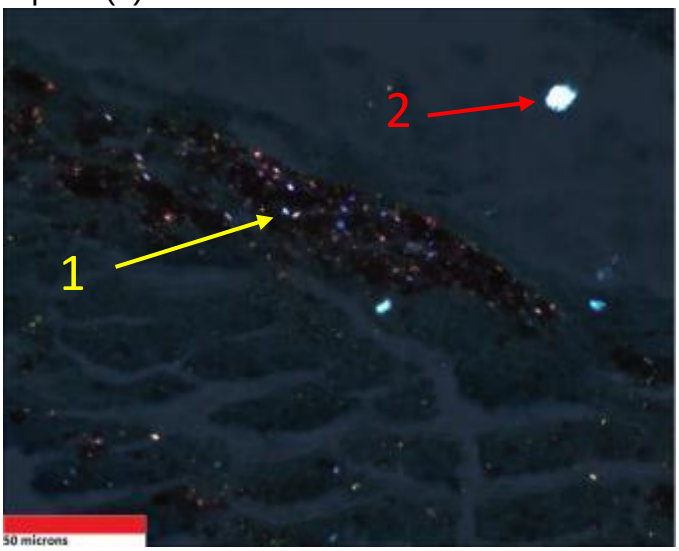

Figure 4.19 DO45 (TB, polarised) showing inorganic particles (1) and a fungal body (2). Scale bar = 50 microns

When the same field is examined with polarised light (figure 4.19), the metachromatic areas of the deposit are revealed to contain birefringent inorganic particles co-deposited with the anthracotic pigment (1). The fungal spore is also birefringent (2).

Figure 4.20a shows further deposits of anthracotic pigment in lung tissue from DO45 stained with H+E. The deposits appear as dark clumps of pigment (1) against a pink background of compacted lung tissue. When the same field is viewed in figure 4.20b with quarter wave plate analysis, birefringent particles (glowing blue and yellow depending on their orientation) are revealed to be co-deposited in the central deposit. The central particle (2) is positively birefringent (yellow) while the other blue particles (3) are negatively birefringent.

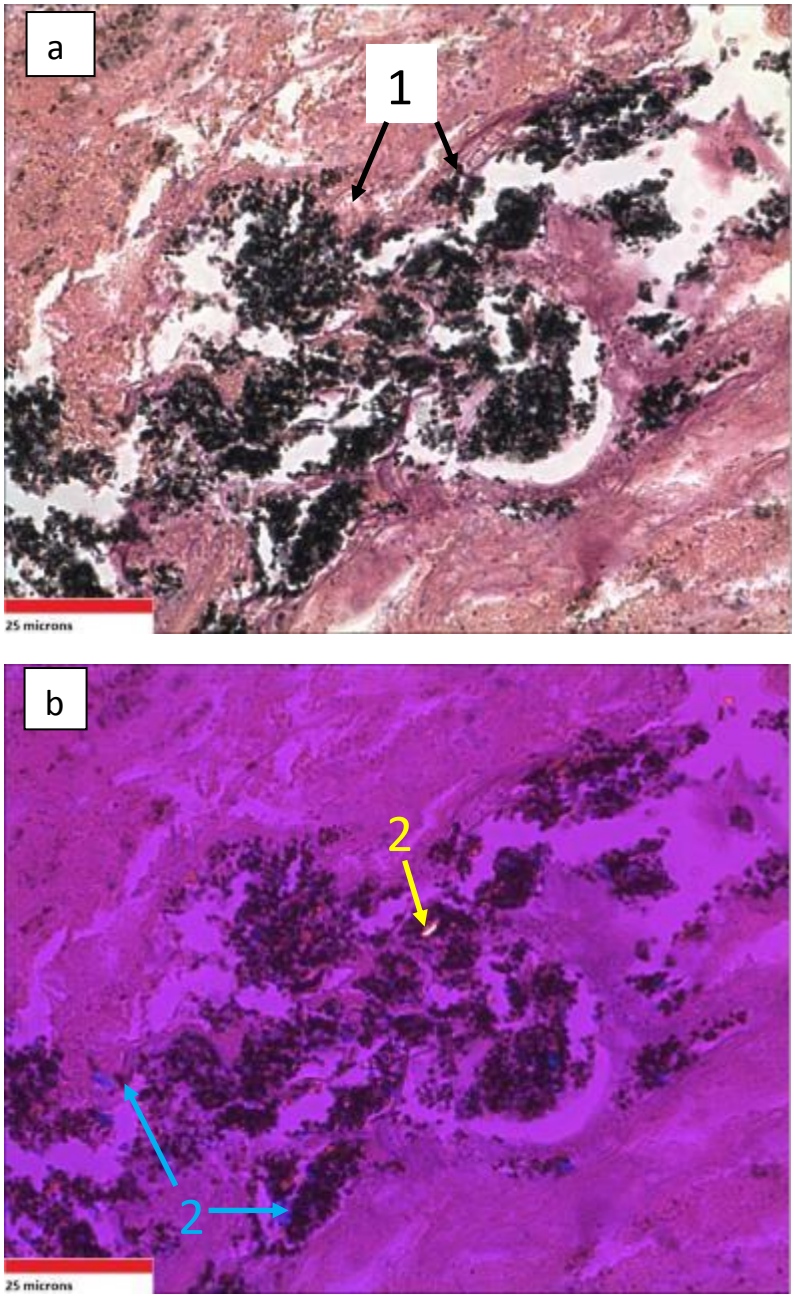

Figure 4.20 An anthracotic deposit (1) with birefringent objects (2 and 3) in a section of DO45 (H+E) a) shows the section under bright field illumination and b) with ¼ wave plate analysis. Scale bar = 25 microns

Sample DO 46

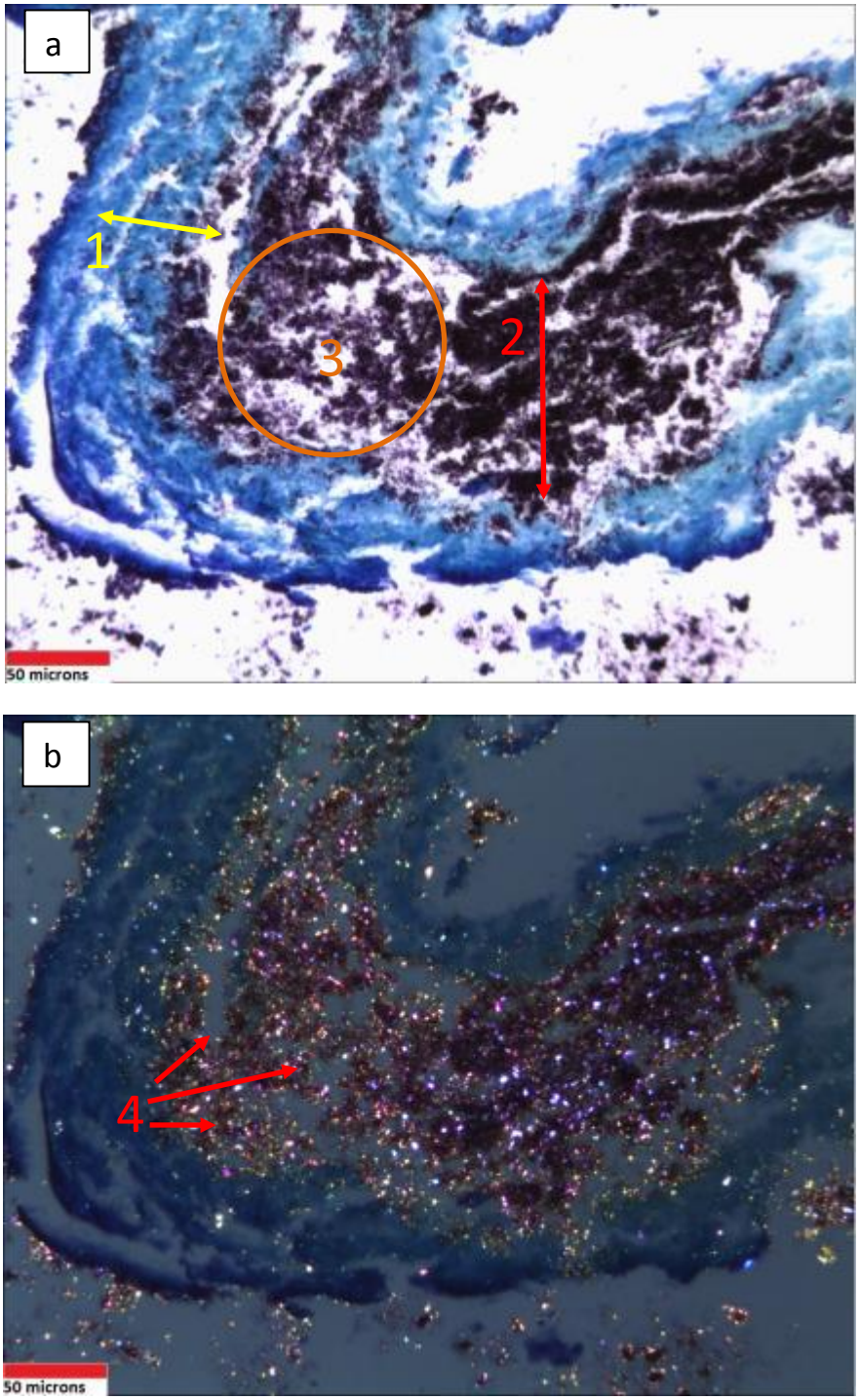

Figure 4.21 Representative images of DO46 viewed with bright field illumination (a) and with polarised light (b). showing bands of compacted, degraded lung (1) tissue and anthracotic deposits (2) with metachromasia (3) where birefringent inorganic particles have been co-deposited (4) (TB). Scale bar = 50 microns

A representative section stained with TB of DO46 can be seen in figure 4.21a. The section consists of bands of badly degraded and compacted interstitial lung tissue (see Introduction section 1.2) (1) with large deposits of anthracotic pigment (2).

There are visible areas of metachromasia (3) within the anthracotic deposits which would suggest the deposits may consist of more than one type of particle. This is confirmed by the presence of birefringent non-organic particles (4) which have been visualised using polarised light in figure 4.21b.

It is possible that this tissue was fibrotic, as a Miller's elastic stain of DO46 (Figure 4.22) reveals the presence of extremely dense elastic fibres (stained blue) spread throughout the lung tissue (stained pink). The density of the fibres seems to increase around the anthracotic deposits.

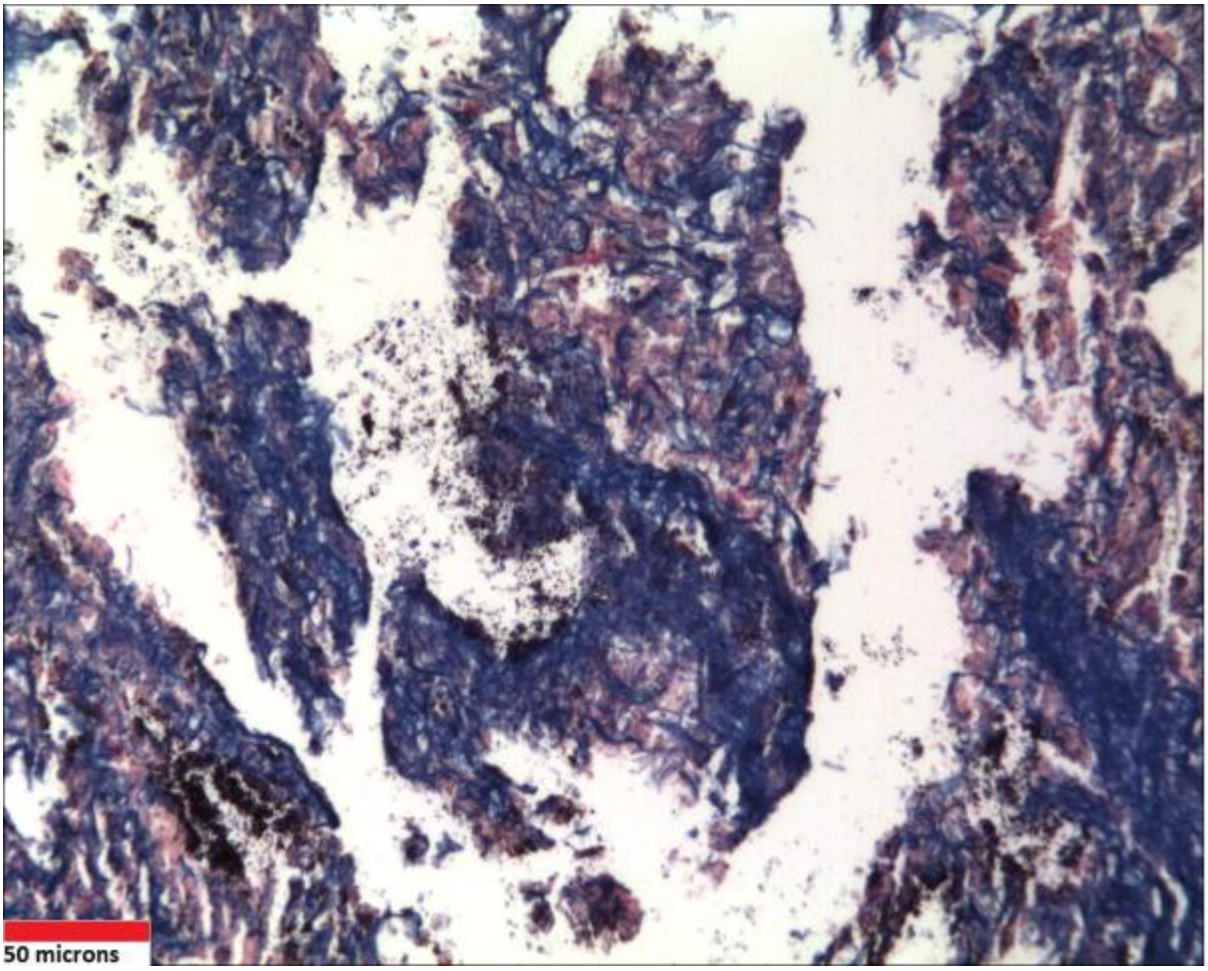

Figure 4.22 A section of DO46 (M). Dense elastic tissue (stained blue/purple) can be seen spread throughout the background of compacted lung tissue (stained pink).

Sample A-4

A representative image of mummified tissue from mummy A-4 can be seen in Figure 4.23. The sample consists of not particularly well preserved interstitial lung tissue (1) with large deposits of a dark soot-like material (2).

A section of this lung tissue can be seen at a higher magnification in Figure 4.24. Small clusters of bacteria from post-mortem infection (1) can be seen as small dark blue circles against the lighter background of interstitial lung tissue. These bacteria must be post-mortem as pre-mortem bacteria would have long since degraded.

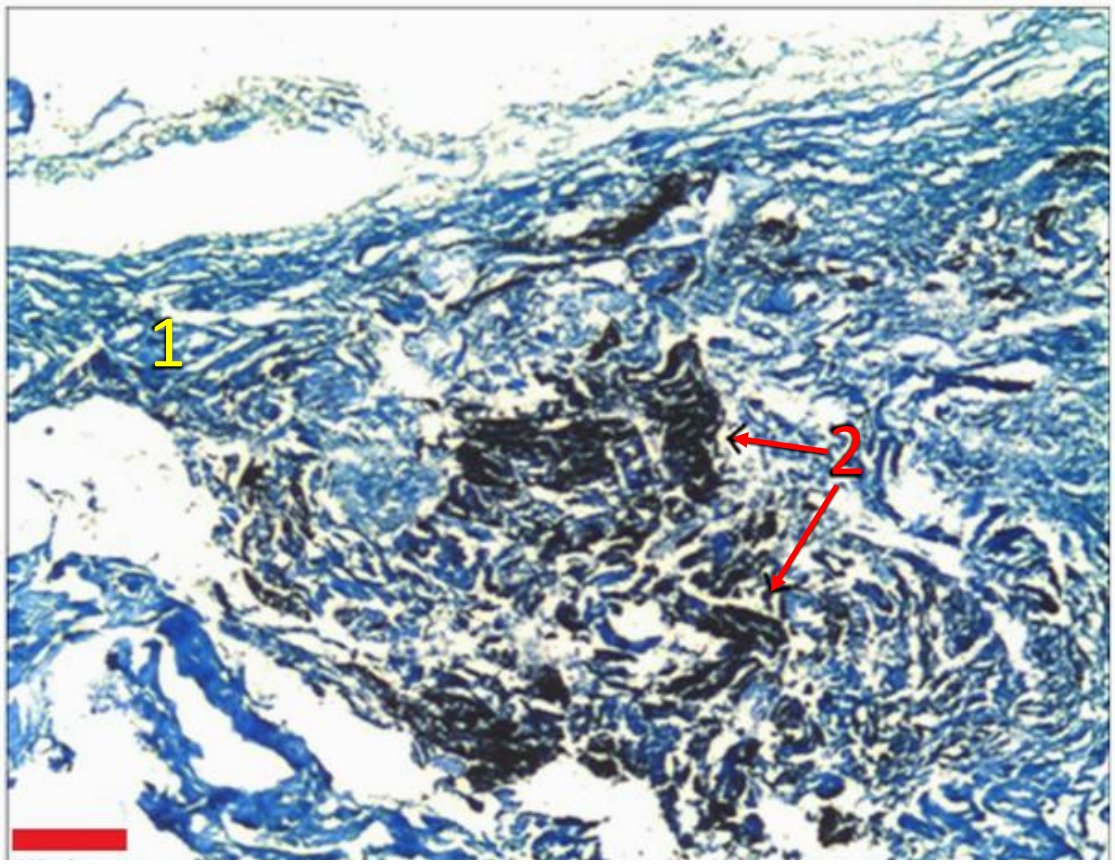

Figure 4.23 A representative image of sample A-4 showing compressed lung tissue (1) and anthracotic pigment (2) TB. Scale bar = 100 microns

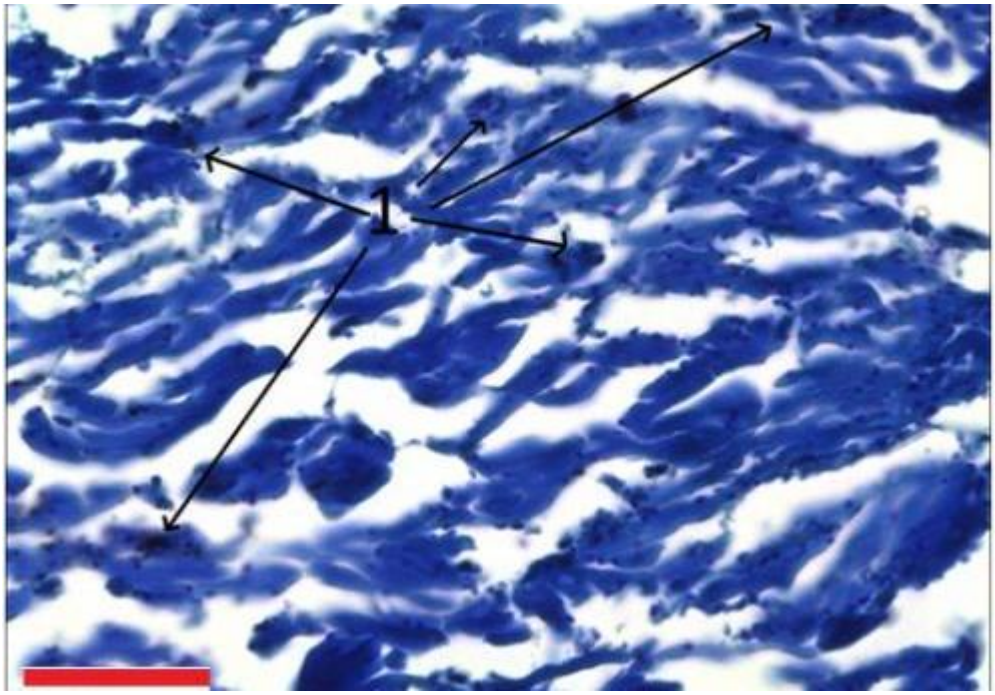

Figure 4.24 An area of mummified lung sample A4 showing the poor state of preservation and presence of bacteria (1) (TB). Scale bar = 50 microns

Further evidence of the poor state of preservation of sample A-4 can be seen at higher magnification in Figure 4.25. Most of the section consists of badly degraded interstitial lung tissue (1) which is surrounded by a large fungal granule (2) and clusters of possible soot material (3). These clusters could possibly be bacteria but they appear darker than the bacteria stained in Figure 4.24, so are probably small clumps of soot. They are in small spherical clumps that could have been caused by collection and storage of anthracotic pigment by alveolar macrophages before the individual died.

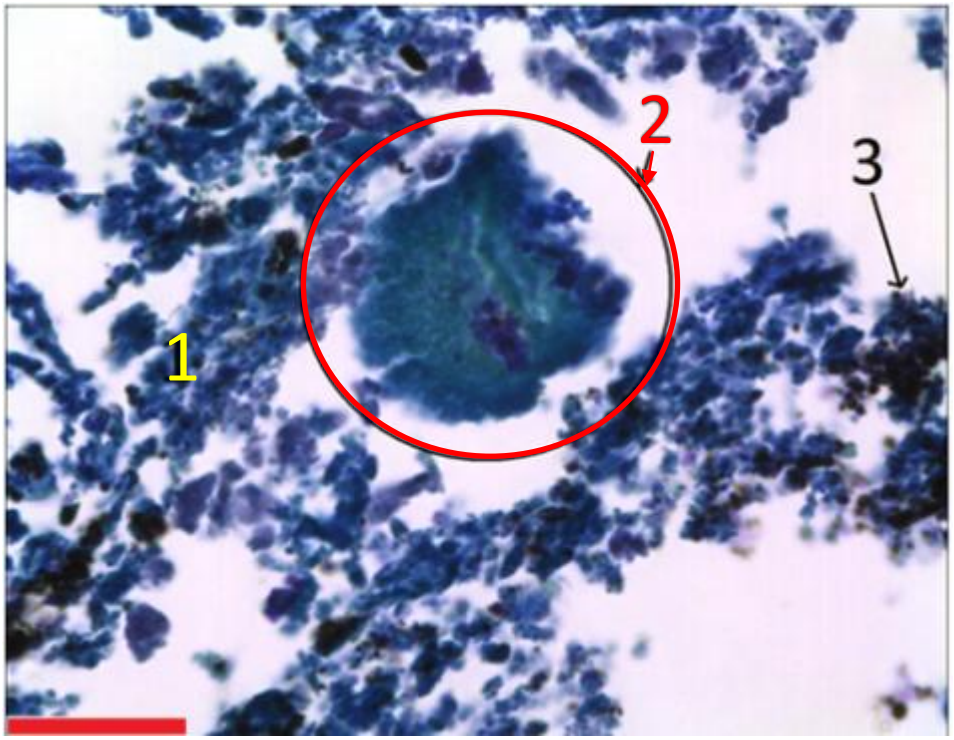

Figure 4.25 A section of degraded A4 tissue (1) showing a fungal granule (2) and small clusters of soot (3) TB. Scale bar = 25 microns

These clumps of soot can be seen in greater detail in figure 4.28a where the individual particles appear to have been deposited and aggregated into large clusters of (1). Areas of purple metachromasia can be seen on the periphery of the large clusters (Figure 4.25, 2). When the same section is examined with polarised light (figure 4.26b), the metachromatic areas (2) are revealed as birefringent particles co-distributed within the clusters of anthracotic pigment (1).

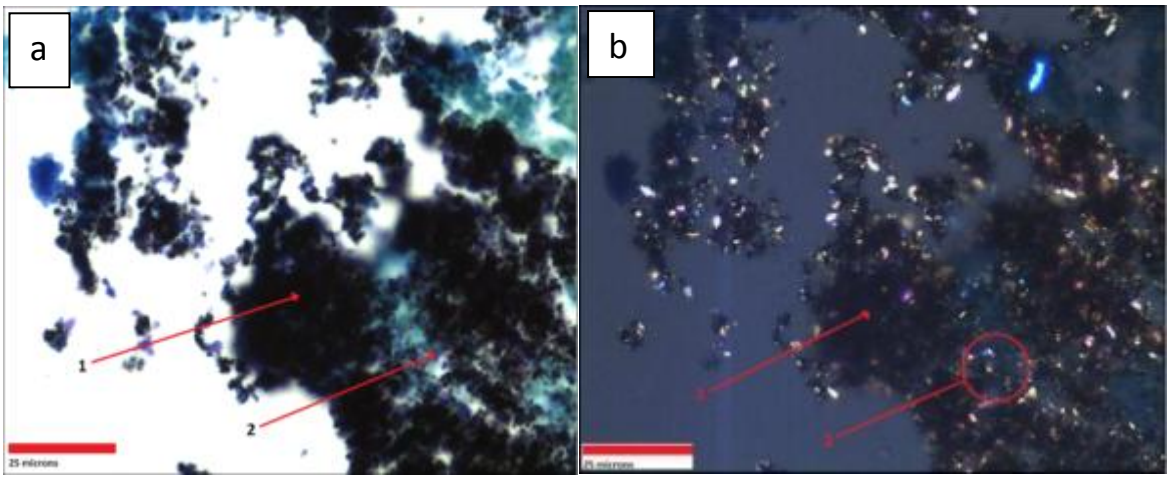

Figure 4.26 A section of mummy A4 lung showing large clusters of anthracotic and birefringent particles (TB 40x) viewed under bright field illumination (a) and under polarised light (b). Scale bars = 25 microns

Sample A13

A representative section of mummified tissue sample A13 can be seen in figure 4.29. The sample consists of areas of densely compacted interstitial lung tissue stained blue (1). In between the bands of tissue there are large deposits of anthracotic pigment (2). The deposits appear to consist of large numbers of small individual particles clumped together. There are numerous tears in the tissue that are probably due to the sectioning method rather the preservation of the tissue.

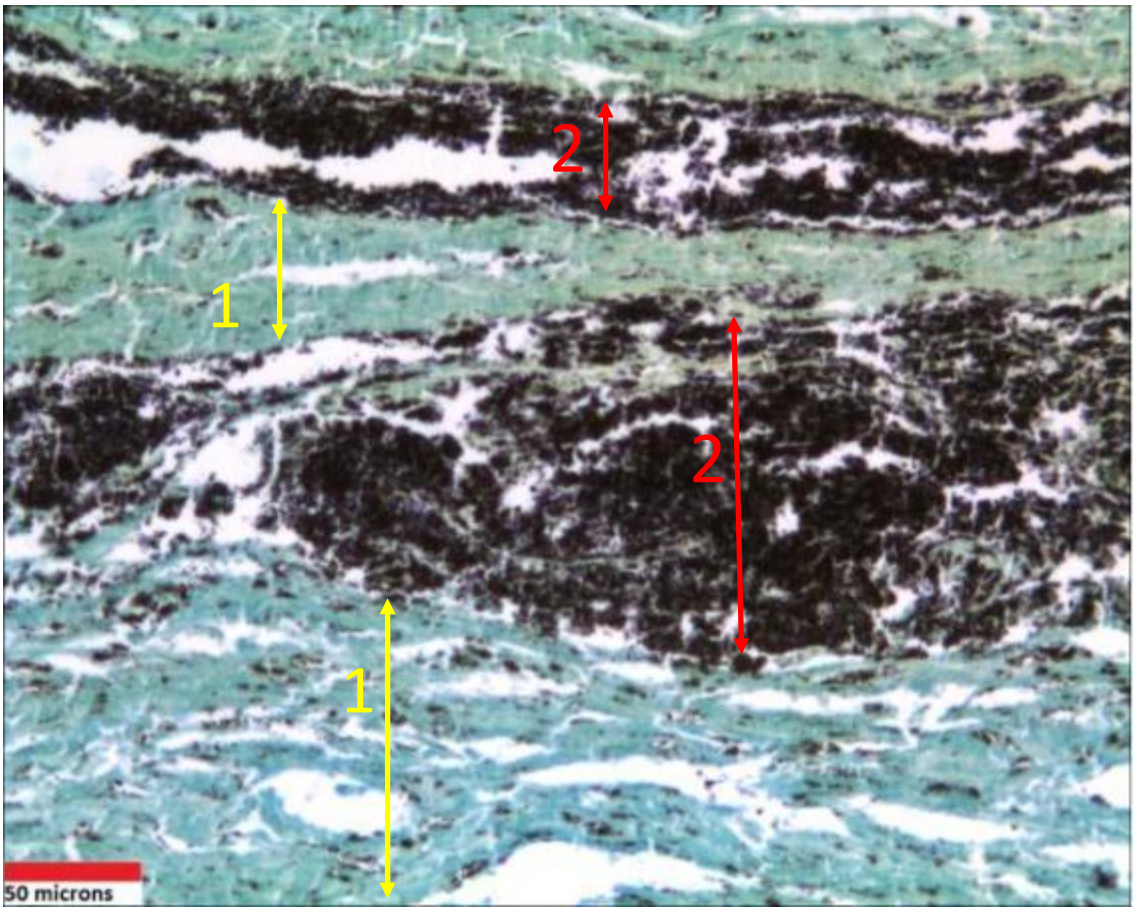

Figure 4.27 Section of A13 mummified tissue showing bands of interstitial lung tissue (1) and large deposits of anthracotic pigment (2) (TB).

When these deposits of anthracotic pigment are viewed at higher magnification in figure 4.28a, it is revealed the larger clumps are composed of smaller individual particles (1) that have probably been collected together through macrophage

action. Areas of purple metachromasia (2) can be seen between the clumps suggesting that the clumps could be composed of different particles with different charging properties. This is confirmed when the same field was examined with polarised light (in figure 4.28b) as birefringent non-organic particles can be seen co-deposited with the anthracotic particles (3).

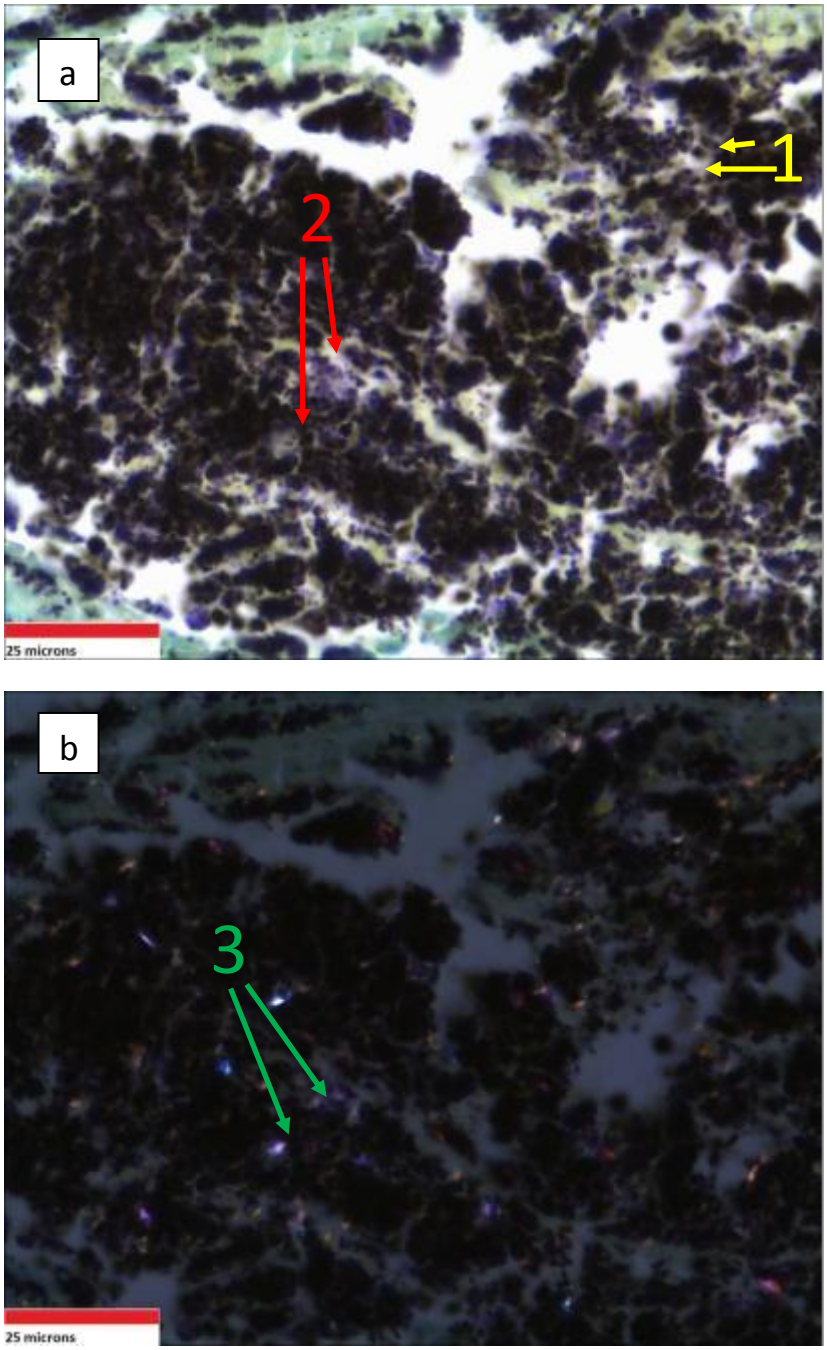

Figure 4.28 High magnification images of the anthracotic deposits in A13 (TB) viewed under bright field illumination (a) and with polarised light (b).

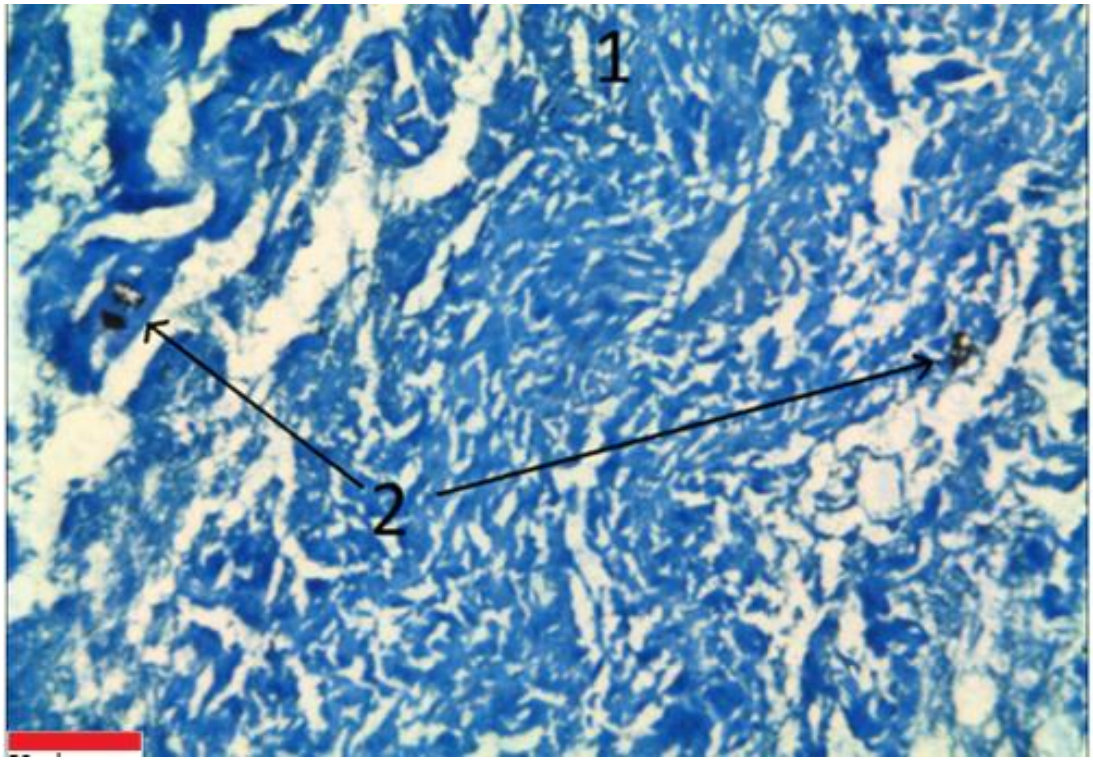

Figure 4.29 A-102 lung tissue with possible staining artefacts (TB). Scale bar = 50 microns.

Sample A102

The general structure of the lung sample from mummy A-102 can be seen in Figure 4.29. It consists of well preserved and rather dense, and possibly fibrotic, interstitial lung tissue (1) which has three very darkly stained areas (2). These areas do not appear to be due to silica or soot and could be artefacts from the mummified tissue reacting with the staining process.

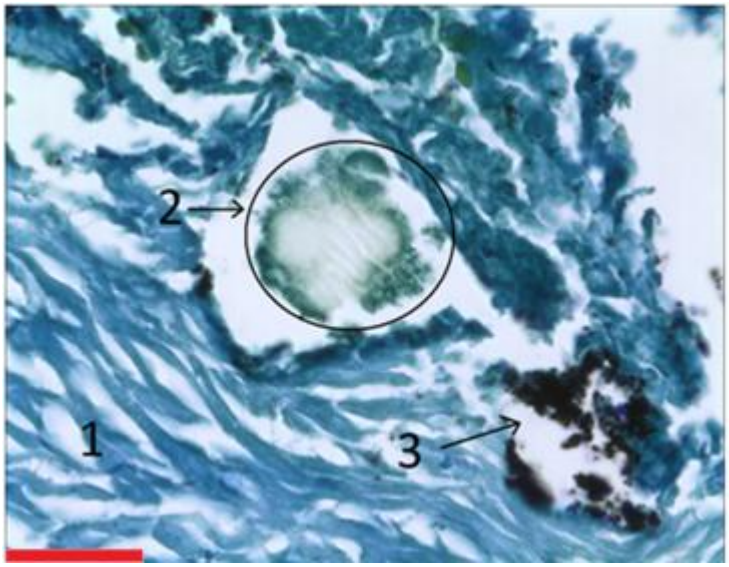

Figure 4.30 Fungal (2) and Bacterial (3) attack of A102 tissue (1) (TB) Scale bar = 25 microns

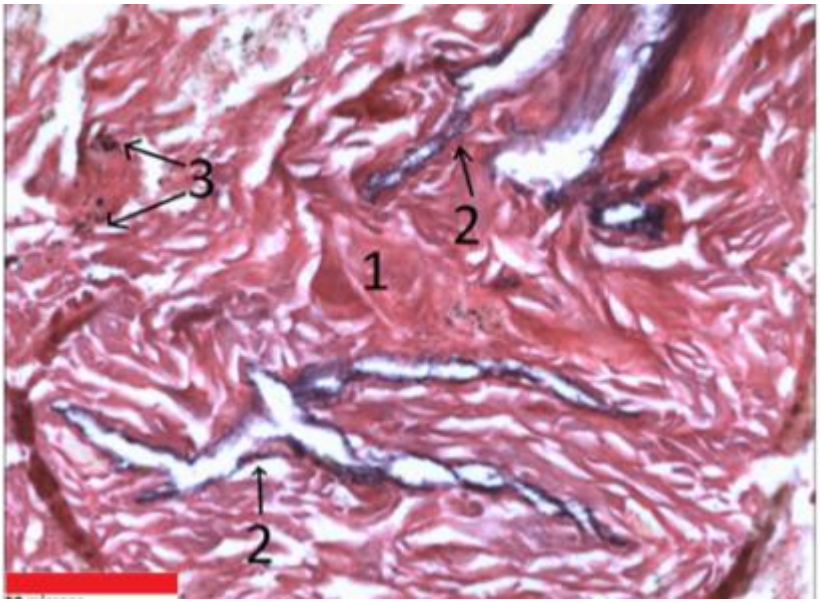

Figure 4.31 A102 Fibrotic tissue with fibrotic tissue (1) alveoli (2) and soot (3). Scale bar = 50 microns

At a higher magnification in figure 4.30, the densely packed tissue (1) has been attacked and degraded on the periphery by a fungal granule (2). There is also a possible soot deposit or bacterial colony (3) In Figure 4.31, dense fibrotic tissue can be seen with the darkly stained elastic walls of what could have been bronchioles or alveoli. There are possible soot deposits in this tissue sample (Figure 4.31).

Sample A105

Figure 4.32 shows a representative image of the sample A105 stained by H+E. All the material has been stained light or dark brown. The tissue or material is so badly degraded that there is no discernible tissue or structures present.

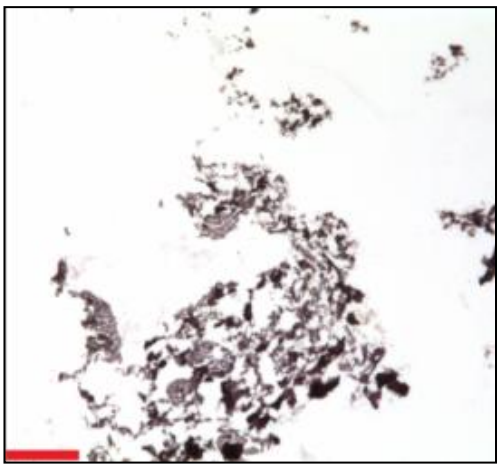

Figure 4.32 Image of sample A105 (H+E). There are no discernible tissues or structures. Scale bar = 50 microns.

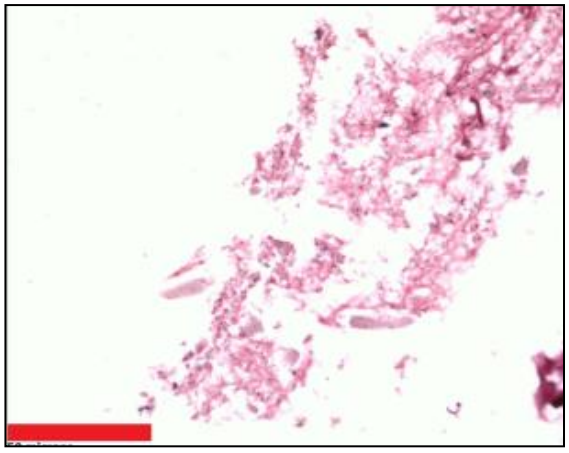

Figure 4.33 Section of A105 showing **no structures or elastic fibres (M).** Scale bar = 50 microns

When stained with Miller's elastic stain, no elastic fibres can be seen in this sample (Figure 4.33). It is concluded that either the sample is not lung tissue or it is too badly degraded to stain.

Sample A108

Figure 3.34 shows a representative image of tissue from mummy A108 stained with TB.

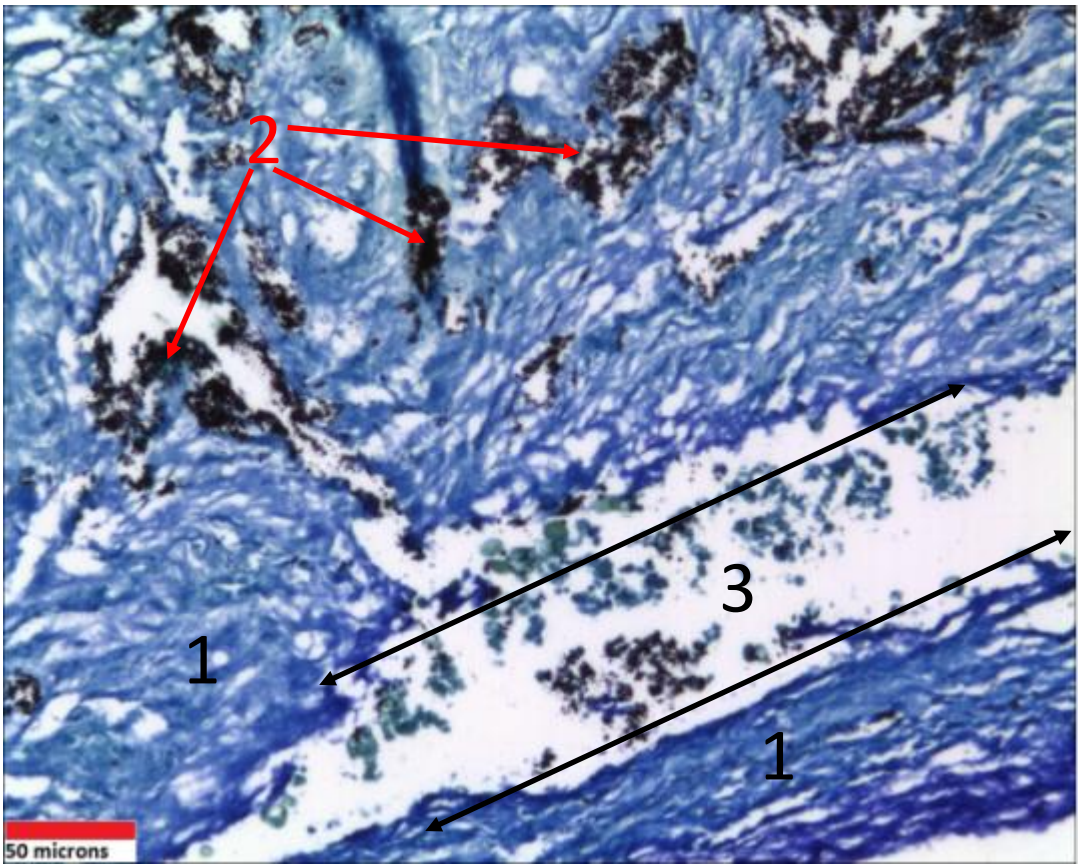

Figure 4.34 Section of A108 (TB) showing interstitial lung tissue (1), anthracotic pigment deposits (2) and fungal bodies (3) in a large tear.

A108 appears to consist of densely compacted intersitial lung tissue (Figure 4.34) stained blue. As well as containing large deposits of anthracotic pigment (2), the tissue has a large tear in the bottom half of the image. This tear could have been caused by the sectioning with the microtome but appears to have been caused or at least exacerbated by the large number of liquefying fungal bodies in that area (3). When the fungal bodies are examined in higher magnification (in figure 3.35) the damage they have caused to the surrounding tissue can be seen.

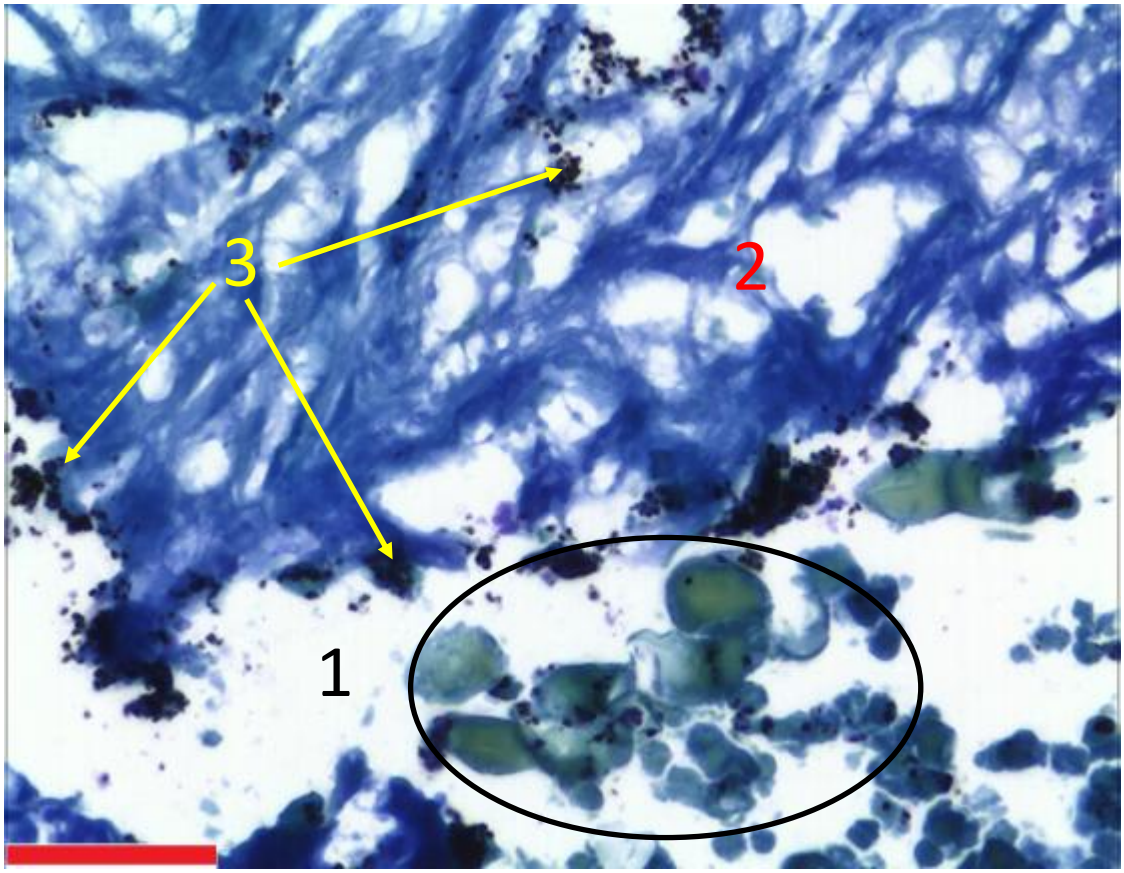

Figure 4.35 Fungal bodies (1) and degraded tissue (2) in A108 (TB). Small particles of anthracotic pigment are also present in and around the tissue (3). Scale bar = 25 microns.

In figure 4.35, the fungal bodies (1) have digested the surrounding tissue resulting in large holes (2) through liquefaction. It is not obvious whether this fungal attack is ancient or more recent following removal of the mummy and/or tissue by the modern excavators.

Figure 4.36a and b show a representative example of an anthracotic deposit at a higher magnification. The deposit consists of a large number of small particles clumped together to produce large clumps of pigmented material. When the same field is viewed with polarised light, birefringent non-organic particles can be seen co-deposited with the anthracotic pigment (Figure 4.36b). This is presumably due to the collection of both types of particle by alveolar macrophages.

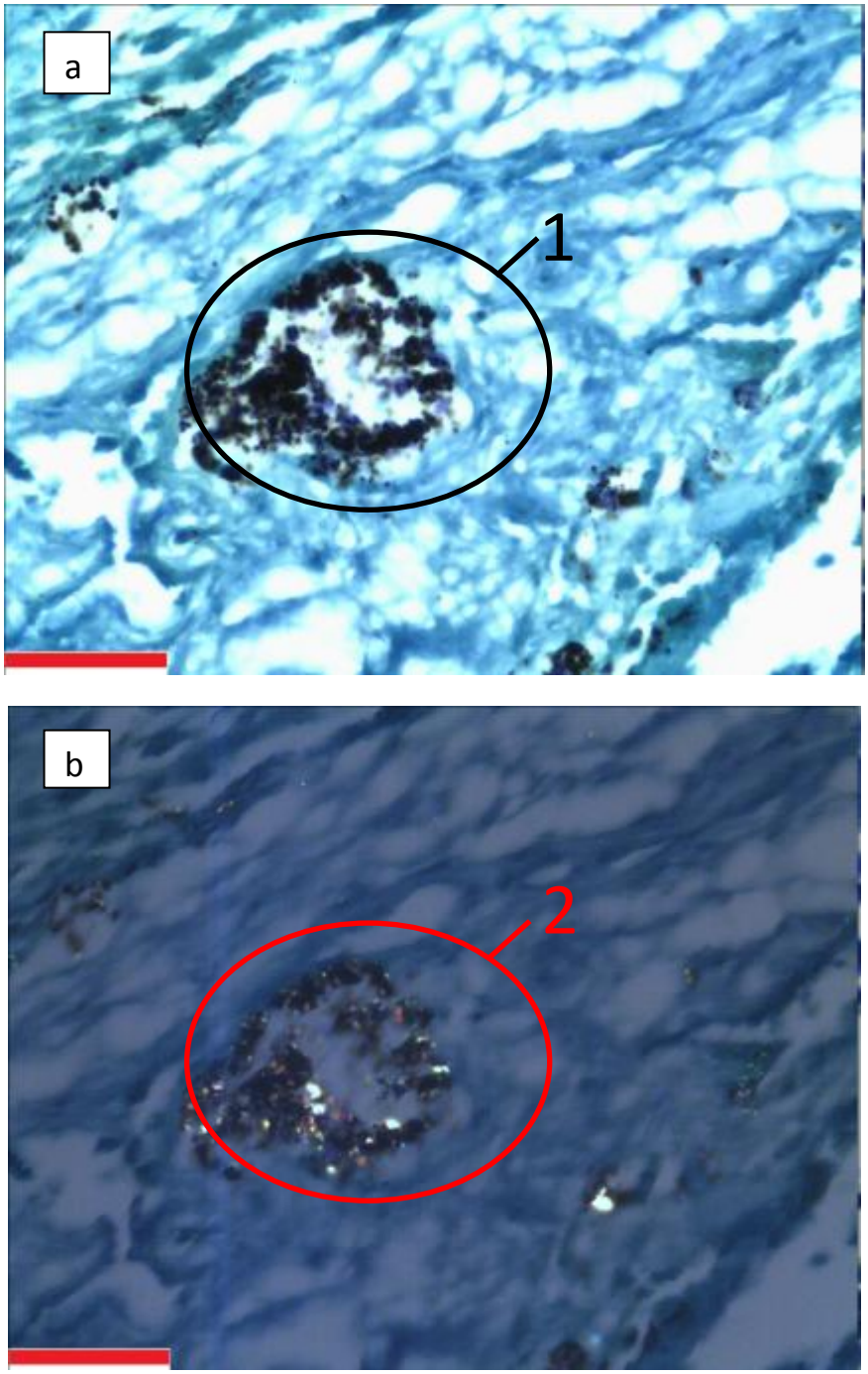

Figure 4.36 High magnification field of anthracotic deposit (1) viewed with bright field illumination (a) and polarised light (b) showing the co-distribution of birefringent particles with the anthracotic pigment (2). Scale bar = 25 microns

Sample A110

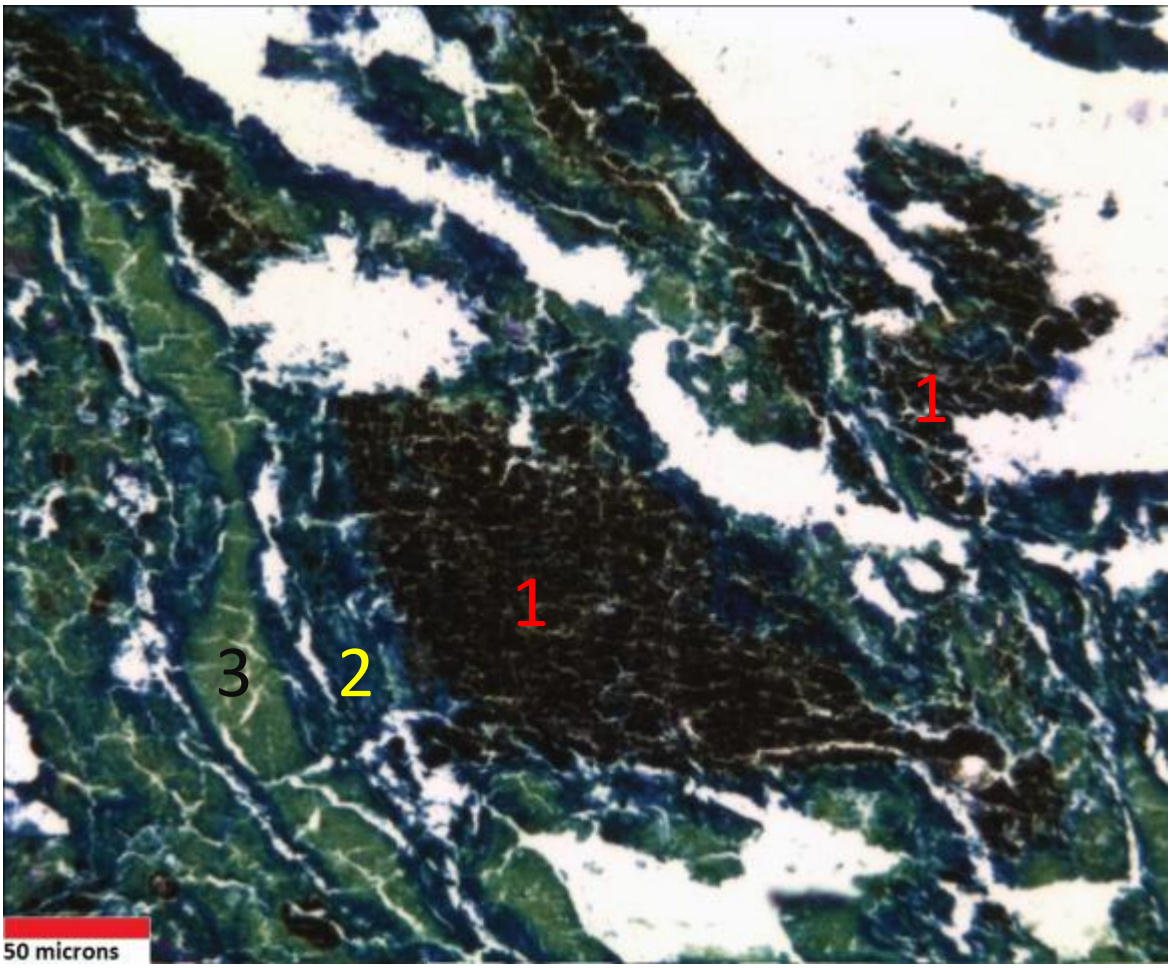

Figure 4.37 Representative image of A110 (TB) showing large dense deposits of anthracotic pigment (1), well stained blue areas of tissue (2) and poorly stained areas of degraded tissue (3).

A representative image of the tissue from mummy A110 can be seen in figure 4.37. Very large and dense deposits of anthracotic pigment (1) are present in this section of mummified lung tissue. The surrounding interstitial lung tissue has large holes and tears and the overall state of preservation appears poor. This is further shown by areas of the tissue which have been poorly stained by TB (3) compared to other areas which are in a better state of preservation and have stained well (2). Further evidence of the poor preservation of this sample can be seen in figure 4.38 where the tissue has almost disintegrated in several areas and no tissue has taken up either the Miller's elastic stain or the counterstain.

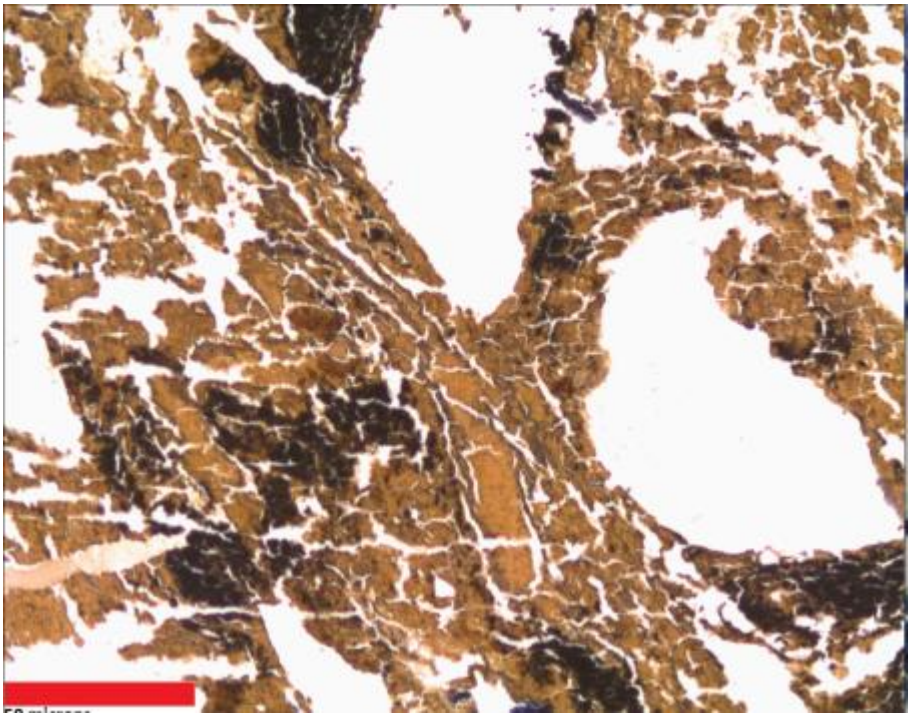

Figure 4.38 Miller's elastic stain of A110 showing large tears and poor state of preservation of the tissue. Note the poor staining of the tissue. Scale bar = 50 microns

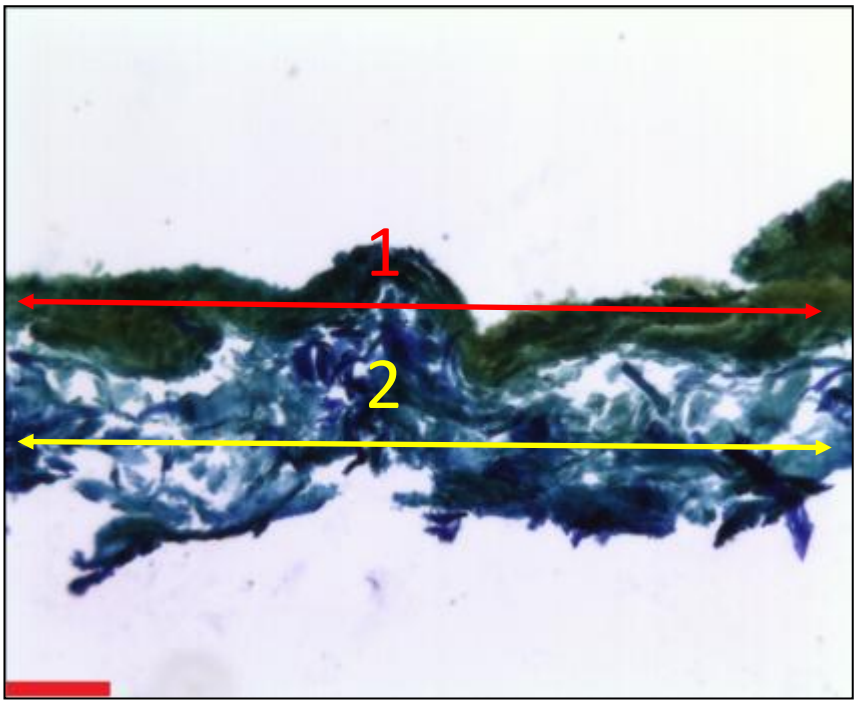

Figure 4.39 Skin sample present in lung tissue block of A110 (TB) showing elastic (1) and collagen (2) layers. Scale bar = 50 microns

The paraffin block of this section had been previously prepared for another study and a second tissue type was contained within the same block. No prior results were available prior to examination. It was found to be a sample of mummified skin. Figure 4.39 shows a transverse section of the skin where the elastic layer (1) and collagen (2) can be seen.

Sample A111

The representative image of A111 shown stained with TB in figure 4.40 indicated that this sample is very badly degraded tissue with large holes and very little distinguishing features.

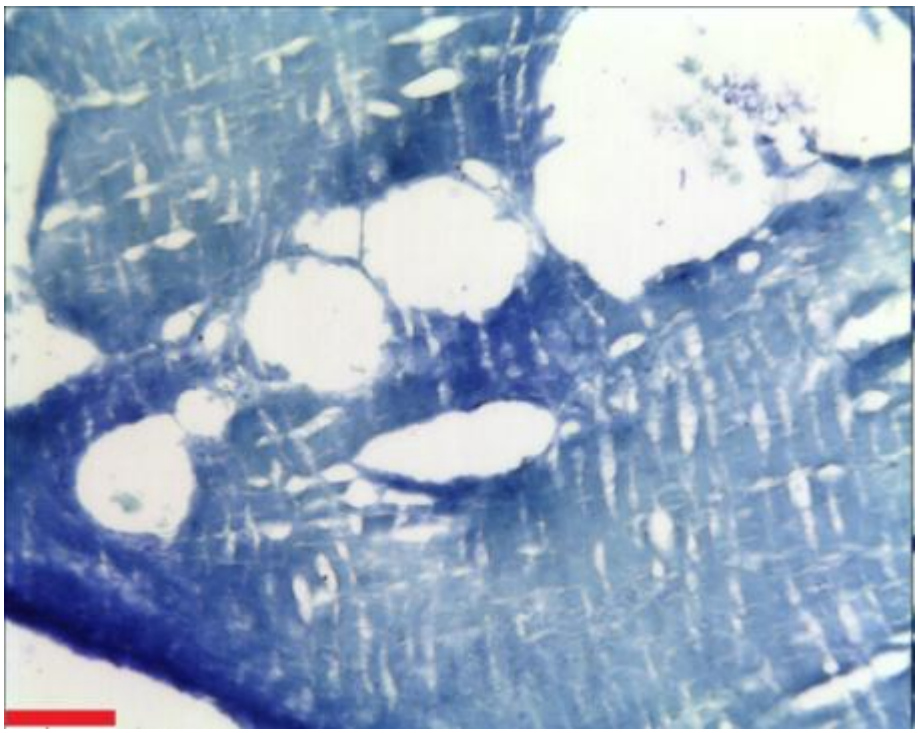

Figure 4.40 Representative image of mummy sample A111 (TB) showing degraded tissue with little or no distinguishing features. Scale bar = 50 microns

When this section was stained with H+E (in figure 4.41), some small anthracotic deposits (1) were revealed to be present in the tissue. Despite the very poor state of preservation, the presence of this anthracotic tissue would suggest that this is indeed lung.

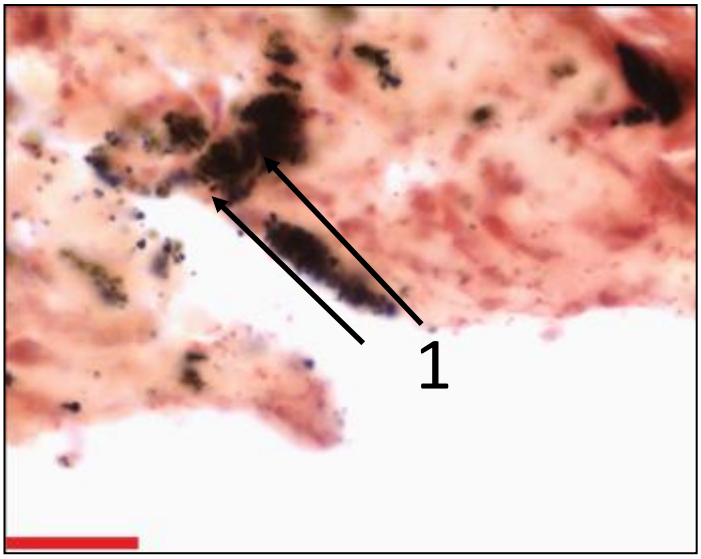

Figure 4.41 Anthracotic deposits (1) in section of A111. When this section was stained with H+E (in figure 3.41), some small anthracotic deposits (1) were revealed to be present in the tissue. The presence of this anthracotic tissue would suggest that this is indeed lung. Scale bar = 25 microns.

Sample A126

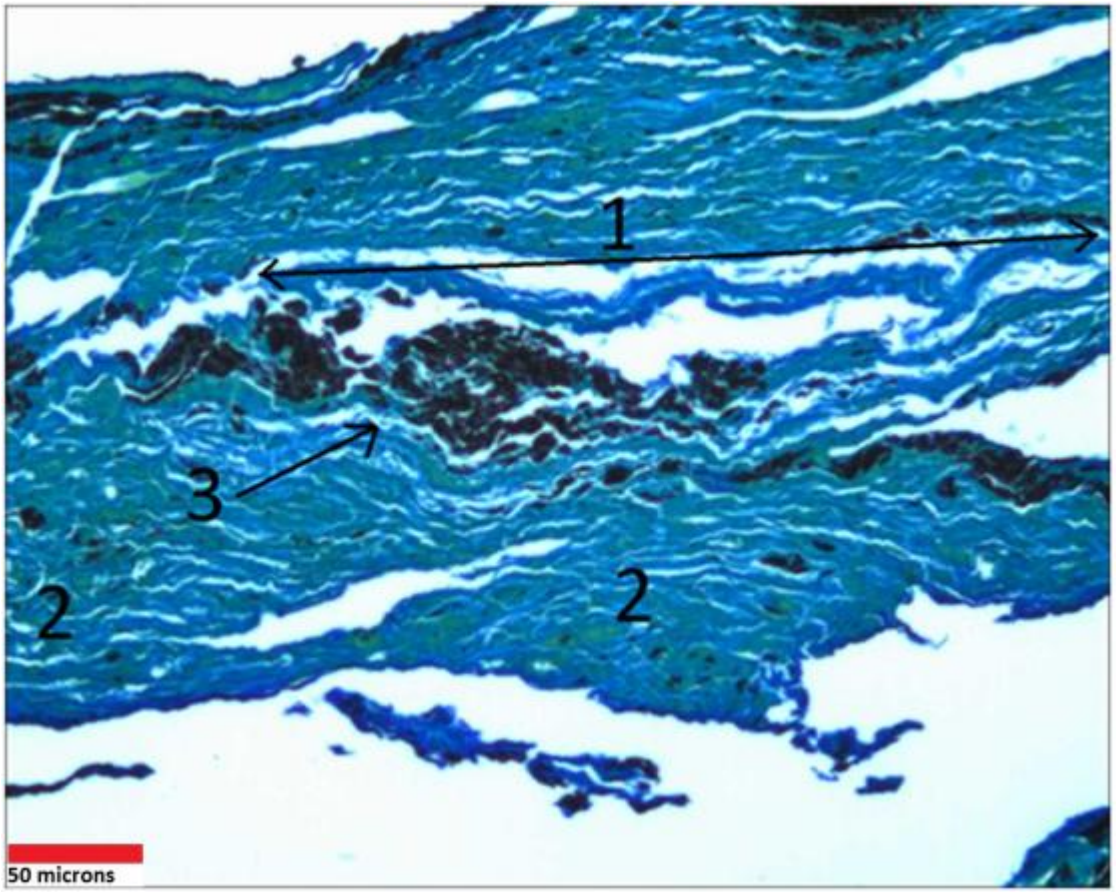

Figure 4.42 Sample A126 (TB) showing possible bronchiole (1), interstitial lung tissue (2) and anthracotic deposits (3).

Figure 4.42 shows a general view of the sample stained with T B. Several features can be seen, including what appears to be a collapsed space (the dark blue line labelled (1). This possibly could have been an alveolus, a small bronchiole or a blood vessel. Interstitial lung tissue, labelled as (2) in Figure 4.42, can be seen surrounding the collapsed space on either side. There is a large deposit of anthracotic pigment, labelled (3), surrounding one side of the collapsed space. The sample is very well preserved and it was decided to carry out additional stains, such as, Martius Scarlet Blue (One-step MSB, see Introduction section 1.3.4) to further differentiate the tissue and features in the sample.

Figures 4.43a and b show the same section of an anthracotic deposit at higher magnification but in different light sources. Figure 4.43a shows the section in bright field illumination and the individual characteristics of the dark brown/black pigments can be seen. The black areas consist of numerous tiny particles that have conglomerated together. This could be evidence of collection by alveolar macrophages in antiquity. Figure 4.43b shows the same section in polarised light. Birefringent (bright shining areas) materials can be seen in and around the soot deposits. This would indicate that non-organic material is present along with the non-birefringent soot. The purple areas around the soot deposits appear to be highly charged.

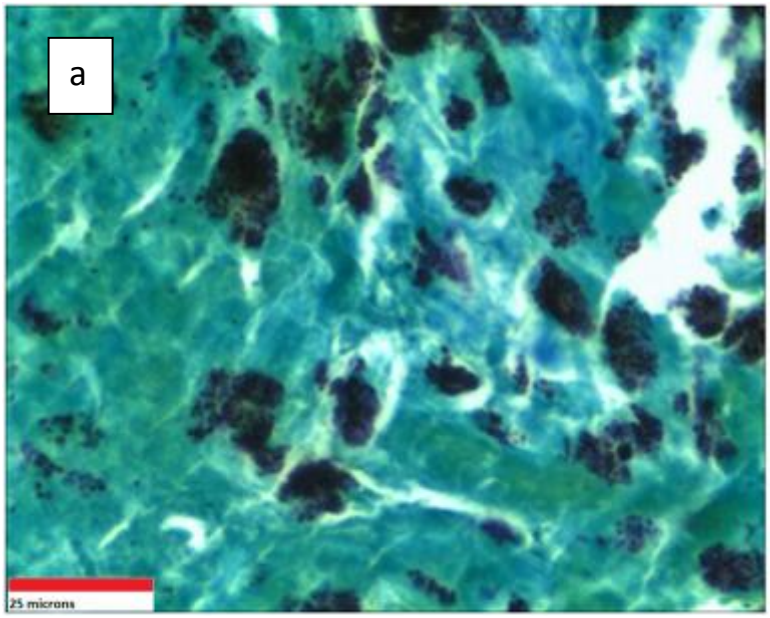

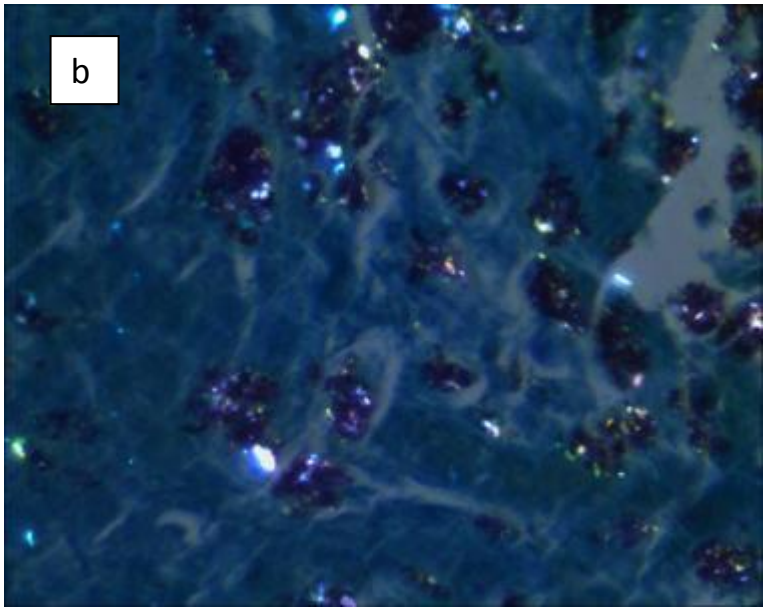

Figure 4.43 Anthracotic pigment in A126 lung tissue showing deposits with bright field illumination (a). Note the birefringent particles within the anthracotic deposits when viewed using polarised light (b). Scale bar = 25 microns.

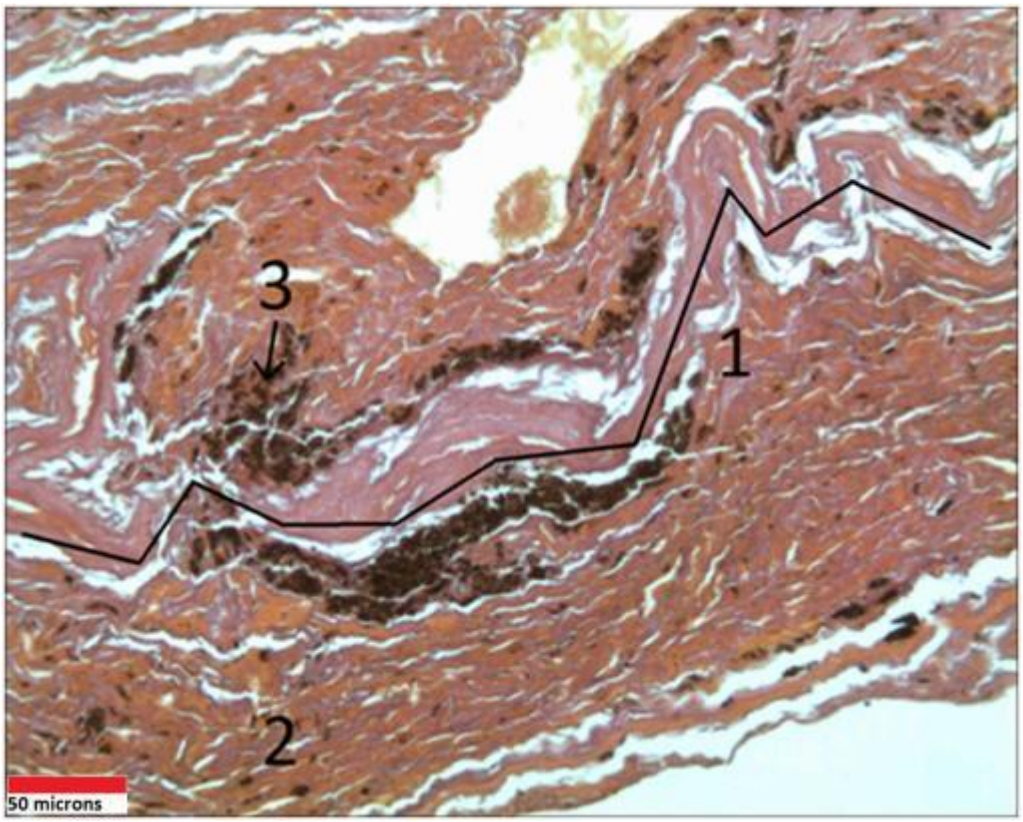

Figure 4.44 Collapsed air space (1) and anthracotic deposits (3) in A126 (stained with H&E). Dense interstitial tissue (2) can also be seen.

Figure 4.44 shows an overview of the sample. Again a collapsed space, labelled as the line (1) can be seen. This collapsed space which could have been a blood vessel, bronchiole or alveolus is surrounded by interstitial tissue (2) and an anthracotic deposit (3). Figure 4.45 is at a higher magnification and clearly shows the border between the collapsed space (1) and the anthracotic deposit (2).

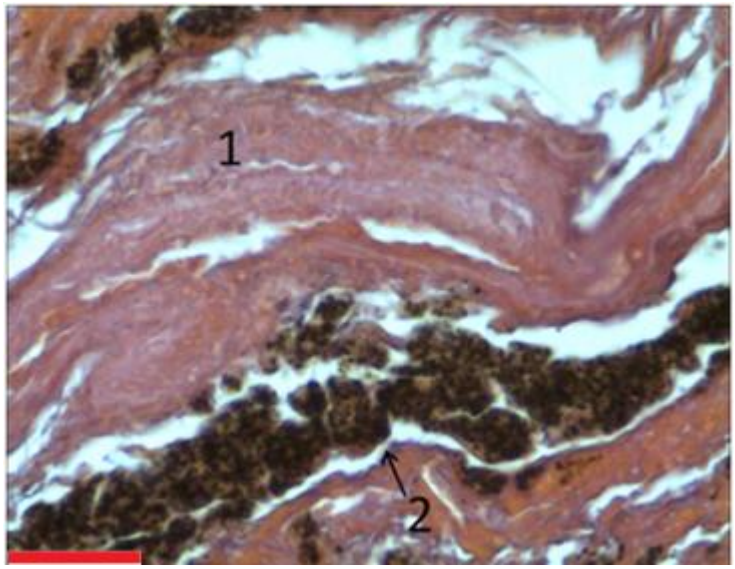

Figure 4.45 A-126 Collapsed air space (1) and anthracotic pigment (2) (H&E). Scale bar = 25 microns

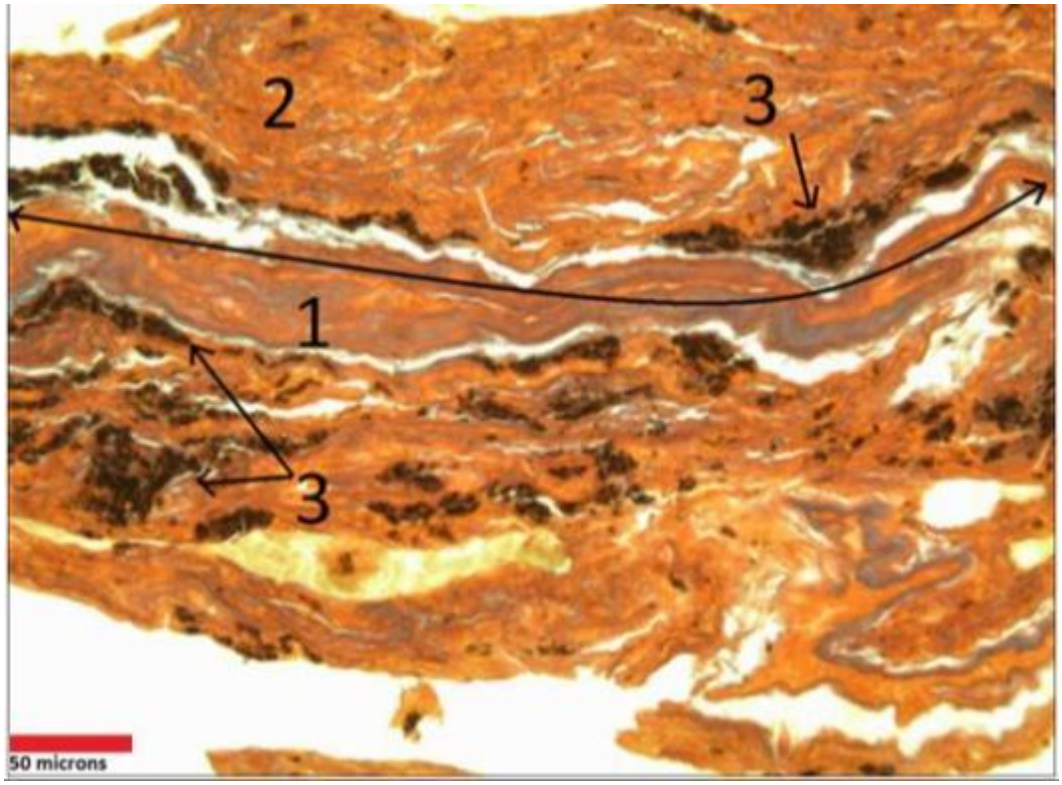

Figure 4.46 A-126 Collapsed air space, lung tissue and soot (MSB)

The Martius Scarlet Blue stain of sample A-126 is shown in Figure 4.46. As with the Toluidine Blue stain, a collapsed space with a lumen and distinguishable walls can be seen (1). The space is surrounded by interstitial tissue (2) and soot deposits (3).

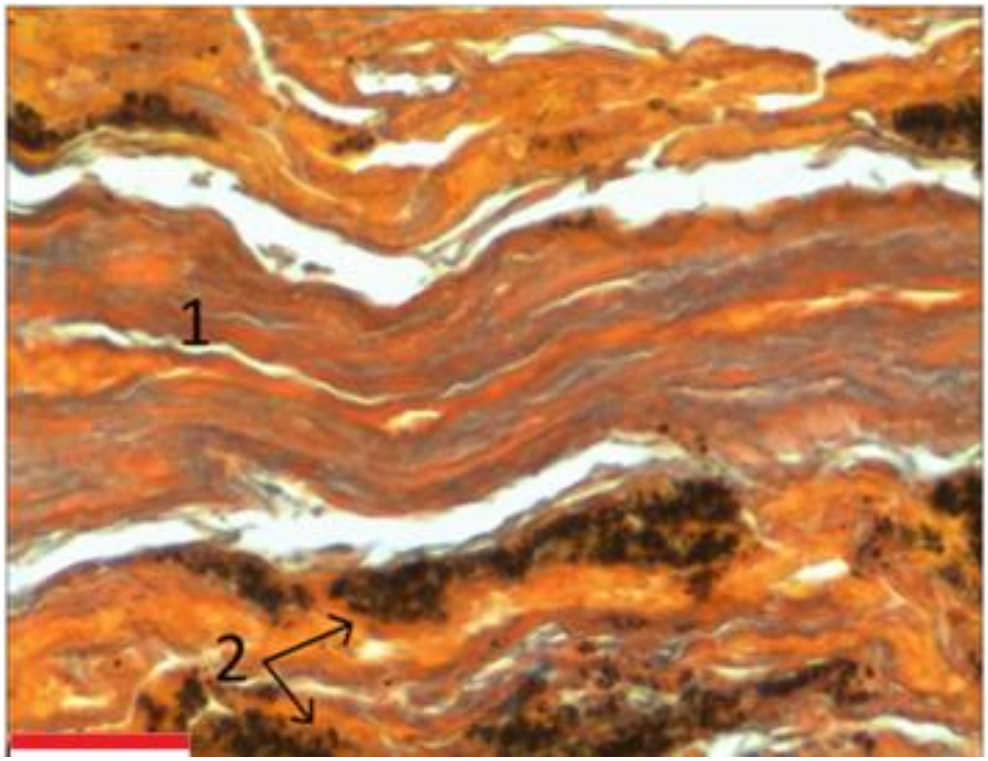

Figure 4.47 Air space (1) and anthracotic deposits (2) in material from A126 (MSB). Scale bar = 25 microns.

Figure 4.47 shows the collapsed air space from Figure 4.46 but at a higher magnification. The air space (1) has visibly distinguishable layers as well as a possible lumen. The collapsed air space is surrounded by anthracotic deposits (2).

Sample A132

A general overview of A132 can be seen in figure 4.48. Plant material (stained green) can be seen on the left hand side of the image. An unidentifiable fibrous tissue (stained blue) can be seen on the right hand side

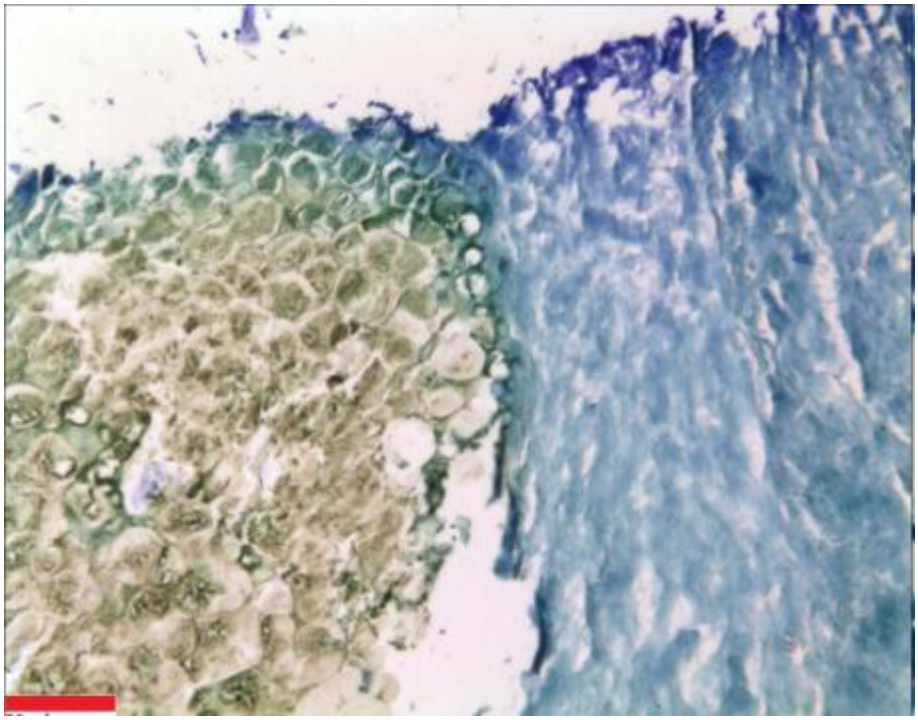

Figure 4.48 Representative image of A132 (TB) showing cellulosic plant material (stained green) on the left and fibrous unidentifiable tissue (stained blue) on the right. Scale bar = 50 microns.

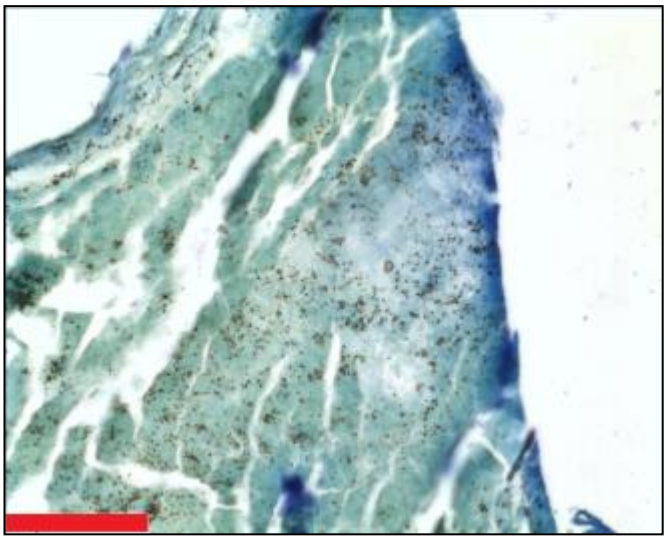

Figure 4.49 Section of A132 with unidentified particles (TB). Scale bar = 50 microns

This section of unidentifiable tissue shown in Figure 4.49 appears to contain small particles of an unidentified nature distributed throughout the tissue. However, when the sections were examined at higher magnification, it is revealed that the particles are small bubble-like artefacts. These artefacts are most commonly produced by incomplete removal of xylene before the section is taken to water.

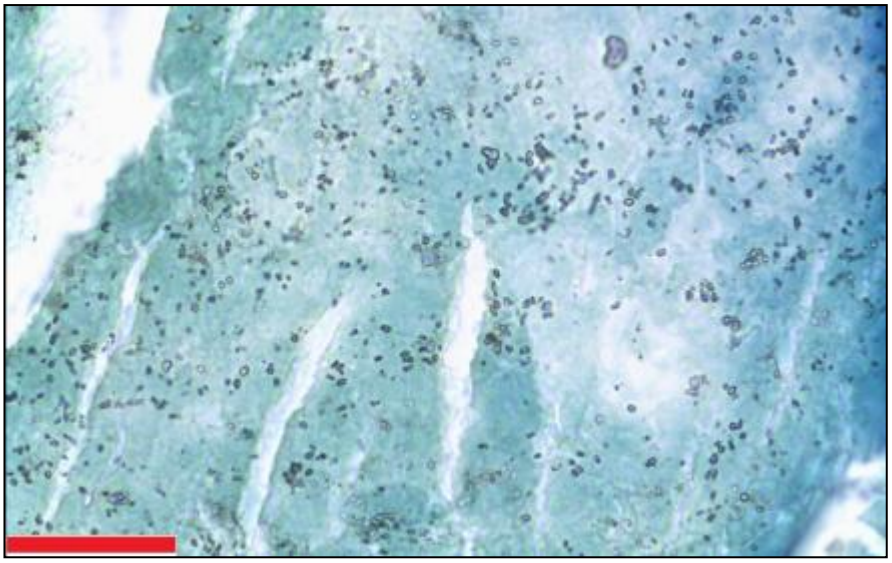

Figure 4.50 Small xylene bubbles in the tissue in A132 (TB). Scale bar = 25 microns.

Due to the presence of cartilage but the lack of anthracotic pigment, the tissue could be from the trachea or the upper bronchus.

Mummies from Thebes and Rifeh

Sample BM 51813

Figure 4.51 shows a representative image of material from 51813.

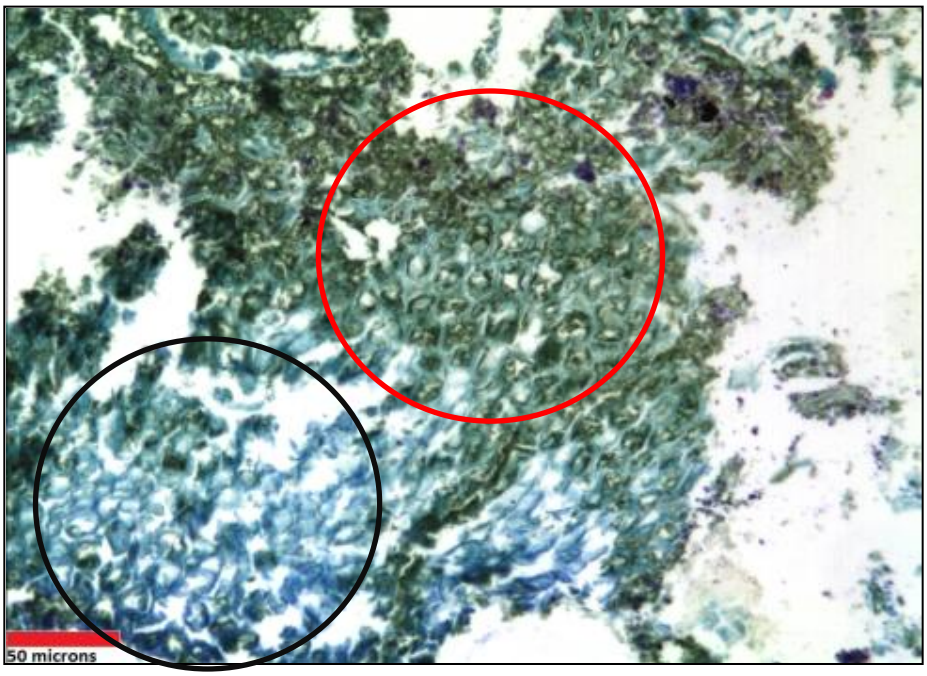

Figure 4.51 Image of 51813 (TB) showing blue-stained cellulose plant cells (black circle) and green-stained plant cells (red circle)

The image shows non-lung tissue that appears to consist of two areas of cellulose plant tissue. The left hand area has stained blue (highlighted in a black circle) by TB whilst the right hand area has stained green (highlighted in a red circle). The difference between these staining behaviours may be due to the state of preservation of different areas of the section or the presence of iron in the section. In Figure 4.52b, where the green area is examined at higher magnification and with polarised light, it is revealed that the cellular walls are birefringent which would be consistent for cellulose-containing plant cells.

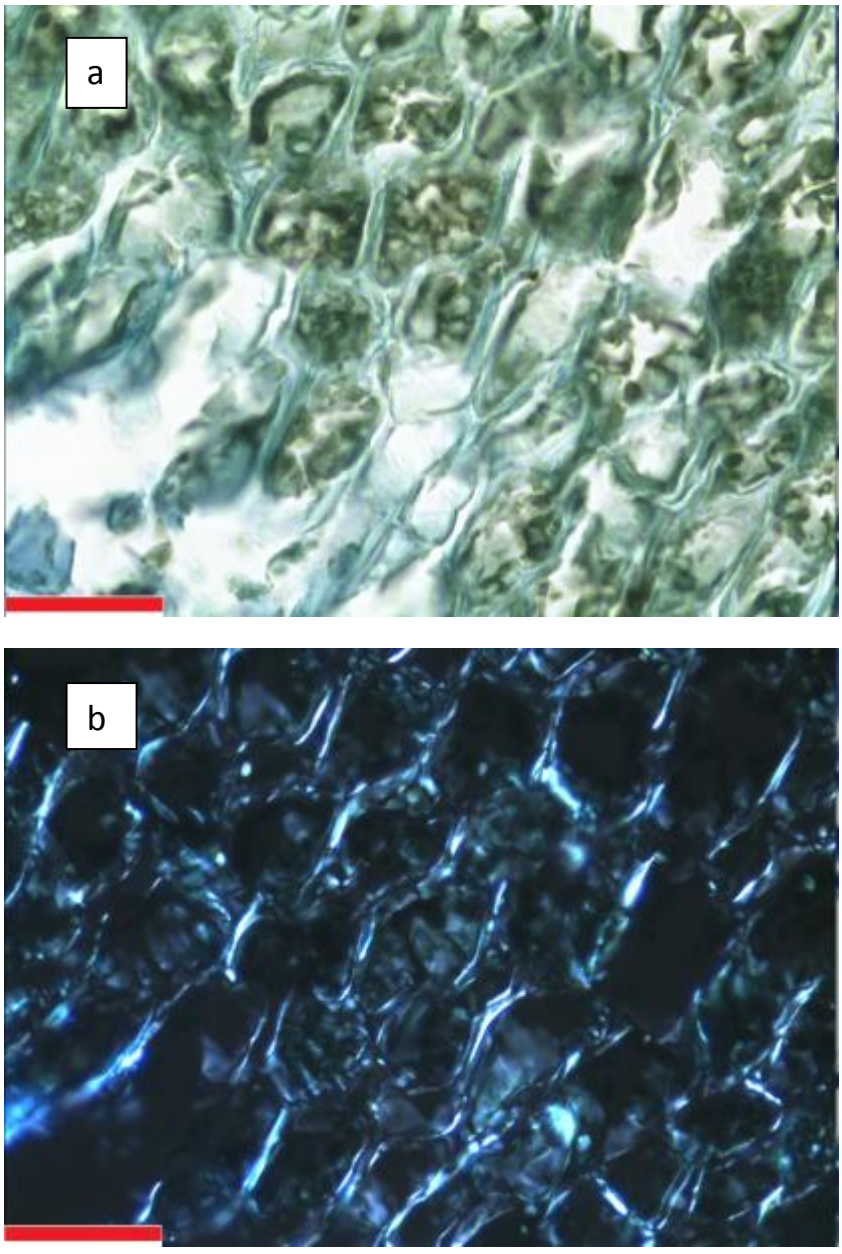

Figure 4.52 The green cellulose plant cells of 51813 (TB) shown with bright field illumination (a) and polarised light (b). Note the birefringence of the cellulose cell walls in (b). Scale bar = 25 microns.

Sample MM 1777

Sample 1777, shown purple and brown stained by H+E in figure 4.53, appears as badly degraded unidentifiable material.

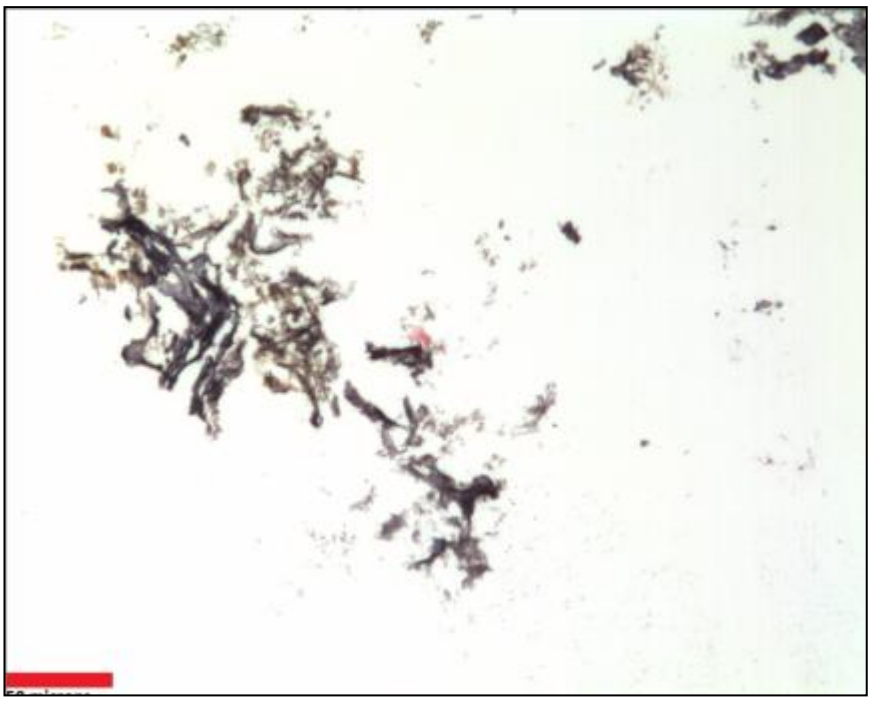

Figure 4.53 Representative image of sample 1777 (H+E). The material is unidentifiable. Scale bar = 50 microns.

Sample MM 11724

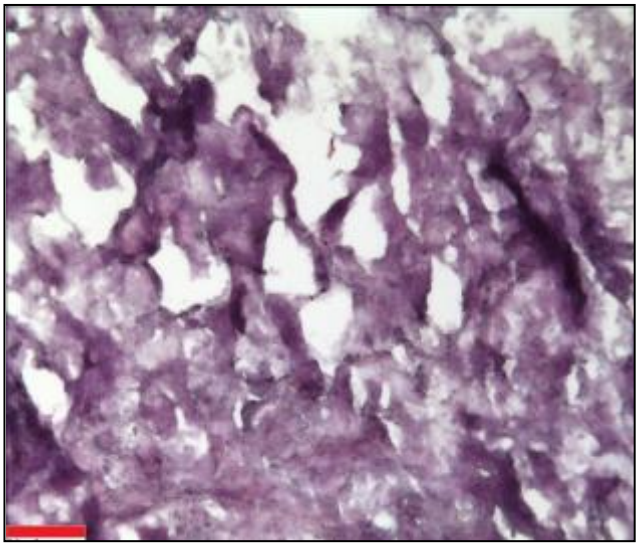

Figure 4.54 Badly degraded and unidentifiable tissue from 11724 (H+E). Scale bar = 50 microns.

The general appearance of tissue from mummy 11724 can be seen in Figure 4.54. The tissue appears as badly degraded purple tissue when stained with haematoxylin and eosin. The holes appear to be from liquefaction or putrefaction rather than tears arising from microtomy. The poor state of preservation of this section means that identification of the tissue is impossible.

Unprovenanced mummies

Sample 34193

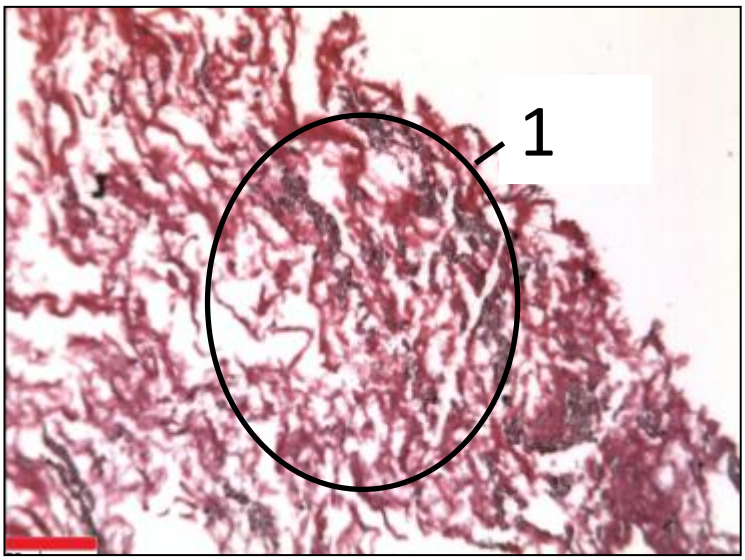

Figure 4.55 Section of mummy 34193 showing degraded tissue and brown substance (1) (H+E). Scale bar = 50 microns.

Figure 4.55 shows a representative image of tissue for sample 34193 stained with haematoxylin and eosin. The unidentifiable tissue appears as red fibres with a brown substance (1) in between the fibres in certain areas. The brown substance is not anthracotic and is unidentifiable. Due to the very poor state of preservation, the tissue is also unidentifiable.

Sample 37949

Figure 4.56 shows a representative image of the sample from 37949. There is very little material in the section and the tissue is unidentifiable.

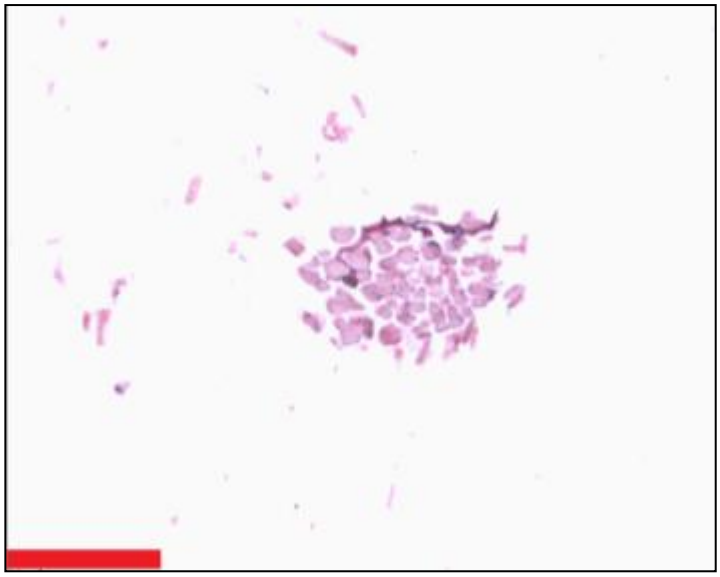

Figure 4.56 Representative image of sample from 37949 (H+E). There is no discernible tissue in the sample. Scale bar = 50 microns.

4.3.2 *Summary of histological examination of mummified material*

Out of the twenty samples labeled as mummified lung material and examined by this study, only nine samples were found to contain identifiable lung tissue. The eleven remaining samples contained plant material, coprolite or were unidentifiable (Table 4.2 and 4.3) The tables also reveal that every lung tissue sample contained anthracotic (soot) and birefringent particles, possibly including phytoliths.

All the samples identified as lung came from the Dakhleh oasis and were spontaneously mummified. Only two unidentified samples came from the Dakhleh excavations and they comprised the youngest age at death (A132 aged 3 to 5 months) and the oldest age at death (A105 aged 50 to 60 years). The lung tissue consists of densely compacted sections of lung tissue with deposits of anthracotic pigment which has been co-deposited with birefringent particles. The best preserved lung samples (A13 and A126) came from males aged between 50 and 20 years old respectively. The only female lung sample (A4) was not well preserved but not severely so compared to male examples from the Oasis.

All the material from the cemeteries at Kulub Narti was identified as coprolite which came from spontaneously mummified corpses. The coprolite consists of plant remains along with unidentifiable, badly degraded material.

All the intentionally mummified material from the elite classes was not identified as lung. Sample BM 51813 from an 19th Dynasty mummy from Thebes was identified as coprolite and the other samples from provenanced mummies (MM 1777 and MM 11724) and those whose origin is known (34193, 3794) contained badly degraded, unidentifiable tissue.

Table 4.2 The identification number and provenance (age, location, and social status) of Dakhleh Oasis samples along with their histological identification along with presence of anthracotic pigment, birefringent particles and phytoliths.

Mummy	Period	Location	Social status	Tissue	Anthracosis	Birefringent	Phytoliths
DO-45	G-R ~200AD	Dakhleh Oasis	Non-elite	Lung	Yes	Yes	Possible
DO-46	G-R ~200AD	Dakhleh Oasis	Non-elite	Lung	Yes	Yes	Possible
A4	Ptolemaic/G-R	Dakhleh Oasis	Non-elite	Lung	Yes	Yes	Possible
A13	Ptolemaic/G-R	Dakhleh Oasis	Non-elite	Lung	Yes	Yes	Possible
A102	Ptolemaic/G-R	Dakhleh Oasis	Non-elite	Lung	Yes	Yes	Possible
A105	Ptolemaic/G-R	Dakhleh Oasis	Non-elite	Unidentifiable/ Possible plant	No	No	No
A108	Ptolemaic/G-R	Dakhleh Oasis	Non-elite	Lung	Yes	Yes	Possible
A110	Ptolemaic/G-R	Dakhleh Oasis	Non-elite	Lung/Skin	Yes	Yes	Possible
A111	Ptolemaic/G-R	Dakhleh Oasis	Non-elite	Possible Lung	Yes	Yes	Possible
A126	Ptolemaic/G-R	Dakhleh Oasis	Non-elite	Lung	Yes	Yes	Possible
A132	Ptolemaic/G-R	Dakhleh Oasis	Non-elite	Unidentifiable	N/A	N/A	N/A

Table 4.3 The identification number and provenance (age, location, and social status) of non-Dakhleh Oasis samples along with their histological identification along with presence of anthracotic pigment, silicosis and phytoliths.

Mummy	Period	Location	Social status	Tissue	Anthracosis	Birefringent	Phytoliths
S82	Christian ~550AD	Kulub Narti	Non-elite	Coprolite	N/A	N/A	N/A
S85	Christian ~550AD	Kulub Narti	Non-elite	Coprolite	N/A	N/A	N/A
S195	Christian ~550AD	Kulub Narti	Non-elite	Coprolite	N/A	N/A	N/A
BM 51813	19th Dynasty	Thebes	Elite	Plant/Coprolite	N/A	N/A	N/A
MM 1777	25th Dynasty	Thebes	Elite	Unidentifiable	N/A	N/A	N/A
MM 11724	12th Dynasty	Rifeh	Elite	Unidentifiable	N/A	N/A	N/A
34193	Unknown	Unknown	Elite	Unidentifiable	N/A	N/A	N/A
37949	Unknown	Unknown	Elite	Unidentifiable	N/A	N/A	N/A

4.4 Shape and size characterisation of particulates by light microscopy

4.4.1 *Modern surrogates*

Surrogate soots

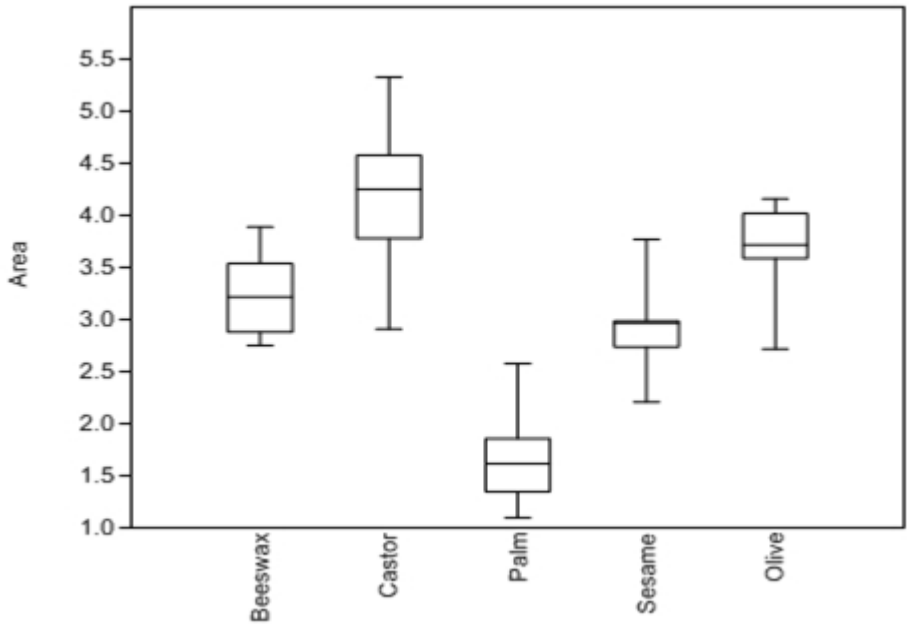

Figure 4.57 Box and whisker plots of the median area of soot particles from combustion of five different fuels. The whiskers show the lowest and maximum recorded values, n = 250.

Figures 4.57 and 4.58 show that the median size of the soot particles from the combustion of all the surrogate fuels are less than 10μm and are, therefore, highly respirable. Statistical analysis reveals that the data are not normally distributed. Palm oil soot appears smaller than the other soots and a Kruskal-Wallis test shows that the difference is significant (probability, P between 0.02 and 0.012). Beeswax, sesame and olive oil soot are similarly sized (P > 0.05). Castor Oil produces soot that is the largest on average of the five fuels examined; it is similar in size to beeswax (P = 0.9; level of significant difference is P > 0.05) but is different (P = 0.06) to sesame oil.

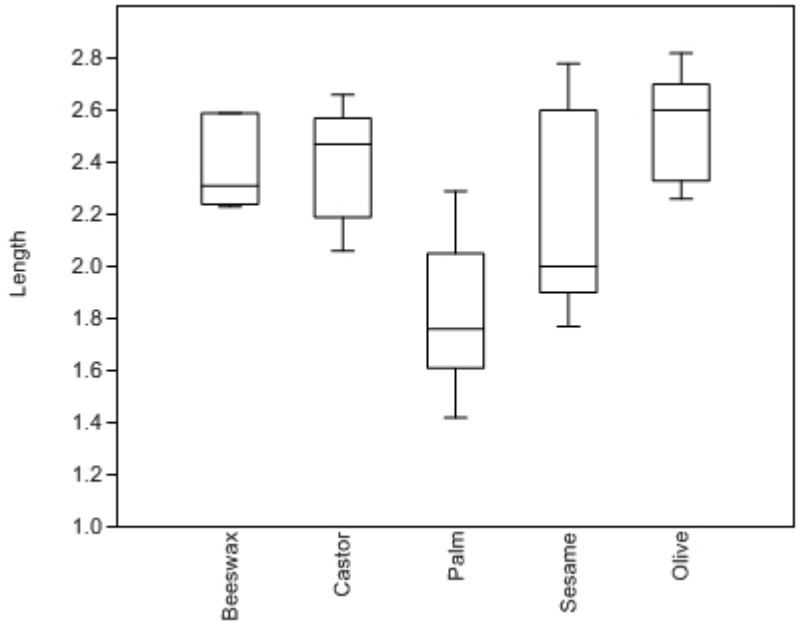

Figure 4.58 Box and whisker plots of the median length of soot particles from combustion of five different fuels. The whiskers show the lowest and maximum recorded values, n = 250.

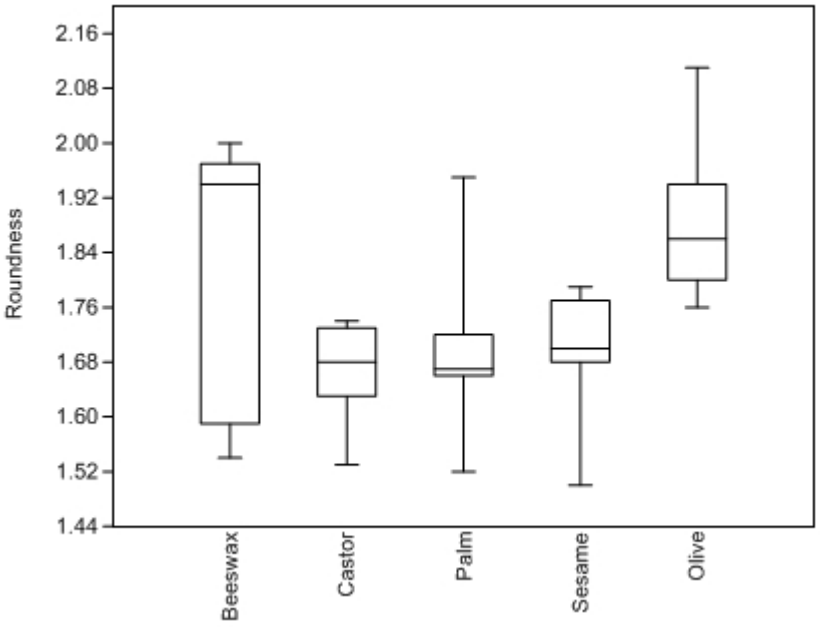

Figure 4.59 Box and whisker plots of the median roundness of soot particles from combustion of five different fuels. The whiskers show the lowest and maximum recorded values, n = 250.

Figure 4.59 shows the average roundness of the five types of soot particles and where a perfect circle give a value of one (1). Statistical analysis reveals that the data are not normally distributed. Comparing the values using a Kruskal-Wallis test

shows that palm oil soot is significantly rounder than olive oil soot (P = 0.013). Sesame oil is also significantly rounder than olive oil soot (P = 0.037). Sesame and palm oil soots are similarly rounded (P = 0.834), as are beeswax and olive oil soots (P = 0.841).

Inorganic particles (sand, mud brick and phytoliths)

Figures 4.60 and 4.61 show that of all the inorganic particles examined, only phytoliths are respirable as the other particulates are too large to enter the lung. All the median sand and mud brick particles are too large to be respirable. Tuna Al Gebel sand in particular is much too large to be respirable. However, these are the mean values and the minimum values are much lower and indicate there are some respirable particles, constituting between 5 and 10% of the total, present in all samples.

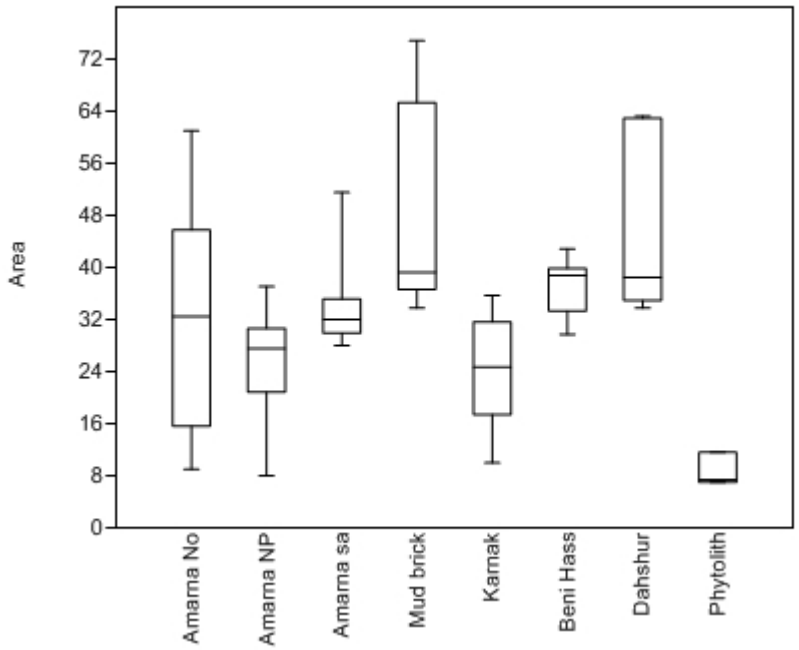

Figure 4.60 Box and whisker plot of median area of sand samples (from Amarna, Amarna North Palace, Beni Hassan, and Karnak), mud brick samples (from Amarna NP, mud brick and Dahshur Pyramid) and phytoliths. The whiskers show the lowest and maximum recorded values, n = 250.

Tuna Al Gebel has been omitted from Figure 4.60 and 4.61 as it is greatly different to the other mean areas. Statistical analysis reveals that the data are not normally distributed. Comparing the values using a Kruskal-Wallis test shows that the two mud bricks are significantly different (P = 0.037). Tuna Al Gebel is significantly

different to all the other sands (P = 0.008). The other sands are very similar (p=0.210 or above). The average area of the phytoliths is significantly smaller than all the other inorganic particles (P = 0.037).

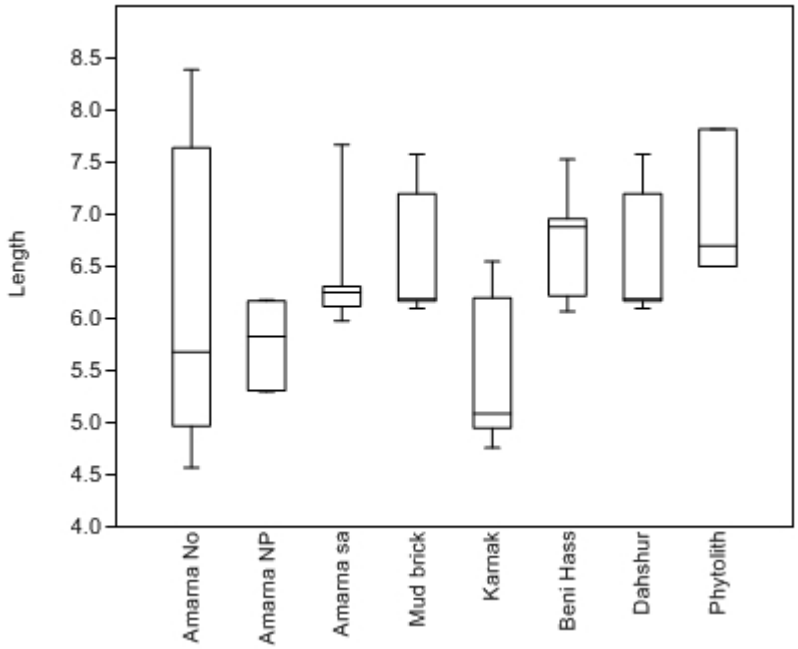

Figure 4.61 Box and whisker plot of median length of sand samples (from Amarna, Amarna North Palace, Beni Hassan, and Karnak), mud brick samples (from Amarna NP, mud brick and Dahshur Pyramid) and phytoliths. The whiskers show the lowest and maximum recorded values, n = 250.

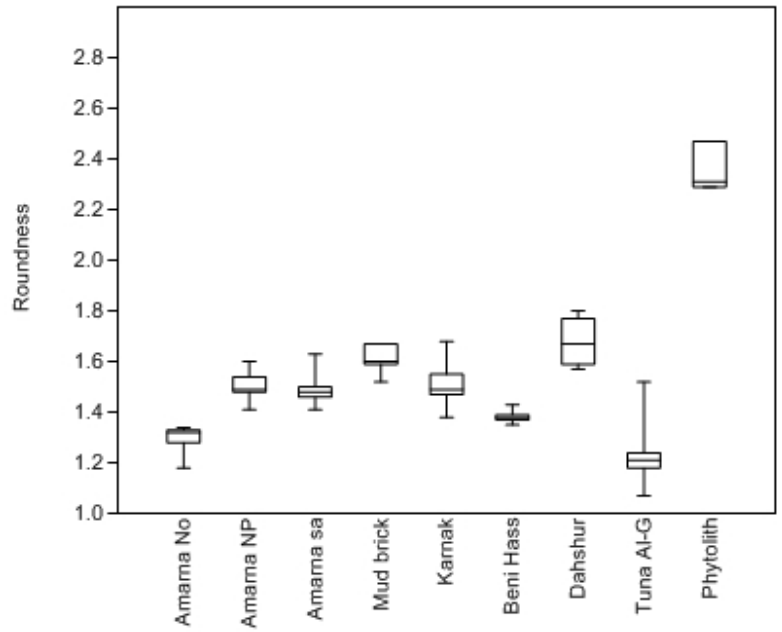

Figure 4.62 Box and whisker plot of median roundness of sand samples (from Amarna, Amarna North Palace, Beni Hassan, and Karnak), mud brick samples

(from Amarna NP, mud brick and Dahshur Pyramid) and phytoliths. The whiskers show the lowest and maximum recorded values, n = 250.

Figure 4.62 shows the median roundness of the five sand, three mud brick particles, and phytoliths, where a perfect circle = 1. Statistical analysis reveals that the data are not normally distributed. Comparing the values using a Kruskal-Wallis test shows that sand from Beni Hassan is significantly rounder than Karnak (p=0.034). Amarna north palace sand is significantly different to all the sands (p=0.012) except for Tuna Al Gebel (p=0.345). Amarna sand is very similar to Karnak sand (p=0.835). The Amarna North Palace brick is significantly rounder than the Dahshur mud brick (p=0.037). Due to their needle-like shape, phytoliths are significantly less round than all the other inorganic particles (p=0.037).

4.4.2 Ancient particles

Pigmented and birefringent particles were analysed separately as the former are likely to be organic (possibly soot) while the latter are of inorganic origin – presumably either phytoliths or sand/mud-brick dust.

Anthracotic pigment particles

Figures 4.63 and 4.64 show that all the extracted anthracotic pigment particles are respirable; i.e., areas which would result in a diameter of less than 10 microns, which confirms that they were respired and not artefacts arising from post-mortem contamination. In all cases the maximum length is considerably less than 10 microns – 0.7 to 1.6 microns (Figure 4.64). The particles from A13 are the largest whilst statistical analysis reveals that the data are not normally distributed. Comparing the values using a Kruskal-Wallis test shows that A13 and mummies A4, A110 and A102 are significantly different (p = 0.051, 0.028 and 0.028 respectively), whilst all the other soots extracted from the remaining mummified lungs are very similar to each other (p = 0.4 to 1).

Figure 4.65 shows the average roundness of the five sand and two mud brick particles, where a perfect circle =1. Statistical analysis reveals that the data are not normally distributed. Comparing the values using a Kruskal-Wallis test shows

that all the roundnesses are similar and not significantly different. The most different are A4 and A13 (p= 0.093) whilst the other particles are similar (p= 0.24 to 1).

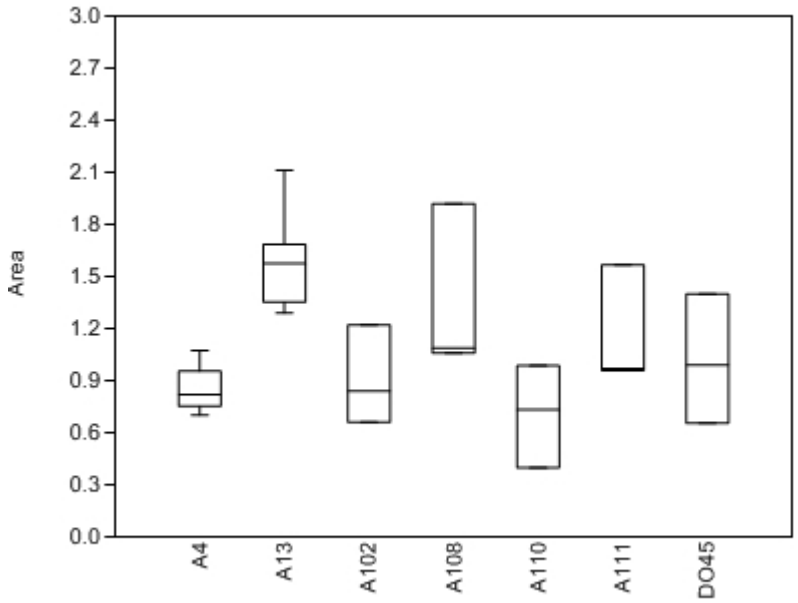

Figure 4.63 Box and whisker plot showing the median area of extracted anthracotic pigment particles from seven mummified lung samples. The whiskers show the lowest and maximum values, n = 250.

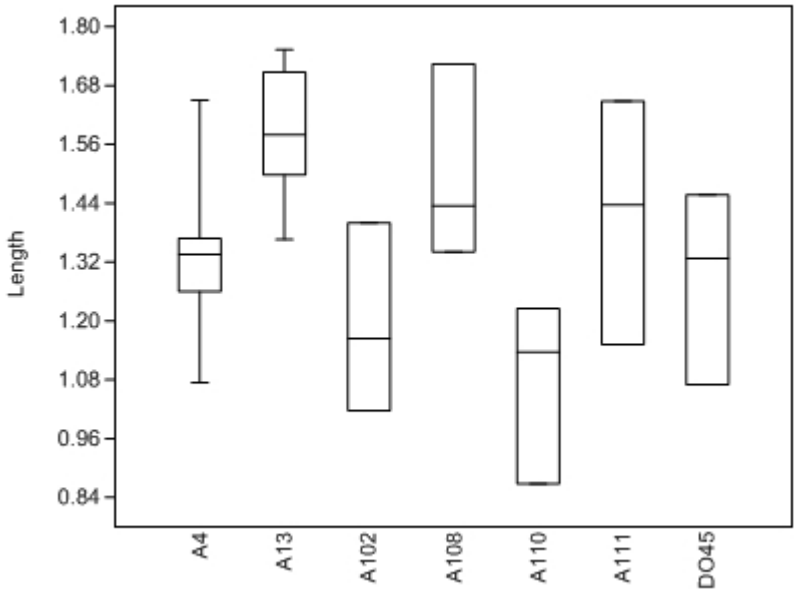

Figure 4.64 Box and whisker plot showing the median length of extracted anthracotic pigment particles from seven mummified lung samples. The whiskers show the lowest and maximum values, n = 250.

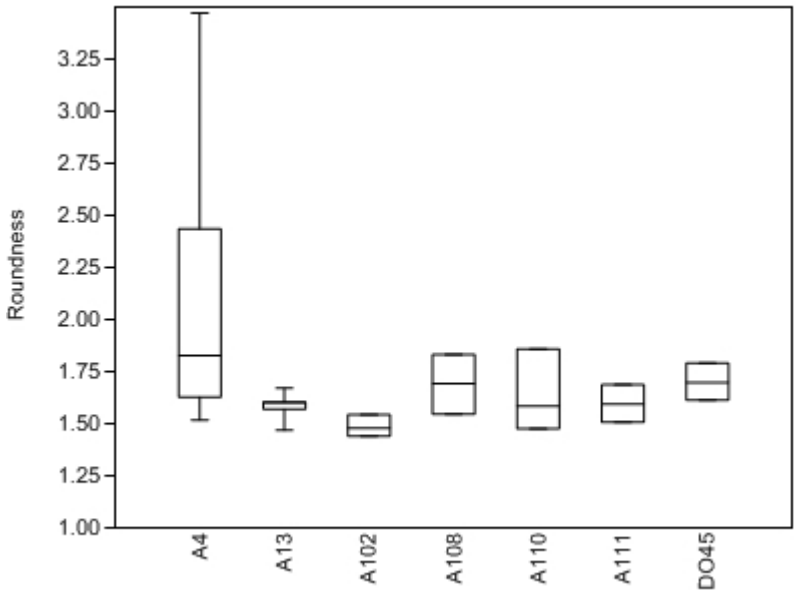

Figure 4.65 Box and whisker plot showing the median roundness of extracted anthracotic pigment particles from seven mummified lung samples. The whiskers show the lowest and maximum values, n = 250.

Birefringent particles

Figure 4.66 shows the median area of birefringent particles extracted from seven samples of mummified lung. All the particles are respirable are less than 10 microns in diameter. These particles are within the respirable range, however, they may also represent post mortem contamination. Statistical analysis reveals that the data are not normally distributed. Comparing the values using a Kruskal-Wallis test shows that all the birefringent particles are similar and not significantly different to each other. The most different are DO45 and A13/A110 ($p = 0.190$) whilst the other particles are very similar to each other ($p = 0.3662$ to 1.0).

Figure 4.69 shows the average area of the five sand and two mud brick particles. Statistical analysis reveals that the data are not normally distributed. Comparing the values using a Mann Whitney U test shows that all the roundness's are similar and not significantly different. The most different are A4 and A102 ($p = 0.100$) whilst the other particles are very similar ($p = 0.245$ to 1).

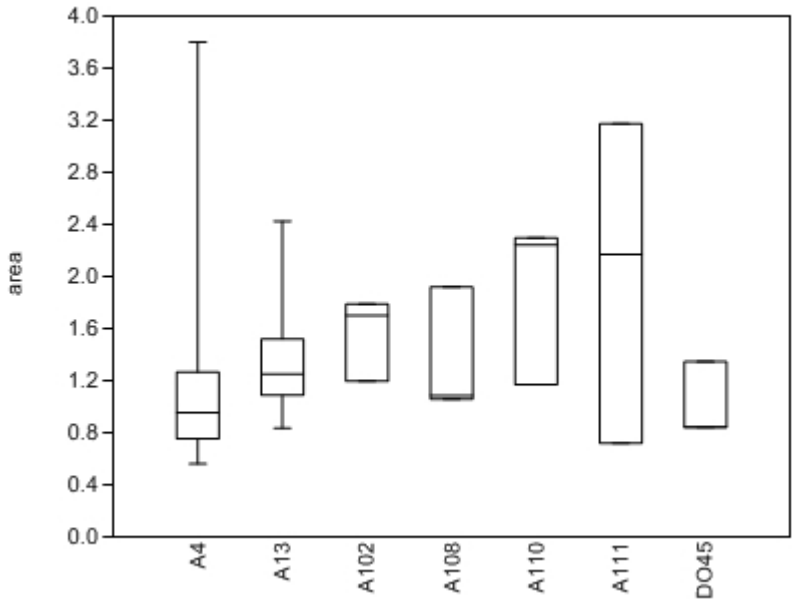

Figure 4.66 Box and whisker plot showing the median area of extracted birefringent particles from seven mummified lung samples. The whiskers show the lowest and maximum values, n = 250.

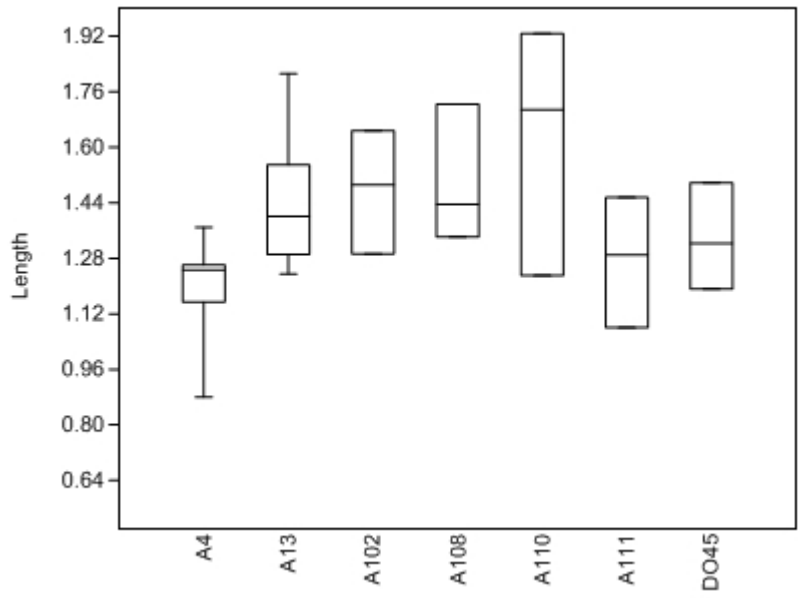

Figure 4.67 Box and whisker plot showing the median area of extracted birefringent particles from seven mummified lung samples. The whiskers show the lowest and maximum values, n = 250.

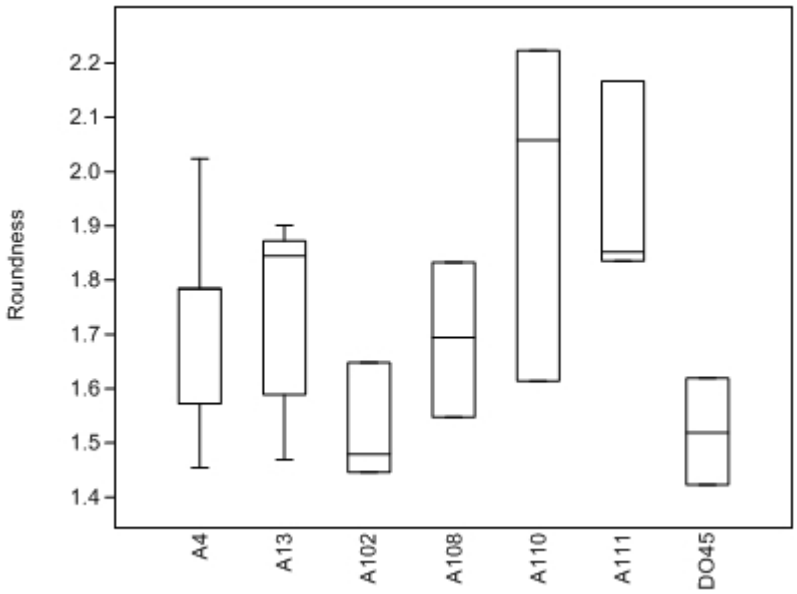

Figure 4.69 Box and whisker plot showing the median area of extracted birefringent particles from seven mummified lung samples. The whiskers show the lowest and maximum values, n = 250.

4.5 Environmental Scanning Electron Microscopy (ESEM)

4.5.1 Surrogate soot

A representative electron micrograph of surrogate soot from Beeswax is shown in figure 4.70. A densely packed layer of light grey small soot particles can be seen against a darker background of the carbon ESEM tab.

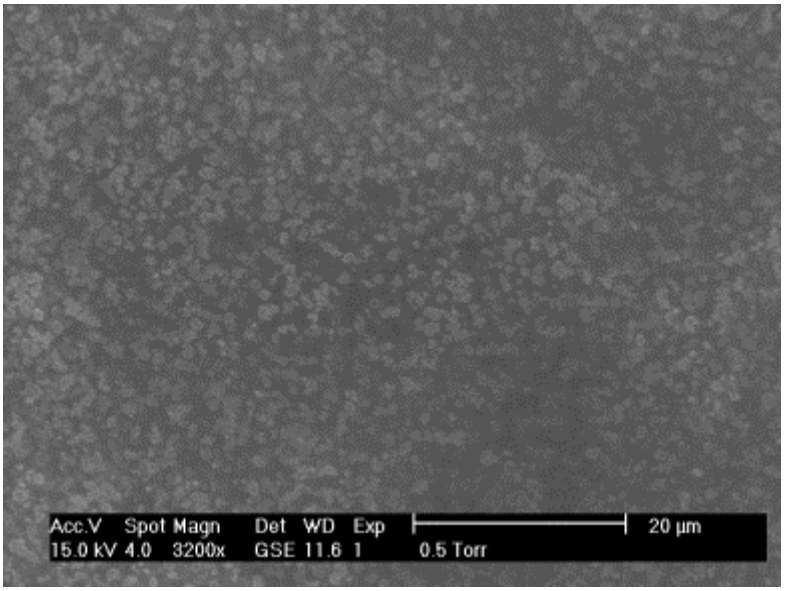

Figure 4.70 A representative electron micrograph of soot from Beeswax (scale bar is 20 microns).

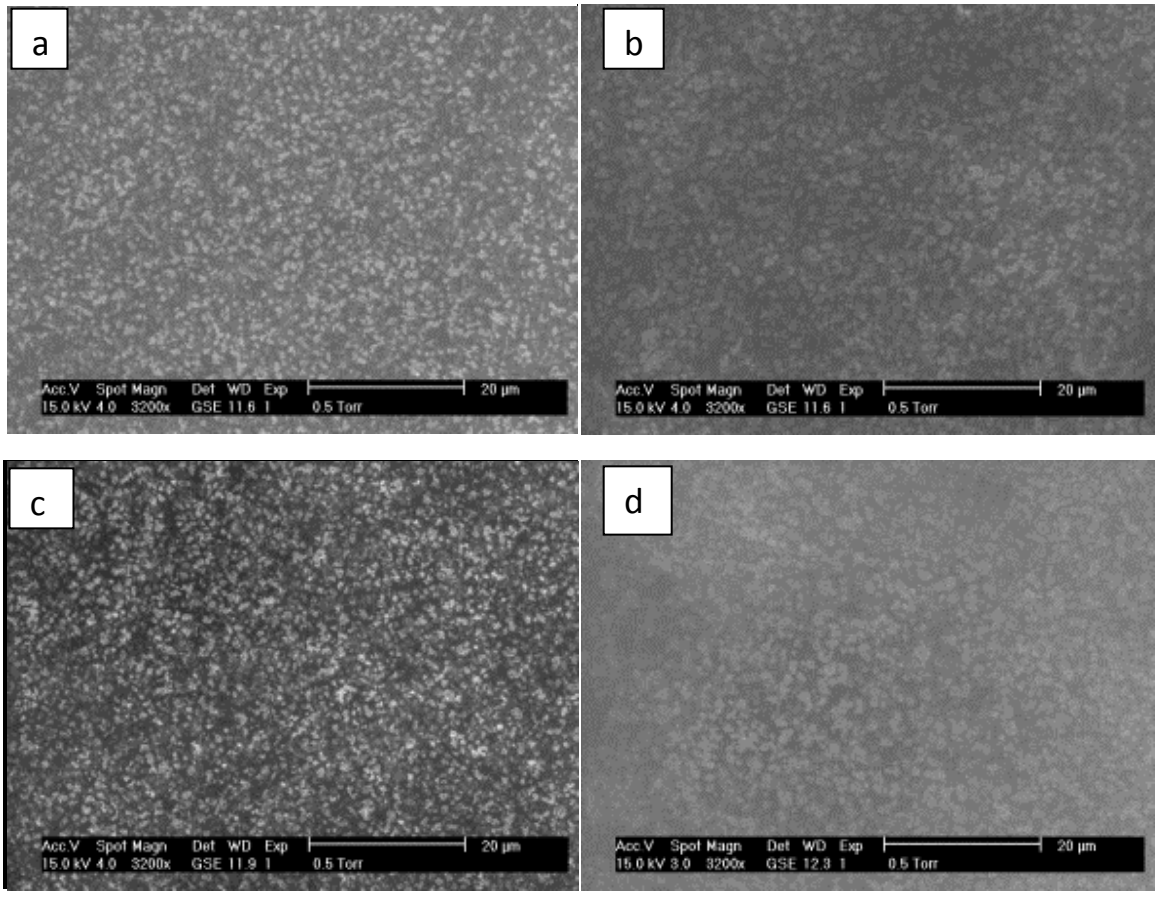

Figure 4.71 Representative images of the surrogate soots from Palm oil (a), Sesame oil (b), Olive oil (c) and Castor oil (d).

The other surrogate soots are extremely similar to each other. They all appear as small grey (false colour image) particles on the dark background of the carbon tab. There are no obvious differences in structure or size, supporting the light microscope observations regarding the similarity of the surrogate soot particles. The difference in contrast in the micrographs, i.e., soot particles from certain samples appear brighter than others, is an artefact due to different contrast settings when the ESEM was capturing micrographs.

4.5.2 *Surrogate inorganic particles*

Sand

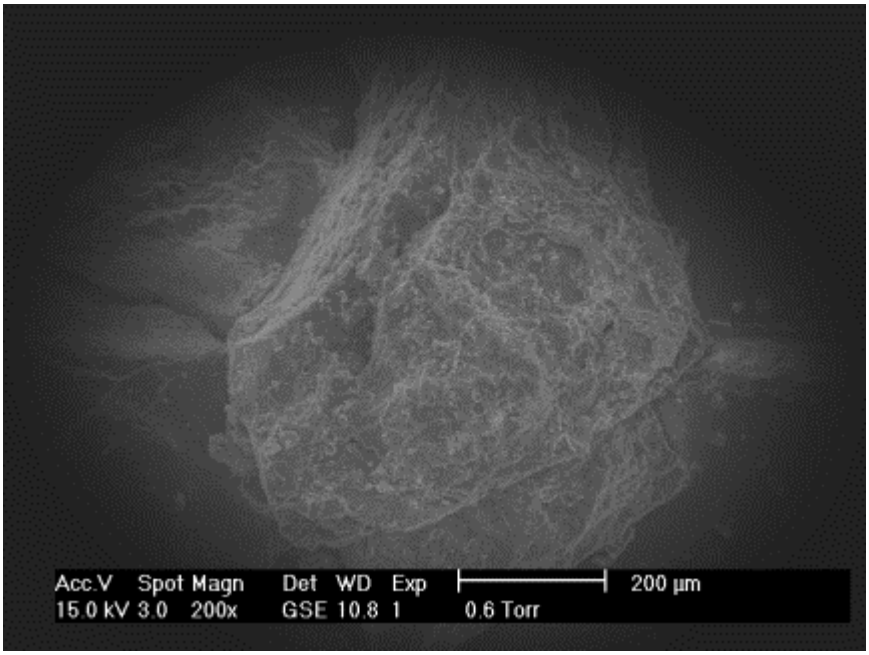

Figure 4.72 Representative micrograph of Amarna sand (scale bar is 200 microns).

Figure 4.72 shows a representative micrograph of sand taken from Amarna in Egypt. Although the grain of sand is large (more than 400 microns in breadth) smaller grains of sand can be seen in the background. The surface of the sand grain is rough and pitted.

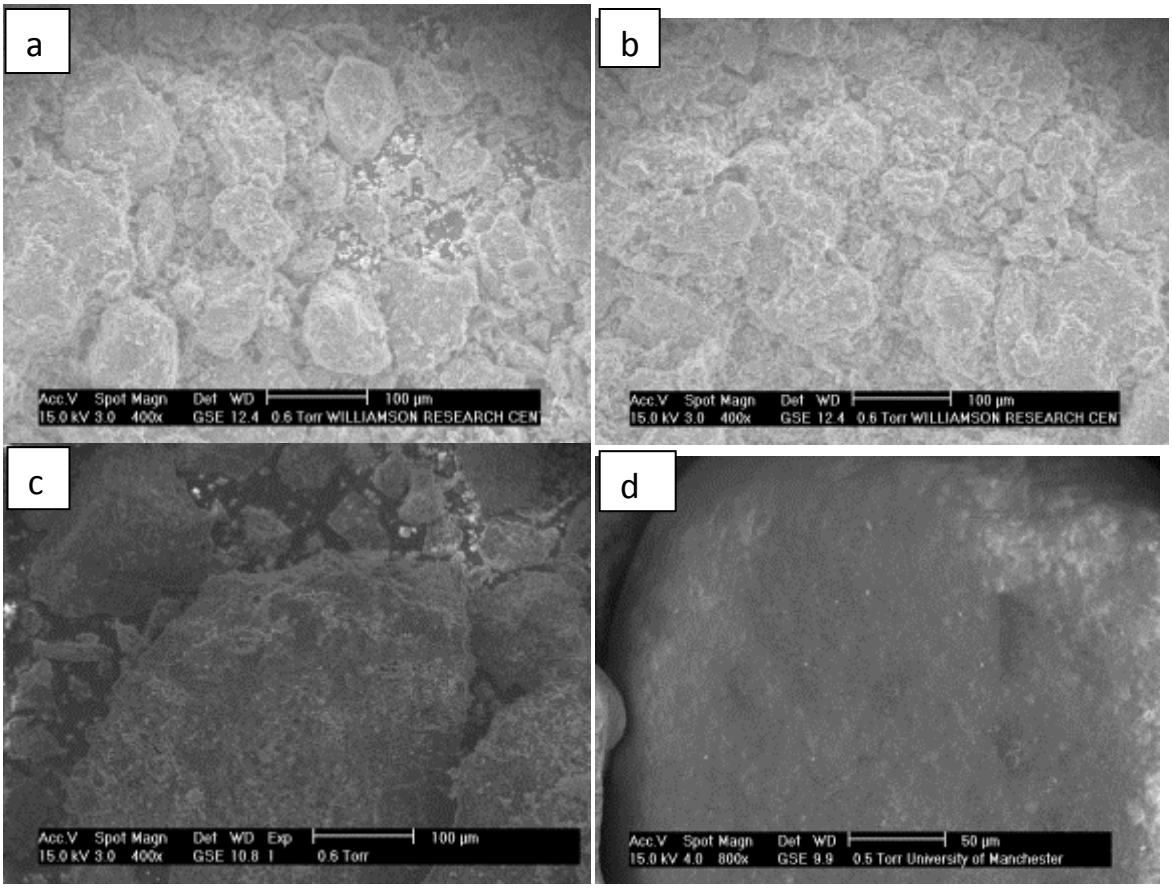

Figure 4.73 Representative micrographs of the sand taken from various sites in Egypt. Micrograph a) shows sand from the Northern Palace at Amarna, b) shows sand from Karnak, c) shows sand from Beni Hassan and d) shows sand from Tuna El-Gebel. The scale bar in a-c) are 100 microns, the scale bar in d) is 50 microns.

Micrographs of sand grains taken from other archaeological sites in Egypt can be seen in figure 4.73. Sands taken from the Northern Palace at Amarna (a), adjacent to the temple at Karnak (b) and Beni Hassan (c) appear very similar to each other. There are grains of multiple sizes which all appear to have rough and pitted surfaces. The sand from Tuna-el-gebel (d) is of a much larger size and appears much smoother than the other sands. The micrograph has been shown at a higher magnification to emphasise the smoother surface of this sand.

Mud bricks

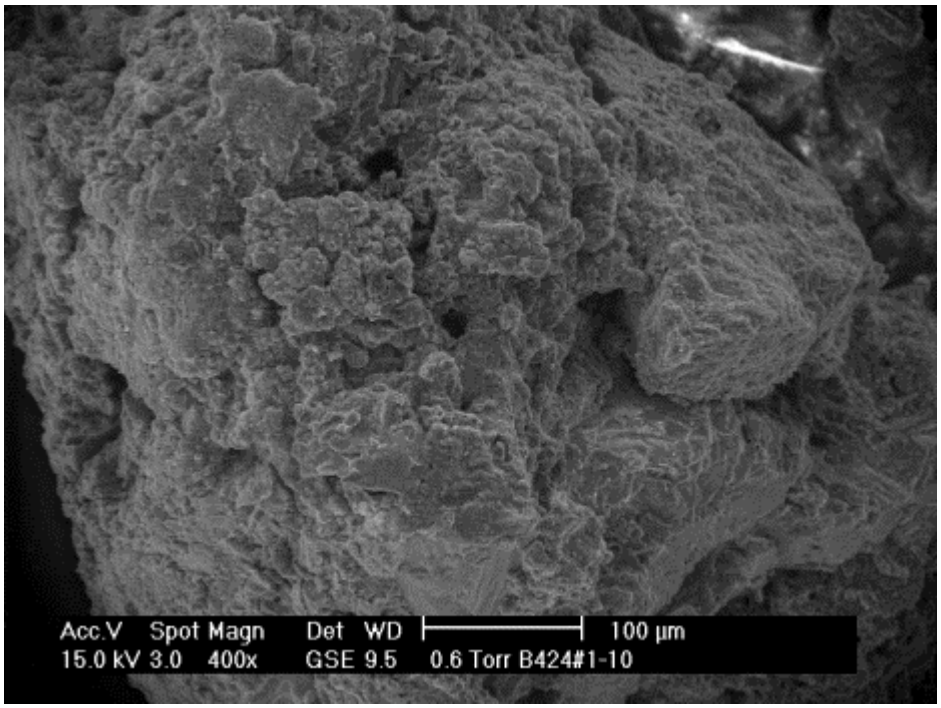

Figure 4.74 Representative micrograph of Amarna North Palace mud brick 1 (scale bar is 100 microns).

The appearance of material from a mud-brick when viewed at high magnification using an ESEM is shown in figure 4.74. The piece of mud brick appears to consist of numerous small irregular particles that are held together by a matrix of finer mud particles. The surface of the mud brick is very rough and pitted. The other two samples of mud brick from the North Palace at Amarna and the Dahshur pyramid are shown in figure 4.75a and b respectively. Again the mud bricks are made of small irregular particles that are held together by the mud matrix. Rectangular crystals are visible in the top left hand side of both images.

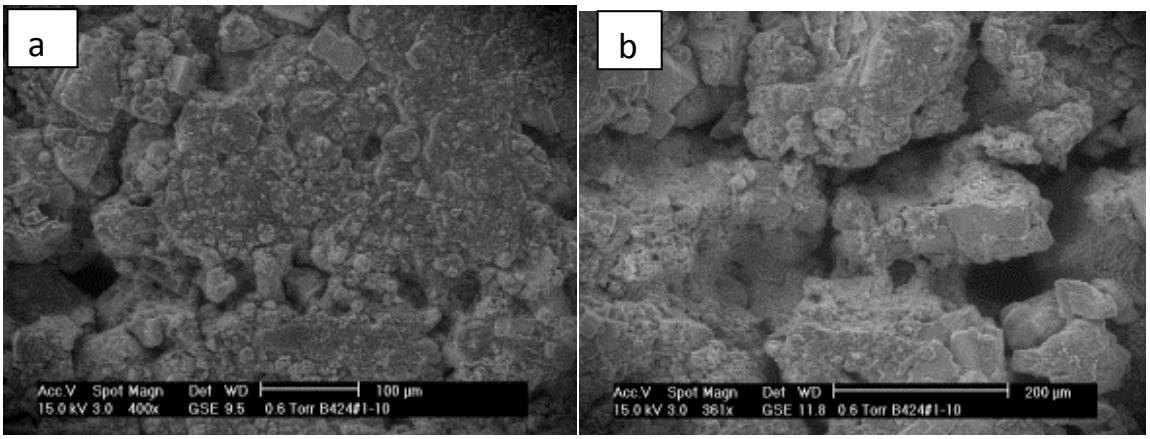

Figure 4.75 Representative micrographs of mud bricks from Amarna North Palace 2 (a) (scale bar is 100 microns) and the Dahshur pyramid (b) (scale bar is 200 microns).

Phytoliths

Figure 4.76 shows representative images from the ashed remains of barley. A large amount of plant debris can be seen, including plant sieve tubes of xylem or phloem (ringed red). When the sieve tube in the centre of 4.76a is viewed at higher magnification in figure 4.76b, a phytolith (1) can be seen in the debris next to the sieve tube (2).

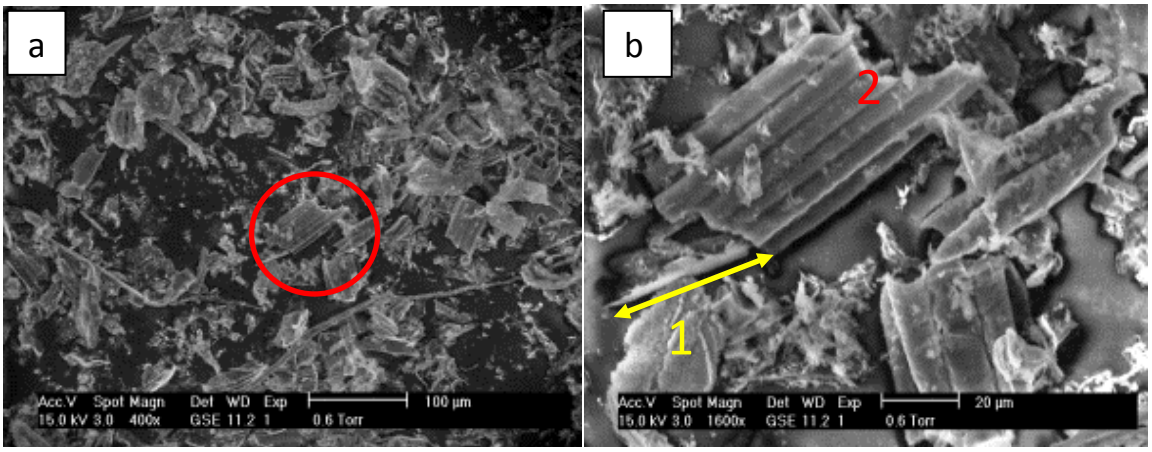

Figure 4.76 Representative micrographs of ashed plant material containing phytoliths. Lots of plant debris including sieve tube elements (ringed red) can be seen in a) (with scale bar of 100 microns). b) shows a phytolith (1) just underneath the sieve tube element (2) (scale bar is 20 microns).

4.5.3 Extracted ancient particles

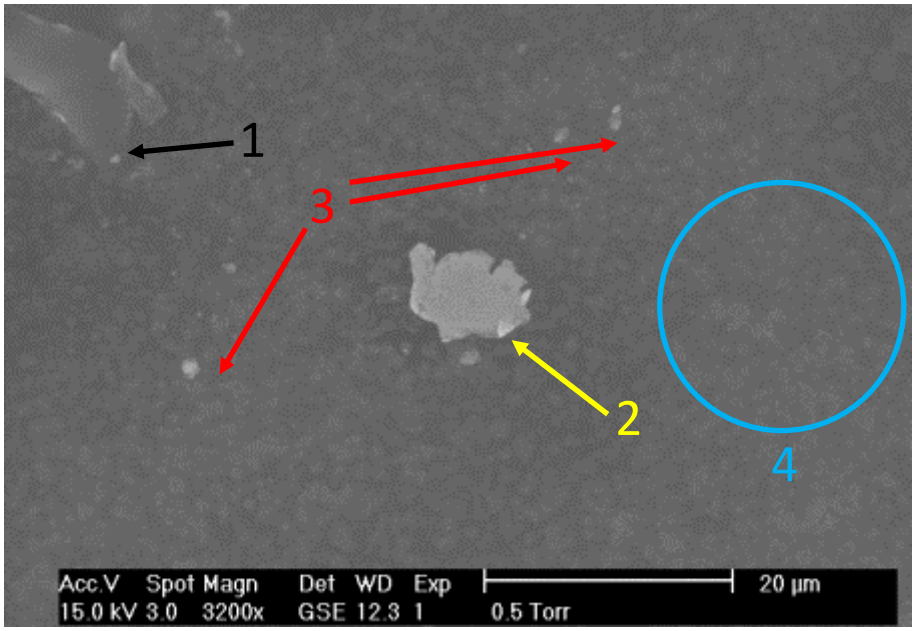

Figure 4.77 Representative micrograph of extracted particles from mummy sample A4. A tear (1) can be seen, along with tissue debris (2), crystals (3) and anthracotic pigment (4).

The representative appearance of particles extracted from mummified lungs (specimen A4) can be seen in figure 4.77. There is a tear at the top left hand of the micrograph (1), a white piece of tissue debris (2), with crystals (3) and anthracotic pigment particles (4) appearing light grey on the darker background of the ESEM sample stub.

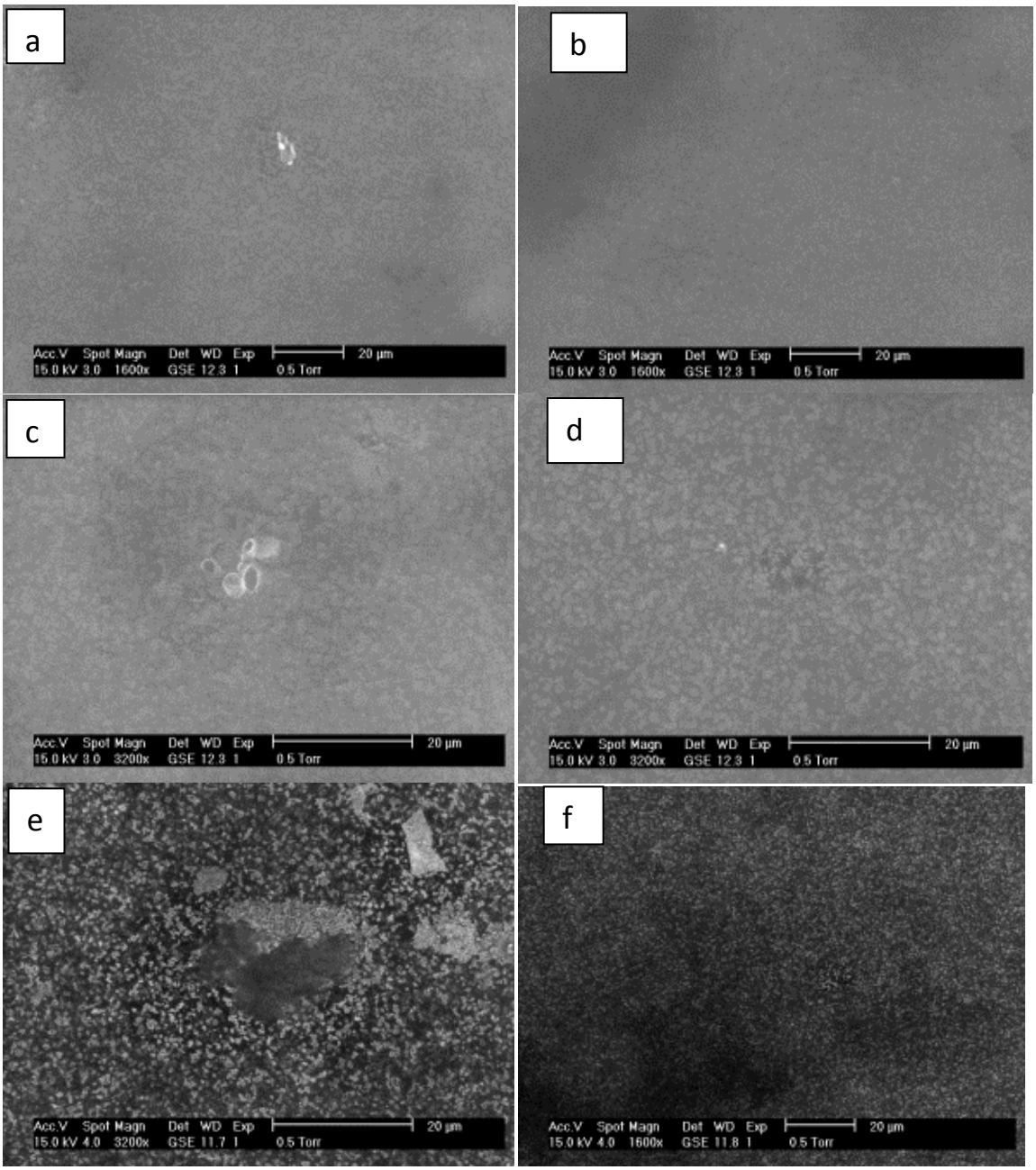

Figure 4.78 Representative micrographs of extracted particles from mummified specimens. a) show mummy A13, b) shows A102, c) shows A108, d) shows A110, e) shows A111 and f) shows DO45. The scale bar is 20 microns.

Figures 4.78a-f show representative images of the extracted birefringent and anthracotic particles from mummified lungs A13, A102, A108, A110, A111 and DO45 respectively. The particles all appear very similar to each other in both appearance and size, and can be visualised as light grey against the dark grey background of the carbon tab.

4.5.4 Ancient tissue

A de-waxed 5 micron section of ancient lung tissue from mummy A13, containing both birefringent and anthracotic pigment particles can be seen in Figure 4.79a and b. The rough surface of the section shows light grey circular and rectangular (1) particles held in a matrix of darker grey tissue background.

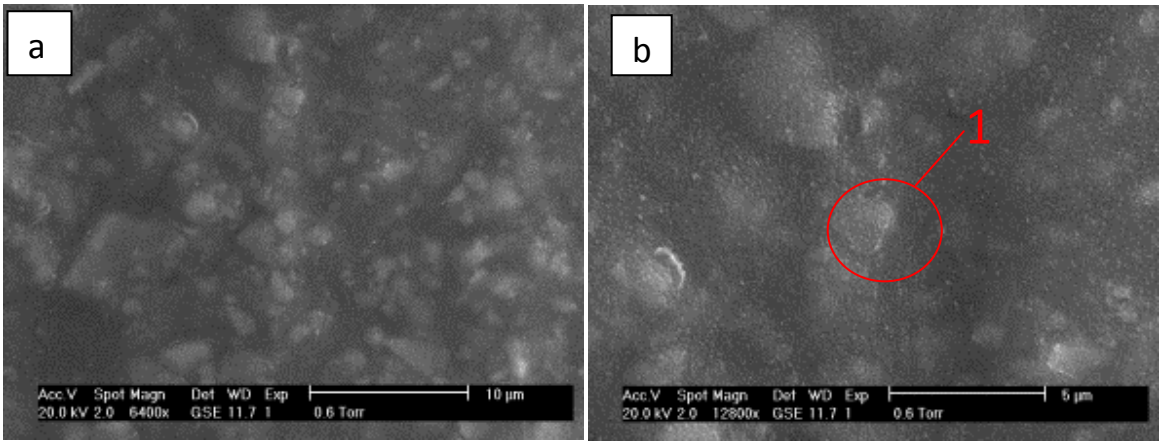

Figure 4.79 the appearance of ancient particles *in situ* in a section of mummified lung tissue A13. The rough surface of the section can be seen in a) where scale bar is 10 microns. b) show a magnified image of the same field showing an individual particle (1) where the scale bar is 5 microns.

3.6 Energy Dispersive X-ray Analysis (EDX)

Electrons hitting matter produce characteristic X-rays from the first micron of the surface of the sample. EDX detects elements on the basis of the energy signature of their X-rays in electron volts from 0 to 40KeV. However, the area of interest for characterisation lies between 0.5 and 10KeV (see Figure 4.80 below). This region is the area shown in the results spectra. The signal is quite 'noisy' which would be expected due to the numerous spectra with most of the counts in the region between 60 and 700 KeV. The initial peak at 1KeV is for carbon and is a standard inclusion across all the spectra obtained using this ESEM.

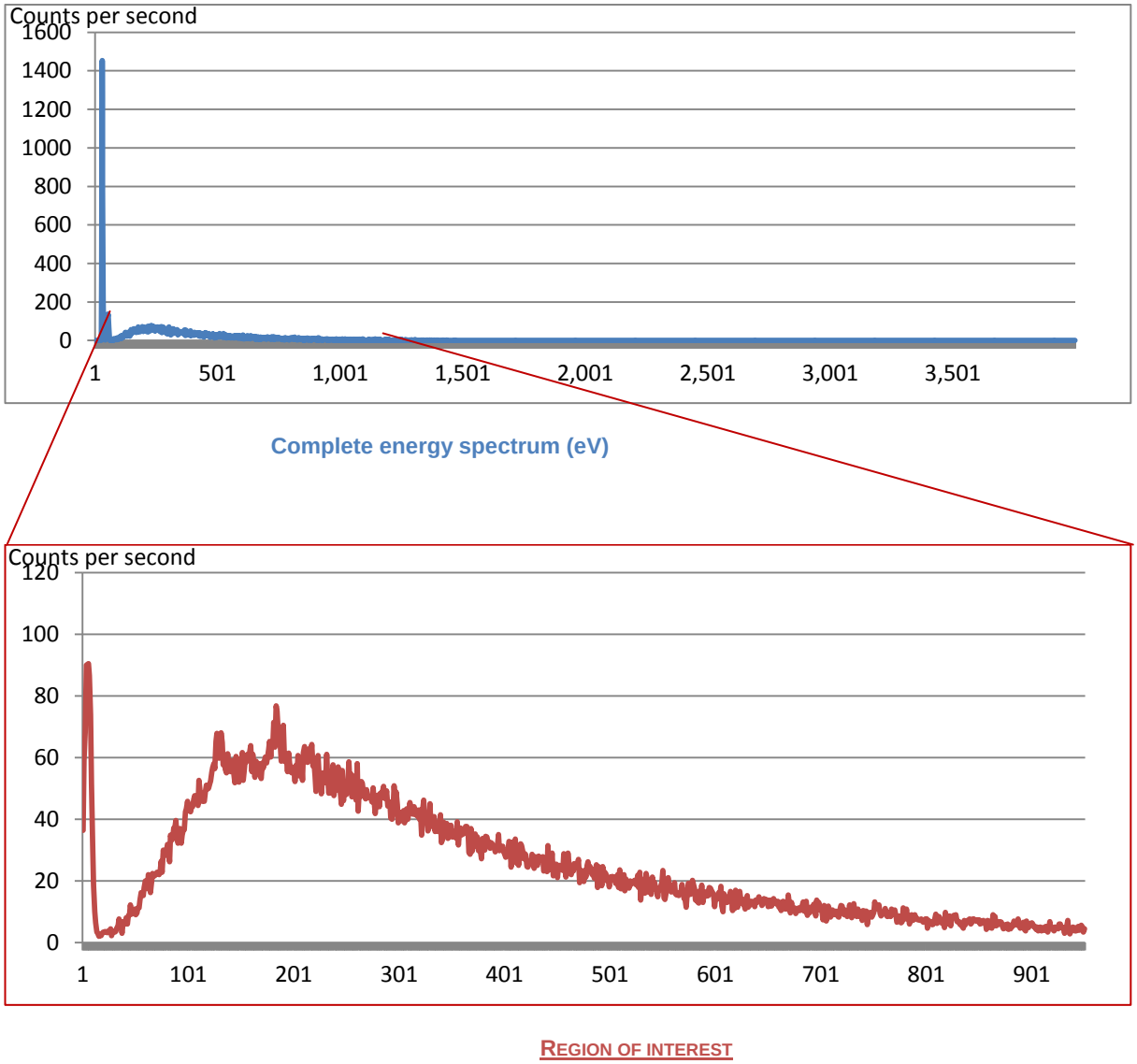

Figure 4.80 Typical EDX spectra of a section of material showing region of interest.

3.6.1 Surrogate soots

Figure 4.81a shows the mean EDX energy spectrum of the surrogate soot produced from the combustion of olive oil. There is a single clear and characteristic peak for Silicon (Si) at 1.74KeV.

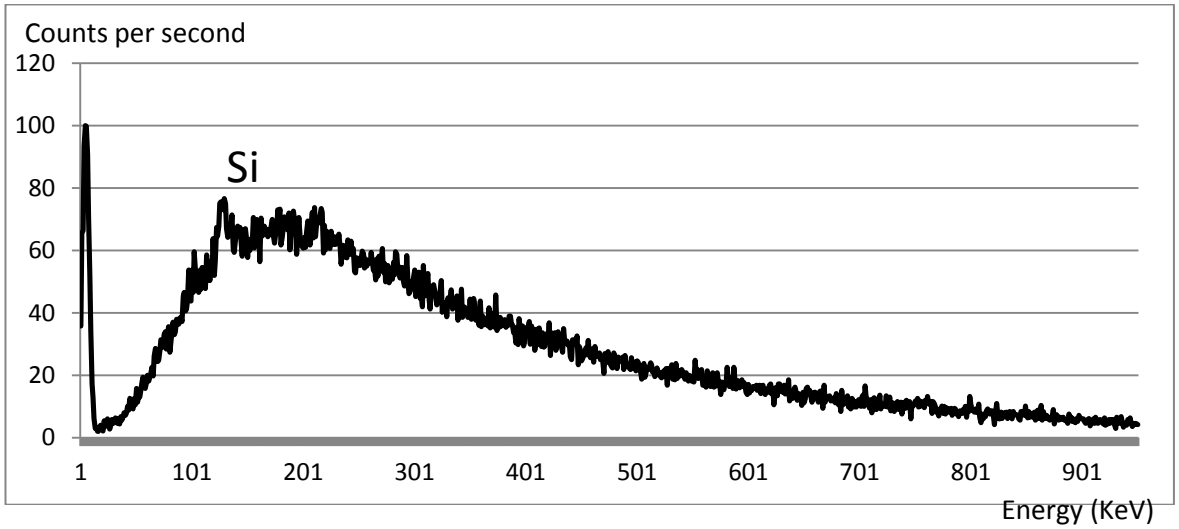

Figure 4.81a: EDX energy spectrum of soot from combustion of olive oil. Magnification = 3200x, acceleration voltage = 15kV, spot size = 4.0, collection time = 100 seconds, n = 5, background corrected.

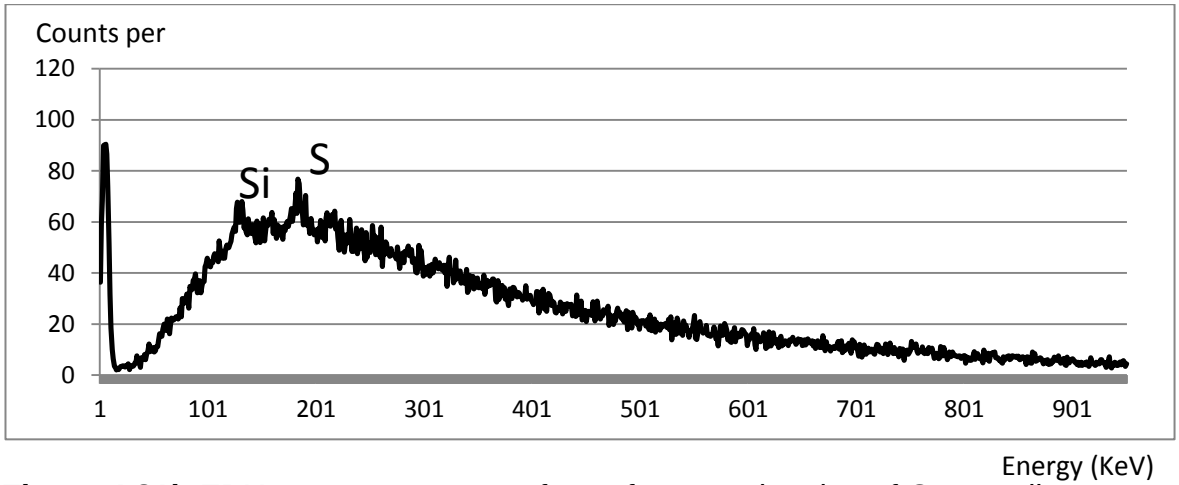

Figure 4.81b EDX energy spectrum of soot from combustion of Castor oil. Conditions are same as figure 4.81a.

Figure 4.81b shows the mean EDX energy spectrum for castor oil soot. In common with olive oil there is a peak for silicon (Si) at 1.74KeV; however, there is an additional peak for sulphur (S) at 2.30KeV.

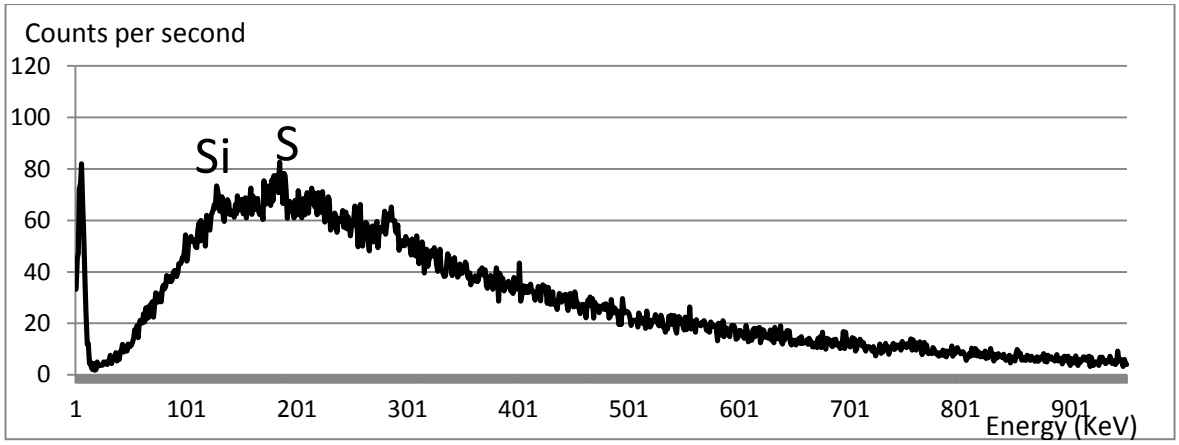

Figure 4.81c EDX enery spectrum of soot from the combustion of Palm oil. Conditions are same as figure 4.81a.

Figure 4.81c shows the mean EDAX energy spectrum for palm oil soot. In common with castor oil soot there is a peak for silicon (Si) at 1.74eV and sulphur (S) at 2.30KeV.

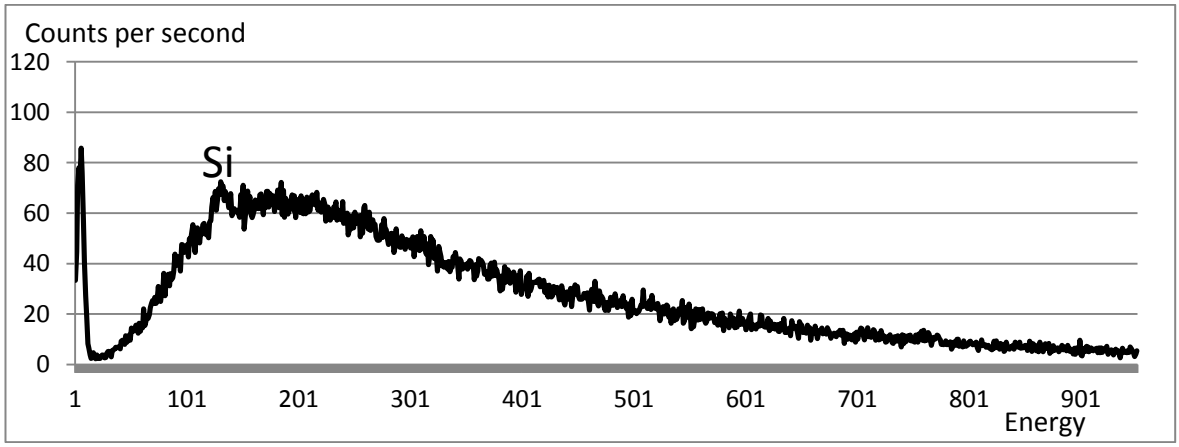

Figure 4.81d EDX energy spectrum of soot from the combustion of Sesame oil. Conditions are same as figure 4.81a.

Figure 4.81d shows the mean EDAX energy spectrum for sesame oil soot. In common with olive oil there is only one identifiable peak - for Silicon (Si) at 1.74KeV.

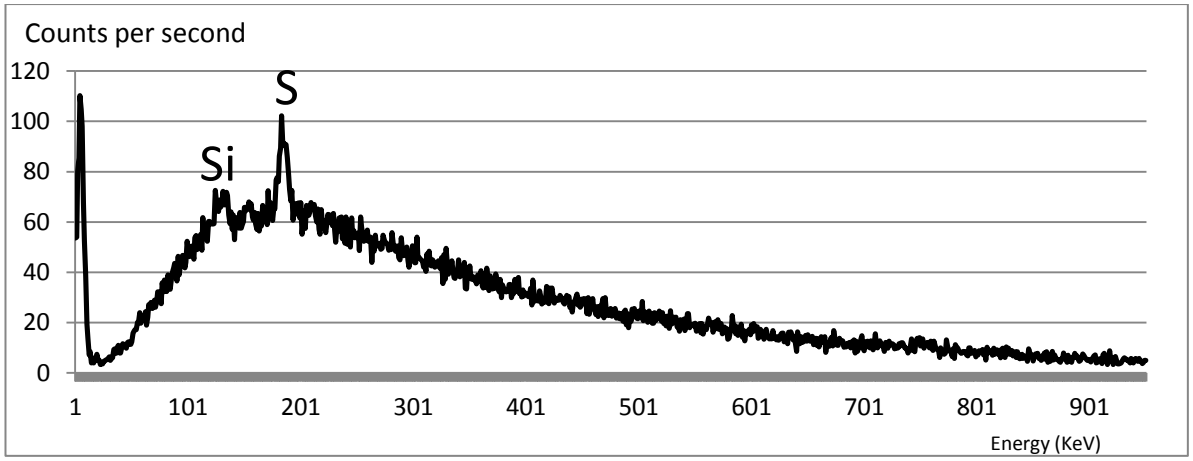

Figure 4.81e EDX energy spectrum of soot from the combustion of Beeswax. Conditions are the same as figure 4.81a.

The mean EDAX energy spectrum of beeswax soot is shown in Figure 4.81e. In common with Castor and Palm oil there is a peak for Silicon (Si) at 1.74KeV and Sulphur (S) at 2.30KeV. However, the sulphur peak appears much larger in intensity than in either Palm or Castor oil.

3.6.2 Modern sands

Figure 4.82a shows the mean EDX energy spectrum of the sand taken from an archaeological site at Amarna.

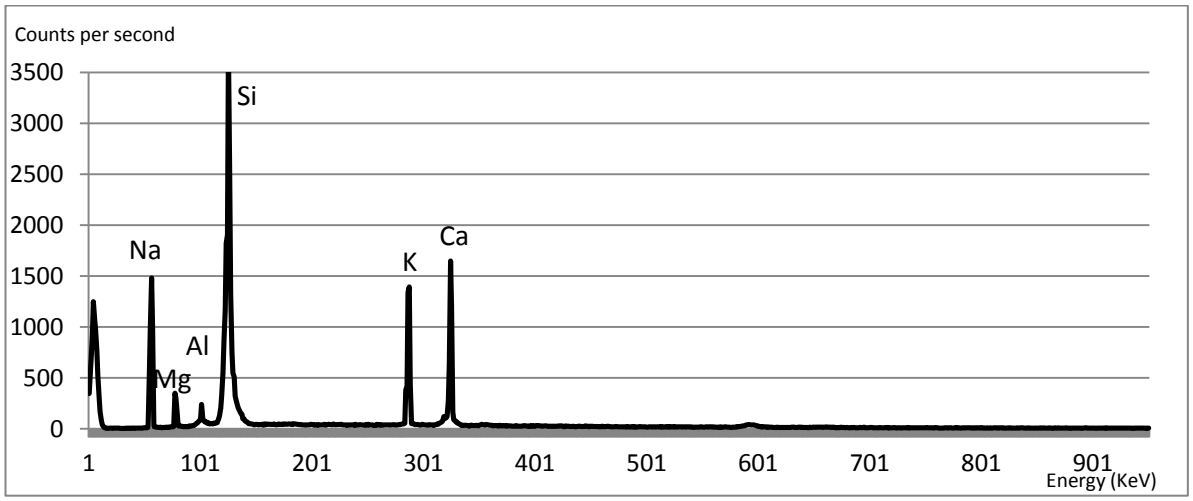

Figure 4.82a EDX energy spectrum of sand from Amarna. Acceleration voltage = 15kV, spot size = 4.0, collection time = 100 seconds, n = 5, background corrected.

There are clear and characteristic peaks for Silicon (Si) at 1.74KeV, Potassium (K) at 3.31KeV and Calcium (Ca) at 3.69KeV. There are small peaks for Magnesium

(Mg) at 1.25 (KeV), Aluminium (Al) at 1.49KeV and Sodium (Na) at 1.04KeV. On average, the counts per second are much higher than the recorded amounts for the surrogate soot.

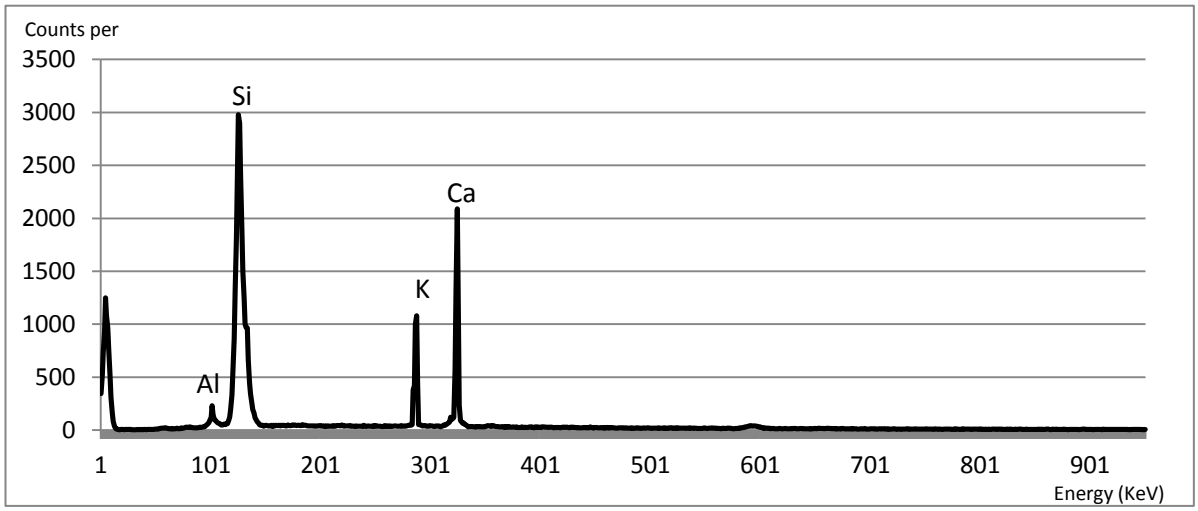

Figure 4.82b EDX energy spectrum of sand from Amarna North Palace. Instrument conditions are the same as figure 4.82a.

The EDX spectrum of Amarna North Palace sand shows its composition to be very similar to Amarna sand (Figures 4.82a and b) except it features no signal for sodium. Amarna North Palace sand has similar peaks for silicon, potassium and calcium, however the peaks have different intensities and the silicon peak has a different shape. There is also a small peak for aluminium.

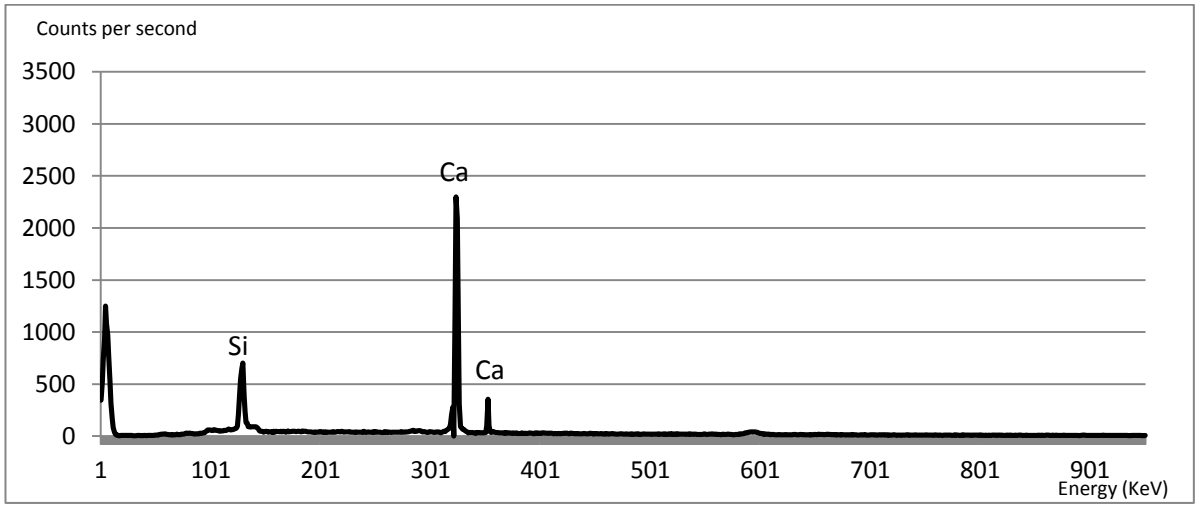

Figure 4.82c EDX energy spectrum of sand from Beni Hassan. Instrument conditions are the same as figure 4.82a.

The EDX of sand from Beni Hassan is shown in Figure 4.82c. The sand only has peaks for silicon and a double peak for calcium.

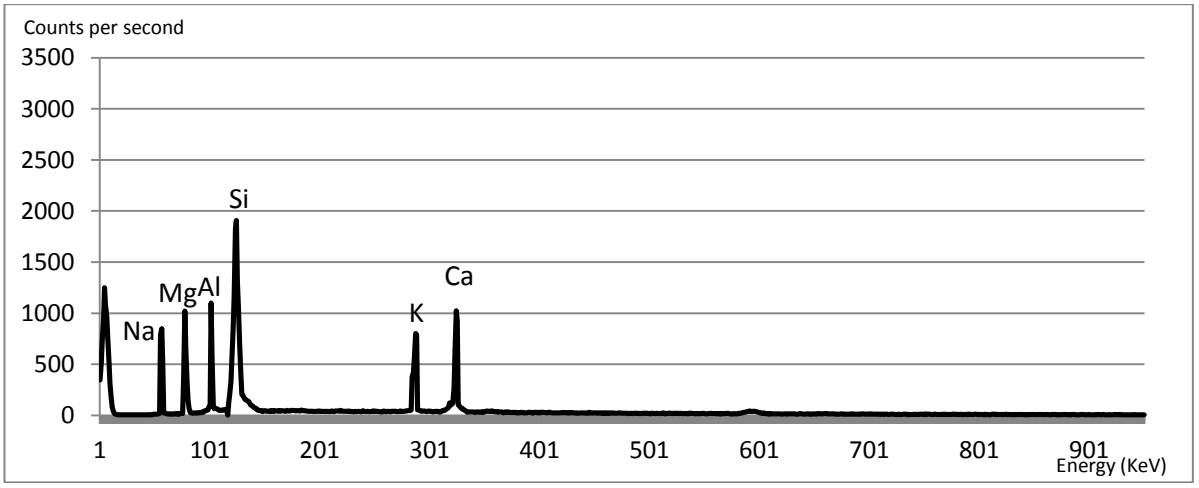

Figure 4.82d EDX energy spectrum of sand from Karnak. Instrument conditions are the same as figure 4.82a.

Sand from Karnak (in figure 4.82d) features a major peak for silicon and other peaks for sodium, magnesium, aluminium, potassium and calcium. Overall, Karnak sand has a lower number of total counts than the other sands.

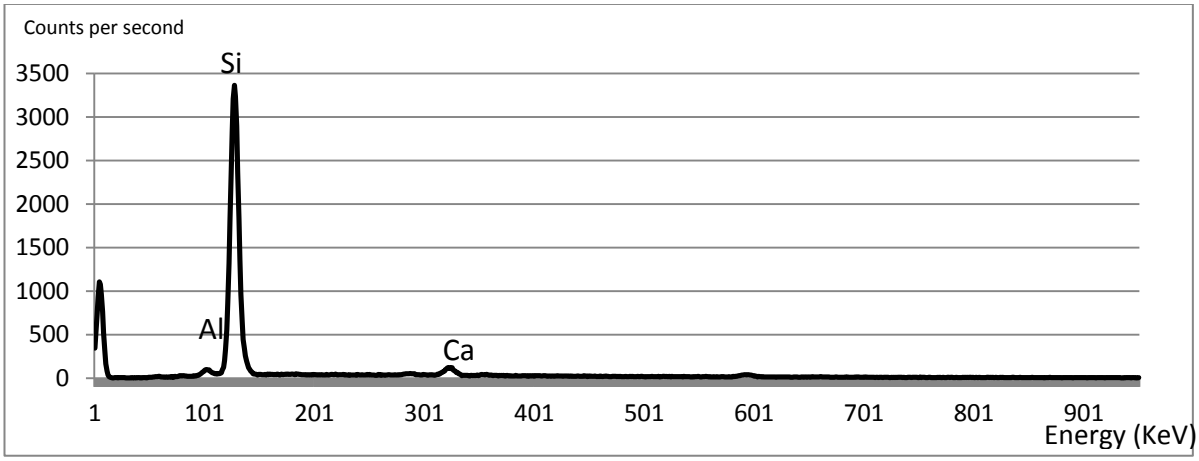

Figure 4.82e The mean EDX energy spectrum of sand from Tuna Al Gebel. Instrument conditions are the same as figure 3.82a.

Figure 4.82e shows the mean EDAX energy spectrum of Tuna Al Gebel sand. There is a very strong characteristic peak for silicon. It has additional small peaks for aluminium and calcium.

4.6.3 Mud bricks

The EDX spectrum for mud brick 1 from Amarna can be seen in figure 4.83a. There are very large peaks for silicon and calcium. There are additional smaller peaks for magnesium, aluminium, phosphorus, sulphur, and chlorine. The additional peaks of potassium and sulphur (compared to the sands) are probably due to the presence of plant material in the mud brick.

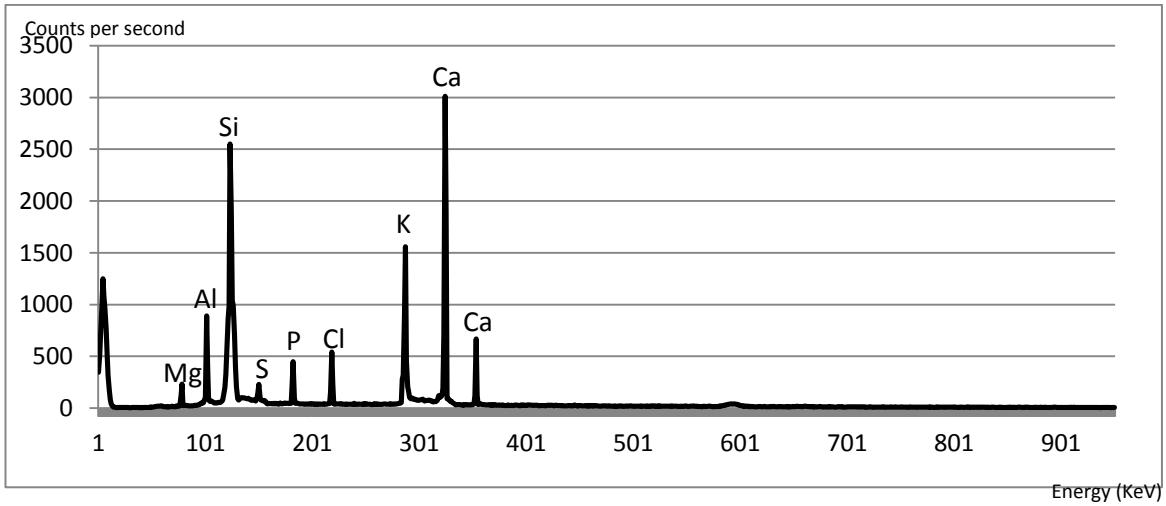

Figure 4.83a The mean EDX energy spectrum of Amarna North Palace Brick 1. Acceleration voltage = 15kV, spot size = 4.0, collection time = 100 seconds, n = 5, background corrected.

Amarna North Palace mud brick 2 has a very similar EDX spectrum to that of mud brick 1, which is unsurprising as they are from the same archaeological site. Although the peaks are similar, the heights of the sulphur, phosphorus, chlorine and secondary calcium peaks are noticeably lower in number or total counts per second.

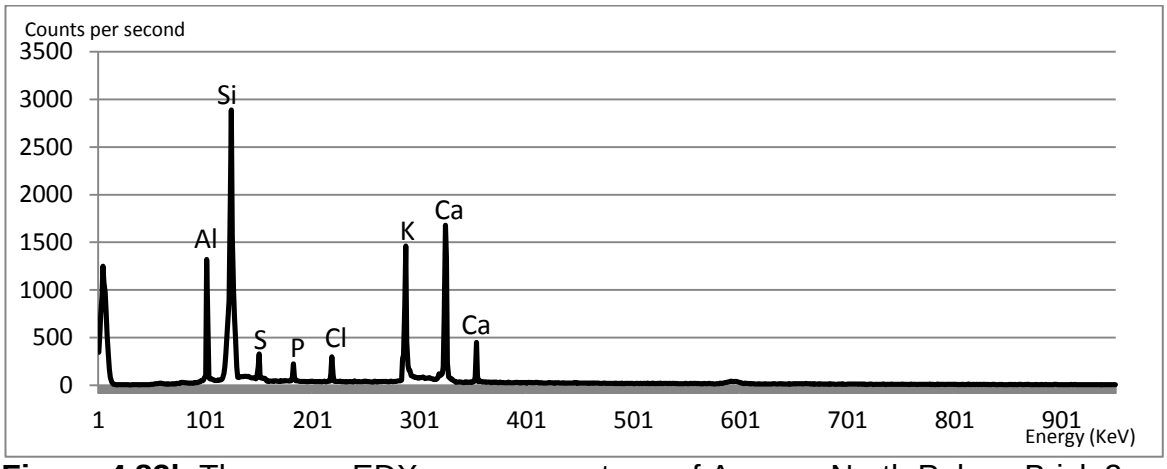

Figure 4.83b The mean EDX energy spectrum of Amarna North Palace Brick 2. Instrument conditions are the same as Figure 4.83a.

The EDX spectrum of a mud brick from the Dahshur pyramid can be seen in figure 4.83c. It is very similar in composition to the other two mud bricks from Amarna. It shares common elements with them, for example, silicon, potassium and calcium but the peak heights are (on average) lower than the second mud brick. It also possesses an additional peak for sodium.

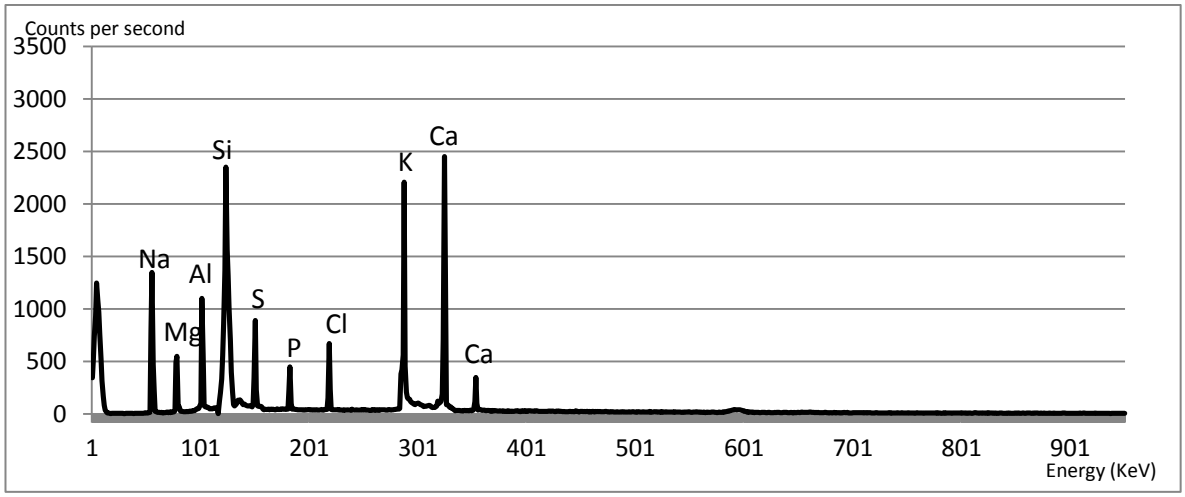

Figure 4.83c The mean EDX energy spectrum of the Dahshur pyramid mud brick. Instrument conditions are the same as figure 4.83a.

4.6.4 Phytoliths

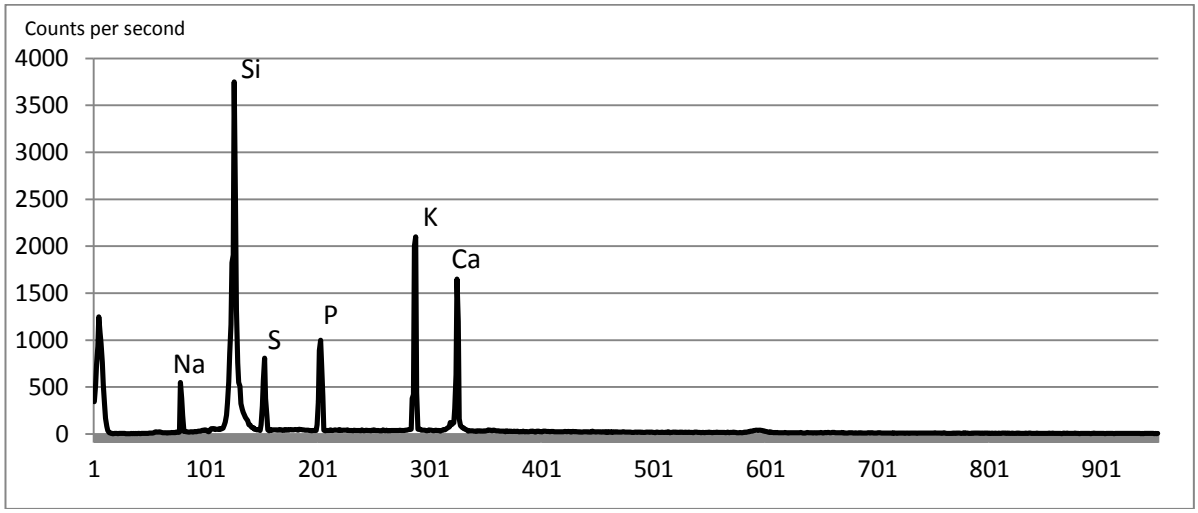

Figure 4.84 The mean EDX energy spectrum of phytoliths from modern barley. Acceleration voltage = 15kV, spot size = 4.0, collection time = 100 seconds, n = 5, background corrected.

The mean EDX spectrum of phytoliths contains strong peaks for silicon, potassium and calcium. There are additional small peaks for sodium, aluminium, sulphur and

phosphorus. This material contains peaks that can all be found in mud brick samples which would be expected as mud brick contained plant material, such as, wheat and chaff.

4.6.5 Extracted particles

The EDX of particles extracted from a section of mummified lung tissue from Mummy A4 can be seen in figure 4.85a. The spectrum contains a large peak for phosphorus and small rounded peaks for sodium, silicon and chlorine.

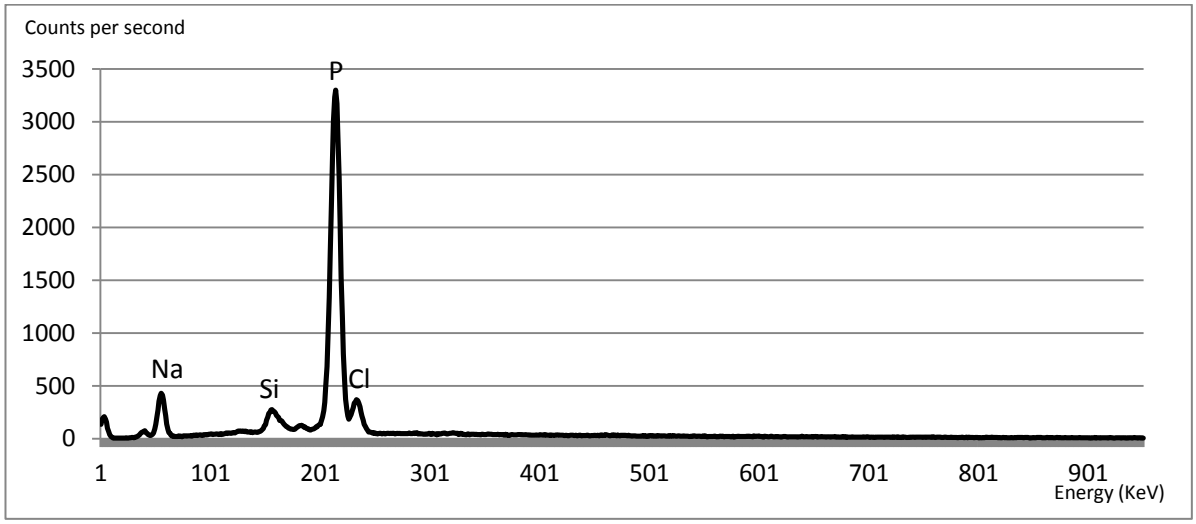

Figure 4.85a The mean EDX energy spectrum of particles extracted from mummy A4. Acceleration voltage = 15kV, spot size = 4.0, collection time = 100 seconds, n = 5, background corrected.

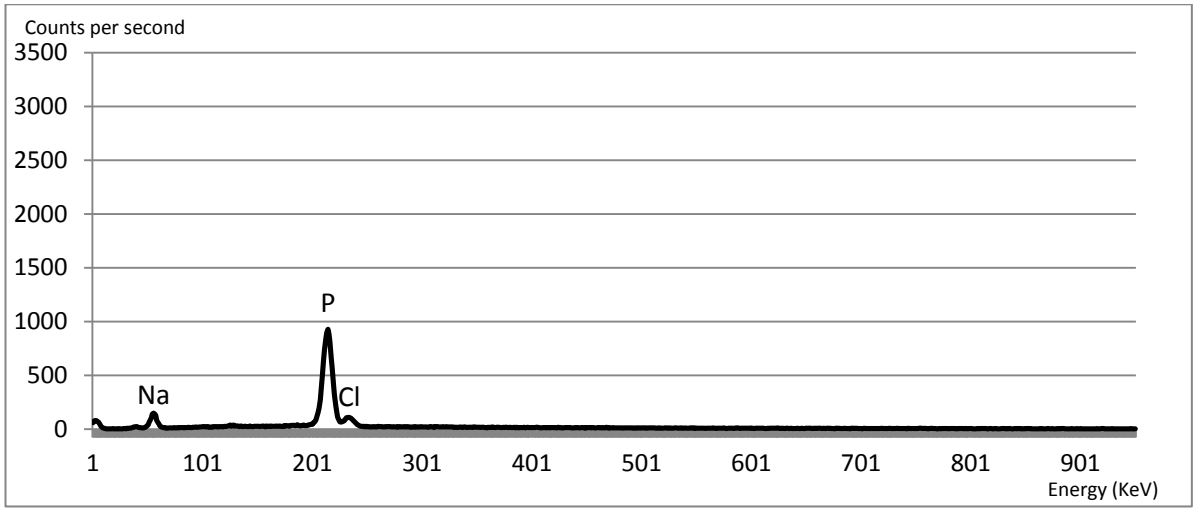

Figure 4.85b The mean EDX energy spectrum of particles extracted from mummy A13. Instrument conditions are the same as Figure 4.85a.

The EDX spectrum for particles extracted from the mummified lungs of mummy A13 is very similar to the spectrum for particles from mummy A4. Although their heights are lower, there are still peaks for sodium, phosphorus and chlorine. There is no visible peak for silicon.

Particles from mummy A102 appear to contain different elements to those found in mummies A13 and A4. The EDX spectrum reveals noticeable peaks for silicon and calcium (Figure 4.85c), along with a very small phosphorus peak.

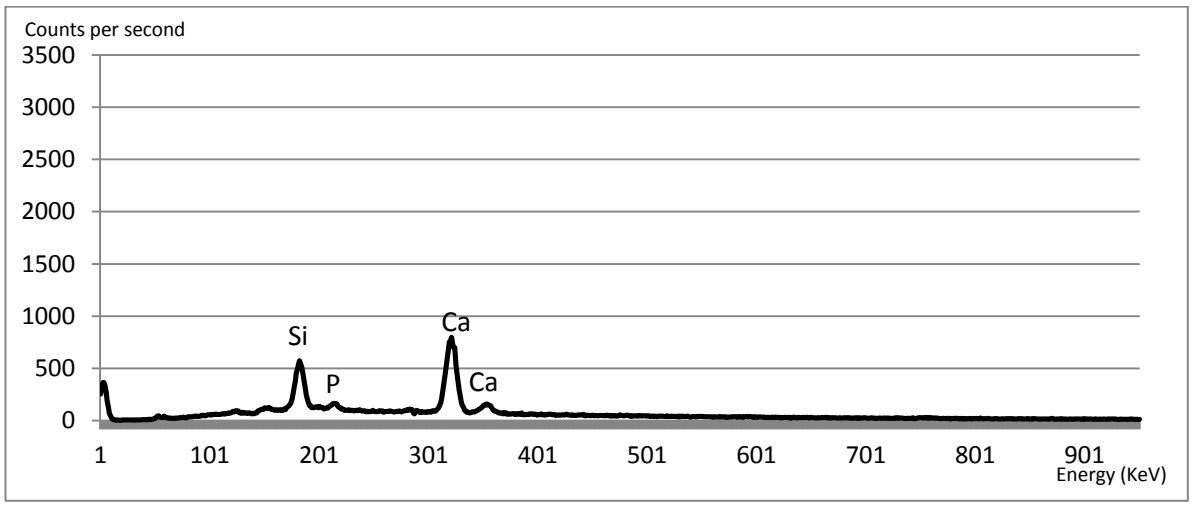

Figure 4.85c The mean EDX energy spectrum of particles extracted from mummy A102. Conditions are the same as figure 4.85a.

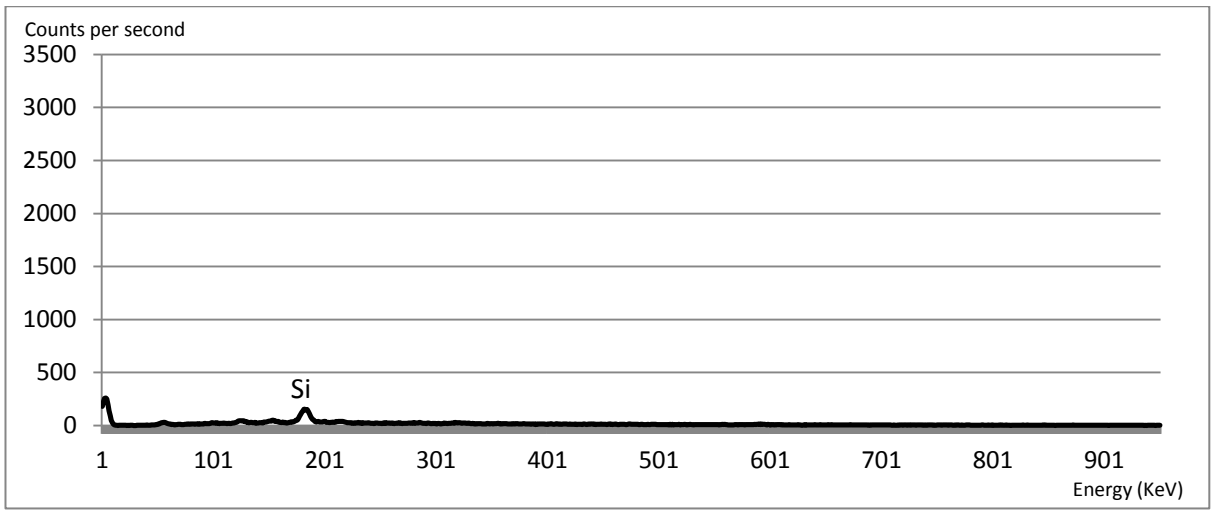

Figure 4.85d The mean EDX energy spectrum of particles extracted from mummy A108. Conditions are the same as figure 4.85a.

Very few counts can be seen in the spectrum of particles collected from mummy A108. There is only a very small peak for silicon and possibly other very weak peaks between 100 and 300 keV.

A silicon peak can again be seen in the EDX spectrum of particles from mummy A110 (Figure 4.85e). Unlike other extracted particle spectra, there is a large area of mass between 50 and 801 KeV which may potentially be quenching small peaks.

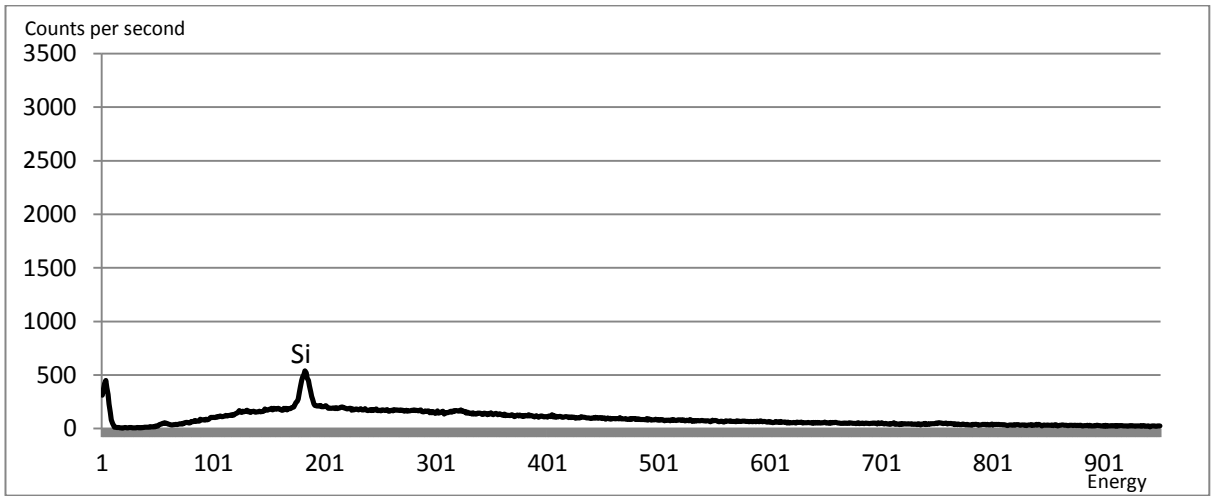

Figure 4.85e The mean EDX energy spectrum of particles extracted from mummy A110. Conditions are the same as figure 4.85a.

Peaks for silicon and phosphorus can be seen in the EDX spectrum of particles from mummy A111 (figure 4.85f). This spectrum is similar to those of A108 and A110.

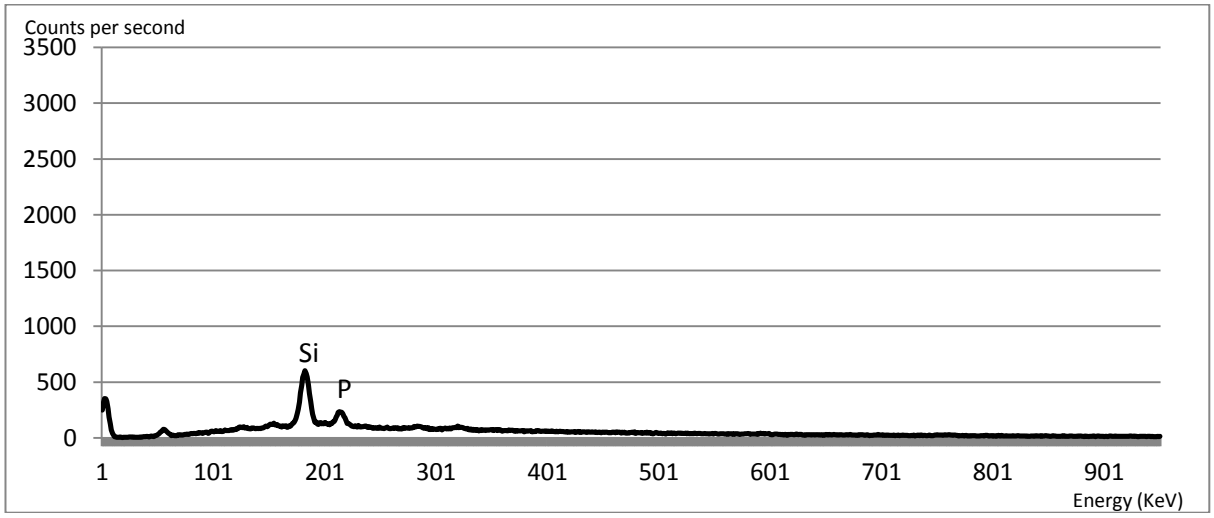

Figure 4.85f The mean EDX energy spectrum of particles extracted from mummy A111. Conditions are the same as figure 4.85a.

The particles extracted from mummy DO45 contain only a small peak for silicon and the complete spectrum (Figure 4.85g) appears very similar to that of mummy A108.

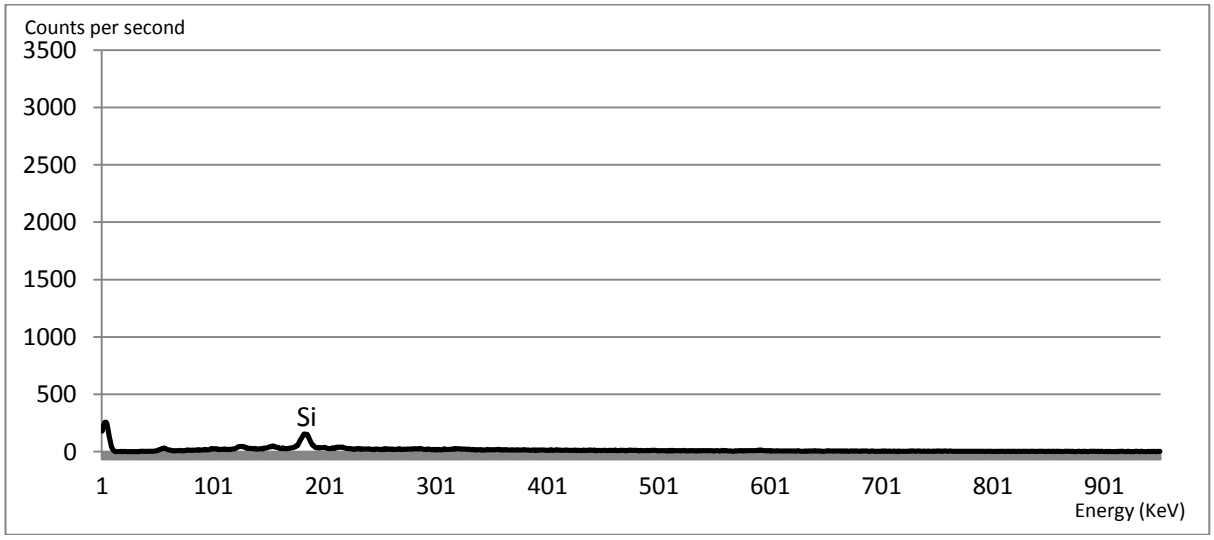

Figure 4.85g The mean EDX energy spectrum of particles extracted from mummy DO45. Conditions are the same as figure 3.85a.

4.7 Inductively Coupled Plasma Mass Spectrometry (ICP-MS)

4.7.1 Modern fuels

Figure 4.86a shows that low concentrations of aluminium boron, copper, iron, manganese, phosphorus and zinc (less than 12ppm) were present in the modern fuels that were combusted to create the surrogate soots. Castor oil is very unusual in that it appears to contain very few elements even at the low detection limits achievable using ICP-MS. As the two most saturated oils, sesame and palm oil contain similar levels phosphorus. Beeswax and olive oil contain much lower levels. Copper was only found in beeswax, and in even smaller amounts in olive oil. There is a small amount (1 ppm) of magnesium in olive oil, and larger amounts present in sesame, palm oil and beeswax. Aluminium was only found in beeswax and boron was only detected in Palm oil.

Other elements are present in higher quantities in the modern fuels. These are shown in Figure 4.86b and include calcium, sodium and sulphur. Beeswax contains a much higher content of sulphur than the oil fuels. Olive oil and beeswax

contain much higher amounts of sodium than the other fuels. Sesame oil and palm oils contain similar amounts of calcium; however beeswax contains a much larger amount. Castor oil contained no detectable calcium, sodium or sulphur.

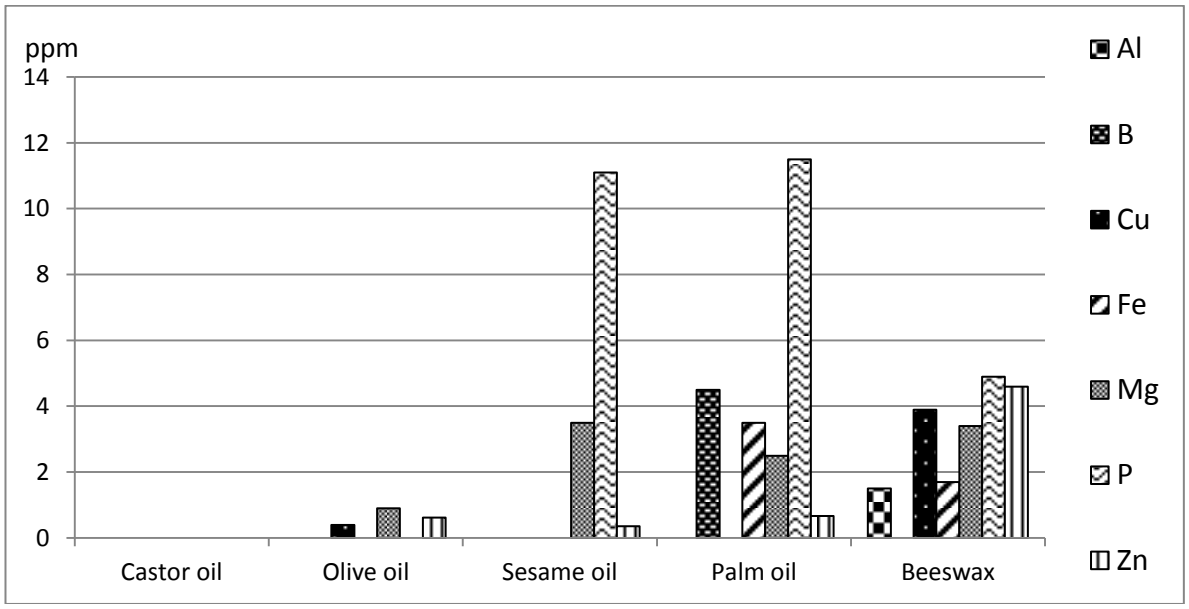

Figure 4.86a Elements lower than 15 ppm in the five modern fuels (castor, olive, sesame, palm oil and beeswax).

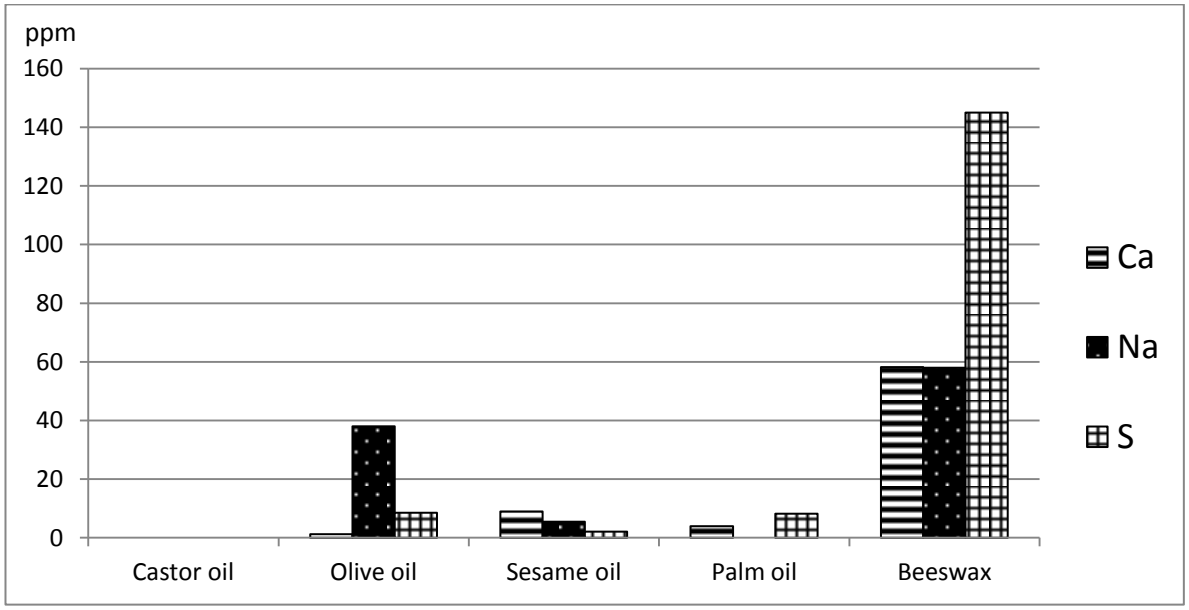

Figure 4.86b Elements in the range between 0 and 150 ppm in the modern fuels (castor, olive, sesame, palm oil and beeswax).

These results show that beeswax has the greatest concentration of the three elements and castor oil having the least.

4.7.2 Surrogate soots

The elements present in surrogate soots produced by the combustion of modern fuels can be seen in Figure 4.87a. Unlike the uncombusted fuel (Section 4.7.1), the combusted soot of castor oil produced detectable signals for various elements.

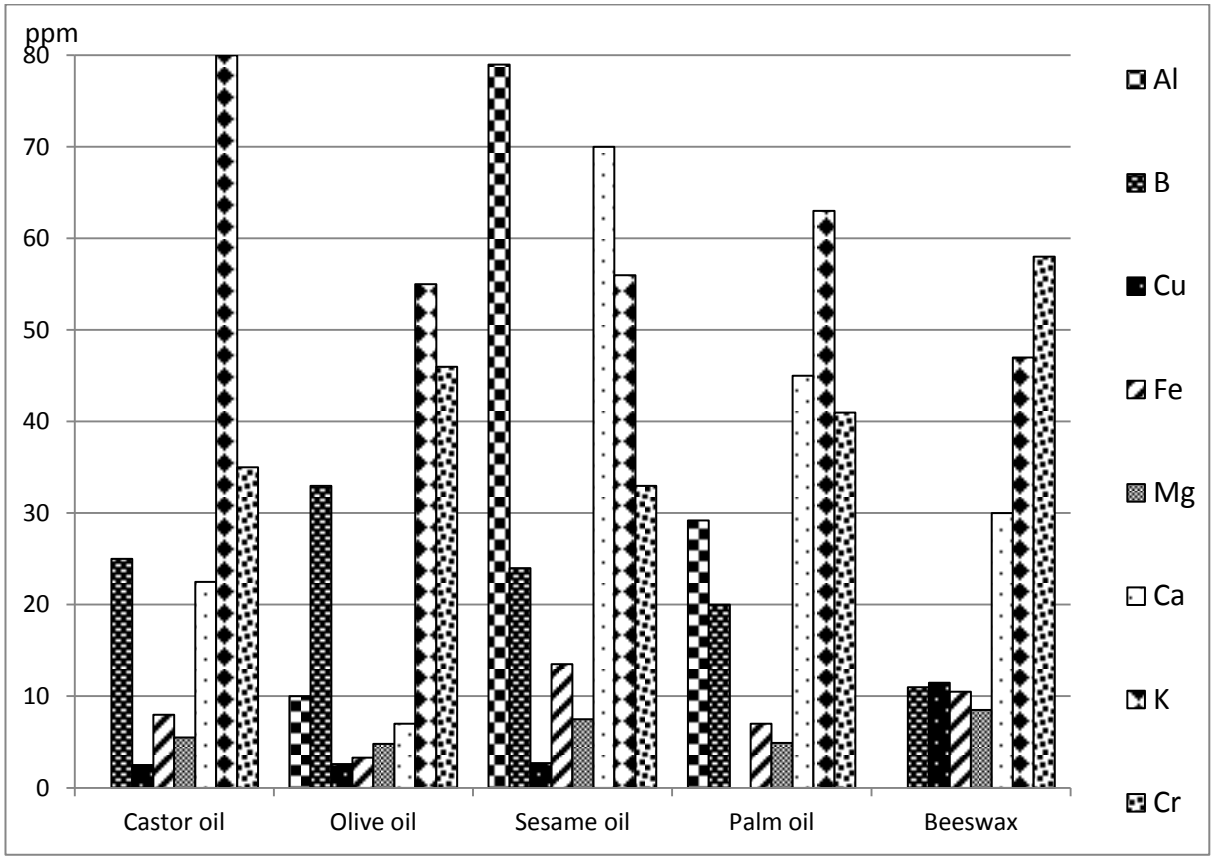

Figure 4.87a Elements present at less than 80 ppm concentration in the surrogate soots from castor, olive, sesame, palm oil and beeswax.

There is no aluminium present in castor oil or beeswax. The strongest signal is for sesame oil resulting in a concentration of 79 ppm whilst olive and palm oil contain much lower amounts (10 and 30ppm). All the oils and beeswax contain boron and it varies between a low of 12 ppm in beeswax to a high of 34ppm in olive oil. There is a relatively large amount of potassium in all the oils and in beeswax. There is a small amount (2 to 12ppm) of copper in all the fuels apart from palm oil. All the fuels contain a small amount of magnesium (4 to 8ppm). Chromium is highest in beeswax with lower amounts in the other fuels. Calcium concentrations are highest in sesame oil (70ppm) and lowest in olive oil.

Figure 4.87b shows elements in the soots at concentrations less than 200ppm. There is a relatively large amount of silicon in all the surrogate soot and varies between 65ppm in beeswax, 85ppm in castor oil, with similar amounts (125ppm) in both olive and palm oil whilst the largest amount (195ppm) is found in sesame oil. The predominantly unsaturated castor oil is the only soot to contain zinc. Sulphur is present in all the fuels with the largest amount (110 ppm) in beeswax.

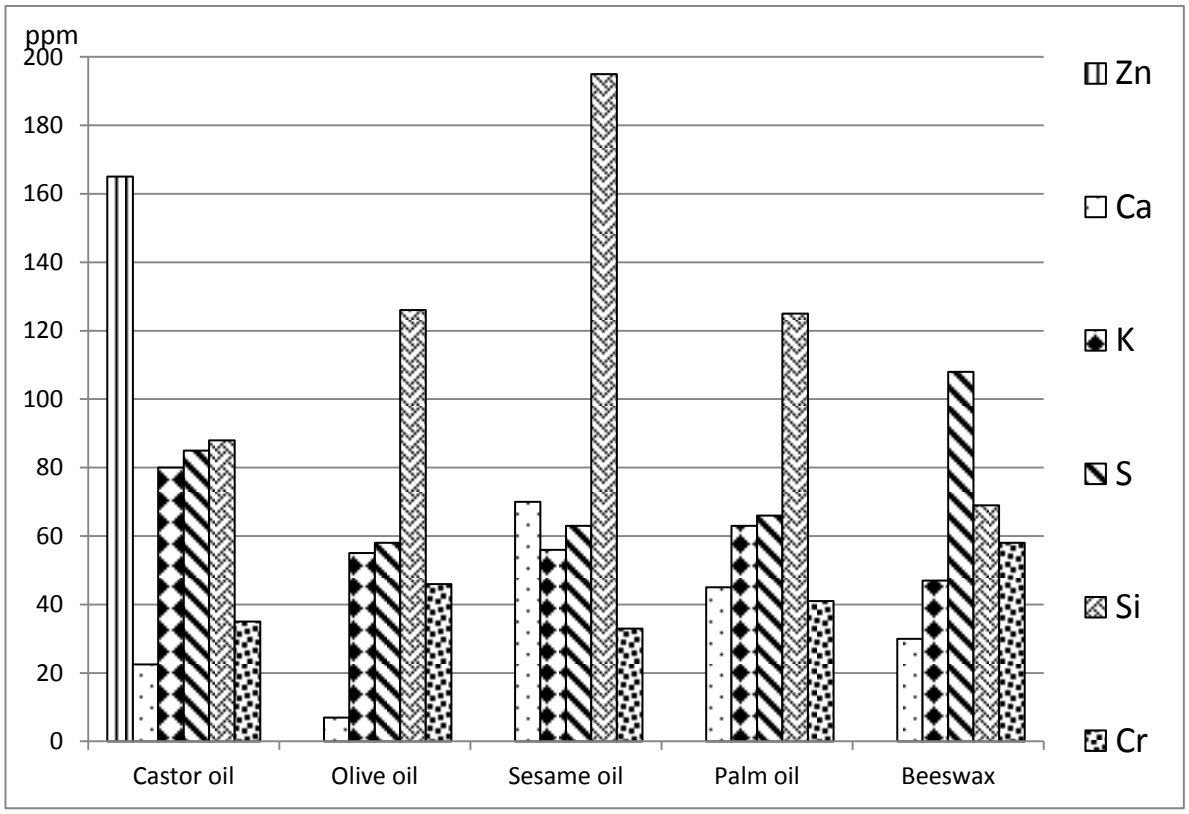

Figure 4.87b Elements at less than 200 ppm concentration in surrogate soots generated from castor, olive, sesame, palm oil and beeswax.

In Figure 4.87c, it can be seen that beeswax contains significantly larger amounts of sodium than all the other fuels. Silicon is the second most common of the elements shown in Figure 4.87c with sesame oil containing the largest amount.

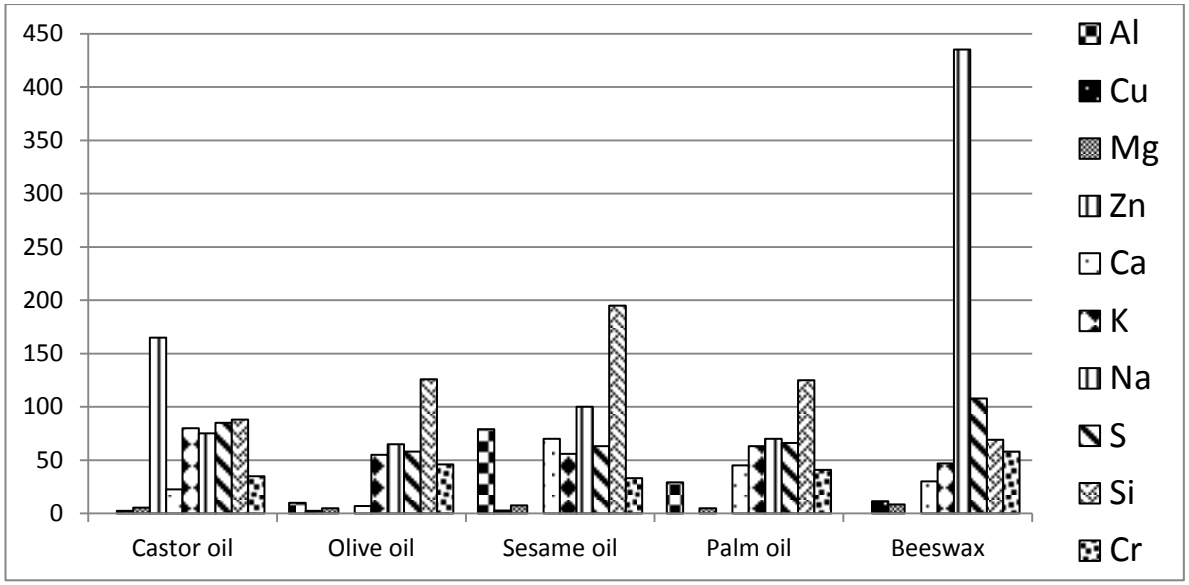

Figure 4.87c Elements in surrogate soot between the range of 0 and 500 ppm

4.7.3 Phytoliths

The elements present in the range up to 8000ppm in phytoliths can be seen in Figure 4.88a. The quantities of elements found in the sample are much higher (often by an order of magnitude) than other sample analysed using ICP-MS.

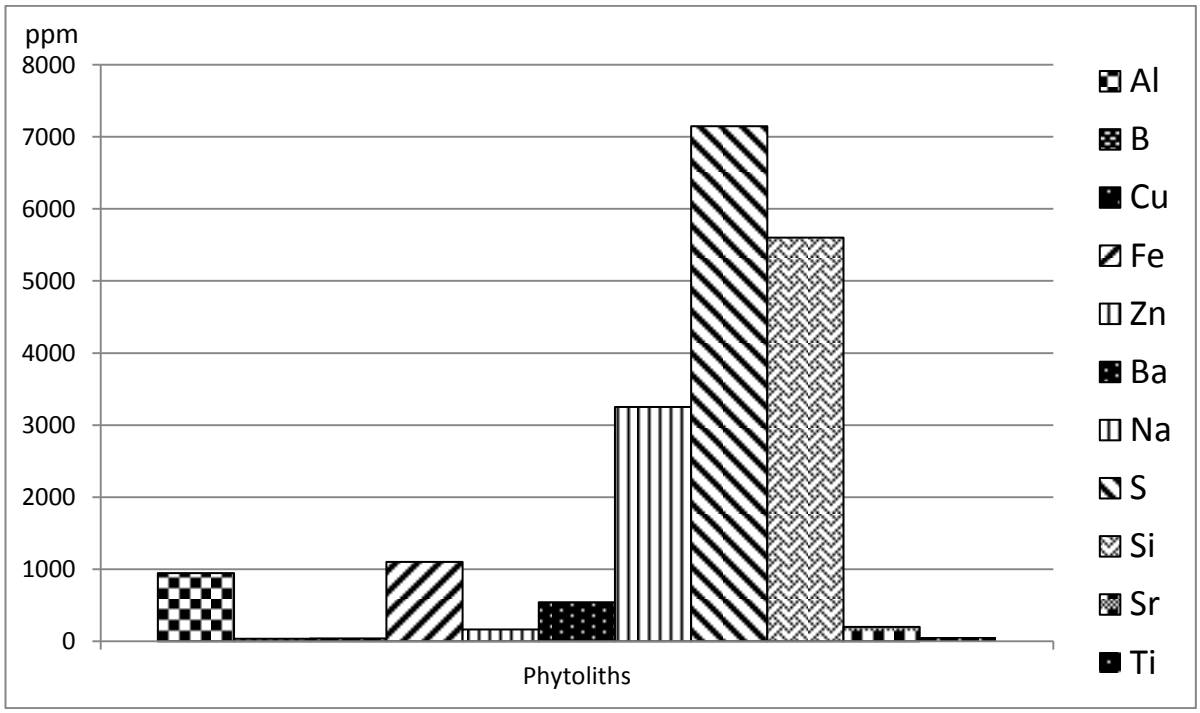

Figure 4.88a Elements present at less than 8,000 ppm in phytoliths.

There is a large amount of silicon (5600 ppm) in the sample, which is not surprising as phytoliths are silicotic structures. The other large signal is sulphur at 7100ppm due to its presence in protein. The third largest concentration is for sodium (3200ppm) whilst aluminium and iron also appear at concentrations around 1000ppm. Barium, strontium and zinc are found at lower concentrations (500ppm or less).

Other elements, such as, potassium (170,000ppm) are present in much higher quantities in phytoliths (Figure 4.88b). There are strong signals for magnesium and phosphorus resulting in concentrations of 9,800 and 16,000ppm respectively, while significant amounts of calcium (62,500ppm) were also recorded in the phytoliths. Phosphorus and magnesium were also present at 10,000 ppm or above.

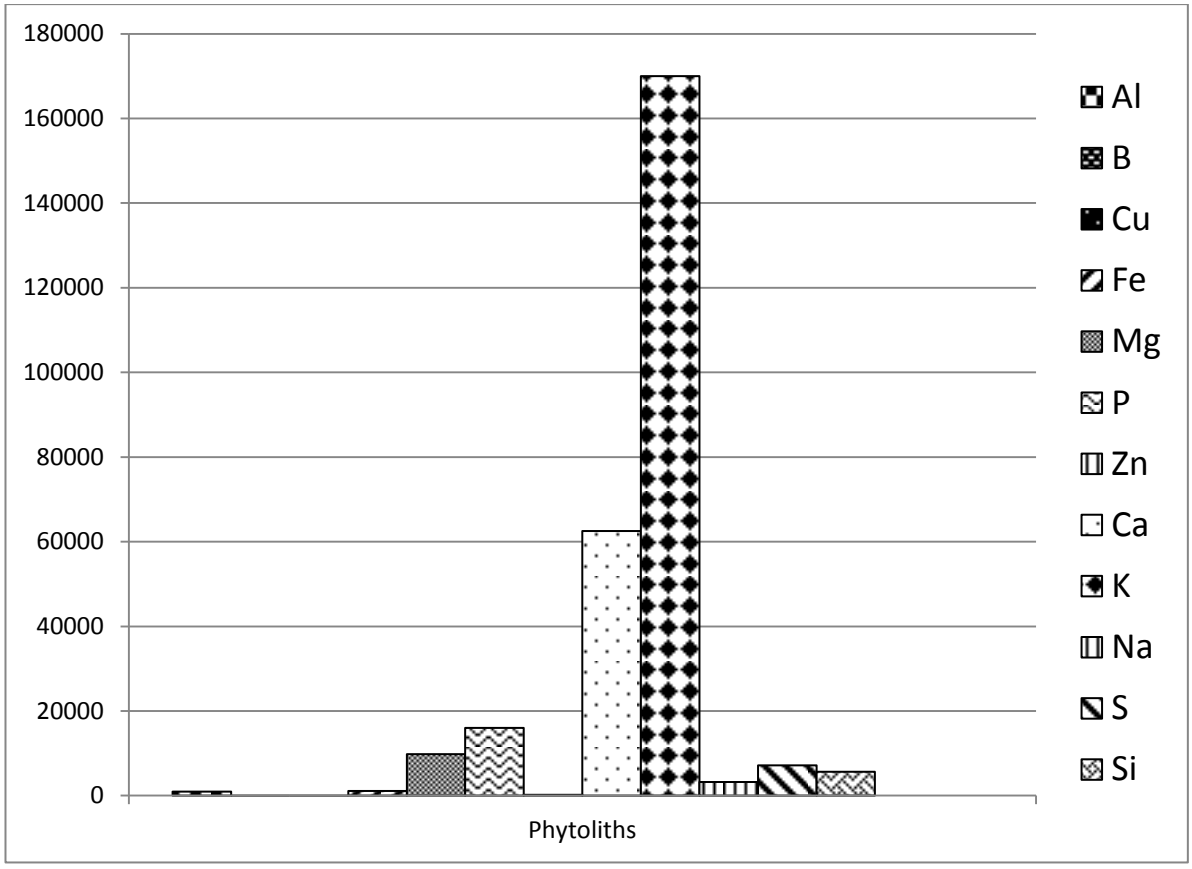

Figure 4.88b Elements present at concentrations of less than 180,000 ppm in phytoliths.

4.7.4 Mummified tissue digests

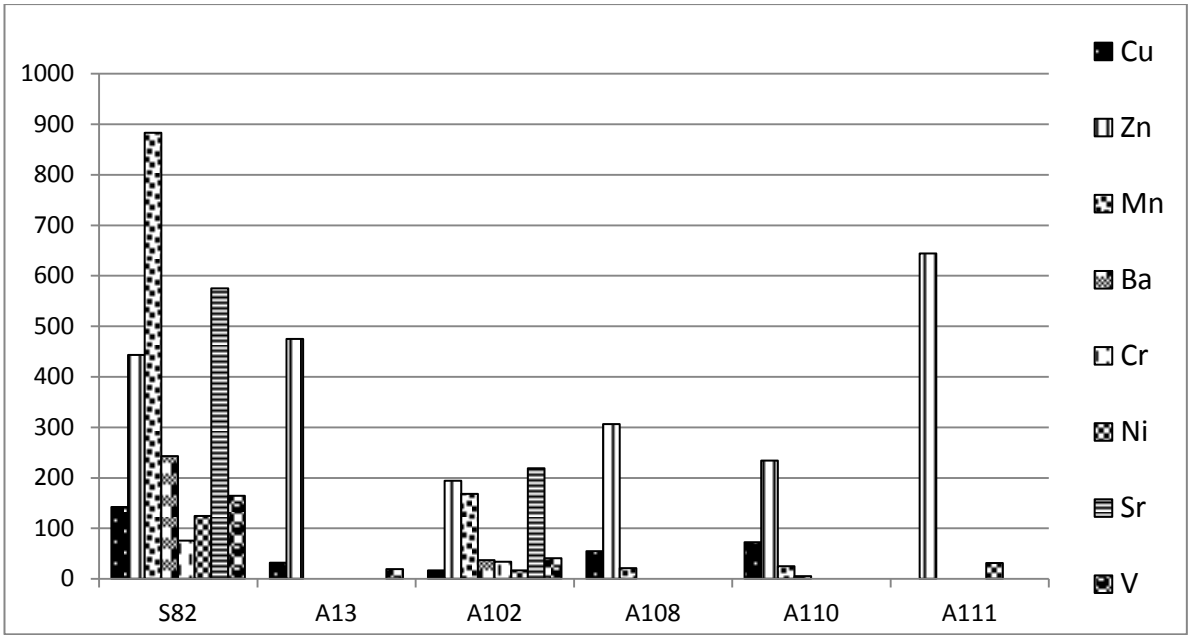

Figure 4.89a Elements present at concentrations of less than 1,000 ppm in tissue digests from five mummified lung samples (A13, A102, A108, A110 and A111) and a control of coprolite (S82).

Figure 4.89a shows the elements present at concentrations of less than 1000ppm in tissue digests from five mummified anthracotic lung samples (A13, A102, A108, A110 and A111) and a control consisting of mummified coprolite (S82). The figure shows that more elements are found in the coprolite, and in higher quantities, than in the mummified lungs. This is not surprising as the former is a mixture of degraded unidentified tissue and, importantly, plant tissue. Metal signatures vary greatly between lung samples. Zinc is present in all the mummified lung samples (194 to 644 ppm in A102 and A101respectively) as well as in the coprolite sample. A111 is the only lung sample to contain nickel. Small amounts of copper can be found in all the mummified samples except for A111, and in the coprolite. A102 contains manganese and strontium though at much lower levels than the control. Manganese is the element that is present at the highest concentration in the coprolite sample, and detectable amounts are found in lung tissue from mummies A102, A108 and A110 (Figure 4.89a).

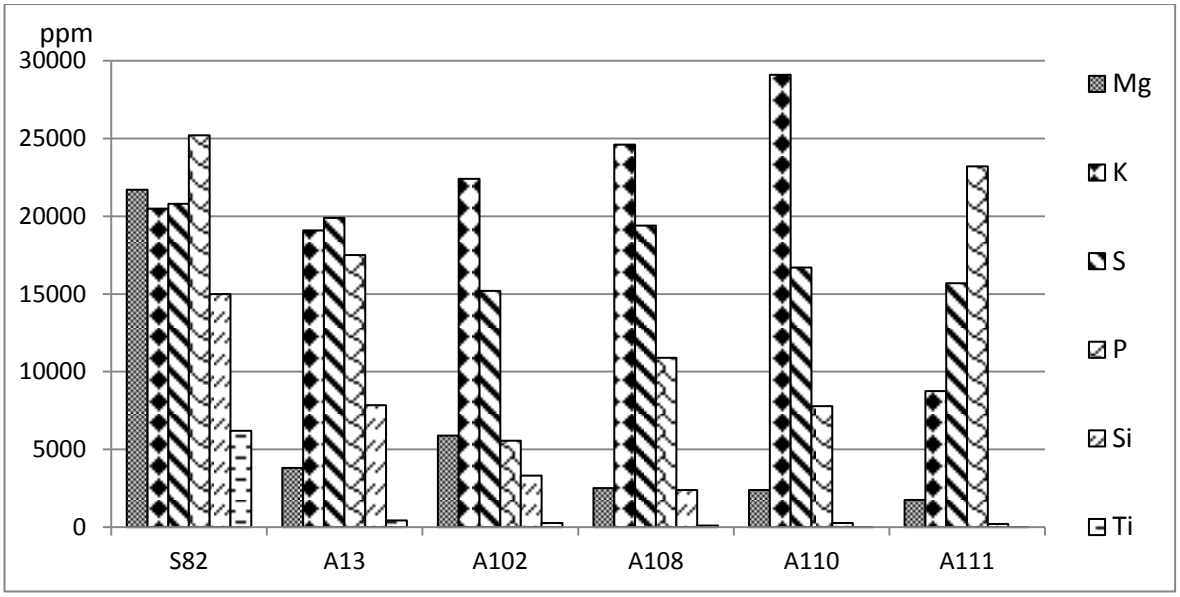

Figure 4.89b Elements present at concentrations below 30,000 ppm in tissue digests from five mummified lung samples (A13, A102, A108, A110 and A111) and a control of coprolite (S82).

Additional elements were present in the tissue digests but in higher quantities (Figure 4.89b) than those listed in Figure 4.89a. Titanium is present in all the mummified lung samples, but at a much lower concentration than in the control coprolite material. There are strong signals for potassium in all the mummified samples with A110 possessing the highest concentration (23,200ppm), which is higher than the control coprolite. Additionally, magnesium is present in all the mummified samples but at much lower quantities than the coprolite sample. Silicon can be found in all the mummified samples but the highest concentrations were recorded in A13, A102 and A108.

Figure 4.89c shows large amounts of sodium in all the mummified lung samples with the largest amount in A108 (39,700ppm). Calcium can be found in all the mummified samples with the highest concentration in A102, but which is still lower than the levels in the coprolite control. All the tissue digests and the control contain similar levels of sulphur (15,000 to 20,000ppm). Potassium was also found in similar levels between all the tissue digests and the control. Aluminium was only found in the coprolite control and in lung samples A13 and A102. There is a very small amount of manganese detectable in the control sample, plus the lung samples A102, A108 and A110.

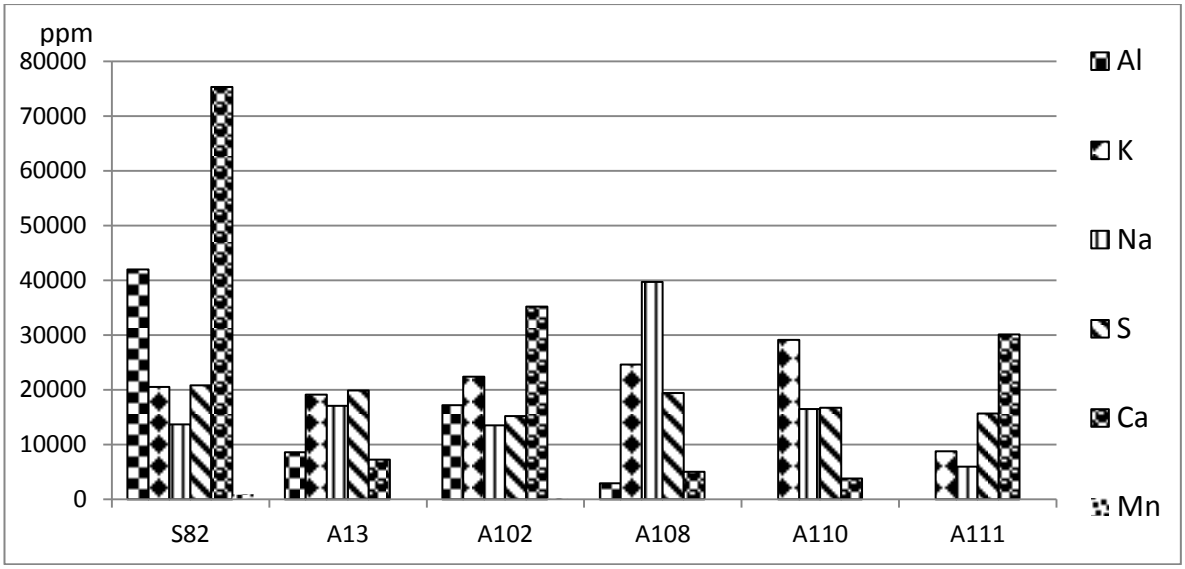

Figure 4.89c Elements ranging between 0 and 80,000 ppm in tissue digests from five mummified lung samples (A13, A102, A108, A110 and A111) and a control (S82).

4.7.5 Particles isolated from mummified tissue

Figure 4.90 shows the elements present in the suspensions of particles extracted from the sonicated mummified lungs. Sodium was the element present in the largest amount, but only in DO45 (8ppm), although this element was also found, but in much lower quantities, in all the other samples extracts. Another element common to all the samples is potassium and was present at concentrations up to 5ppm. Iron was found in all the extracted particles except those from mummy A108 and DO46. Phosphorus had a concentration of 2.8ppm in DO45 but was not detected in any other particle suspension. Magnesium was present at a concentration of 1.5ppm in sample DO45 but was also found in minute amounts in the other particle suspensions. Copper was detected in very small amounts in sample A4. Aluminium was only present in very small amounts in two samples - A4 and A102. The largest amount of zinc was found in sample A4 although it was present in very small quantities in all the other samples. The largest concentration of sulphur was found in DO45 (2.3ppm) but was also detectable in the other samples. Manganese (1ppm) was only detected in sample DO46.

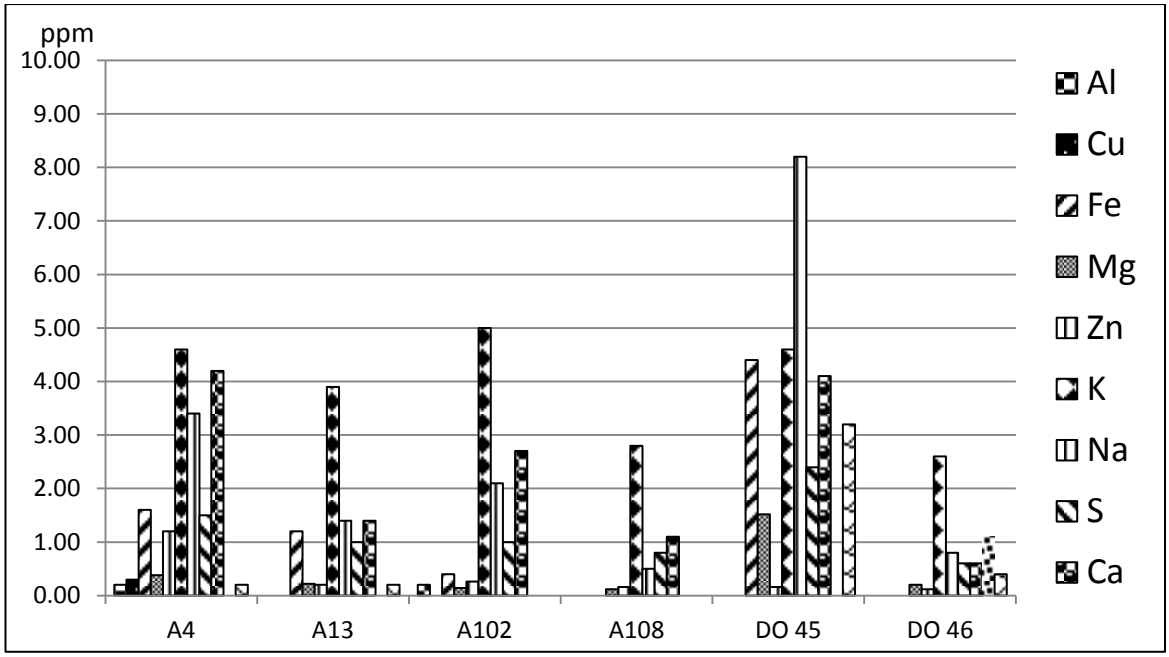

Figure 4.90 Elements from five mummified lung samples (A4, A13, A102, A108, DO45 and DO46).

4.8 *Laser Ablative Inductively Coupled Plasma Mass Spectrometry (LA-ICP-MS)*

4.8.1 Modern sand samples

As previously mentioned in the introduction (see Chapter 1, Section 1.5.9) the following elements were scanned: magnesium (Mg), calcium (Ca), strontium (Sr), titanium (Ti), vanadium (V), chromium (Cr), manganese (Mn), iron (Fe), cobalt (Co), nickel (Ni), copper (Cu), zinc (Zn), cadmium (Cd), mercury (Hg), aluminium (Al), silicon (Si), phosphorus (P), lead (Pb) and uranium (U).

Amarna

Figure 4.91a shows the mass spectrum of a sand sample from an archaeological site near Amarna. The two most dominant signals are for magnesium and aluminium and they follow each other closely suggesting that most of the sand material is composed of aluminium and magnesium. There is a weaker peak for manganese at 38 seconds, and the background contains elements such as iron and nickel.

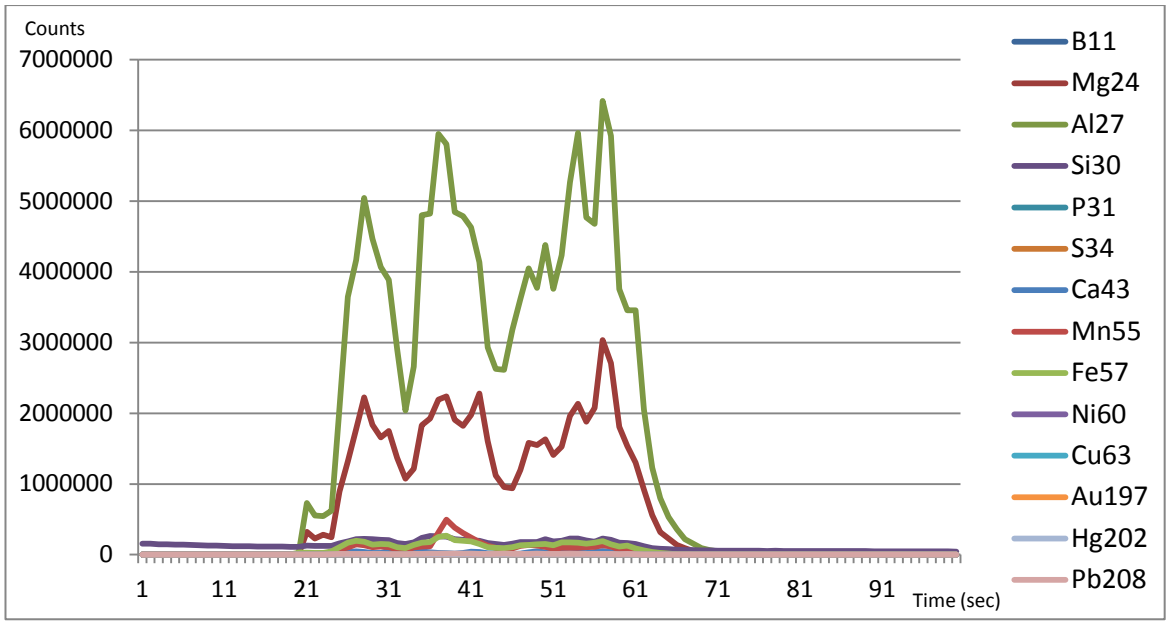

Figure 4.91a Mass spectrum of sand from Amarna. The sample ran from 20 to 70 seconds.

Amarna North Palace

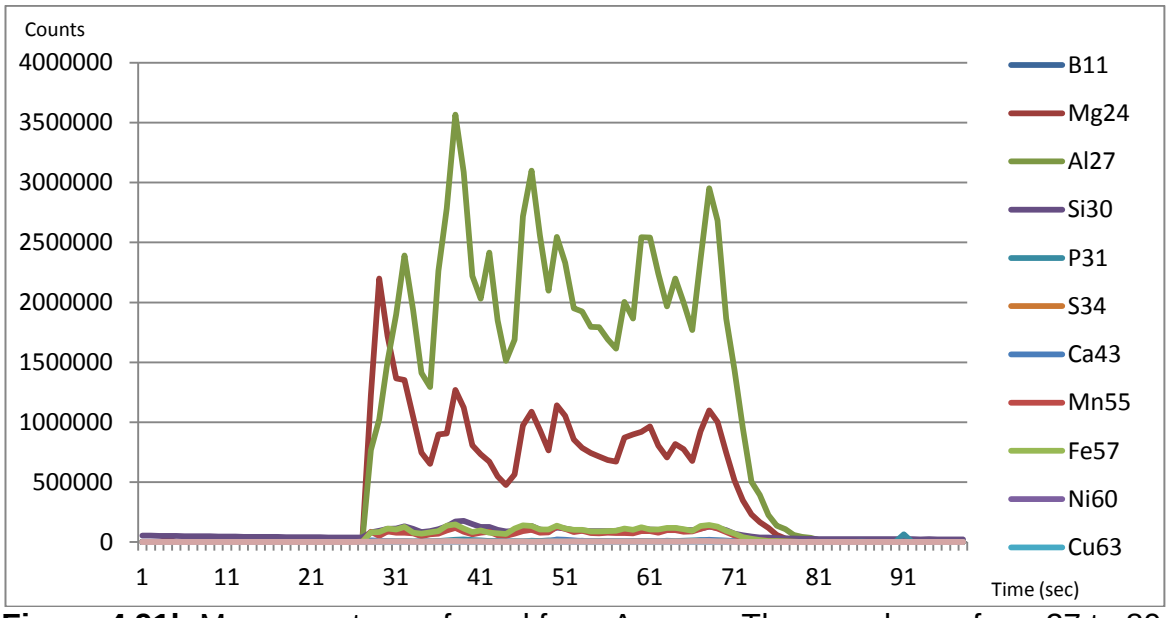

Figure 4.91b Mass spectrum of sand from Amarna. The sample ran from 27 to 80 seconds.

In common with Amarna sand, the sand from the Amarna northern palace contains very strong signals for aluminium and magnesium (Figure 4.91b). The background contains variations in the levels of silicon, iron, and sulphur across the length of the sample.

Karnak

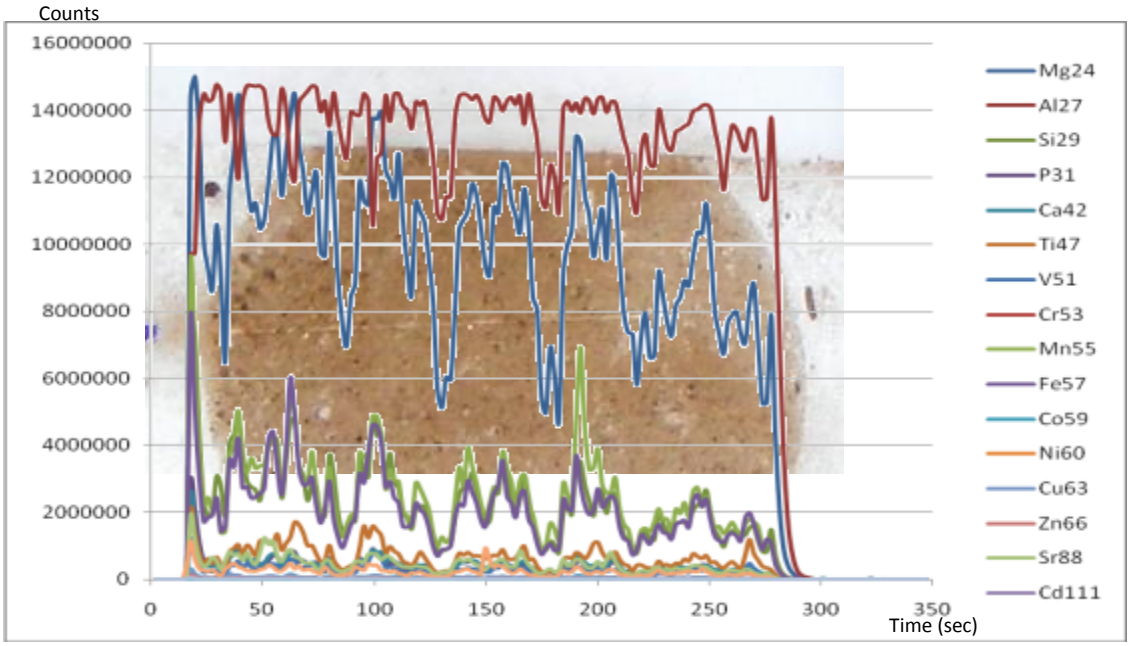

Figure 4.91c Mass spectrum of sand sample from Karnak. The mass spectrum of the sample has been superimposed over the sample stub to show the variation in the sample as it was scanned from 10 to 290 seconds.

Figure 4.91c shows the mass spectrum of sand sample from Karnak. The mass spectrum of the sample has been superimposed over an image of the sample stub to show the variation in the sample as it was scanned (the laser line is visible in the sand). Like the other sands, there are large signals for aluminium and magnesium. There are additional strong peaks for silicon and phosphorus. The silicon peak appears to follow the peaks and troughs of the aluminium curve and suggests there may be aluminosilicates in the sample.

Tune Al-gebel

The mass spectrum of sand from Tuna Al-gebel can be seen in Figure 4.91d. It has very strong peaks for magnesium and aluminium which is consistent with the other sands. It has a peak for silicon which seems to mirror the aluminium and magnesium profiles.

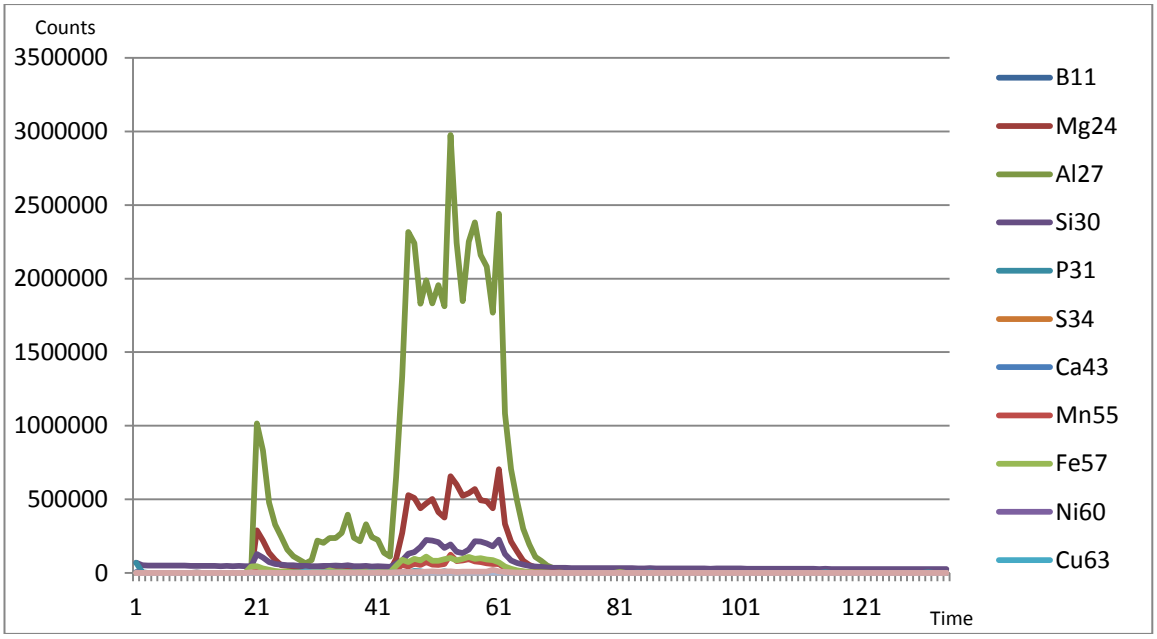

Figure 4.91d Mass spectrum of sand from Tuna Al-gebel. The sample ran from 20 to 70 seconds.

4.8.2 Sections of ancient lung tissue

The following elements were scanned for: Magnesium (Mg), calcium (Ca), manganese (Mn), iron (Fe), nickel (Ni), copper (Cu), aluminium (Al), silicon (Si), phosphorus (P), lead (Pb), gold (Au), and mercury (Hg).

Control – non lung mummified tissue 34193A

Figure 4.92a shows a large signal for magnesium as the laser was fired across the sample. The magnesium signal in this non-lung sample which contained unidentifiable material is much stronger than the signals for any other elements which appear to be present in very small amounts.

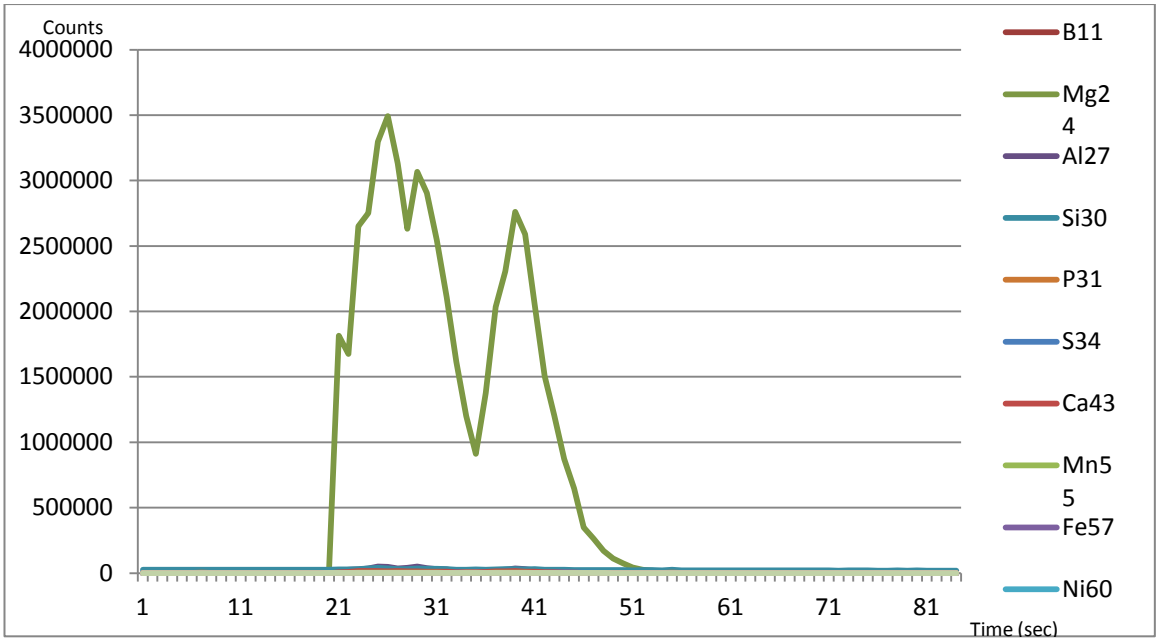

Figure 4.92a Mass spectrum of control (non lung) mummified tissue sample 34193A. The sample started at 20 seconds and ended at 50 seconds.

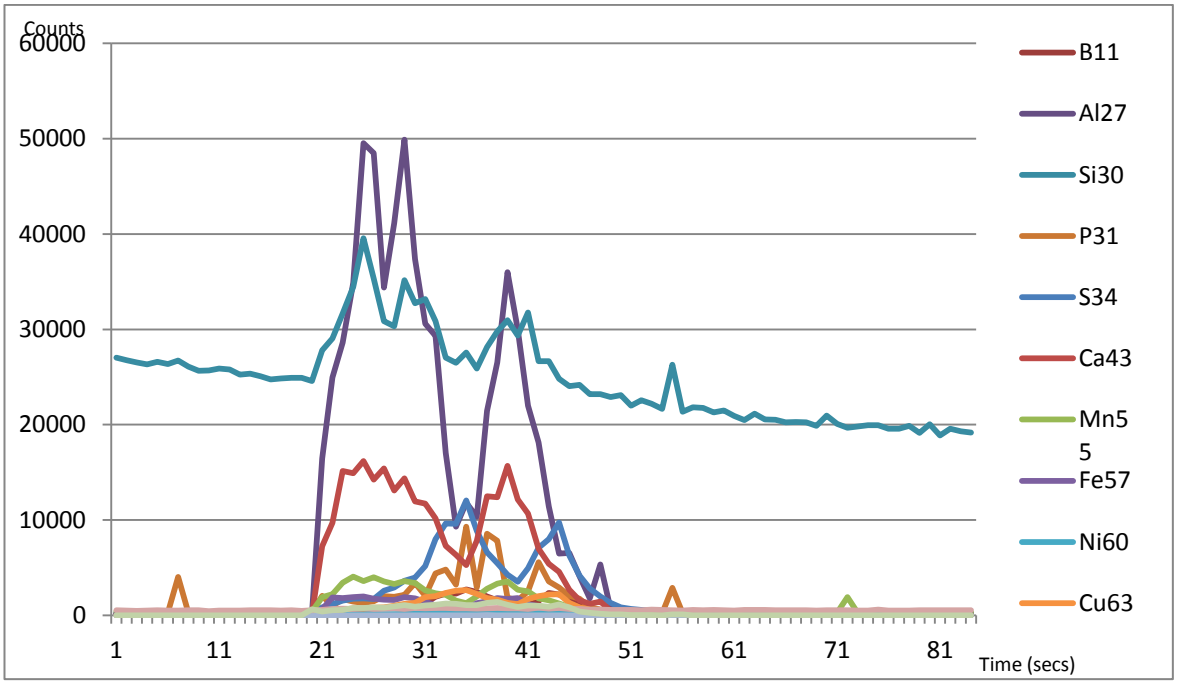

Figure 4.92b Mass spectrum (with Mg subtracted) of control (non lung) mummified tissue sample 34193A. The sample started at 20 seconds and ended at 53 seconds.

When the magnesium peak is subtracted (Figure 4.92b) the underlying elemental signals can be observed. The baseline of the silicon signal appears to be much higher than the other elements. Its trend appears to be a slow decline as time increases but it does contain three peaks within the sample. These three peaks also correspond to three peaks in the aluminium signal. This suggests there are alumino-silicates in the sample. Calcium and sulphur also have peaks at the same times suggesting that calcium sulphates or other combinations of elements may also be present in the unidentifiable material.

A13

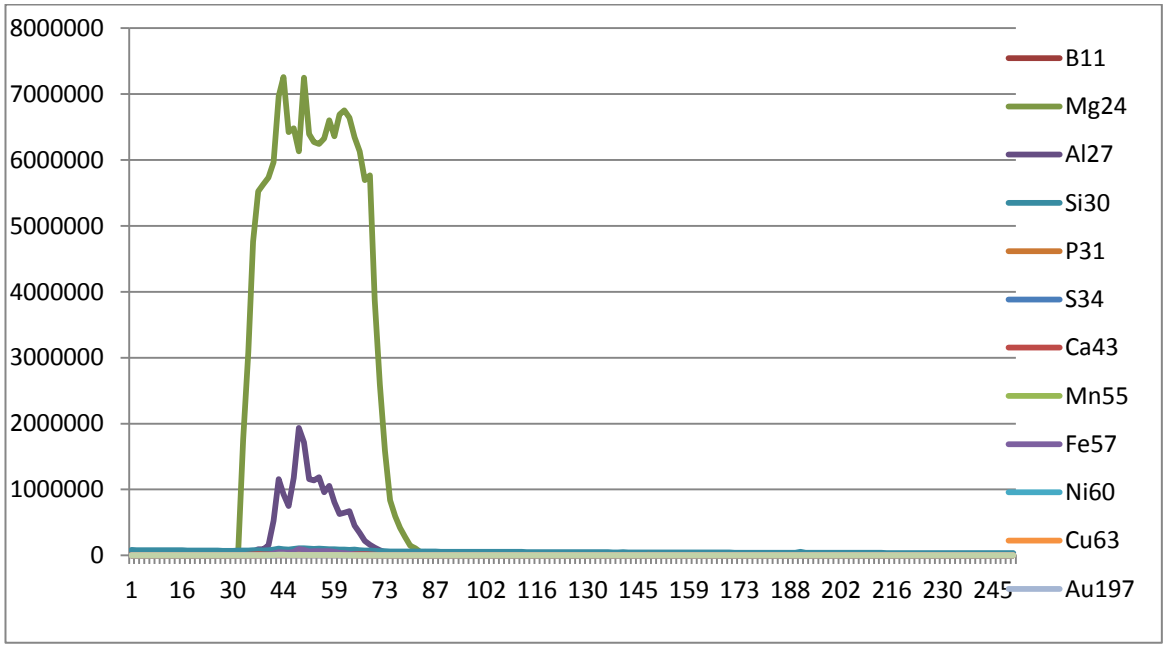

Figure 4.93a Mass spectrum of mummified tissue sample A13. The sample started at 30 seconds and ended at 85 seconds.

The mass spectrum of mummified lung sample A13 can be seen in Figure 4.93a. Again large signals for magnesium and aluminium can be seen. Their signals are several orders of magnitude higher than for the other elements. The mass spectrum with magnesium and aluminium deducted can be seen in Figure 4.93b.

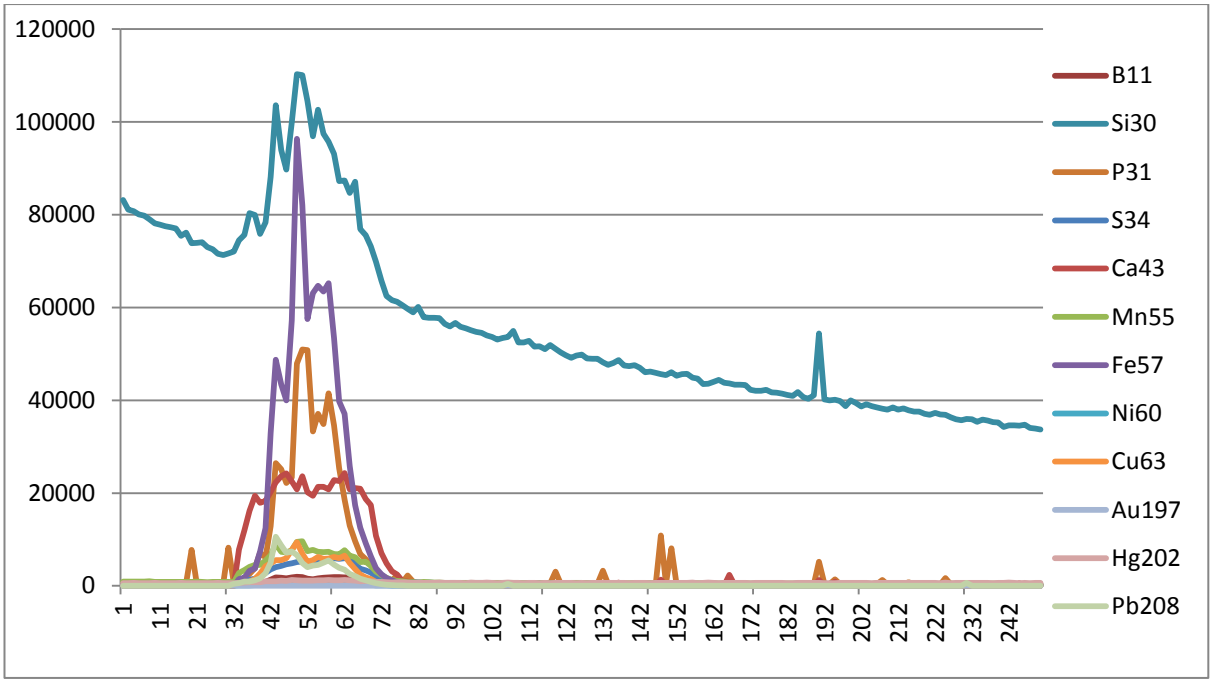

Figure 4.93b Mass spectrum of mummified lung sample A13 with Mg and Al subtracted. The sample started at 30 and ended 85 seconds.

There is again a strong signal for silicon throughout the mass spectrum. The trend of the silicon signal is that of a decline but it has several peaks throughout the sample. These peaks correspond well with the peaks of the calcium signal. The signals from iron and phosphate also closely resemble each other. Lead and copper also show small peaks in the sample.

4.9 Electron Probe Micro-Analysis (EPMA)

In this method, a resin-mounted sample of mummified lung tissue was mapped for specific elements by EPMA. The tissue appears as a uniform light blue and the sample stub appears as a dark blue/black background. The distribution of aluminium, silicon, calcium and magnesium can be seen in Figure 4.94 whilst Figure 4.95 shows the location of iron, phosphorus, sulphur and lead.

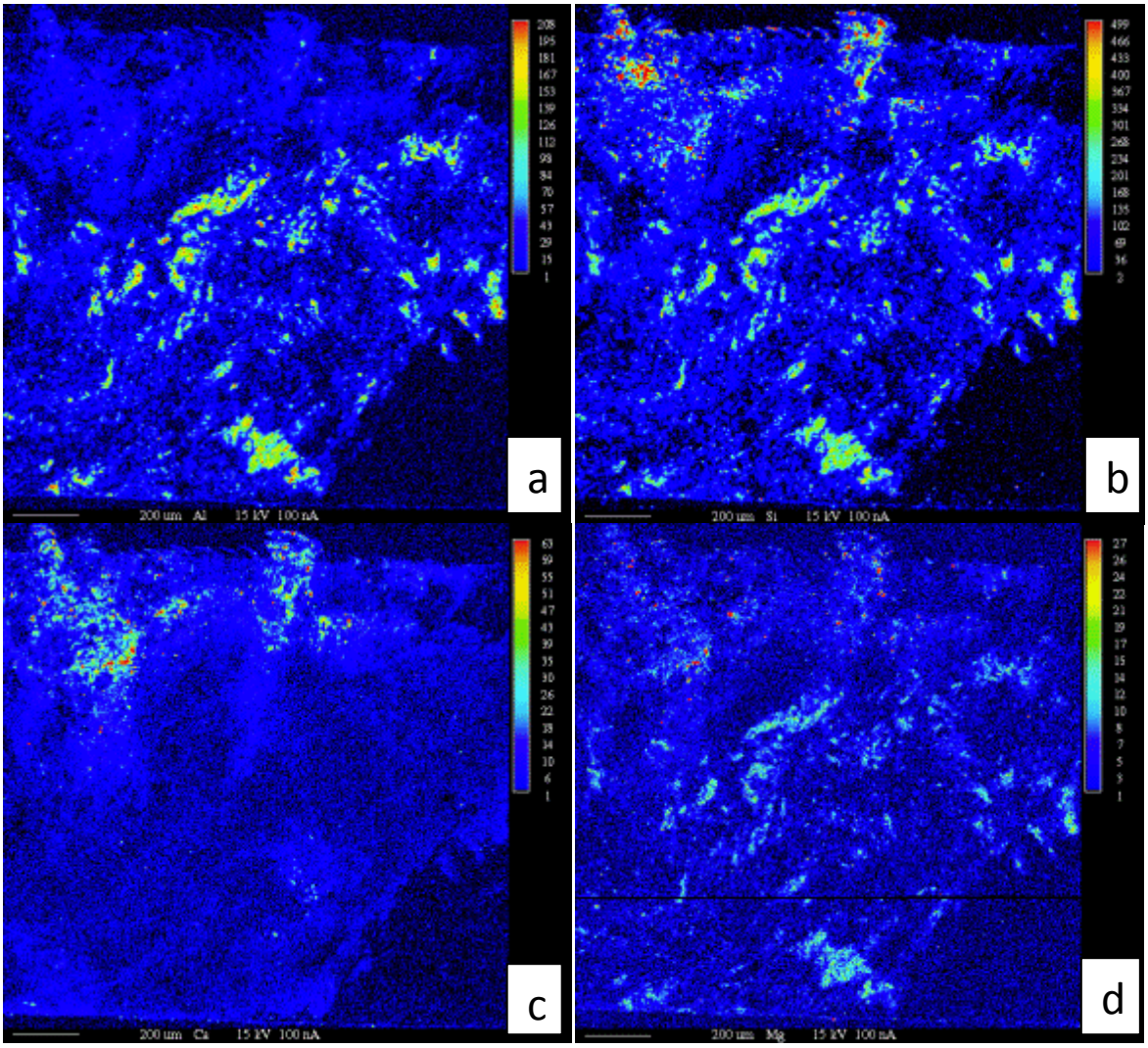

Figure 4.94 Elemental maps of a resin-mounted section of mummified lung sample A13 where the brighter colours (e.g. red or yellow) indicate high intensities of elements and dark colours (e.g. blue or black) indicate low intensities. a) shows aluminium, b) silicon, c) calcium and d) magnesium. Scale bar is 200 microns, and 1 pixel = 1 micron.

Figure 4.94a and b show that for the lower half of the lung section, aluminium and silicon closely co-distributed as there are no signals of aluminium without a corresponding signal for silicon. However, silicon has some additional signals in the top half of the tissue. These additional signals are in the same areas as the signals from calcium (Figure 4.94c). Magnesium (Figure 4.94d) appears to co-distribute with silicon and magnesium in the bottom half of the lung section and with silicon and calcium in the top half.

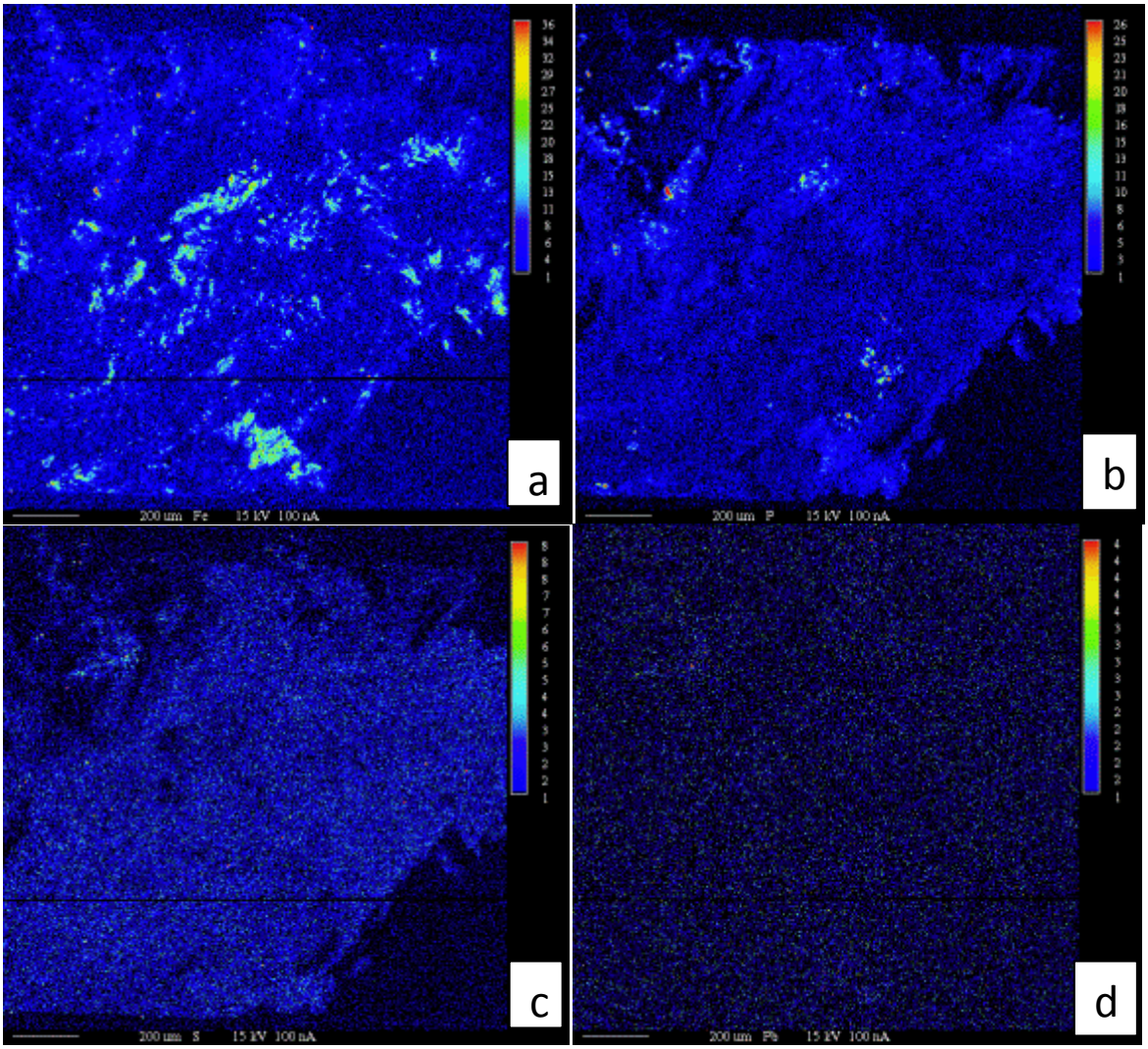

Figure 4.95 Elemental maps of a resin-mounted section of mummified lung sample A13 where the brighter colours (e.g. red or yellow) indicate high intensities of elements and dark colours (e.g. blue or black) indicate low intensities. a) shows Iron, b) phosphorus, c) sulphur and d) lead. Scale bar is 200 microns, and 1 pixel = 1 micron.

Figure 4.95a shows that iron appears to co-distribute predominantly with aluminium (Figure 4.94a) and also areas of silicon and magnesium (Figures 4.94b and d). Phosphorus has few signals and appears not to co-distribute with any particular element (figure 4.95b) and so may be contained within the organic tissue matrix. Sulphur shows a light blue background in the tissue but has no strong signal (figure 4.95c); again the small amounts present may be of organic origin. Lead is present in such small amounts that the element has no signal and does not even reveal the light blue background of the tissue.

4.10 Raman Spectroscopy

4.10.1 Uncombusted surrogate fuels

The non-baseline corrected data for uncombusted surrogate oils and beeswax can be seen in figure 4.96a. Olive oil produced the highest absorption and shares peaks at 850, 1100, 1300, 1450 and 1650cm^{-1} with castor and sesame oil. Beeswax and palm oil produce broad “humps” with no discernible peaks.

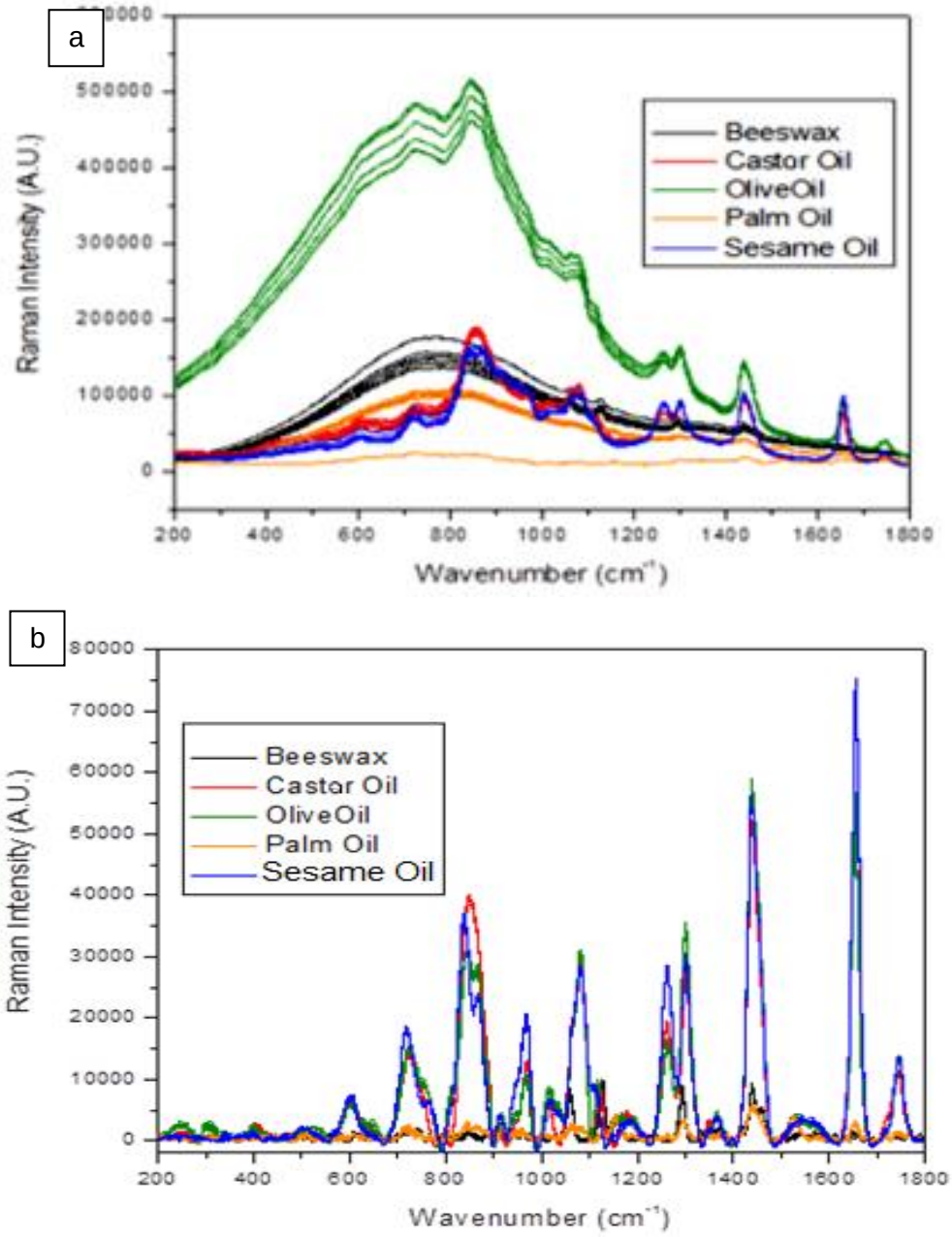

Figure 4.96 Baseline uncorrected (a) and corrected (b) data for uncombusted surrogate fuels and beeswax (n=5).

When the data are baseline corrected (Figure 4.96b) castor, sesame and olive oil show clear shared peaks at wavenumbers 850, 1100, 1300, 1450 and 1650cm^{-1} but again the signals produced by palm oil and beeswax are too 'noisy' to allow direct comparison between all the fuels.

A non-scaled comparison can be seen in Figure 4.97. Comparison of Raman intensity is not possible but differences in features and band positions can be observed. For example, sesame, castor and olive oil all possess small hump peaks at 1500-1600 cm^{-1} whereas beeswax and palm oil contain a small double peak. Overall, sesame, castor and olive oil all appear similar although small differences in certain peak shapes can be seen. Palm oil and beeswax also appear similar to the other fuels but the signals are noticeably noisier.

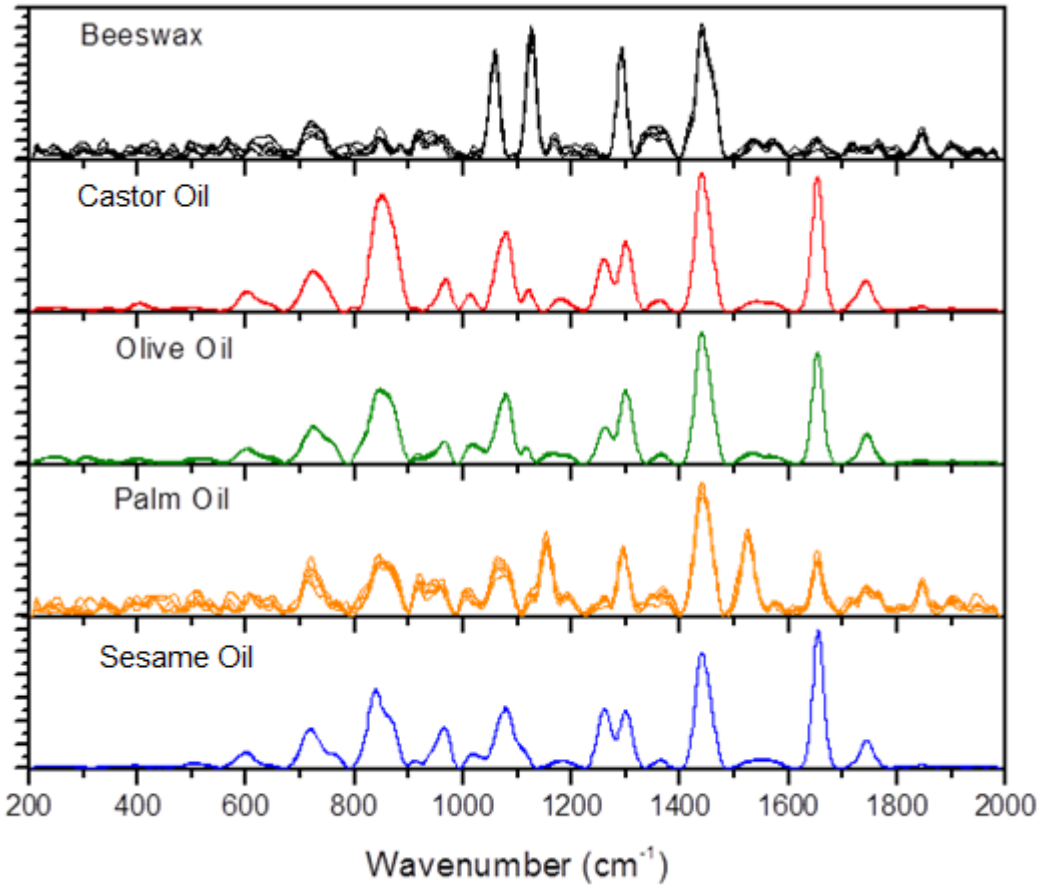

Figure 4.97 Non-scaled comparison of the uncombusted fuels used to create surrogate soots (n=5).

4.10.2 Surrogate soots

Figure 4.98 shows Intensity and bands present in samples of surrogate soot (n=4). Spectra could not be produced for palm and olive oil soot. All three fuels look similar to each other and possess similar peaks at 1200, 1650, 1800 and 1900 cm^{-1}. The only difference between the 3 fuels is the difference in peak shape at 1250-1450cm^{-1} where beeswax possesses a double peak and castor and sesame oil only contain a single peak.

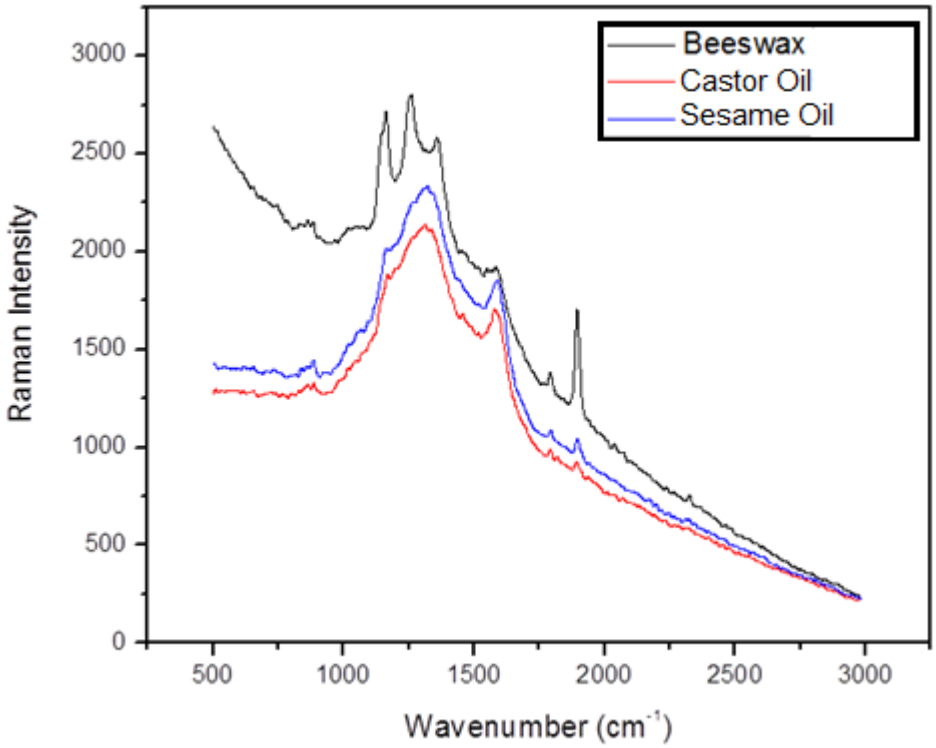

Figure 4.98 Non-baseline corrected data for surrogate soots (n=5). Spectra for palm and olive oil could not be produced.

4.10.3 Ancient lung tissue

Spectra could not be produced from interrogation of ancient tissue section with a raman laser.

4.11 Fourier Transformed InfraRed Spectroscopy

4.11.1 Surrogate oils

Figure 4.99a shows the FT-IR spectra obtained from the surrogate fuels. Beeswax is solid at room temperature and could not be analysed in this manner. Apart from apparent differences in the region of 800-1500cm^{-1} and olive oil featuring a hump between 3200 and 3700 cm^{-1}, all the spectra are very similar. Figure 4.98b shows the separated spectra allowing differences in peak shape to be observed.

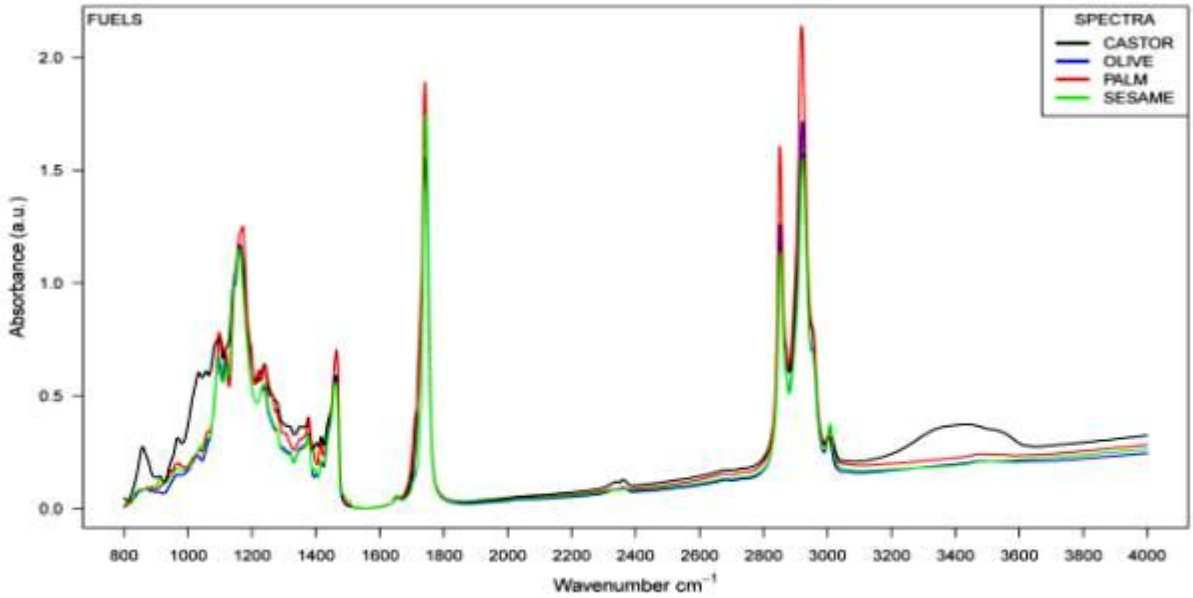

Figure 4.99a FT-IR spectra of oils used to create surrogate soots (background subtracted).

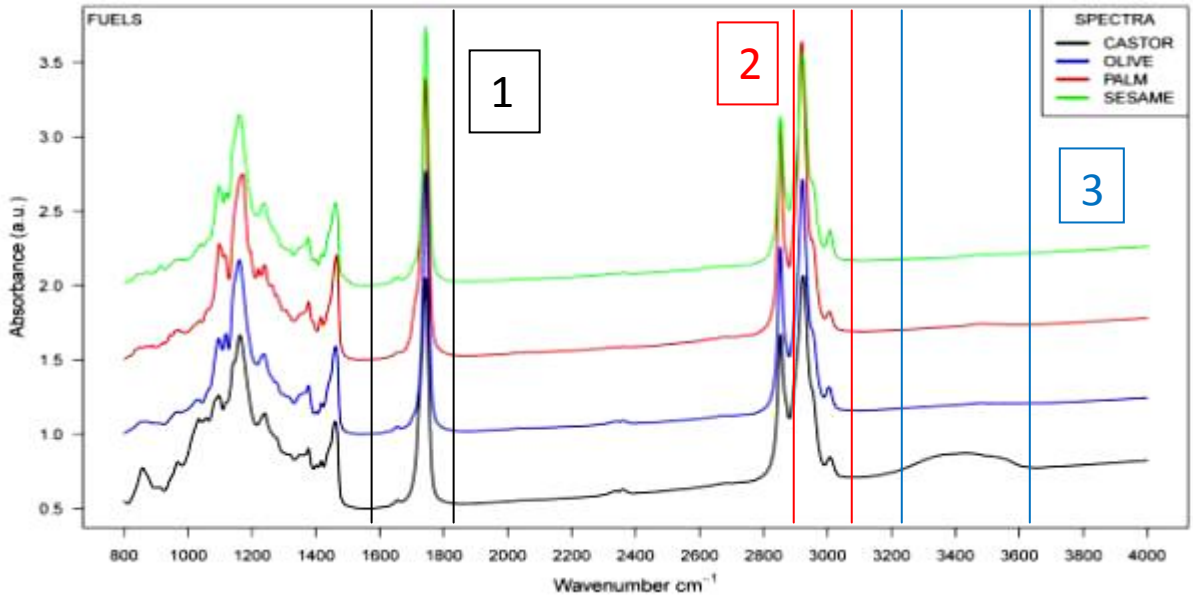

Figure 4.99b Separated FT-IR spectra of oils allowing differences in peak shapes (regions 1, 2 and 3) to be observed (background subtracted)

From figure 4.99b, it can be seen that there are differences in peaks between the different oils. The differences in the region of 800-1500cm^{-1} have been removed by the scaling and separation process. There is a slight difference in peaks in region (1) where palm oil appears to have a hump where other fuels have a smooth line. In region (2), the second peak appears to have different hump shapes on the way down. This is the fatty acid region. In region (3) (the polysaccharide region) castor oil possesses a broad hump whereas the other fuels do not.

Figure 4.99c shows a principal component analysis (PCA) plot of the fuels. Principal component analysis is a mathematical procedure that allows a set of possibly correlated observations (the FTRI spectra) to be transformed into uncorrelated linear values (the symbols on the plot). When plotted, the proximity of the symbols (of the same type) to each other shows their variance and the proximity of the different symbols shows their statistical similarity. This plot shows that the standard deviation and variance of each sample is very low. The least saturated oil (castor) is very different to the most saturated oil (palm) whilst the middle oils are very similar.

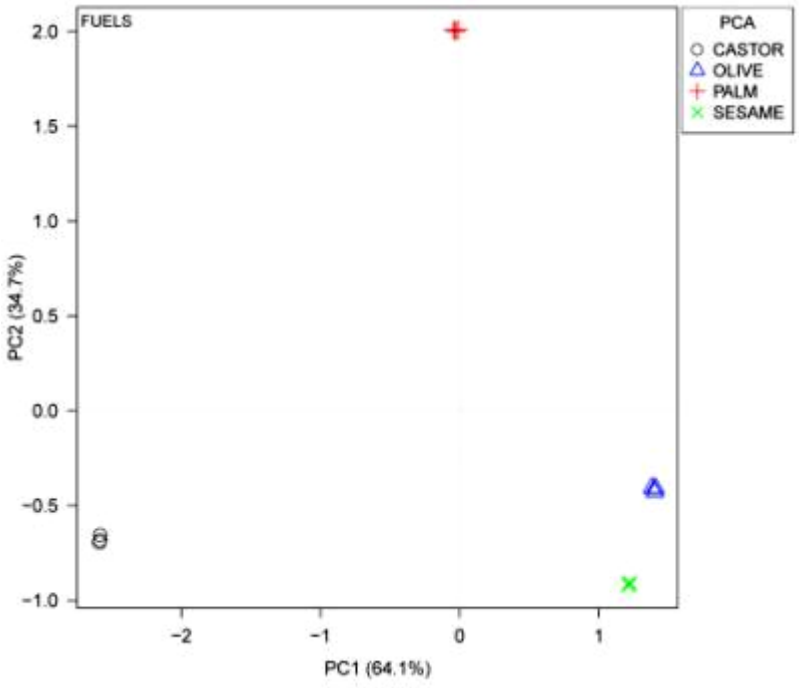

Figure 4.99c PCA plot showing variance within replicates of samples and the overall similarities between the different fuels.

4.11.2 Section of mummified lung A13

The FT-IR spectra of different areas (anthracotic, suspected silicotic and particle-free tissue) can be seen in figure 4.100a. The region of 900 to 1869cm^{-1} is too noisy for direct comparison; however there may be differences in the peaks in region (1) which corresponds to the boundaries of the fatty acid and polysaccharide regions. Figure 4.99b shows the PCA plot of the spectra. Unlike the oils, there is a significant amount of variance between the different tissue replicates, and between the anthracotic and silicotic regions. However the spectra does show that the anthracotic, silicotic and tissue regions are different to each other.

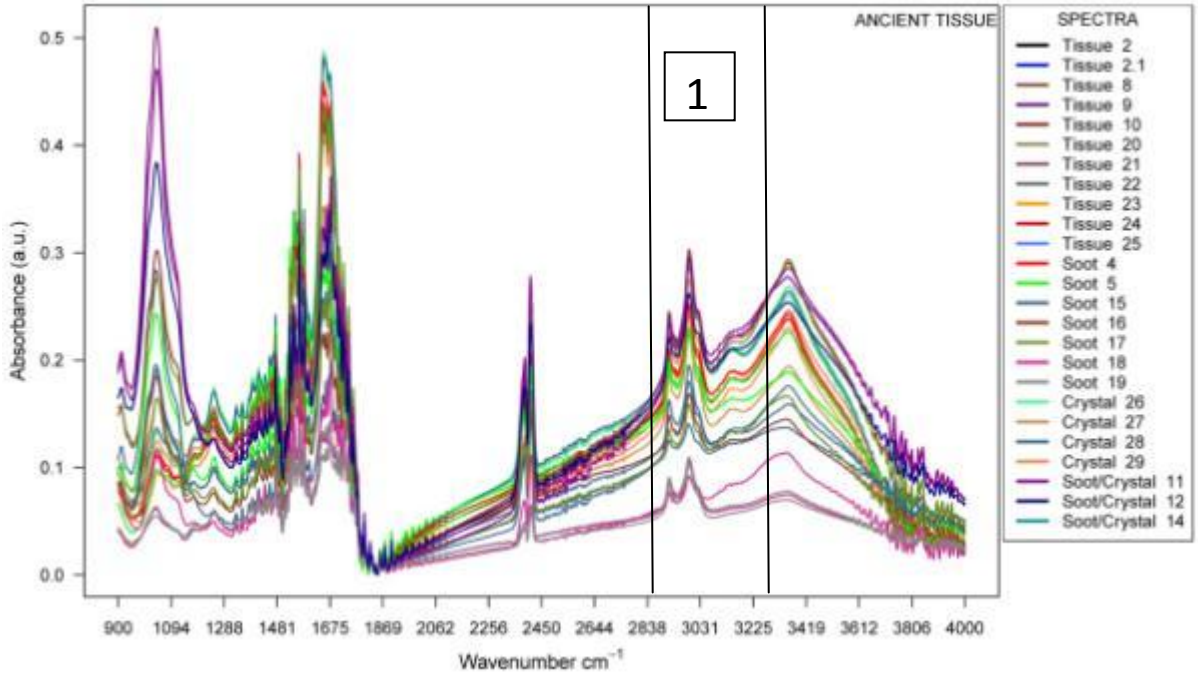

Figure 4.100a FT-IR spectra of different regions of a section of mummified lung from mummy A13 (background subtracted). Differences can be seen in region (1).

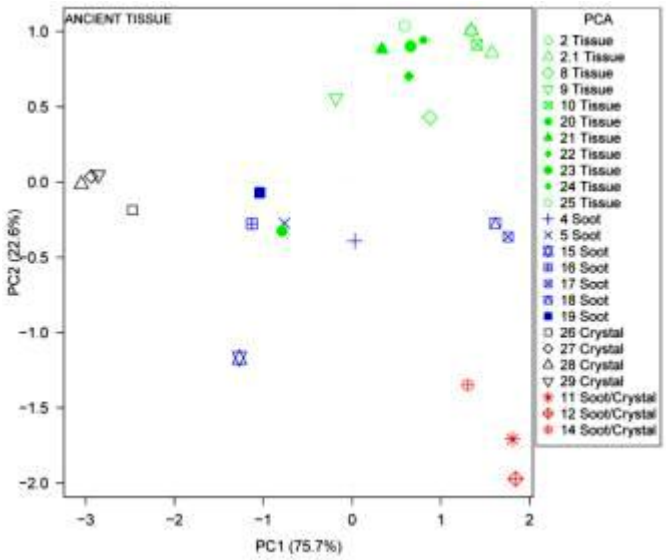

Figure 4.100b Principal component analysis plot showing how variance within replicates of samples and the overall similarities between the different areas of the section.

4.11.3 Extracted ancient particles

The FT-IR spectra of suspensions of particles extracted from different mummies can be seen in figure 4.101a. There may be differences in the peaks in region (1) where A4, DO45 and A108 appear to have peaks where the other suspensions do not. Region (2) also appears to show variation between the different suspensions. Figure 4.101b shows the PCA plot of these spectra. There is a larger amount of variance between the different replicates of the suspensions than in either the oils or the mummified tissue regions. This indicates that this technique may be suitable for this type of sample.

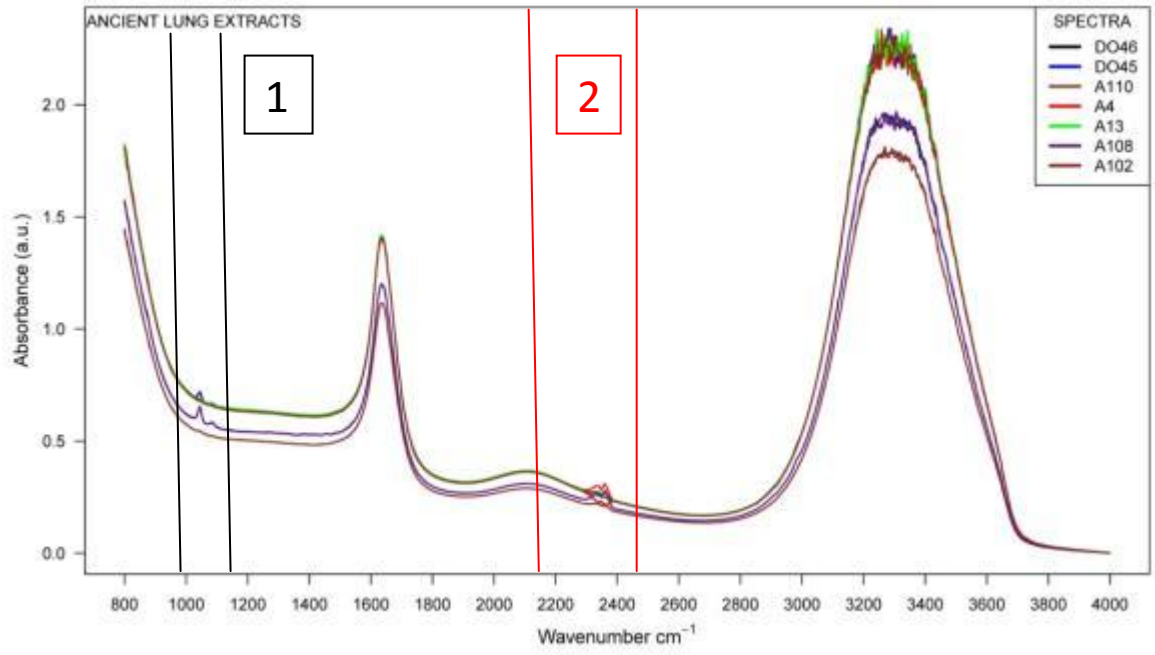

Figure 4.101a FT-IR spectra of suspensions of particles from different mummified lungs (background subtracted). Differences can be seen in region (1) and (2).

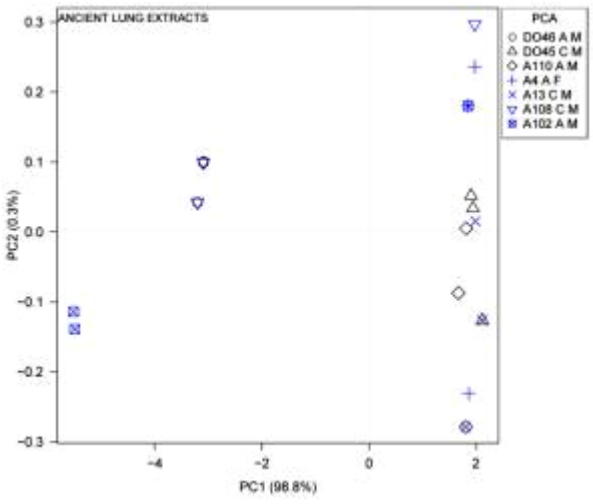

Figure 4.101b Principal component analysis plot showing how variance within replicates of samples and the overall similarities between the different particle extracts.

Chapter 5

Discussion

As previously mentioned in the introduction chapter, the ancient Egyptians suffered from a variety of lung diseases. The degree and type of disease would have depended on the individual and their exposure to disease causing particles. The particle composition in many ways is a permanent record of the environmental, occupational and social status of the individual during life and at the time of death. Differences in the shape, size and elemental composition of these particles will give insight into the provenance of the particles inhaled during the person's lifetime. With such a wide variety of diseases and potential sources of disease-causing particles, it is essential to have as many samples of mummified lungs as possible. Not only does this make the study statistically viable but also allows for the disease and particles of different groups of individuals to be compared.

The twenty samples of mummified lung for this study were obtained through the International Mummy Tissue Bank at the University of Manchester. This unique facility possesses over one thousand samples of mummified tissue from Egypt and Nubia which has been donated by universities, museums and private collections (Lambert-Zazulak et al, 2003). The resource pool for mummified Egyptian tissue for scientific analysis is not being replenished due to the long standing political opposition to the removal of mummified human tissue from Egypt. Fortunately, Sudan, which was part of the ancient Egyptian empire, has less strict rules on the removal of human tissue than Egypt and some of the material in this study came from Sudan. Ideally, if numbers of specimens had been sufficient a multi-centre investigation would have been undertaken. This would have given additional information to this study. However, it was decided to have a single population and to investigate these by histological and analytical techniques which would lead to a greater understanding of the inter-personal and community commonalities and differences.

During the practical investigation of my Master's thesis, I examined specimens from eight Canopic jars to establish the presence of funerary plant remains. It was expected that the use of funerary plants in wrapping internal organs was a standard procedure although this has not been fully established. No plant remains were found in the specimens histologically examined. It was established that the

tissue specimens were mostly lung based on their micro-anatomical structure and the presence of anthracotic and silicotic particles.

My Master's thesis was a limited study whose main aim was to identify histological tissue. It became apparent that the particles were not homogeneous in size, shape or distribution.

A histological screening study was carried out to positively identify samples which could be subsequently used for analytical techniques. Initially the Toluidine blue staining technique was used to visualise the micro-anatomy of the tissue, however, the drawback with this was the state of preservation was so poor in many specimens that individual components of the tissue, such as, alveoli could not be positively identified. Therefore it was impossible to positively identify any mummified tissue as lung.

The structure of lung from a modern environment was compared to other possible types of tissue, such as, liver which could have been contained in the canopic jars. Lung is a unique organ that contains many tubular and vascular structures, of which each has a characteristic configuration of elastic fibres which are known to be very resistant to putrefaction and degradation. The classical way to demonstrate elastic fibres in histological preparations is using a variation on the elastic Van Giesen (EVG) where the elastic fibres are stained with an elastic stain and counter-stained with a Picro-dye complex. From previous work by Allan Hicks in his MSc thesis in which he compared numerous EVG configurations on mummified tissue (Hicks, 2004). He demonstrated that the most effective combination was Miller's elastic stain coupled with the counter-stain Picro Sirius.

The three most common vascular structures in the lung are arterioles, venules and bronchioles. Arterioles are the mid-stage between large arteries and small capillaries and possess small, almost circular lumen. They contain large amounts of elastic fibre in the tunica media (the middle lining of the vessel) to counteract the high pressure caused by the systolic heartbeat. It also contains larger amounts of smooth muscle to further compensate for this pressure. Venules are small veins and have much larger and irregular shaped lumen than arterioles. Their tunica media contains much less elastic fibre as they function at much lower pressure than arterioles. Bronchioles transport air throughout the lung. They decrease in

size the further they travel from the bronchus and terminate in alveoli. Unlike the larger bronchioles which possess hyaline cartilage to maintain their shape, the smaller bronchioles have increased amounts of elastic fibre in their lamina propia (the inner lining layer of the vessel) to perform this function. The bronchioles terminate in alveoli which are small gas-filled sacs whose structure give them a large surface area where blood/gas interactions occur. These sacs possess elastic fibres to allow them to expand and contract during respiration. Although two of these four structures are not unique to lung, observing their presence and elastic configurations along with anthracotic or silicotic particles will lead to the positive identification of ancient lung tissue.

A second pilot study was then carried out which used different stains (Haemalum and Eosin, Toluidine blue, and Miller's elastic) to evaluate the tissue and any particles held within the tissue. Multiple stains were used as the different stains reveal information complementary to each other and there is not one stain that can reveal all the required information about the tissue and particles. Haemalum and Eosin was carried out as it is the standard staining procedure used in histology laboratories around the world. Haemalum stains the nuclei in the section black/blue whilst the eosin counterstains the rest of the tissue pink. Whilst this is a very powerful stain for modern tissue, its usefulness for analysing mummified tissue is greatly reduced as most, if not all, nuclei in mummified tissue have degraded. Haemalum and Eosin usually results in whatever degraded tissue is present being stained solely by eosin. Additionally this staining procedure may add aluminium and sulphur derived from the aluminium potassium and aluminium sulphate which are used as the mordant in the stain solution which would interfere with subsequent elemental analysis. Another problem with this staining reaction is that it is performed at pH 4.0., at this pH any acid soluble compounds such as limestone (calcium carbonate) will be dissolved and any released calcium would combine with the haemalum stain to produce an insoluble "calcium lake" masking other components.

Toluidine blue is very suitable for this study as not only does it display the architecture of the mummified tissues, it also clearly displays the anthracotic and silicotic particles in the tissue. Toluidine blue powder is generally supplied as the zinc salt of Toluidine blue and therefore with any subsequent elemental analytical

techniques on stained sections care would have to be taken that zinc had not been added to the tissue by this staining technique. The metachromatic property of the Toluidine blue stain can also reveal additional information about the particles held within the tissue. When an area stains purple with Toluidine blue, it means that the area possesses a substance that has allowed the dye molecules to form aggregates that absorb a different wavelength of light (in this case purple) to individual dye molecules that absorb blue light. Metachromasia can therefore demonstrate chemical differences in either tissue or particles across a seemingly uniform section of tissue. This stain operates at a pH of 4.2 which is not acidic enough to dissociate most inorganic rock compounds for example, gypsum, but could have removed limestone. These inorganic rocks would have come from the surrounding environment of the individual and could be used to suggest the individuals' geographical location.

Miller's elastic, although very useful for visualising elastic fibres and lung vascular structures, is not suited for demonstrating particles in the tissue. This is due to the addition of many chemicals used in the staining procedure for example, potassium permanganate which is used in the staining technique to oxidise the elastic fibres in preparation for the Miller's elastic stain which could under certain circumstances oxidise inorganic or organic particles inducing a change in their elemental composition or physical appearance. Picric acid is a chemical that binds actively to metallic groups forming picrates which are often soluble and have the potential to remove some inorganic or organic components. Additionally these substances could have altered or added various compounds or chemical groups to any organic or inorganic particles present in the section. The length of time involved in staining process (at least seven hours) also increases the probability that particles or indeed whole sections of tissue may slip off the slide into the staining mixture.

As well as allowing the visualization of particles and the identification of the tissue type, these three stains allowed the assessment of disease states in the lung tissue. In a modern Egyptian one would expect to find diseases, such as, tuberculosis, emphysema, anthracosis and silicosis. Tuberculosis would be difficult, if not impossible to diagnose in ancient tissues as its pathogonomic features, discrete granulomas, would have not survived either mummification process because of pronounced tissue degradation and tissue compression.

Additionally the effects of mycolic acid produced by *M. Tuberculosis* would not be evident for the same reasons. Emphysema, where the alveolar sacs have been destroyed or coalesced meaning they can no longer function would be impossible to observe as most preserved lung tissue is so degraded and compacted that individual alveoli cannot be distinguished. For anthracosis and silicosis, the particles must be less than ten microns in aerodynamic diameter in order to enter the lungs. Any larger particles will be removed by nasal mucus or the mucocilliary escalator (Introduction section 1.2.3). When the foreign particles rest in the lungs, they are phagocytosed by alveolar macrophages. These macrophages will remove cellulosic or proteinaceous particles; however silicon and carbon cannot be broken down so the macrophages accumulate them in certain areas of the lung, coalesce and break down forming large areas of aggregated particles. The breakdown of the macrophages can damage the alveoli creating permanently air-filled bullae which are formed by the breakdown of alveolar walls forming large spaces containing the anthracotic and silicotic particles. As the soft tissues' immune and physical reactions to disease are not well preserved in either spontaneous or artificially mummified bodies, the only diseases which can be examined are those who possess pathogonomic features that can resist degradation. Anthracosis and silicosis with their chemically resistive anthracotic and silicotic particles are two such diseases that have been previously found in mummified tissue (Tapp, 1979; Walker et al, 1987).

Before the mummified lung tissue was examined histologically for a second time, it was decided to optimise the sample preparation and staining techniques on a biological model as mummified material is a finite resource that is hard to obtain and ethically undesirable to waste. After examination of the first pilot study, it was also observed that the ancient particles are aggregated together and they would have to be extracted and isolated to provide optimum specimens for further size, shape and elemental analysis. Additionally, it is not known to what extent either mummification process altered the organic and inorganic particles within the lung. A novel biological model was designed to optimise the staining and extraction techniques and allow the morphological and elemental changes of particles within mummified lung tissue to be studied. The lungs were obtained from rats killed as

part of a separate study into cardiac myocytes. Not only is this model ethically sound but it also provided a use for laboratory animal tissue that would have otherwise been disposed of. In an ideal situation the particles would have been introduced into the lung by respiration or at least by insufflation of the dry particles as would have happened in life, however, as the lungs were from a dead animal this was not possible. The solution to this was to use a pipette to pump surrogate particles (in suspension with a saline solution) in and out of the lungs via the bronchus. The particles would then stay in the lungs as they were mummified. The main caveat with the model would be the lack of biological reaction, ie, immune response or phagocytosis of particles by macrophages, to the particles by the rat lung tissue as the animal was dead at the time of the particles being introduced.

Once the biological model had been designed, both inorganic and organic surrogate particles were needed. The inorganic surrogates were produced from lightly-crushed modelling clay which were then taken into a saline suspension by agitation of the clay in saline. There would have been more variation in the inorganic particles the ancient Egyptians were exposed to, for example, desert sand, particles from processing of stone, but modelling clay was chosen as it was readily available and very easy to put into suspension with saline solution. Other modern surrogates, such as, sands from Egypt, mud bricks and phytoliths were considered but it was decided to only introduce one inorganic particle into the biological model to simplify the extraction and analysis process. Phytoliths were extracted from barley in an established technique which mimics the crop burning process which should result in respirable phytoliths (Becklake, 2007).

For the organic surrogates, it was decided to combust fuels using modern lamps styled in an ancient Egyptian fashion, using double-twisted cotton wicks like those found at Amarna (see Introduction section 1.3.3). Although the selected modern fuels were thought to be the same as those used by the ancient Egyptians, they were obtained from modern commercial sources. The modern fuels would have been hydraulically pressed, filtered and sometimes distilled which would result in a much purer product than the ancient Egyptians possessed. These impurities, for example, plant matter, sand or stone from the grinding mill, may have resulted in different burning characteristics such as, sootiness, temperature of the flame and

viscosity (wick flow). Even the elemental composition may have changed depending on the production methods, for example, certain acids and alcohols only leeching out of seeds when they are crushed by a hydraulic press. The modern recreation lamps for this study were provided by an outreach programme with Mossley Hollins High School where students in arts and science clubs researched the designs for the burning vessels, produced them from fired clay, evaluated the burning properties of the fuels and ensured that soot was produced by collecting it on a cold metal plate held over the flame. Unlike the inorganic surrogates, the organic surrogates from the modern fuels needed to be captured from the smoke plume before it could be put into the biological model.

There are many methods of soot capture available including suction onto a filter, immersion in water, capture by water spray or collection on a glass plate held over the flame. Each method has an effect on the size, shape and possible composition of the surrogate soot particles so it is important that the correct method is chosen for the correct analytical technique. For the biological model, the main consideration was the size and shape of the soots. They needed to be fully combusted, respirable individual particles of soot just like those that the ancient Egyptians would have been exposed to. The soots also needed to be suspended in a water solution as they were introduced into the rat lungs. The suction onto a filter and collection on glass plate methods were judged not appropriate as they would produce large clumps of aggregates of soot and it could not be guaranteed that the fuel had been fully combusted. The immersion in water and spray capture methods were more promising that they required less sample preparation as the soot was already collected in suspension with water. Initially a hookah-like collector was developed which used an aspirator to draw the lamp's smoke plume through a funnel via a plastic tube into water where the soot was captured. The method was very inefficient and the soot produced was very hydrophobic and aggregated where subsequent analysis was impossible. Instead a spray capture method was developed where a water spray using a garden sprayer was passed through the smoke plume at the tip of the lamp flame, the spray being captured in a beaker opposite to the spray source. Additionally, a small amount of detergent (sodium lauryl sulphate) was mixed with the water spray to try to keep the soot particles separate. There are several advantages to this method: firstly the spray

covers the entire smoke plume and rapidly captures the majority of the soot produced by the flame. The spray can be moved so it doesn't put out the flame or produce partially combusted fuel. The captured soot is already suspended in water which can be easily stored or to which salt can be added (to produce a saline solution). The final advantage is that the added detergent ensures that the collected soot is non-hydrophobic with fewer aggregates.

After the organic and inorganic surrogate particles had been produced, their suitability for the biological model needed to be established. This was achieved by characterising their size and shape through light microscopy. The light microscope images were then analysed using a software package called Leica Quantimet software.

The appearance of these surrogate soots can be seen in section 4.1.1. These surrogate soots were mounted in xam mounting medium which is xylene based mounting medium which is immiscible with water. The advantages of using xam are that the refractive index of xam is 1.52 which is higher than water and allows surrogate particles to be imaged more clearly (Iramm, 2012). Secondly the use of a non-water based mounting medium reduces the effect of brownian motion on the particles and again allows them to be imaged easily.

The surrogate soots are shown to consist predominantly of individual soot particles with several aggregates. Although all five fuels appear very similar, sesame oil, olive oil and beeswax contain the largest number of aggregates whereas the most and least saturated oils, palm and castor oil contained the lowest number indicating the degree of saturation affects the sootiness of the flame. Fuels that consist primarily of an extreme of hydrogen saturation (palmitic acid in palm oil) or non-hydrogen saturation (ricinoleic acid in castor oil) may burn more consistently ensuring that the soot particles do not adsorb any oil residues and aggregate as easily. The middle-range saturated oils, sesame and olive oil, consist of a mixture of compounds of varying saturation producing a less consistent flame resulting in aggregated oily soot particles. Beeswax is composed of chemical components whose degree of saturation is unknown; however, it appears to produce soot similar to that of the mid-range oils. Further variation between these surrogate

soots can be seen in size and shape analysis in Results section 4.4.1. All the surrogate soot particles are potentially highly respirable, i.e., less than 10 microns in aerodynamic diameter. If dependence on artificial illumination was widespread in ancient Egypt then most Egyptians would possess these particles in their lungs. This is due to the lack of ventilation in their houses (figure 1.4a and b) which would have ensured the slow removal of smoke from illumination and cooking sources, leaving a residual suspension of soot in the domestic environment. The majority of Egyptian society would have been exposed to this soot-rich atmosphere as the "Khamsin" wind season with its frequent strong sandstorms would have forced the population indoors for weeks at a time (Mair, 2008). If differences between the soots can be observed, then the identity of the soots in ancient lungs could be discerned. The identity of these soots along with their provenance, ie, the periods of history they were popular in or the social group that used them could elucidate social details about the mummy. Castor oil with the lowest degree of saturation produced the largest sized soot particle (4.2 μm^2) whilst the heavily saturated palm oil produced the smallest soot (1.7 μm^2). These differences are presumably down to the temperature of the lamp flame where the higher the degree of saturation of the fuel, the higher the temperature and therefore, the finer the soot particle produced. The other oils and beewax which were similar in aggregation behaviour also produced soots which were similar in size. These differences between soots produced from fuels with different degrees of saturation also extend to the roundnesses. When the roundnesses of these surrogate soots were compared, palm oil and castor oil produced the roundest soot particles. Beeswax and olive oil soots were significantly less round however sesame oil was quite similar in size to both castor and olive oil soot.

The areas and roundness of these soots were calculated from the images by the Quantimet software. This software used feret diameters (shown in figure 3.6) to measure the areas, lengths, breadths and roundnesses of coloured pixels occupied by the soots (Leica, 1994).

This size and shape analysis approach was also extended to the examination of the inorganic surrogate particles which included modern sand samples from Egypt,

fragments of ancient mud bricks and extracted phytoliths. The methodology for appearance, size and shape analysis of the inorganic surrogate particles was the same as the organic particles except they were mounted in glycerin whose refractive index enhances the visualisation of birefringent particles. Their appearance can be seen in section 4.1.2. The appearance of the modern sands can be classified into two categories depending on the type of rock and geographical location; sands with 3 different grain types which would apply to Amarna, Amarna north palace, Beni Hassan and Karnak sand and sands with two grains which applies only to sand from Tuna El-Gebel. The first category all appear similar and consist of sharp angular grains of varying sizes. The second category consists of large rounded grains of two different colours. The archaeological sites of the first category are all located within the Nile valley region whereas Tuna El-Gebel is situated on the border of the desert and these results show the difference between these two types of valley and open desert sand. The three mud bricks can also be classified into two categories by their appearance; the two mud bricks from Amarna North Palace consist of three types of grains with a large amount of variation in size. The Dahshur pyramid complex mud brick consists of only two types of much smaller grains. Mud bricks were usually manufactured near to the site of building construction and these differences in appearance highlight the geographical and geological differences between the two archaeological sites. The phytoliths can only be visualised easily in polarised light as they appear translucent in bright field illumination. In polarised light, the phytolith appears as a long, thin needle-like structure. It is completely unlike any other inorganic surrogate particle.

Further differences between the inorganic surrogates can be demonstrated in the size and shape analysis (section 4.4.1). Of all the samples, only the phytoliths lie within the respirable range (less than 10 microns in aerodynamic diameter) on average. This agrees with a previous study of phytoliths which suggested that phytoliths are released in a respirable form during crop burning (Becklake, 2007). However, when the minimum values of the size measurements are considered, five to ten percent of all the sand and mud brick samples, except sand from Tuna El-Gebel, were in the respirable range. This suggests that ancient Egyptians living in the Nile valley areas, which would have been the majority of the population,

could have respired sand and mud brick particles. Inorganic particles and their associated diseases must have been widespread in ancient Egypt as most, if not all Egyptians were exposed to both mud-bricks and the desert every day of their lives. Egyptians would have encountered the Nile valley sands every day as they travelled or simply carried out their business. Most buildings and homes in Egypt were constructed out of mud bricks so this would have been an extremely widespread source of respirable inorganic particles. Women and infants would have been especially at risk with mud brick dust; children would be crawling around on the floor during their infancy whilst women would have spent a lot of time in the home environment. As the Egyptians would have respired a large amount of inorganic particles during their lifetime, if differences between the different sands and mud-bricks can be demonstrated then this would possibly allow the identification of particles (and their mummies) to a specific geographical area. When considering the average values, only the rounded desert sand from Tuna El-Gebel is significantly larger to the other samples. All the smaller, more angular grained sand samples from the Nile valley are roughly the same average area and length. The mud bricks can again be divided into two groups; the Amarna mud bricks and the Dahshur brick. The Dahshur mud brick consists of larger particles on average than the Amarna mud bricks which is surprising as the images suggest the opposite. This may be due to the Amarna mud bricks possessing a broader range of sized particles which may lower the average.

Additional differences between the samples can be demonstrated through the roundness characterisation. Phytoliths are significantly less round than all the other samples which is unsurprising given their needle-like shape. Although Tuna El-Gebel sand was the largest size, it is also the most round sand particle. This is consistent with desert erosion where particles are rounded after colliding with other sand grains when being moved around by wind. The other sands are not from the desert and are less round which is consistent with their appearance and provenance. The Amarna mud bricks are of similar roundness which is not surprising given that they are from the same archaeological site and were used in buildings that were constructed at the same time. The Dahshur mud brick particles possess similar high roundnesses to the other mud bricks. This suggests that mud brick material came from non-desert sources due to the angular nature of the

particles. These sources could have included sites near rivers/irrigation which could have provided the water necessary for manufacturing the brick.

Once the particles of the olive oil soot and the modelling clay which were suspended in saline (at a concentration of 0.5g/ml) had been characterised by their size and shape and deemed suitable for the biological model, they were introduced into the rat lungs. The rat lungs were artificially mummified using a formulated artificial natron and a dehydrating oven before being rehydrated after twenty-eight days. Table 4.1 shows the weight reduction due to the mummification process. The minimum weight reduction was 68% indicating that the method worked well and removed a lot of water from the tissue.

At this point, it was necessary to develop the particle extraction procedure before the tissue and particles from the biological model could be analysed. This is necessary as anthracotic and silicotic particles would have been phagocytosed by alveolar macrophages and collected into large aggregated deposits (see Introduction section 1.2.3). An ideal extraction method would release the particles from the tissue and allow them to be isolated for subsequent analysis without altering the particles' chemical and physical structure. Initially tissue digestion using the papaya plant-derived enzyme papain was attempted. This method has been used successfully with ancient DNA extractions and is frequently used to separate out diatoms from modern lung tissue particularly in the forensic examination of drowning victims. Although the enzyme was successful in breaking down the lung tissue, subsequent bacterial colonisation made analysis of the extracted particles very complicated. Papain was chosen as its optimal pH is 6 to 7. Other enzymes, such as, trypsin, require a more acidic pH which could dissociate certain inorganic particles like calcium carbonate inside the tissue. After the failure of the tissue digestion protocol, a sonication method was designed where an ultrasonic cleaner was used to agitate the ancient particles out of thin sections of mummified lung tissue. When the section of lung was cut by a microtome, the particles within the tissue were held in place by the paraffin wax and weak bonding with the tissue. With the paraffin wax removed, the ultrasonic cleaner provided enough agitation to break the loose bonding between the particles and tissue, thus liberating the particles. Centrifugation of the sample moves the particles and tissue into a pellet which was washed with multiple

washes of xylene and alcohol to result in a suspension of extracted particles in water. Disadvantages of this methodology are the possibility of losing particles in-between every wash when the supernatant is removed, and the possible inclusion of mummified tissue that may complicate size and shape analysis.

After rehydration, sections of mummified rat lung were taken and prepared for histological examination. The rat lungs were stained with Toluidine blue and the resulting light microscope images can be seen in Results section 4.2.1. None of the rat lungs contain either organic or non-organic surrogates. There are several reasons why this could have happened. The amount of particle solution introduced into the lungs may have not been sufficient enough to ensure a large number of analysable particles were present in the lungs. The surrogate material may simply have been deposited in another area of the lungs that were not sectioned in this tissue block. The residual air held in the rat lungs may have slowly forced the particle suspension to ooze out after inspiration had taken place. Another possibility is that the suspension was too viscous to travel far into the lungs. Additionally the rat lungs all show alveolar damage consistent with emphysema, ie, the alveoli have burst. This was presumably due to excess pressure applied by the pipette during the inspiration process. However, it is also possible that the section of tissue came from an alveolar duct and this area was naturally devoid of regular alveolar structures. This means that the changes in physical and chemical properties of lung particles have not been elucidated by this biological model. If the model were to be repeated, a diluted and more viscous suspension of particles would be carefully inspirated into the lungs with a carefully monitored amount of force. The three rat lung samples demonstrate possible signs of an immune response against an infection just before death. As mentioned previously, due to desiccation, compression and degradation over thousands of years, an immune response of this type will not have been preserved in mummified lung tissue from Egypt. It is possible that the immune response may be type II alveolar cells secreting surfactant.

After the biological model experiment was concluded, the second multi-stain study was carried out on the twenty mummified ancient Egyptian lung samples. The

histological images of these sections can be seen in Results section 4.3.1. Only nine of these samples labeled as “lung” were found to contain positively identifiable lung tissue. The other eleven samples consisted of coprolite containing degraded unidentifiable tissue and plant material. This information has been previously summarised in tables 4.2 and 4.3 in Results section 4.3.2.

The material from Kulub Narti, mummies S82, S85 and S195, were all identified as coprolite. Representative images of these samples can be seen in figures 4.11, 4.14 and 4.16a respectively. The figures all demonstrate the characteristic features of coprolite: degraded and fragmented plant material intermixed with unidentifiable particles and degraded tissue. The fragmented plant material consisting of damaged xylem or phloem sieve tubes has been damaged through the processes of mastication and digestion. Sample 51813 also contains plant material. Its representative image (figure 4.51) shows better preserved xylem and phloem than the Kulub Narti specimens which would be expected as it has not been subject to digestion processes. Mummy A105 (figure 4.32) is also identified as possible plant material and this material is much more degraded than either the coprolite or BM 51813 material. Mummies A132, MM 1777, MM11724, 34193, and 37949 are all unidentifiable and their representative images show badly degraded tissue which possesses no obvious identifying structures.

One of the aims of this study was to assess the differences in quality of preservation of lung tissue and their associated particles across the different types of mummification (intentional and spontaneous). It appears that all the intentionally mummified lung samples obtained for this study cannot be identified as lung tissue. This does not mean that intentional mummification cannot provide examples of well-preserved lung tissue. There are many potential reasons why the identities of mummified samples might not match their provenanced information; the samples may not have been directly sampled from the mummy itself or the individual taking the samples may have lacked the experience to identify the correct tissues in a mummy. There may be lots of variation in a small sample, for example, BM51813 has been previously examined and found to contain lung with anthracotic pigments (Walker et al, 1987). However, it is possible that the material supplied for this study was from a different section of the canopic jar that did not contain lung. Canopic jars may also have been unintentionally misidentified by

ancient embalmers if they put the wrong set of mummified organs in the wrong jar by mistake. The unidentifiable material in this study may have been further degraded by improper storage in a museum. Additional dangers to mummified material in museums include misguided attempts at conservation and pests. Poor attempts at conservation can not only damage mummies but also introduce elemental contaminants which may hinder scientific analysis. Pests, such as *Tyrophagus putrescentiae*, may feed on fungi present on improperly stored mummies, leaving behind their exoskeletons which act as food for further fungal colonization. A fungal granule liquefying mummified tissue from mummy A102 can be seen in figure 4.30. Additionally the *Tyrophagus putrescentiae* faeces present on tissue could be misinterpreted as anthracotic pigment.

All the tissue positively identified as lung came from non-elite naturally mummified mummies buried at the Kellis cemeteries in the Dakhleh Oasis. As previously mentioned, sampling of mummified tissue is important. These samples were from preserved mummies whose organs were easy to visualize and taken by a very experienced scientist (Prof A. Aufderheide). Only two samples from the Dakhleh oasis were unidentifiable and they comprised the youngest age at death (male mummy A132, aged 3 to 5 months) and the joint oldest age at death (male mummy A105, aged 50 to 60 years). These two samples represent the age groups that are most likely to suffer from infection. If the infant or old man (for his time period) were to have a necrotizing condition, such as, septicaemia, the enzymes released by the disease causing bacteria could damage organ systems and lower the overall state of preservation. If bacteria were also present in the lung, for example, pneumonia, they would greatly lower the state of preservation as well.

An image of poorly degraded lung tissue from mummy A4 is shown in figure 4.24. The tissue consists of small semi-continuous lengths of TB stained tissue. The tissue is sparsely distributed with many voids and spaces. No vascular features can be demonstrated. Additionally, a fungal granule (figure 4.25) in the process of liquefying surrounding mummified tissue has been demonstrated. In contrast to this, a representative image of well preserved lung material (EVG stained) from mummy DO45 can be seen in figure 4.17. This lung tissue is demonstrated as

large compressed bands of interstitial tissue which has been stained pink. The degree of compression is such that no discrete alveoli can be distinguished. Despite this, the large amount of elastic fibres and presence of a possible bronchiole along with anthracotic pigment allow this tissue to be identified as lung. There are small tears throughout the tissue that may have been produced as an artefact from microtomy. This is when non-uniform hardness in the tissue causes the blade to jump as it cuts and create micro-tears in the tissue section.

There are large deposits of anthracotic pigment contained within the tissue. When seen at higher magnification in figure 4.18 (stained by TB) the deposits consist of lots of small individual particles conglomerated together. This is consistent with phagocytosis by alveolar macrophages and indicates that the material was present in the lungs some time before death. Metachromasia in between the large conglomerates suggests there may be particles of different composition and charge affecting the binding properties of the Toluidine dye. When viewed with polarised light (in figure 4.19) birefringent particles can be seen co-deposited within the anthracotic pigments which would explain the presence of metachromasia.

An aim of this study was to assess evidence of disease of particulate origin in ancient Egyptian lung tissue. All the positively identified lung material studied in this project contains anthracotic and birefringent particles although the size, distribution and degree of deposits vary from specimen to specimen. The co-distribution of the anthracotic and silicotic particles is characteristic of phagocytosis by alveolar macrophages, and indicates the particles were present in the tissue pre-mortem. All nine mummified individuals suffered from some degree of anthracosis and silicosis, surprisingly, even the youngest individual.

Another aim of this study was to characterize the particles found in ancient Egyptian lung tissue, with comparison to surrogate (modern) particles. To this end, the particles present in seven of the nine mummified lungs were extracted, imaged and characterised by size and shape. Only seven of the nine mummified samples

had extracts taken because the other two sample tissue blocks, DO46 and A126, did not contain enough tissue to allow for extraction to be carried out.

The size and shape characterisation can be seen in Results section 4.4.2. As would be expected all the extracted anthracotic particles are highly respirable, ie, less than 10 microns in aerodynamic diameter. This means that all the anthracotic particles contained within the mummified lungs must have been inhaled when the individual was alive and are not post-mortem contamination. The largest anthracotic pigments were found in mummy A13 (with an area of 1.6μm^2) and the smallest were found in A110 (0.71μm^2). The only significant differences between the areas or the lengths of the extracted anthracotic particles exists between A13 and A4, A110 and A102 meaning that the majority of the particles cannot be distinguished from each other by differences in size. It is possible that given a larger sample number, more individuals could be distinguished from each other. It is unfortunate that no provenance exists concerning the Dakhleh Oasis mummies as this could shed light on why there is a difference between them. Aside from social factors, such as, profession and social status, which may have dictated the type of particle that they were exposed to, there remain the factors of age and gender. The largest particles were extracted from the oldest mummy at time of death (A13 which was fifty to sixty years old) and the smallest were taken from the second oldest (A110, thirty to forty years old) so the size of particle does not appear to depend on the age of the mummy and therefore the degree of exposure. This is because you'd expect the degree of particle exposure to increase with the individuals' age as they would have more time to inhale particles. The study's sole female mummy does possess soot that is significantly different to the soot from male mummies however, the low number of samples (n=1 for this factor) makes a comparison of gender statistically non-viable. Apart from sample A13 there is not much variation in the size of particles extracted from the different male mummies. It could be that this small soot particle was the optimal size of soot that could be deposited in the lungs. Any larger particles may have not been able to be deposited this far into the lung and would have been removed by the body's many defences against foreign particles.

The ancient anthracotic particles are much smaller than the surrogate soots produced for this study. This is to be expected as the surrogate spray capture method captured soot directly from the smoke plume whereas it is doubtful that the ancient Egyptians would have been breathing in smoke directly above the flame of any illumination or cooking source for any considerable amount of time. They would have inhaled a much finer suspension of soot particles contained within the domestic environment due to settling of the larger particles and the lack of ventilation in their houses.

Comparison of the roundness of these extracted anthracotic particles shows that this property shows no significant differences between the different mummies. The anthracotic particles present in the female mummy A4 are significantly less round than the anthracotic particles contained within male mummies. This could suggest that soots produced and inhaled from primarily cooking sources could be different to the soot produced by illumination used by male professions, for example, scribes, tomb painters, etc. The extracted particles are more rounded overall than the surrogates. It could be that the finer, more rounded anthracotic particles found in mummified tissue would have travelled through the air further than the larger, more angular surrogate soot captured from the lamp smoke plume. Additionally smaller, rounded particles would have stayed in suspension in the air for longer thus increasing their chances of being deposited in the lungs. However, only one female was examined and so the gender distribution cannot be ascertained.

The size and shape results from the extracted birefringent, non-organic particles can be seen in section 4.4.2. Like the anthracotic particles, they are all much lower than the ten micron aerodynamic diameter limit. The largest particles (area of $2\mu m^2$) in A111, a 20 to 25 year old mummy, whilst the smallest were found in DO45 (male mummy of unknown age at death). There are no significant differences between the birefringent particle sizes in the mummies. The size of particle does not appear to depend on the age at time of death and therefore the degree of exposure. The degree of particle exposure should increase with the individuals' age as they would have more time to inhale particles and have a macrophage reaction. Mummy A4, the study's only female mummy, does not have birefringent particles that are significantly different to the birefringent particles from male mummies. The low number of samples (n=1) makes a comparison of gender

statistically non-viable. The overall size of these extracted particles is much lower than the surrogate inorganic particles. This may be because the optimal size for birefringent particles held in a suspension of particles of mud bricks within domestic building environments, or the sand hurled around in a sandstorm is much lower than the average size of the particles.

Potential phytoliths were found in one mummified lung sample, DO45. These phytoliths can be seen in figure 4.20 where they appear as long, needle-like structure that are very similar in size and shape to the surrogate phytolith in figure 4.6. Additionally the needle-like structures in DO45 share the same positively birefringent properties as the surrogate which strongly implies they are phytoliths. They are also in the same size region as the surrogate phytoliths. The presence of phytoliths in this individual may indicate that he was a farmer working in the fields and or was at least exposed to burning crops. Another potential source of phytoliths would be the burning of phytolith-containing plant material in the domestic environment.

Like the area and length, statistical analysis of extracted birefringent particles shows that there are no significant differences in the roundnesses between mummies. Overall the particles are less round than the surrogate inorganic particles collected for this study. This could be due to the nature and source of the surrogate particles as they were collected from the surrounding landscape where sand samples would have been created by natural erosion over a long period of time. These ancient birefringent particles may be from manipulation and cutting of stone which would have produced sharper and more angular particles.

In order to achieve a more detailed comparison between the extracted ancient particles and the surrogates, further size, shape and elemental information was visualised and investigated using electron microscopy and various analytical methods.

When the surrogate organic particles were examined and visualised using ESEM (Results section 3.5.1), it was found that the general size and appearance of the surrogates was very similar across all the fuels. The surrogate appeared as light

grey irregular shaped particles on a dark background. This supports the size and shape analysis by light microscopy which came to the same conclusions. The surrogate inorganic particles were examined using ESEM (Results section 3.5.2) and again the results corroborated the light microscopy size and shape analysis. However additional surface information, such as the rough and pitted nature of the sand particles could be seen using ESEM. The nature of the mud-brick surface with random orientations of particles and the needle-like structure of phytoliths were also shown in more detail than with light microscopy. This additional surface information and the higher magnifications (compared to light microscopy) make it useful for examining the particles. Its main disadvantage is that the black and white images produced by ESEM make tissues and certain particles much harder to visualise than brightly stained or unstained light microscopy images.

Some difficulty was encountered when the extracted ancient particles and a section of ancient tissue were examined (Results section 4.5.4 and 4.5.5 respectively). Small sections of tissue were found in the extracted ancient particles, however the greatest problem was telling the difference between the anthracotic and birefringence particles as they appeared very similar. Light microscopy is probably better suited for analysing these extracts as polarised light can be easily used to distinguish between the two types of particles. A possible area of future work would be into separating out these extracted particles so that only anthracotic particles are present in one area of the ESEM sample stub and birefringent particles in another area. This would make analysis much easier. Despite the difficulty with visualising the particles, the general shape and appearance of these extracted particles agrees with the size and shape analysis conducted with light microscopy. Visualising anthracotic and inorganic particles in lung tissue is very difficult to achieve using ESEM. This is due to the nature of ESEM images where only the surface detail can be seen. The particles present themselves as rough, irregular shapes sticking out of the smoother background of lung tissue (figure 3.79a and b). Only where the particles are exposed by sectioning can they be visualised by ESEM.

The limits of characterisation by visual examination of size and shape had now been reached. Further classification would have to be achieved through analysing the elements and chemical bonds present in the extracted particles and comparing them against the surrogates.

The first elemental method to be used was EDX. EDX is qualitative meaning it can tell you the elements that are present in the sample but not their exact quantities. The advantages of EDX are that it is quick and a specific area or particle can be targeted for analysis. The limitations of EDX are that it is a relatively insensitive technique especially compared to bulk analysis methods, such as, mass spectrometry. When the surrogate soot particles produced through the spray capture method were examined using EDX, it was found that they contained very high signals for sulphur and sodium. This contamination was found in all the samples examined leading to the idea that there had been a contamination problem in all specimens of organic particles. When the methodology of production of the soot particles was examined the only real difference between the organic and inorganic particles was their collection. In order to minimise soot aggregation a detergent was used, this detergent being sodium lauryl sulphate which contains the two elements suspected of contamination. A run of the soot collector was run and the particles although aggregated were analysed. The results showing a large reduction of the signal for sodium and sulphur indicated it was the detergent that was causing the contamination problem. It was decided that an easier method be used.

Therefore surrogate soots examined by EDX in this study were prepared using glass plate collection. Although the size and shape of the surrogate would be wrong (which is irrelevant as they have already been characterised), there would be no contamination. This emphasises the importance of tailoring the sample preparation to suit the analytical method, i.e., it doesn't introduce contamination of artefacts that will complicate or influence the interpretation of results.

When the surrogate soots were examined using EDX (Results section 4.6.1), very little differences were found between the different fuels. Very low signal counts were detected from the surrogates which is unsurprising as completely combusted soot should not contain an overabundance of elements. The surrogate soots possessed either sulphur, silicon or both. No other elements were detected. The soot from palm oil (the most saturated oil) contained signals for both as did the least saturated oil, castor oil. The middle-ranged saturated oils, sesame and olive oil, only contained a peak for silicon. Beeswax had a peak for silicon and the highest intensity sulphur peak. All the EDX data had large areas of noise under the peaks indicating that there may be hidden weak signals from other elements and that this technique is just not sensitive enough to detect them.

The inorganic surrogates produced much stronger signals than the surrogate soots and correspondingly they produced much cleaner looking EDX spectra. There is a degree of variation between the different sand samples. This would be expected as the light microscope and ESEM examination of the sands revealed them to be composed of lots of different coloured and sized grains. Sand from Amarna has strong characteristic peaks for silicon, potassium and calcium. There are small peaks for magnesium, aluminium and sodium. This would indicate the rock is primarily an aluminosilicate with some possible dolomite (magnesium and calcium). The sodium was presumably bound to chlorine in the form of sodium chloride. The potassium may also be bound to chlorine but may have been from some plant material mixed in with the sand. Sand from Amarna North Palace again contains strong peaks for silicon and calcium with weaker potassium and a very weak aluminium signal. The presence of silicon and the absence of aluminium indicates that the silicon is primarily bound to oxygen which cannot be detected. This form of Si and O_2 is known as the mineral silica. This shows the large variation that can exist between two sand samples that were taken from locations only five miles apart from each other. Sand from Beni Hassan contains a strong double peak for calcium and a much weaker peak for silicon. The calcium was presumably bound to carbonate (the carbon element of which would be invisible to the detector) and this sample is probably limestone. Karnak sand is very similar to Amarna sand and contains a major peak for silicon and other peaks

for sodium, magnesium, aluminium, potassium and calcium. Tuna El-Gebel is primary an aluminosilicate with a small peak for calcium.

For the mud bricks, the two Amarna bricks had very large peaks for silicon and calcium smaller peaks for magnesium, aluminium, phosphorus, sulphur, and chlorine. Therefore Amarna bricks are mainly composed of silica and carbonates. The additional peaks of chlorine and sulphur (compared to the surrogate sands) are probably due to the presence of plant material in the mud bricks. The Dahshur pyramid block is very similar to the Amarna mud bricks but contains a peak for sodium (which could be bound to the chlorine). The phytoliths contain strong peaks for silicon, potassium and calcium. There are additional small peaks for sodium, aluminium, sulphur and phosphorus. Phytoliths shares peaks with the mud brick samples which would be expected as mud brick contained phytolith-rich plant material, such as, wheat and chaff.

The extracted particles can be seen in section 4.6.5. Particles from the female mummy A4 contain a large peak for phosphorus and small rounded peaks for sodium, silicon and chlorine. The most likely explanation is that the phosphorous is in combination with the sodium producing a sodium phosphate. It should again be noted that the height of the peak indicates the quantity of the element, however, this varies from element to element. For example a peak height of 10 for sodium and a peak height of 10 for potassium does not mean there is the same quantity of both elements, this being dependant on the energy of the x-rays produced by the electron beam. Particles from mummy A13 are very similar although they lack a silicon peak. Indicating this sample had no silicates or silica in the particles. Particles from mummy A102 appear to contain different elements to those in the other mummies. It has peaks for silicon and calcium along with a very small phosphorus peak indicating it may contain some inorganic calcium-based particles and silicates. The EDX spectrum of particles from mummy A111 shows peaks for both silicon and phosphorus. A108, A110 and DO45 only possess peaks for silicon, although the silicon peak in A110 has a higher intensity than A108 and DO45. It is unclear whether this silicon peak could be from anthracotic particles, as most of the surrogate fuels contained silicon, or whether it is from inorganic

particles. The variations that can be shown by EDX include differences in elemental composition and also relative intensity. Overall EDX appeared to work much better with the surrogate inorganic material than on the organic material as would be expected in the fact that the majority of inorganic compounds are composed of specific elemental combinations and the organic soots are composed mainly of carbon, hydrogen and oxygen. This indicated that another method should be employed to examine the ancient and surrogate organic particles.

After it was observed that EDX was the good method for examining surrogate and extracted anthracotic particles but with the limitations of the technique being its lack of quantification and relatively poor detection limits. Another technique relying on the solubilisation of the sample and the subsequent ionisation by passing it through a plasma where the ions were then measured in a quadropole mass spectrometer was used. This method (ICP-MS) has a much increased sensitivity but has the disadvantage that elements under investigation have to be predetermined and that all of the sample has to be in solution this precluding any comparison between individual particles. ICP-MS was used to examine the surrogate fuels, the soots, tissue digests, and extracted particles.

The raw fuel results can be seen in Results section 4.7.1. The least saturated oil, castor oil produced a clean spectrum with no elements other than carbon, oxygen and hydrogen present. This would indicate that the oil is very pure and contains no significant elements. Beeswax contained the largest number of elements and the strongest signals, including the only signal for aluminium and copper out of all the fuels. The presence of these elements in relatively high concentrations is possibly due to the presence of pollen proteins. It is unknown how much elemental variation exists between beeswax from different geographical locations. The most saturated and viscous fuel, palm oil, contained the second largest amount of elements including phosphorus, iron and was the only fuel to contain boron. The mid-range fuels contained elements common to all the fuels, for example, calcium, sodium and sulphur although the levels varied between fuels.

The soots produced from the combustion of these fuels was also analysed using ICP-MS and the results from this can be seen in Results section 4.7.2. Unlike the fuel, the castor oil soot contains various elements. The reason for this is due to the

amount of fuel needed to produce soot. Lots of fuel needs to be burnt in order to produce a relatively small amount of soot. If there are only trace elements in the unburnt fuel, then burning the fuel will condense the elements down and therefore increase the abundance of elements present in the soot. The unsaturated castor oil is the only soot to contain zinc. There is a relatively large amount of silicon in all the surrogate soot and the largest amount found in sesame oil. Sulphur is present in all the fuels with the largest amount in beeswax. Unlike the raw fuels where only palm oil contained boron, all the combusted soots now possess it but at lower concentrations. There is a relatively large amount of potassium and silicon in all the soots. The most saturated oil, palm oil, is the only soot not to contain copper. These results show how different soots are to their uncombusted fuels.

Phytoliths were also analysed using ICP-MS and the results are shown in Results section 4.7.3.

Phytoliths contain large amounts of silicon, unsurprisingly, as they are silicon-based structures. They also contain large amounts of sodium, potassium, magnesium calcium, aluminium and iron. There are trace amounts of strontium, zinc and barium. Phytoliths contain lots of elements that are present in the surrogate soots and fuels, except for strontium and barium. These two elements may work as key identifiers for phytoliths in ancient samples. It is to be expected that plant derived tissues contain a spectrum of elements which will reflect the growing conditions of the plant where it will generally absorb elements and may preferentially absorb specific elements.

After analysing the modern material, ancient tissue digestions and extracts were analysed with ICP-MS to show any mummification contaminants that may be present in mummified tissue and also to illustrate what elements may be lost during the extraction process. The results of the ancient tissue (along with a control of coprolite) digestions are shown in Results section 4.7.4.

More elements can be found in the coprolite control sample than in the mummified lungs. This is not surprising as the coprolite is a mixture of degraded tissue, plant tissue and various other substances that have been excreted out of the human

body. The identifying elements for the different lung digests may be the metal signatures which vary greatly between lung samples.
The coprolite and lung digests all contain zinc. A111 is the only lung sample to contain nickel and not copper. A102 contains manganese and strontium though at much lower levels than the control. Titanium is present in all the mummified lung samples, but at a much lower concentration than in the control coprolite material. There are strong signals for potassium in all the mummified samples with A110 possessing the highest concentration (23,200ppm), which is higher than the control coprolite. Additionally, magnesium is present in all the mummified samples but at much lower quantities than the coprolite sample. Silicon can be found in all the mummified samples as can sodium. Calcium can be found in all the mummified samples with the highest concentration in A102, but which is still lower than the levels in the coprolite control. All the tissue digests and the control contain similar levels of sulphur and potassium. Aluminium was only found in the coprolite control and in lung samples A13 and A102. There is a small amount of manganese in the lung samples A102, A108, A110 and the control.
The results of the ancient particle extracts can be seen in Results section 4.7.5. The extracts contained much lower amounts of elements than the tissue digests which one would expect as the tissue digest would also include elements from the lung tissue that would be missing from the extracted particle suspension.

Sodium was present in all the samples. Another element common to all the samples is potassium. Iron was found in all the extracted particles except those from mummy A108 and DO46. Sample DO45 alone contained phosphorus. Magnesium was found in minute amounts in all the particle suspensions and at a higher level in DO46. Copper was detected in very small amounts in sample A4. A4 and A102 were the only samples to contain aluminium. The largest amount of zinc was found in sample A4 although it was present in very small quantities in all the other samples. The largest concentration of sulphur was found in DO45 but was also detectable in the other samples. Elements, such as magnesium, manganese, aluminium and copper are probably indicative of inorganic materials. Copper could be present from copper smelting although it has been found in surrogate soots, for example. Despite the presence of sodium and other trace

elements in these samples, it is unlikely to indicate the presence of natron as its identifying element is boron (Currie, 2008) and also could have been washed out (in solution) during the extraction process.

Although ICP-MS is a much more sensitive technique for elemental analysis with the surrogate soots and ancient particle extractions than EDX, it is not without its limitations. There is the polyatomic mass interference effect where signals of low atomic number elements can overlap (and effectively combine) and produce a false signal of a higher atomic number element. For example, two oxygen signals (which each have an atomic number of 16) can combine to produce a false signal for sulphur (atomic number 32) (May and Wiedmeyer, 1998). Although no solutions have been found to this problem, several approaches, including collision induced dissociation, have been suggested to reduce its effects (Jackson, et al. 2003). Additional problems include the high detection limit for silicon and the undetectability of halide elements. Additionally the signal strength detected in this method can depend on the natural abundance of the ion.

For example, when analyzing for calcium it is often the case that calcium is the major element present. If this is the case then the isotope of calcium ^{44}Ca which has a natural abundance of 2% is quantified as opposed to the major isotope ^{40}Ca which has a natural abundance of 96%. This method mitigates the potential to swamp minor elemental signals by a massive ^{40}Ca peak.

The results for LA-ICP-MS examination of modern sand samples can be seen in Results section 4.8.1. All four sands appear to contain large signals of magnesium and aluminium. Where the sands differ is in the other elements underneath these two large signals. It appears the sands can be divided into two groups; sands with strong silicon peaks and sand without strong silicon peaks. Karnak sand would belong to the first group as it possesses strong peaks for silicon and phosphorus. The silicon peak appears to follow the peaks and troughs of the aluminium curve and suggests there is co-distribution of these two elements in the form of the mineral aluminosilicate. Additionally, sand from Tuna El-Gebel also possesses peaks for silicon which seems to mirror the aluminium and magnesium profiles, again indicating aluminosilicates. Sands from Amarna and Amarna North Palace would belong to the second group. The Amarna sand contains variations and

peaks in manganese and iron and nickel. Amarna North Palace sand has variations in the levels of silicon, iron, and sulphur across the length of the sample.

Results of the scans of anthracotic ancient tissue and an accompanying control can be seen in Results section 4.8.2. Both samples contain a large magnesium signal not seen in other analytical techniques. This suggests that the magnesium signal may be a systematic contaminant through all the LA-ICP-MS samples. Additionally in both samples, the baseline of the silicon signal appears to be much higher than the other elements. Its trend appears to be a slow decline as time increases but it does contain three peaks within the sample, this change in signal was attributed to the ablated plume attaching and contaminating the internal componants of the instrument. . These three peaks also correspond to three peaks in the aluminium signal. This suggests there are alumino-silicates in the sample. Calcium and sulphur also have peaks that co-distribute suggesting that calcium sulphate in the form of gypsum or other combinations of elements may also be present in the unidentifiable material.

Mummy A13 also has silicon peaks throughout the sample. These peaks correspond well with the peaks of the calcium signal. The signals from iron and phosphate also closely resemble each other. Lead and copper also show small peaks in the sample which suggests that mummy A13 may have been exposed to copper from smelting processes or lead from lead working.

This method has several limitations which make it not particularly suitable for examining mummified tissue or preparations of particles. Like ICP-MS, a major limitation of this method is the polyatomic mass interference effect which could explain the large magnesium signal throughout all the samples. This magnesium signal could be composed of a carbon couplet where two carbon^{12}s combine to give a false signal of magnesium^{24} (May and Wiedmeyer, 1998). Carbon is ubiquitous and sources could have included the mylar substrate, the adhesive used to adhere particle to the Mylar. Additionally the signal strength detected in this method can depend on the natural abundance of the ion. For example, calcium is ubiquitous in rocks and inorganic samples. To prevent quenching of the elements by a huge calcium signal, the LA-ICP-MS is programmed to detect the Ca^{44} isotope with only 2% natural abundancy. Therefore, the calcium signal you

detect is only 2% of the actual calcium present in the sample providing that there has been no isotopic contamination. Although this method is far more sensitive than EDX, EDX is more focally accurate as the electron beam coupled with a scanning electron microscope allowed individual particles or small groups of particles to be analysed whereas the laser ablator spot of 100 micron size allowed only larger areas of mixed particles to be examined. The spot size of 100 microns was used to analyse particles of less than 10 microns which could have led to signal dilution as what should have been a sharp, well defined peak was drawn out over a larger time frame by the size of the laser. When examining preparations of particles, the energy transfer from the laser was apparent and caused the section to vibrate and eject particles off the mylar substrate. A laser with a smaller spot size could be used to remedy these two problems. This too has its disadvantages as although the laser would then be more focally accurate, it would be less powerful and less efficient at ablating the sample.

The LA-ICP-MS results not only provided elemental data on mummified tissue but suggested possible areas of particle distribution through varying peaks of different elements as the laser passed through the mummified tissue. EPMA was chosen to provide more information and help elucidate the distribution patterns of elements within mummified tissue.

The results of WD-EPMA can be seen in Results section 4.9. WD-EPMA having the advantage of mapping the surface of the sample at high spatial and elemental resolution has major advantages, however, sample preparation is problematic. The co-distribution of aluminium and silicon together was expected as their affinity for each other is well known. Sand is commonly composed of alumino-silicates and indeed the modern surrogates from Amarna especially are composed of alumino-silicates. Silicon does not exclusively co-distribute with aluminium as it has co-distributed with iron, calcium and magnesium in the top half of the tissue. Aluminium also seem to distribute with magnesium. Iron appears to co-distribute predominantly with aluminium and also certain areas of silicon and magnesium. This indicates that there may be at least three types of particles present for example, an alumino-silicate, dolomite (magnesium and calcium carbonate) and haemosiderin (iron-based compound deposited in immune reactions). The distribution maps show that the particles are located in packed deposits at specific

points rather than homogeneously dispersed throughout the mummified tissue. This type of deposition behaviour is characteristic of selective phagocytosis by alveolar macrophages, where the macrophages would engulf the particle, and travel to a specific area in the lungs before coalescing and laying down the particles. Phosphorus and sulphur have few signals and appear not to co-distribute with any other elements. These elements may be contained within the organic tissue. WD-EPMA shows that there is no lead in the sample, which directly contradicts the LA-ICP-MS. It is very possible that there are further particles of lead within the lung tissue of A13 but this method is only probing the surface layers of the specimen and may not penetrate far enough into the tissue to find them. EPMA has produced detailed maps of the distribution of these elements in mummified lungs and therefore, the elements localised within the inorganic and organic particles. However, a major limitation for its use with mummified material is the requirement for the sample to be embedded in resin. Although the method is non-destructive, embedding the sample in resin makes the material difficult or impossible to use for analysis by other techniques. Analysis using this method was not extended to other mummified lung samples as not enough spare tissue was available.

After EDX spectra of the surrogate soots and extracted anthracotic particles failed to reveal much information on their elemental content, it was decided to try a different approach to see if the soot could be identified through Raman spectroscopy and characterised by interaction of their chemical bonds with the Raman laser. It was hoped that even if the bonds themselves could not be identified, then the bonds could still act as a fingerprint. The fuels were analysed first to assess differences between the fuel and its associated soot. The analysis (Results section 4.10.1) revealed that Raman spectroscopy could be applied successfully to the oils and beeswax. The data revealed that even though the fuels looked similar, they each possessed differences in absorbance band shape and breadth which could potentially be used to identify it. When the surrogate soots were analysed, it was revealed that few bonds had survived the combustion process leaving insufficient band “fingerprints” to positively identify the surrogate soots. Additionally two of the surrogates did not react when interrogated by the

Raman laser and did not produce data for a spectrum. This same scenario occurred when a section of mummified lung tissue was examined. The main limitation for this technique is that the Raman Effect is very weak, with only 1 in every 10^6 to 10^8 photons undergoing inelastic scattering (Ellis and Goodacre, 2006). Additionally the Raman laser needs to be focussed exactly onto the sample. If not focussed correctly, the objective lens can interfere with signal collection.

After Raman spectroscopy failed to successfully analyse the bonds in surrogate and ancient anthracotic particles, it was suggested that a similar technique, FT-IR, would be able to overcome these problems. Again the surrogate fuels were characterised in an attempt to demonstrate the differences between the fuels and their associated soots. The results of the FT-IR analysis (Results section 4.11.1) of the fuels provided three areas where differences in absorbance peak shape could be used to characterise and identify the fuel (figure 4.99b). However, when surrogate soots were examined using FT-IR no valid spectra could be produced. Background and anthracotic areas of a histological section of mummified lung from mummy A13 were interrogated with a FT-IR beam. The spectra produced (figure 4.100a) from the different areas demonstrated a small change in peak shape between the background tissue and anthracotic deposits. Analysis of the raw data showed that the results contained too much variance between sample replicates for this peak change to be considered accurate. It was thought that reproducibility and accuracy could be improved if the particles were analysed without the presence of tissue. Analysis of the extracted ancient particles showed two possible areas of identification (figure 4.101a) however statistical analysis of the raw data showed the variance of the replicates was greater than before. Although FT-IR is a rapid technique that can be used on a variety of sample types, its lack of reproducible results when analysing ancient particles and surrogate soots mean it is not suitable for this project.

The original hypothesis of this study was to examine the lungs of ancient Egyptians for signs of particles and their associated diseases. The lungs act as a

permanent scientific record of the living conditions and environment of the individual. By examining the particles and establishing their aetiology it was hoped that new details of social and economic conditions could be elucidated. The need for this project exists because the only evidence thus far comes from transcriptional and archaeological sources rather than a scientific investigation of tissues belonging to individuals of that era.

The aims of this study were as follows:

"*To assess differences in quality of preservation of lung tissue and their associated particles across the different types of mummification (intentional and spontaneous*)."

This was achieved by using a pilot and subsequent multi-stain histological study to evaluate the state of preservation and confirm the identity of mummified lung tissue samples obtained through the International Mummy Tissue Bank at the University of Manchester. Over half the mummified samples did not contain tissue that corresponded with their provenanced identity. This was due to mislabelling either in antiquity or at time of sampling. Mummified lung tissue was only sourced from spontaneously mummified individuals meaning a comparison of preservation states between the different mummification methods was not possible.

Another aim was "*to assess evidence of disease of particulate origin in ancient Egyptian lung tissue*."

A multi-stain histological study was used to evaluate the presence and degree of particle deposits in the mummified samples. Stains, such as, Toluidine blue, can be used to successfully demonstrate the anthracotic particles present in the ancient tissue whilst polarised light can demonstrate the birefringent inorganic particles.

A further aim was "to characterise the particles found in ancient Egyptian lung tissue, including with reference to surrogate (modern) particles". Surrogate soot particles were produced from fuels to act as a comparison against the ancient anthracotic particles. Sands from Egypt, mud-brick fragments and phytoliths were collected to act as comparisons against inorganic particles. A biological model was developed to assess changes made to particles during intentional mummification

process. This model also provided surrogate tissue for optimisation of staining methods and the development of particle extraction. A sonication method was developed to extract ancient particles from mummified lung tissue. Once extracted these particles were characterised and compared in situ and ex situ by size, shape and elemental composition. The size and shape characterisation was achieved through examination of ancient particles through light and electron microscopy. The elemental characterisation employed various analytical methods including bulk analysis techniques such as ICP-MS and focal techniques, such as, EDX and LA-ICP-MS. Other methods, such as, Raman spectroscopy and FT-IR could not be appropriately applied to the characterisation of ancient particles.

After characterisation, the next aim was to "*use this information as an indicator of the social status and living conditions of ancient Egyptians*".

Unfortunately elemental, physical and morphological characterisation of the particles did not show enough variation and identifying factors to allow individuals to be distinguished from each other by their lung particle content. The study was limited by the number of samples of ancient lung that could be obtained for examination.

If this study were to be repeated, it would be essential to obtain a higher number of samples.

The final aim was "*to review evidence for use of artificial lighting and cooking in enclosed environments (and hence exposure from the resulting soot) in ancient Egypt by the examination of archaeological records".*

Inscriptional evidence and excavation records were examined to try and establish the availability of artificial lighting and cooking in enclosed environments by different social groups and hence the extent of exposure of the population as a whole. Artificial lighting was probably widespread in ancient Egyptian culture as evidenced by popular culture examples such as "the tale of the Two Brothers" and inventory list evidence from workman villages like Deir el-Medina.

Chapter 6

Conclusions and Future Work

Conclusions

The original hypothesis of this study cannot be supported. This is primarily due to the low number of mummified lungs that were available to be studied. A larger sample size would not only provide greater numbers of ancient organic and inorganic particles for characterisation, but allow interpersonal relationships and global commonalities in populations to be demonstrated.

A multi-stain histological study was successfully applied to mummified tissue allowing lung tissue to be identified by its characteristic micro-anatomical features and components. Histological stains have demonstrated that the distribution of particle deposits within ancient lung tissues are the result of alveolar macrophages phagocytosis and other biological processes before death. Both the organic and inorganic particles have been shown to be less than 10 microns in aerodynamic diameter implying they were respired pre-mortem. One mummified sample could be distinguished from the others, however, lack of provenance means details surrounding this detail could not be elucidated. Surrogate soots and some of the smaller grains of samples of Egyptian sands, mud-bricks and phytoliths have all been shown to be within the respirable range and could be potential sources of these ancient particles.

Elemental characterisation of the ancient particles by both bulk and focal analysis methods did not show enough variation and characteristic identifying factors to allow individuals to be distinguished from each other by their lung particle content.

Literary evidence has been reviewed showing that artificial illumination was widely available in ancient Egyptian society.

Future work

The main area for future work would be performing a similar study with a much larger sample size. More specimens could be obtained by co-operating with academics and scientific institutions in Egypt and using their facilities to carry out the scientific analysis.

A larger sample size would allow the study of populations not only from different geographical locations but also from different time periods. This could establish whether the degree of exposure to different fuels (and therefore the extent of their usage) varies not only from area to area but over the different periods of Egyptian history. Additionally more samples would allow the effect of gender, age, and social class bias on lung particle content to be thoroughly explored. For example, a gender study could show that females had a higher degree of exposure to cooking fuel soots than males or a social study could demonstrate the differences in sand and phytolith exposure between outdoor workers and the nobility.

A method of separation of anthracotic and birefringent particles from ancient mummified lungs using methods such as specific density would also be developed to aid subsequent analysis.

References

Abdel-Maksoud, G;, and El-Amin, A.R., (2011) “A review on the materials used during the mummification processes in ancient Egypt” Mediterranean archaeology and archaeometry11 (2): 129 – 150.

Adams, W.Y., Adams, N.K. *et al.* 1999. *Kulubnarti III. The Cemeteries.* Sudan Archaeological Research Society 4, London.

Allen, R.C., (1997) “Agriculture and the origins of the state in ancient Egypt”, *Explorations in Economic History* 34 (2): 135-154.

Anderson, J.R., (2008) “A Mamluk coin from Kulubnarti, Sudan”, *British Museum studies in Egypt and the Sudan* 10: 65-71.

Arnold, D., (1996) *Die Temple Agyptens*, Augsberg, Bechtermunz Verlag.

Arnold, D., (2001) *The Encyclopaedia of ancient Egyptian architecture*, London, I.B. Tauris.

Artal-Sanz, M., Samara, C., Syntichaki, P., and Tavernakis, N., (2006) “Lysosomal biogenesis and function is critical for necrotic cell death in Caenorhabditis Elegans”, *Journal of Cell Biology*, 173 (2): 231-239.

Aston, B., Harrell, J., and Shaw, I., (2000) “*Stone*” in P.T., Nicholson and I., Shaw (Eds.), Ancient Egyptian materials and technology, Cambridge, Cambridge university press.

Aufderheide, A.C., (2003) *The scientific study of mummies*. Cambridge, Cambridge University Press.

Aufderheide, A.C., Cartmell, L., and Zlonis, M., (2004) “*Bio-anthropological features of human mummies in Kellis 1 cemetery: The database for mummification methods*” in Bowen, G.E., Hope, C.A., *The Oasis Papers 3. Proceedings of the Third International Conference on the Dakhleh Oasis Project.* Dakhleh Oasis Project: Monograph 14. Oxford, Oxbow Books.

Bagchi, N., (1992) “What makes silica so toxic?” British Journal of Industrial Medicine, 49: 163-166.

Bancroft, J., and Stevens, A., (1996) *Theory and Practice of Histological Techniques* (4th Ed), London, Churchill Livingstone.

Becklake, M., (2007) “Grain dust and lung health: Not just a nuisance dust” Canadian Respiratory Journal, 14 (7): 423-425.

Bedigian, D., and Harlan, J.R., (1985) “Sesamin, sesamolinand the origin of sesame”, Biochemical Systematics and Ecology 13 (2): 133-139.

Bradbury, H.S.M., and Bracegurdle, B., (1998) *Introduction to light Microscopy*, London, Garland Science.

Brier, B., (1996) “*Egyptian Mummies: Unravelling the Secrets of an Ancient Art”*, London, O’Mara publishing.

Brier, B., and Wade, R.S., (2001) “Surgical procedures during ancient Egyptian mummification”, *Chunga (Arica)* 33 (1)

British Museum, (2009) **"***Canopic chest and jars of Henutmehyt*", http://www.britishmuseum.org/explore/highlights/highlight_objects/aes/c/canopic_chest_and_jars_of_henu.aspx, accessed 5/7/09.

Budge, E.A.W., (1895) The Book of the Dead, New Jersey, Gramercy books.

Canadian Museum of Civilization, (2010) "The Soul", http://www.civilization.ca/cmc/exhibitions/civil/egypt/egcr05e.shtml, accessed 24/10/10.

Capasso, L., (2000) "Indoor pollution and respiratory diseases in Ancient Rome", The Lancet, 356 (9243): 1774.

Cassel, S.L., Eisenbarth, S.C., Iyer, S.S., Sadler, J.J., Colegio, O.R., Tephly, L.A., Carter, A.B., Rothman, P.B., Flavell, R.A., Sutterwala, F.S., (2008) "The Nalp3 inflammasome is essential for the development of silicosis", *Proceedings of the National Academy of Sciences of The United States of America 105 (26): 9035-9040.*

Cerny, J., (1973) *A community of workmen at Thebes in the Ramesside Period*, Cairo, L'Institut Francais D'Archeologie Orientale.

Cesarani, F., Martina, M.C., and Ferraris, A., (2003) "Whole-body three-dimensional multidetector CT of 13 Egyptian human mummies". *American Journal of Roentgenology* 180(3): 597–606

Christie, W.W., (2012) "Fatty acids: Hydroxy and other oxygenated", *lipidibrary.aocs.org*, accessed 12/03/11.

Clarke, S.W., and Pavia, D., (1980) "Lung mucus production and mucociliary clearance: methods of assessment." *The British journal of Clinical Pharmacology*, 9(6): 537–546.

CNX.org, (2012) http://cnx.org/content/m22326/latest/graphics6.jpg, accessed 12/03/12.

Cockburn, A and E., (1985) *Mummies, Disease and Ancient Cultures*, Cambridge, Cambridge University Press.

Copley, M.S., Bland, H.A., Rose, P., Horton, M., and Evershed, R.P., (2005) "Gas chromatographic, mass spectrometric and stable carbon isotopic investigations of organic residues of plant oils and animal fats employed as illuminants in archaeological lamps from Egypt." *The Analyst*, 130: 860-871.

Corbelli, J., (2006) *The Art of Death in Graeco-Roman Egypt*, Oxford, Osprey Publishing.

Currie, K., (2006) "Sections of mummy – Histological investigation of ancient Egyptian remains", *The Biomedical Scientist*, April 2006: 328-331.

Currie, K., (2008) "*Analytical elemental fingerprinting of natron and its detection in ancient Egyptian mummified remains* ", Unpublished PhD Thesis, Manchester, University of Manchester.

Dass, C., (1994), "*Mass Spectrometry: Instrumentation and techniques*", in D.M., Desiderio (Ed.), Mass Spectrometry – Clinical and Biomedical applications Volume 2, New York, Plenum Press.

David, A.R., (1978) *Mysteries of the mummies: The story of the Manchester University investigation*, London, Book Club Associates.

David A.R., and David A.E., (1995) “Preservation of human mummified specimens” in C.Collins (Ed.), *The Care and Conservation of Palaeontological Material*. Oxford, Butterworth-Heinemann Ltd.

David, A.R., (1999) “*Handbook to life in ancient Egypt*” Oxford, Oxford University Press.

David, A.R., (2008) “Egyptian Mummies: An Overview” in A.R. David (Ed.), *Egyptian Mummies and Modern Science*. New York, Cambridge University Press.

Davies, N., (1929). “The town house in ancient Egypt” *Metropolitan Museum Studies*, 1: 233-55

Drury, R.A.B., and Wallington, E.A., (1980) *Carleton’s Histological Technique*, Toronto, Canada, Oxford University Press.

Dunnill, M.S., Parums, D.V., and Bates, J., (1996) “Diseases of the Ear and Respiratory tract” in D.V. Parums (Ed.), *Essential clinical pathology*, Oxford, Blackwell Science.

Ellis, D.I., and Goodacre, R., (2006) “Metabolic fingerprinting in disease diagnosis: biomedical applications of infrared and Raman spectroscopy”, *The Analyst*, 131: 875-885.

Erman, A., (1894) *Life in Ancient Egypt,* New York, Dover Publications.

Ezzamel, M., (2004) “Work organisation in the Middle Kingdom, Ancient Egypt”, Organization 11 (4): 497-539.

Feldtkeller, E., Lemmel, E-M., and Russell, A.S., (2003) “Ankylosing spondylitis in the pharaohs of ancient Egypt”, *Rheumatology International*, 23: 1-5.

Fischer, H.G., (1977) "The Evolution of Composite Hieroglyphs in Ancient Egypt." *Metropolitan Museum Journal*, 12.

Garner, R., (1979) “Experimental mummification” in A.R., David (ed) *The Manchester Museum Mummy Project*, Manchester.

Grobbelaar, J.P., and Bateman, E.D., (1991) “Hut lung: a domestically acquired pneumoconiosis of mixed aetiology in rural women”, *Thorax* 46: 334-340.

Gross, J.H., (2004), *Mass Spectrometry: A textbook*, Berlin, Springer-Vergal Science and Business media.

Harrell, J.A., and Lewan, M.D., (2002), “*Sources of mummy bitumen in ancient Egypt and Palestine*”, Archaeometry, 44 (2): 285-293.

Harris, J.E., and Weeks, K.R., (1973) “*X-raying the Pharaohs*”, New York, Scribners.

Hayes, W., (1953). "Notes on the Government of Egypt in the Late Middle Kingdom" *Journal of Near Eastern Studies* 12: 31–39.

Heller, M.J., Burgart, L.J., Teneyck, C,J., Anderson, M.K., Greiner, T.C., and Robinson, R.A., (1991) “An efficient method for the extraction of DNA from formalin-fixed, paraffin embedded tissue by sonication” Biotechniques, 11: 372-377.

Hicks, A., (2004) *A comparative study of the staining properties of elastin in rehydrated mummified tissue*, Unpublished Masters Thesis, Manchester, University of Manchester.

Hirata, K., (2005) “Radiographic findings in ancient Egyptian mummies” *X-rays for Arhaeology 2005*: 259-261.

Hubschmann, C., (2010) “Who inhabited Dakhleh Oasis: Searching for an Oasis identity in Pharaonic Egypt”, Papers from the Institute of Archaeology, Vol 20: 341.

Kay, A., (1996) “*California's Push to End Global Warming*”, http://healthandcleanair.org/newsletters/issue9.html, accessed 5/7/09.

Kaper, O.E., and Zoest, C.V., (2006) *Treasures of the Dakhleh Oasis*, Cairo, Nederlands-Vlaams Instituut.

Kemp, B., (2000) “*Soil (including mud-brick architecture)*” in P.T., Nicholson and I., Shaw (Eds.), Ancient Egyptian materials and technology, Cambridge, Cambridge university press.

Kiernan, J.A., (1981) *Histological and Histochemical Methods: Theory and Practice*. Oxford, Pergamon Press.

Klatt, E.C., (2009) “*Pulmonary pathology*”, http://library.med.utah.edu/WebPath/LUNGHTML/LUNG084.html, accessed 5/7/09.

Jackson, G.P., King, F.L., and Duckworth, D.C., (2003) “Efficient polyatomic interference reduction in plasma-source spectrometry via collision induced dissociation”, *Journal of Analytical Atomic Spectometry*, 18: 1026-1032.

Lambert-Zazulak, P., (2000) “The International Ancient Egyptian Mummy Tissue Bank at the Manchester Museum,” *Antiquity*, 74: 44-48.

Lang, M.R., Fiaux, G.W., Gillooly, M., Stewart, J.A., Hulmes, D.J.S., and Lamb, D., (1994) “*Collagen content of alveolar wall tissue in emphysematous and non-emphysematous lungs*”, Thorax – an international journal of respiratory medicine, 49: 319-326.

Leica, (1994) “*Quantimet 600 User Manual*” Leica Cambridge Ltd, Cambridge, UK,

Lucas, A., (1962) Ancient Egyptian Materials, Montana USA, Kessinger Publishing.

Manniche, L., (1999) *Sacred Luxuries*, New York, Cornell University Press.

McCreesh,N.C., Gize, A.P.,Denton, J., and David, A.R., (2011). “Hair analysis: a Tool for Identifiying Pathological and Social Information,”*Yearbook of Mummy Studies*, 1(1)

McDowell, A.G., (1990) *Jurisdiction in the Workmen’s community of Deir El-Medina*, Leiden, Nederlands Instiut voor het Nabije Oosten.

McManus, J.F.A., (1946) “Histological demonstration of mucin after periodic acid”, *Nature* (London), 158: 202.

Mailer, R., (2006) “Chemistry and quality of Olive oil”, *New South Wales Department of Primary Industries:* 227.

Mair, C., (2008) “*Lighting the dark: Artificial lighting in Dynastic Egypt*”, Unpublished Certificate in Egyptology Thesis, Manchester, University of Manchester.

May, T.W., and Wiedmayer, R.H., (1998) “A table of polyatomic interferences in ICP-MS” Journal of Atomic Spectroscopy, 19 (5): 150-155.

Meinardus, O.F., (2003) *Two thousand years of Coptic Christianity: New Edition*, Cairo, The American University in Cairo Press.

Mekhota, A-M., and Vermehren, M., (2005) “Determination of optimal rehydration, fixation and staining methods for histological and immunohistochemical analysis of mummified soft tissues”, *Biotechnic and Histochemistry*, 80 (1): 7-13.

Meyer, C., (1997) “Bir Umm Fawakhir: Insights into ancient Egyptian mining” Journal of the Minerals, Metals,and Materials society, 49 (3): 64-68.

Miller, P.J., (1971) “An elastic stain”, *Medical Laboratory Technology*, 28 (2):148-149.

Molinero, A.L., Morales, A., Villareal, A., and Castillo, J.R., (1997) “Gaseous sample introduction for the determination of silicon by ICP-AES”, Fresenius’ Journal of Analytical Chemistry, 358 (5): 599-603.

Mulhern, D.M., (2000) “Rib modelling dynamics in a skeletal population from Kulubnarti, Nubia”, *American Journal of Physical Anthropology* 111:519-530.

Murray, M.A., (2000) “*Cereal production and processing*” in P.T., Nicholson and I., Shaw (Eds.), Ancient Egyptian materials and technology, Cambridge, Cambridge university press.

Nerlich, A.G., Parsche, F., Wiest, I., Schramel, P., and Lohrs, U., (1995) “Extensive pulmonary haemorrhage in an Egyptian mummy”, *Virchows Arhiv*, 427 (4): 423-429.

Nicholson P.T., and Shaw, I., (2000), *Ancient Egyptian materials and technology*, Cambridge, Cambridge university press.

Nikon, (2009) “*Human Pathology Digital Image Gallery*”, http://www.microscopyu.com/staticgallery/pathology/anthracosis10x01.html, accessed 6/7/09.

Notter, R.H., (2000) *Lung surfactants: Basic science and clinical applications*. New York, Marcel Dekker.

Nunn, J.F., (1996) *Ancient Egyptian Medicine,* Norman,OK, USA, University of Oklahoma Press.

Nzikou, J.M., Atos, J.E. Moussounga, C.B. Ndangui, A. Kimboguila, Th. Silou, M. Linder, M., and Desobry, S., (2009) “Characterisation of *Moringa olifeira* seed oil

variety Congo Brazzaville” *Journal of Food Technology* 7(3): 59-65.

Ogden, J., (2000) “*Metals*” in P.T., Nicholson and I., Shaw (Eds.), Ancient Egyptian materials and technology, Cambridge, Cambridge university press.

Parr, J.F., Lentfer, C.J., and Boyd, W.E., (2001). “A comparative analysis of wet and dry ashing techniques for the extraction of phytoliths from modern plant material”. *Journal of Archaeological Science* 28, 875-886

Petrie Museum, (2009a) "*Museum number – UC34739*" http://www.petrie.ucl.ac.uk/detail/details/index_no_login.php?objectid=UC34739&accesscheck=/detail/details/index.php, accessed 7/7/09.

Petrie Museum, (2009b) "*Museum number – UC34977*" http://www.petrie.ucl.ac.uk/detail/details/index_no_login.php?objectid=UC34977&accesscheck=/detail/details/index.php, accessed 7/7/09.

Petrie Museum, (2009c) "*Museum number – UC45601*" http://www.petrie.ucl.ac.uk/detail/details/index_no_login.php?objectid=UC45601&accesscheck=/detail/details/index.php, accessed 7/7/09.

Petrie, W.M.F, Quibell, J.E., and Spurrell, F., (1895) *Naqada and Ballas*, London, British school of Archaeology in Egypt.

Pettijohn, F.J., Potter, P.E., and Siever, R., (1987) *Sand and Sandstone*. New York, Springer.

Piperno, D.R., (2006) "*Phytoliths: A Comprehensive Guide for Archaeologists and Paleoecologists* ", United States, AltaMira Press.

Potts, M., (1994) "Desiccation tolerance of prokaryotes" *Microbiological Reviews*, 58 (4): 755-805.

Quirke, S., and Spencer, J., (1992) *The British Museum book of Ancient Egypt*. London, British Museum Press.

Rawlinson, G., (1880) *The History of Herodotus: A new English version with copious notes and appendices*. London, J. Murray.

Reed, S.J.B., (2005) *Electron Microprobe Analysis and Scanning Electron Microscopy in Geology*. Cambridge, Cambridge University Press.

Reisner, G.A., (1934) "The history of the Egyptian Mastaba" *Extrait des Memoires de l'Institut Francais LXVI*, Cairo, Imprimerie de l'institut Français.

Riyad, H., (1973) *Mummification in ancient Egypt and the celebration of the hundredth anniversary of the discovery of the royal mummies in the Valley of the Kings at Thebes*, Cairo, Ministry of Culture.

Robins, F.W., (1939) "The lamps of ancient Egypt", *Journal of Egyptian Archaeology, 25: 184-187.*

Robins, G., (1993) Women in ancient Egypt, Harvard USA, Harvard University Press

Robinson, J.W., and Frame, G.M., (2004) *Undergraduate Instrumental Analysis.* New York, Marcel Dekker.

Rosen, A.R., (1998) "*Catalhoyuk 1998 Archive Report*" http://www.catalhoyuk.com/archive_reports/1998/ar98_08.html, accessed 7/7/09.

Rubins, J.B., (2003) "Alveolar Macrophages: wielding the double-edged sword of inflammation", *American Journal of Respiratory and Critical Care Medicine*, 167: 103-104.

Ruffer, M.A., (1911) "Histological studies on Egyptian mummies", *Mémoires présentés a l'institut Égyptien et publies sous les auspices de S. A. Abbas II*, 6.

Saint George's University of London (2013) "Lung structure and function" http://www.elu.sgul.ac.uk/rehash/guest/scorm/244/package/content/alveoli.htm, accessed 31/1/13.

Santhanam, N., Balu, M, and Sreevatsan, S., (2012) "Production and uses of key castor oil oleochemicals" *Castoroil.in*.

Seidlmeyer, S., (2000) "The First Intermediate Period" in Shaw, I., (ed) "*The Oxford History of Ancient Egypt*", Oxford, Oxford University Press.

Serpico, M., (2000) "*Resins, Amber and Bitumen*", in P.T., Nicholson and I., Shaw (Eds.), Ancient Egyptian materials and technology, Cambridge, Cambridge university press.

Serpico, M., (2009) "*Armana project: Organic Residues*", http://www.amarnaproject.com/pages/recent_projects/environmental/organic.shtml , accessed 10/6/09.

Serpico, M., and White, R., (2000) "*Oil, fat and wax*", in P.T., Nicholson and I., Shaw (Eds.), Ancient Egyptian materials and technology, Cambridge, Cambridge university press.

Shaw, A.F.B., (1938) "A histological study of the mummy of Har-Mose, the singer of the eighteenth dynasty." *Journal of Pathological Bacteriology*, 47: 115-123.

Shaw, I., (2000) "*The Oxford History of Ancient Egypt*", Oxford, Oxford University Press.

Sheldrick, P., (2007) "The People of the Dakhleh Oasis", *Ancient Egypt Magazine*, April/May 2007: 19-26.

Shier, L.A., (1978) Terracotta lamps from Karanis, Egypt: Excavations of the Univserity of Michigan, Boston, USA, University of Michigan Press.

Simpson, W.K., Faulkner, R.O., and Wente, E.F., (1973) The literature of ancient Egypt, London, Yale University Press.

Smith, J.R., (1953) "Salt", Nutrition Reviews 11 (2): 33-36.

Smith, G.D., and Clark, R.J.H (2004) "Raman microscopy in archaeological science", *Journal of Archaeological Science* 31: 1137-1160.

Stanley, N.N., Alper, R., Cunningham, E.L., Cherniack, N.S., and Kefalides, N.A., (1975) "Effects of a molecular change in collagen on lung structure and mechanical function" *The Journal of Clinical Investigation*, 55(6): 1195–1201.

Strouhal, E., Nemeckova, A., and Kouba, M., (2003) "Palaeopathology of Iufaa and other persons found beside his shaft tomb at Abusir (Egypt)", *International Journal of Osteoarchaeology*, 13 (6): 331-338.

Suthren, R., (2007) “Sand SEM”, http://www.virtual-geology.info/sedimentology/sandsem.html, accessed 12/3/12.

Tapp, E., Curry, A., and Anfield, C., (1975) “Letter: Sand pneumoconiosis in an Egyptian mummy”, *British Medical Journal*, 2(5965): 276.

Tapp, E., (1979) “Disease in the Manchester mummies” In A.R. David (Ed.) *The Manchester Museum mummy project*, Manchester, Manchester Museum Press.

Taylor, J.J., and Griffith, F., (1894) *The Tomb of Paheri*, London, Egypt Exploration Fund.

Turner, B.L., Edwards, Quinn, E.A., Kingston, J.D., and Van Gerven, D.P., (1997) “Age-related variation in Isoptic Indicators of diet at medieval Kulubnarti in Sudanese Nubia”, *International Journal of Osteoarchaeology* 17 (1): 1-25

Turner-Walker and Peacock, (2008) “Preliminary results of bone diagenesis in Scandinavian bogs” *Palaeogeography, Palaeoclimatology, Palaeoecology*, 266 (3-4): 151-159

Tyldesley, J., (1996) Hatchepsut, *The Female Pharaoh*, England, Penguin Group.

Uponreflection.com (2009) “Hieroglyphic H”, http://www.uponreflection.co.uk/hieroglyphics/egyptian_hieroglyphics_h.htm, accessed 9/10/09.

U.S. National Cancer Institute., (2006) “*Anatomy of the lung*”, http://training.seer.cancer.gov/module_anatomy/images/illu_bronchi_lungs.jpg, accessed 07/01/09.

Vass, A., (2010) “Dust to Dust”, *Scientific American*, 303: 56-59.

Vogelsang-Eastwood, G., (2000) “*Textiles*” in P.T., Nicholson and I., Shaw (Eds.), Ancient Egyptian materials and technology, Cambridge, Cambridge university press.

Walker, R., Parsche, F., Bierbrier, M., and McKerrow, J.H., (1987) “Tissue identification and histologic study of six lung specimens from Egyptian mummies”, *American journal of physical Anthropology*, 72 (1): 42-48.

Weeks, K., (2000) “KV 5: a preliminary report, revised edition (2006), New York, The American University in Cairo Press.

Ward, H.E., and Nicholas, T.E., (1984) “Alveolar type I and II cells”, *Australian and New Zealand Journal of Medicine*, 14 (5 suppl 3): 731-734.

Wilson, J.A., (1965) *The culture of Ancient Egypt*, Chicago USA, University of Chicago press.

Wolman, M., (1971) “Amyloid its nature and molecular structure: Comparison of a new toluidine blue polarised light method with traditional procedures”, *Laboratory Investigation*, 25 (4): 104-110.
Zimmerman, M.R., (1972) “Histological examination of experimentally

mummified tissues” *American Journal of Physical Anthropology* 37: 271-280.

Zimmerman, M.R., (2010) Personal Communication.